AD-A049 796 HARRIS CORP MELBOURNE FLA ELECTRONIC SYSTEMS DIV F/G 9/4
DIGITAL IMAGERY TEST SET.(U)
NOV 77 R H COFER, A R MARTIN
UNCLASSIFIED RADC-TR-77-371 F30602-76-C-0296 NL

1 OF 3
AD A049798



AD A049798

DDC FILE COPY

RADC-TR-77-371
Final Technical Report
November 1977

DIGITAL IMAGERY TEST SET

Dr. Rufus H. Cofer, Jr.
Mr. Albert R. Martin

Harris Corporation

DDC
FEB 10 1978
F

Approved for public release; distribution unlimited.

ROME AIR DEVELOPMENT CENTER
Air Force Systems Command
Griffiss Air Force Base, New York 13441

This report has been reviewed by the RADC Information Office (OI) and is releasable to the National Technical Information Service (NTIS). At NTIS it will be releasable to the general public, including foreign nations.

RADC-TR-77-371 has been reviewed and is approved for publication.

APPROVED: Andrew R. Pirich

ANDREW R. PIRICH
Project Engineer

APPROVED: Howard Davis

HOWARD DAVIS
Technical Director
Intelligence & Reconnaissance Division

FOR THE COMMANDER: John P. Huss

JOHN P. HUSS
Acting Chief, Plans Office

If your address has changed or if you wish to be removed from the RADC mailing list, or if the addressee is no longer employed by your organization, please notify RADC (IERE) Griffiss AFB NY 13441. This will assist us in maintaining a current mailing list.

Do not return this copy. Retain or destroy.

UNCLASSIFIED

SECURITY CLASSIFICATION OF THIS PAGE (When Data Entered)

REPORT DOCUMENTATION PAGE	READ INSTRUCTIONS BEFORE COMPLETING FORM
1. REPORT NUMBER: RADC-TR-77-371	2. GOVT ACCESSION NO. / 3. RECIPIENT'S CATALOG NUMBER
4. TITLE (and Subtitle): DIGITAL IMAGERY TEST SET.	5. TYPE OF REPORT & PERIOD COVERED: Final Technical Report. Jun 76 — Jun 77
	6. PERFORMING ORG. REPORT NUMBER: N/A
7. AUTHOR(S): Rufus H. Cofer, Jr Albert R. Martin	8. CONTRACT OR GRANT NUMBER(s): F30602-76-C-0296
9. PERFORMING ORGANIZATION NAME AND ADDRESS: Harris Corporation Electronic Systems Division Melbourne FL 32901	10. PROGRAM ELEMENT, PROJECT, TASK AREA & WORK UNIT NUMBERS: 62702F 6244 10
11. CONTROLLING OFFICE NAME AND ADDRESS: Rome Air Development Center (IRRE) Griffiss AFB NY 13441	12. REPORT DATE: Nov 77 13. NUMBER OF PAGES: 286 12 287p.
14. MONITORING AGENCY NAME & ADDRESS (if different from Controlling Office): Same	15. SECURITY CLASS. (of this report): UNCLASSIFIED 15a. DECLASSIFICATION/DOWNGRADING SCHEDULE: N/A

16. DISTRIBUTION STATEMENT (of this Report)

Approved for public release; distribution unlimited.

DDC
FEB 10 1978
F

17. DISTRIBUTION STATEMENT (of the abstract entered in Block 20, if different from Report)

Same

18. SUPPLEMENTARY NOTES

RADC Project Engineer: Andrew R. Pirich (IRRE)

19. KEY WORDS (Continue on reverse side if necessary and identify by block number)

Image quality	Spatial
Digital image	Quantization
Image test set	Sampling
Test image	Gray-level mapping

20. ABSTRACT (Continue on reverse side if necessary and identify by block number)

This exploratory development provides the initial concepts for a digital imagery test set from which subsequent detailed specifications would result. The difficult questions of image evaluation and quality were explored with the following categories of performance suggested for the test set criteria; amplitude response, frequency response, geometric fidelity, and noise. Both subjective tests with an experienced photointerpreter and objective tests using test pattern concepts were made. Computer programs were generated to simulate digital

→ next page

DD FORM 1 JAN 73 1473 EDITION OF 1 NOV 65 IS OBSOLETE

UNCLASSIFIED

SECURITY CLASSIFICATION OF THIS PAGE (When Data Entered)

408972

imagery degradations for the subjective tests, and these programs could be extended to include sensor simulations. The use of Moire' patterns provided simple objective tests as a result of the array structure of 2-dimensional digital imagery. Further development is recommended in exploring the trade-offs between MTF response and aliasing distortion.

ABSTRACT

The work described in this report provides basic information which will allow partial production of a standardized image quality test set. Factors affecting the production of a standardized imagery test set concerned digital image processing procedures and image reconstruction. Imagery consisting of one scene from a Texas Instruments FLIR sensor tape, one scene from a UPD-4 coverage of Griffiss AFB, NY and two scenes from a Wild RC-8 Mapping camera were qualitatively evaluated by a photo interpreter from Rome Research Corp. (Mr. Petroski). The imagery was evaluated both in hard copy (digitized scenes with perturbation on film) and soft copy (digitized scenes with perturbations using the RADC/Image Processing Facility). A total of 144 images was derived from four test scenes and were evaluated against an original set of imagery that was used as a base for comparison.

The information gathered included relationships between perturbations and image quality as expressed by per cent utility under perturbation, isopreference contours (pleasing to the eye) across modes of perturbation, verbal description of effects, and image quality as a transitive (comparative) characteristic.

Results indicate that the combination of sampling rate inclusive of source (sensor) imagery characteristics, structure (characteristics of display) and optimization (modulation transfer function) of the entire digital (processing) system, and the physiology of the visual system, lead to bounds on digital image quality.

ACCESSION for
NTIS [x]
DDC B.ff Section [ ]
UNANNOUNCED [ ]
JUSTIFICATION
BY
DISTRIBUTION/AVAILABILITY CODES
Dist. SPECIAL
A

TABLE OF CONTENTS

Section	Title	Page
I	INTRODUCTION	9
II	THE IMAGERY CHAIN	11
	A. The Natural Imagery Source	13
	B. The Observer	20
	C. Major Components of the Digital Imagery Processing Subsystem	33
	D. The Digital Image Conversion Process	37
	E. Digital Image Processor	39
	F. Image Evaluation	41
	G. Image Quality	43
III	SCANNERS AND REPRODUCERS	47
	A. Spatial Sampling and Reconstruction	47
	1. The Nyquist Sampling Theorem and Time-Limited Real Signals	48
	2. Image Resolution and Aliasing	49
	3. Aliasing Considerations in Image Resolution Reduction	54
	B. Quantization of Image Sources	60
	1. Three Approaches to Quantizing	60
	2. The Quantizing Performance Metric . . .	63
	3. Source Coding Subject to a Fidelity Criterion: Shannon's Rate-Distortion Theory	64
	C. Practical Digital Image Degradation Mechanisms	68

TABLE OF CONTENTS (Continued)

Section	Title	Page
IV	SUBJECTIVE EFFECTS OF SELECTED DIGITAL DEGRADATIONS	79
	A. Testing	79
	B. Preliminary Image Comparative Test Sets	80
	C. Results	84
V	POSSIBLE DIGITAL IMAGE SYSTEM OBJECTIVE TEST PATTERNS	127
	A. Measurement of Sampling Rate	127
	B. Measurement of MTF	132
	C. Measurement of Sampling Inhomogeneities	139
	D. Measurement of Reproducer Sampling Structure	143
	E. Observation of Systematic and Random Image Perturbations	145
	F. Determination of the Imagery System Gray-Level Mapping and Number of Levels of Quantization	145
VI	RESULTS AND CONCLUSIONS	147
	REFERENCES	151
	BIBLIOGRAPHY	153
	APPENDIXES	
	A Digital Imagery Test Set Program Documentation	161
	B Subjective Effects of Selected Digital Degradations	238
	C Interpretation of Moire' Pattern Formation as a Digital Sampling Process	269

TABLE OF CONTENTS (Continued)

Section	Title	Page
	APPENDIXES (Con't)	
D	Mathematics of Moire' Plotting	278
E	Measurement of MTF by the Observer	283

LIST OF ILLUSTRATIONS

Figure	Title	Page
2-1	The Natural Imagery Chain	12
2-2	Inclusion of Imagery Processing into the Natural Imagery Chain	12
2-3	A Simplified Representation of the Natural Imagery Source	14
2-4	Image Gray Level as a Function of Spatial Position (One Dimension Assumed)	17
2-5	Autocorrelation Curves Corresponding to BLRC Spectra with Normalized Corner Frequency ω_c/ω_o as a Parameter	21
2-6	Spectrum of Low Resolution Vertical Digitized Photograph	22
2-7	Spectrum of Infrared Image of Parked Image	23
2-8	Spectrum of Synthetic Aperture Radar Image over Griffiss AFB, NY	24
2-9	A Simplified Representation of the Human Observer	25
2-10	Intensity Profiles Illustrating "Brightness Constancy".	27
2-11	Subjective Brightness as a Function of Image Luminance	29
2-12	Backward Detector Inhibition Model	30
2-13	Overall Spatial Frequency Response for Several Values of Sinusoidal Modulation m	31
2-14	Ability to See as a Function of Visual Parameters	32
2-15	The Structure of the Digital Image Processing Subsystem	34

LIST OF ILLUSTRATIONS (Continued)

Figure	Title	Page
2-16	Abstract Representation of the Action Taken by a Digital Image Processing Subsystem	35
2-17	Results of an Arbitrary Digital Image Processing Action	40
2-18	Evaluation of a Digital Imagery Subsystem	42
3-1	Sampled Imagery System with Aliasing	50
3-2	Example of Aliasing	52
3-3	Sampled Imagery System, Sampling Frequency Adjusted to Prevent Aliasing	53
3-4	Sampled Imagery System, Prefiltered to Prevent Aliasing	55
3-5	Sampled Imagery System, Using Decimation and Interpolation, Degraded by Aliasing Effects . . .	56
3-6	Sampled Imagery System Two-Dimensionally Filtered to Prevent Aliasing	58
3-7	Nonideal Two-Dimensional Low-Pass Filtering Using Uniformly Weighted Input Values	59
3-8	Scanner and Reproducer Gray Level Mappings	61
3-9	Development of the Composite Gray Level Mapping . .	62
3-10	Data Rates Required to Send Uniform Quantizer Outputs to a Receiver as a Function of ϵ^2/A. Also Shown are Curves of Quantizer Output Entropy $H_Q(V)$ vs. ϵ^2/A as V_{max} is varied for M=10,20,40	65
4-1	Master Digital Images	81
4-2	Additive Gaussian Spot Noise Applied to a High Resolution B/W Vertical Digitized Photograph	85
4-3	Additive Gaussian Line Noise Applied to a High Resolution B/W Vertical Digitized Photograph	87

LIST OF ILLUSTRATIONS (Continued)

Figure	Title	Page
4-4	Varying the Sampling of a High Resolution B/W Vertical Digitized Photograph Under High Aliasing	89
4-5	Varying the Sampling of a High Resolution B/W Vertical Digitized Photograph Under Reduced Aliasing	90
4-6	Additive Gaussian Spot Noise Applied to a Low Resolution B/W Vertical Digitized Photograph	91
4-7	Additive Gaussian Line Noise Applied to a Low Resolution B/W Vertical Digitized Photograph	93
4-8	Gaussian Line Jitter applied to a Low Resolution B/W Vertical Digitized Photograph	95
4-9	Varying the Quantization of a Low Resolution B/W Vertical Digital Photograph	97
4-10	Varying the Sampling of a Low Resolution B/W Vertical Digitized Photograph Under High Aliasing	98
4-11	Varying the Sampling of a Low Resolution B/W Vertical Digitized Photograph Under Reduced Aliasing	99
4-12	Additive Gaussian Spot Noise Applied to an Infrared Image of Parked Aircraft	100
4-13	Additive Gaussian Line Noise Applied to an Infrared Image of Parked Aircraft	102
4-14	Gaussian Line Jitter Applied to an Infrared Image of Parked Aircraft	104
4-15	Varying the Quantization of an Infrared Image of Parked Aircraft	106

LIST OF ILLUSTRATIONS (Continued)

Figure	Title	Page
4-16	Varying the Sampling of an Infrared Image of Parked Aircraft Under High Aliasing	107
4-17	Varying the Sampling of an Infrared Image of Parked Aircraft Under Reduced Aliasing . . .	108
4-18	Additive Gaussian Spot Noise Applied to a Synthetic Aperture Radar Image	109
4-19	Additive Gaussian Line Noise Applied to a Synthetic Aperture Radar Image	111
4-20	Gaussian Line Jitter Applied to a Synthetic Aperture Radar Image	113
4-21	Varying the Quantization of a Synthetic Aperture Radar Image	115
4-22	Varying the Sampling of a Synthetic Aperture Radar Image Under High Aliasing	116
4-23	Varying the Sampling of a Synthetic Aperture Radar Image Under Reduced Aliasing	117
4-24	Effect of Additive Gaussian Spot Noise	118
4-25	Effect of Additive Gaussian Line Noise	118
4-26	Effects of Jitter	119
4-27	Effects of Number Gray Levels	119
4-28	Effect of Sampling Rate, High Aliasing	120
4-29	Effect of Sampling Rate, Low Aliasing	120
4-30	Effect of Additive Gaussian Spot Noise (Hardcopy vs. Softcopy)	124
4-31	Effect of Additive Guassian Line Noise (Hardcopy vs. Softcopy)	124
4-32	Effects of Jitter (Hardcopy vs. Softcopy)	125
4-33	Effects of Number Gray Levels (Hardcopy vs. Softcopy)	125
5-1	Input Sampling Rates Test Pattern	128
5-2	Comparative Sampling Rate	129
5-3	Example Results of Sampling Rate Test	131

LIST OF ILLUSTRATIONS (Continued)

Figure	Title	Page
5-4	Determination of Spatial Sampling Reproduction Rate	133
5-5	Precise Determination of Spatial Sampling Reproduction Rate	134
5-6	A Reproduced Chirped Test Image	136
5-7	Comparison of Chirped Spatial Frequency Test Charts	137
5-8	Example Derivations of MTF from the Chirped Spatial Frequency Test	137
5-9	A Test Image for Scan Reproduction	140
5-10	The Reproduced Version of Figure 5-9 with Scan Nonhomogeneity	141
5-11	Example of Moire' Scan Nonlinearity	142
5-12	Mathematical Spot Test *Image*	144
5-13	Example Results of Structural Determination	144
A-1	CPL Hardware Configuration	164
A-2	The DITS Test Set System	165
A-3	The Digital Processing Subsystem	166
A-4	The Digital Display Subsystem	167
A-5	Data Formats	170
C-1	The Spatial Frequency Representation of the Image of Figure 5-1	271
C-2	Rotated Version of the Input Test Pattern of Figure 5-1	272
C-3	The Local Origins of the Replicating Effects of the Image of Figure C-2 Used as a Sampler	273
C-4	The Spatial Frequency Distribution of the Image of Figure 5-4	274
C-5	Modulation Transfer Functions of Visual System (at Retina)	276
C-6	Relative Response of the Eye to the Spatial Frequency Distribution of Figure 5-4	277

SECTION I

INTRODUCTION

Digital processing techniques have become commonplace in their applications to imaging systems such that the need is long overdue for a digital imagery test set. The objective of this exploratory investigation is to determine preliminary criteria for such a test set. Necessary prerequisites which are first investigated include considerations of image quality, detailed analysis of the elements peculiar to digital imagery and subjective tests of imagery degraded by basic digital parameters.

The image quality considerations are introduced in Section II wherein an imagery source, digital processor, and observer are each evaluated as elements in the imagery chain. The representation of imagery by digital techniques and the processing of digital imagery is placed in proper perspective by considering the source characteristics such as its spectral properties, and the observer characteristics.

The sampling and reconstruction of two-dimensional imagery signals are the basic functions peculiar to digital imagery and these are analyzed in Section III. Aliasing and quantization noise are emphasized.

Section IV provides the conditions for and the results of subjective tests. A trained photointerpreter is used to evaluate the effects of basic digital degradations. Different imagery sources are used and include visual, FLIR and SAR. Digital degradations include additive noise, line jitter, quantization, and aliasing.

Finally, in Section V preliminary criteria for the digital imagery test set are given and several examples of candidate tests are provided. The use of Moire' patterns, which are ideally suited for analyzing the structure of digital image patterns, is included in this Section.

EVALUATION

Surprisingly little is found in the open literature on digital image quality. This preliminary investigation including both subjective and objective techniques forms a basis for the definition of a digital imagery test set.

The recommended test set criteria should include measurements in four categories of system performance: non-linear amplitude transfer characteristic, non-uniform MTF response (for frequencies up to one-half the Nyquist frequency), non-linear geometric response, and noise effects in general.

Digital imagery, based on its periodic or array structure, has interesting properties which provide simple tests for many, if not all, of the categories of system performance.

A wide variety of alternatives were considered in the search for dominant factors of digital image quality. These included physiology of the visual system, source imagery characteristics, structure and optimizations of digital image systems, and experimental evaluation of a preliminary subjective digital image test set.

A list of the objective digital image quality factors was determined:

a. Image extent in number of pixels.

b. Image sampling rate.

c. Image sampling structure.

d. System MTF (Modulation Transfer Function) below the Nyquist rate.

e. Prefilter MTF response above the Nyquist rate.

f. Postfilter MTF response above the Nyquist rate.

g. Number of quantization levels.

h. Quantization intervals.

i. Gray level reconstruction (false contouring).

Preliminary objective test images suitable for non-mechanized use by an observer were developed to determine the presence or absence of many of the image quality factors listed above. The most novel of these are relatively unique being based upon Moire' pattern comparisons against reference images. A quick guide to system MTF up to the Nyquist limit was also presented.

The following is required in the continuation of efforts to develop a standardized digital image test set:

a. Subjective evaluation of the complete set of objective image quality factors previously listed.

b. Development of finished forms of test imagery from the preliminary concepts described.

c. A survey of current state-of-the-art digital image subsystems in reference to the list of objective image factors.

d. Digital image processing procedures and algorithms and their inherent affect upon image quality.

e. Display technology concerning the modulation transfer function and equipment characteristics as they pertain to image quality assessment.

f. Image reconstruction equipment as they pertain to the production of a standardized imagery test set.

This initial study has provided the framework for a digital image test set with continuing efforts recommended for detailed specifications and construction of a test set. One development which was started in this effort and worth exploring further is the relationship between MTF response and aliased distortion. In addition, this study has generated computer programs for the subjective evaluation of digital degradations which would prove useful for simulating the performance of the sensor portion of the total digital imaging system.

Andrew P. Pirich

ANDREW PIRICH
Project Engineer

SECTION II

THE IMAGERY CHAIN

The objective of this Section is to provide introductory discussions of a digital imagery system in order to define the criteria for a Test Set. The essential elements, or functions, of an imagery system are first discussed, and are then followed by considerations of performance. Thus, the notions of imagery evaluation and image quality, so important to the test set definition, are first introduced.

The linking of imagery information between an input source and the output observer is termed an imagery chain. The simplest case in which only a source and observer are present is called the natural imagery chain as depicted by the Figure of 2-1. The observer is a human who visually observes the source representation be it FLIR, synthetic aperature radar, or a visual photographic sensor. The human, being the end user of the imagery information, is the final judge of what constitutes "good" performance. This subjective nature of this performance and the limited body of knowledge on the psycho-visual aspects of the human observer presents a rather primitive, although to-date adequate, status.

An image processing function when added between the source and observer constitutes the general imagery chain of Figure 2-2. With the mushrooming of computer technology and the ability to process, or transform, imagery information almost at will, the basic questions of imagery evaluation and performance become more paramount. For example, the image quality, presumed for a given observer's task, can be drastically altered by controlling the detailed spectral response of the imagery. The developments of digital image processing have advanced to the point where basic questions of image quality, especially digital image quality, need to be answered.

This Section provides an introduction to the essential

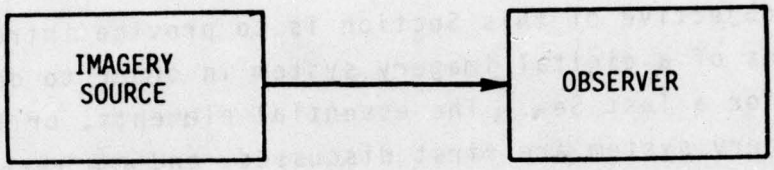


Figure 2-1. The Natural Imagery Chain

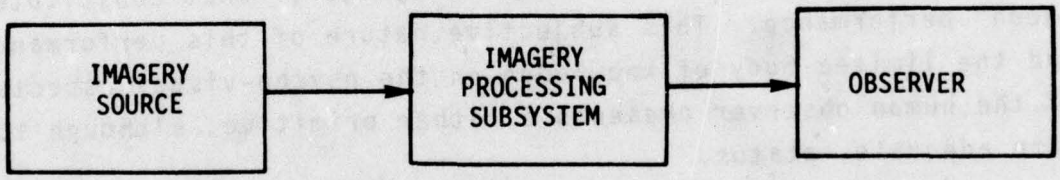


Figure 2-2. Inclusion of Imagery Processing
Into the Natural Imagery Chain

functions of the digital imagery chain in the following paragraphs. The source and observer of the natural imagery chain are discussed in Sections II-A and II-B respectively. The governing characteristics of the image processing subsystem under consideration here will be digital, rather than photographic, electric, or acoustic in nature. The fundamental characteristics of the digital image processing subsystem are discussed in Sections II-C, II-D and II-E. In each of these subsections the broader view is taken in lieu of more specific and detailed concentration upon the narrow present state-of-the-art considerations. These narrower considerations are addressed in Section III.

Once a digital processing subsystem has been inserted into the natural imagery chain, the impact on performance must be evaluated. Imagery evaluation procedures are considered in Section II-F. The question of what constitutes image quality will also be found relevant at this point. The prime indication of the state of relevant knowledge is that no consistent definition or measurable indicator of image quality has yet emerged. This problem is further considered in Section II-G.

A. THE NATURAL IMAGERY SOURCE

Not totally as conjecture, the natural imagery source can be pictured as shown in Figure 2-3. With some abstraction, various naturalistic relationships combine with laws of nature to produce objects; i.e., material bodies of specified composition occupying specified positions in space. These material bodies, as a function of their material properties, produce potential visual features. Usually these features are surface phenomena (shape, size, roughness, texture) but are occasionally volumetric phenomena (glow, translucence, density). Under self- or external illumination, these features are converted to a luminous field, and then are subject to various atmospheric and optical effects. Upon being subjected to a final perspective

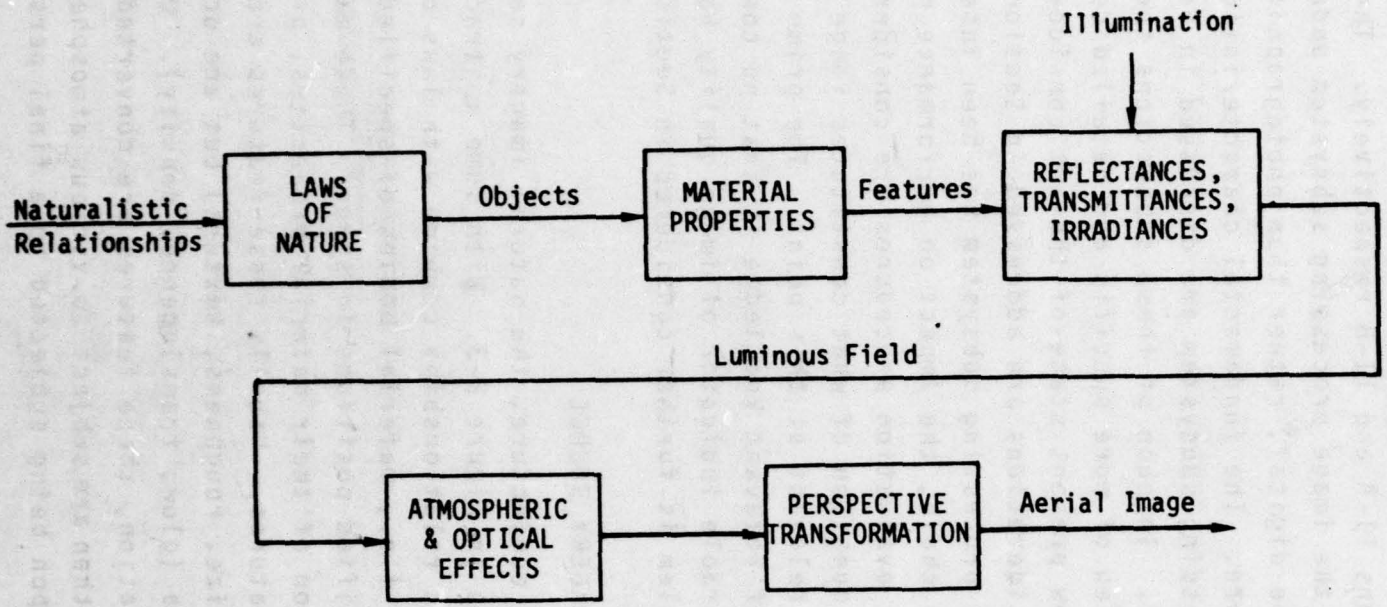


Figure 2-3. A Simplified Representation of the Natural Imagery Source

transformation, the luminous field is considered an aerial image suitable for input to man or machine.

The simpler portions of the natural imagery source have been reduced to theory. Certainly the nature of projective transforms has been understood for a few centuries. The various atmospheric and optical effects have been catalogued and to a large degree manageably reduced to formula. Basic laws of interrelationship of reflectance, transmittance and absorption as a function of illumination have been developed. In effect, all of the image modifiers of the image source are reasonably well understood. What is insufficiently well understood is the basic structural information contained in the image. For instance, it is not presently possible to reduce to formula answers to the questions: "How are the image reflectance and transmittance functions of the image features developed?" or "How are the object functions of the environmental relationships developed?"

Present efforts toward characterization of the structural information of an image is simplistic. Nevertheless the data so derived is useful in determining the impact of current state-of-the-art image processing subsystems. The characterizations include measurement and/or modelling of the image spectrum, amplitude distribution, second-order statistics, etc.

The spatial imagery spectrum is currently the most useful form of structural data to be extracted from the image. This spectrum data which varies with classes of source imagery is particularly useful in determining desirable digital sampling frequencies, filter rolloffs, and bandwidth reduction parameters. The approach taken here is to intuitively arrive at an appropriate model for image source spectra and then demonstrate that the model is consistent with the actual spectra of several image sources. One dimensional signals are assumed; however, the results are easily extended to two dimensions as required.

Consider the hypothetical one-dimensional image gray level profile shown in Figure 2-4. The various gray levels could correspond to different objects in a scene, each having a different gray shade value. The transitions then are the object boundaries.

In order to develop the image source model, it is necessary to determine the probability of one or more gray level boundary transitions in an interval of length τ. In a scene, these gray level transitions usually occur at the boundaries of material objects. Since the boundaries of objects in one part of the scene do not affect the boundaries in another part of the scene, and these boundaries are randomly distributed in most natural or man-made scenes, the boundaries are easily seen to be Poisson distributed. We shall assume that for a given class of imagery, there are α gray level transition boundaries per unit length; of course, α can vary from one class of imagery to the next.

With these assumptions the probability of k transitions in the interval τ is given by

$$P_k(\tau) = (\alpha\tau)^k \, e^{-\alpha\tau}/k! \ ,$$

in which case it can be shown that the probability of no transitions in τ is $P_o(\tau)=e^{-\alpha\tau}$. (It should be noted that we are considering the probability density function for the number of gray level transitions in an interval τ; this is not to be confused with the probability density function for the gray levels themselves.)

The autocovariance function, $C(\tau)$, is given by the definition

$$C(\tau) = E\{(f(x)-Ef(x))(f(x+\tau)-Ef(x+\tau))\}$$

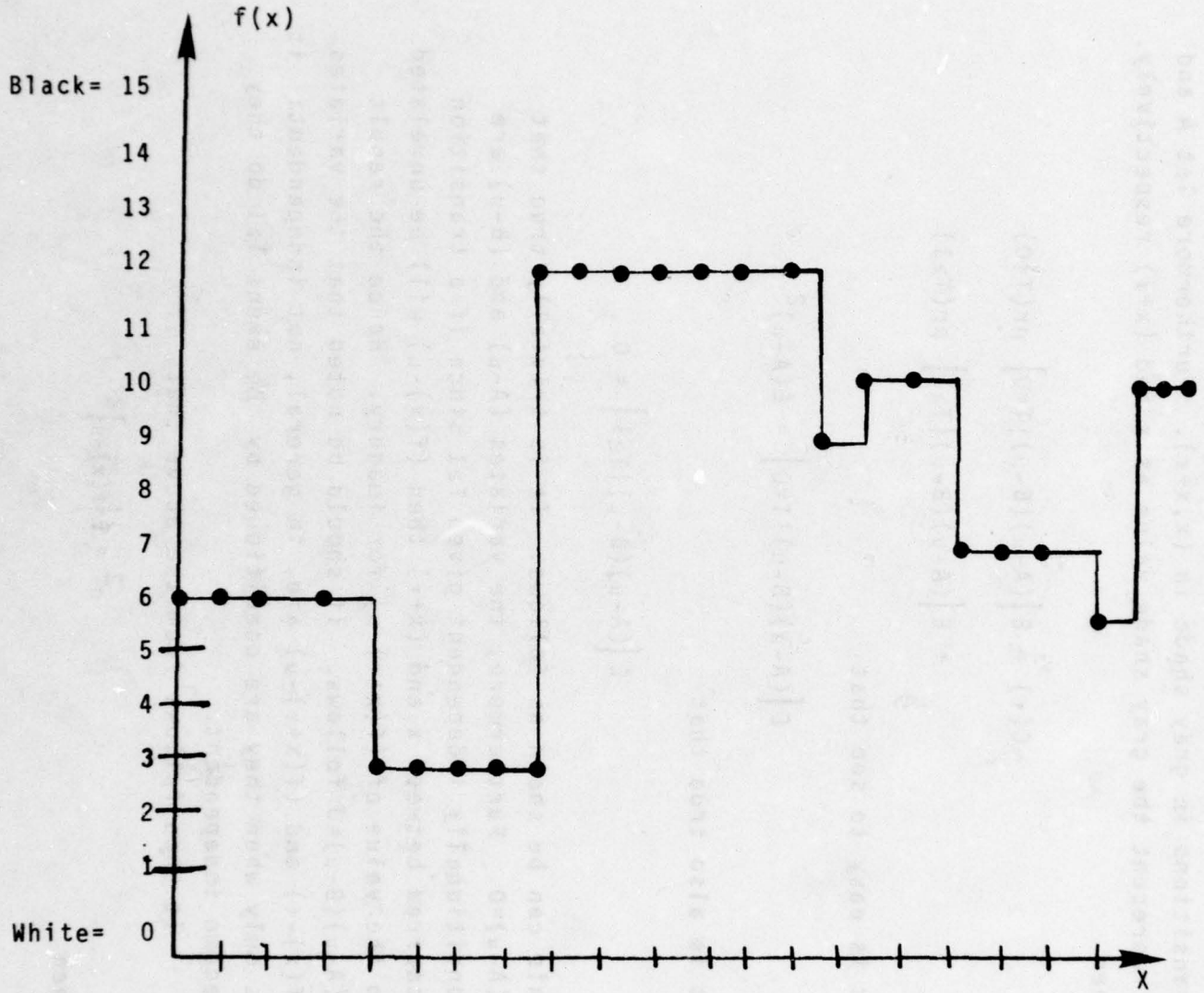


Figure 2-4. Image Gray Level as a Function of Spatial Position (One Dimension Assumed)

where $E\{\cdot\}$ denotes the expectation operator. It will be assumed that $Ef(x)=Ef(x+\tau)=\mu$. Let T denote the number of transitions in gray shade in $(x,x+\tau)$. Furthermore let A and B represent the gray shade value at x and $(x+\tau)$ respectively. Then

$$C(\tau) = E\left[(A-\mu)(B-\mu)\,|\,T=0\right]\ pr(T=0)$$

$$+\ E\left[(A-\mu)(B-\mu)\,|\,T\geq 1\right]\ pr(T\geq 1)$$

It is easy to see that

$$E\left[(A-\mu)(B-\mu)\,|\,T=0\right] = E(A-\mu)^2 \ .$$

It is also true that

$$E\left[(A-\mu)(B-\mu)\,|\,T\geq 1\right] = 0 \ .$$

This can be shown as follows. It is trivially true that $E(A-\mu)=0$. Furthermore, the variates $(A-\mu)$ and $(B-\mu)$ are conditionally independent given $T\geq 1$ since if a transition occurred between x and $(x+\tau)$ then $(f(x)-\mu)$ will be unrelated to the value of $(f(x+\tau)-\mu)$ for imagery. Hence the result $E(A-\mu)(B-\mu)=0$ follows. It should be noted that the variates $(f(x)-\tau)$ and $(f(x+\tau)-\mu)$ are, in general, not independent: it is only when they are conditioned by the event $T\geq 1$ do they become independent.

It then follows from the above that, if

$$\sigma^2 = E\left[f(x)-\mu\right]^2$$

then

$$C(\tau) = E\left[f(x)-\mu\right]^2 e^{-\alpha|\tau|}$$

so that

$$S(\omega) = \sigma^2 \frac{2\alpha}{\omega^2+\alpha^2} = F\{\sigma^2 e^{-\alpha|\tau|}\} .$$

In this case the image spectrum rolls off at 6 dB/octave (20 dB/decade) and is characterized by a 3 dB corner frequency of $\omega_c=\alpha$ radians/sec. This type of spectrum is referred to an RC spectrum since it would also result from passing white noise through an RC lowpass filter. It has thus been shown that an RC spectrum is a plausible model for imagery source spectra.

In order to demonstrate the validity of the RC model, it is necessary to compare actual imagery source spectra to the RC spectrum model. The results of real-time spectral analysis of analog television signals [1] indicate that television signal spectra rolloff at 6 dB/octave until the upper frequency limit of the bandlimited television signal is reached. Further support for this model for source imagery spectra was obtained during the study by computing and examining the Discrete Fourier Transform (DFT) of horizontal, vertical, and diagonal lines of several images of interest from Section IV. It should be noted that these DFT's are not the source spectra but are based upon a representation of the source spectra obtained after scanning, sampling, and quantizing the original source image. This scanning and sampling process introduces secondary bandlimitings due to the lowpass nature of optical lens and the finite bandwidth of photodetectors and the associated electrical circuitry. More importantly, the original image was undoubtedly purposely bandlimited (prefiltered) to less than one-half the sampling rate before sampling and quantizing to minimize aliasing degradations. For these reasons, the spectrum that exists just prior to sampling and quantizing is more properly called bandlimited RC (BLRC). O'Neal [2] has derived an analytical expression for the autocorrelation of BLRC spectra, with the corner frequency (normalized by total bandwidth) as a parameter. Autocorrelation

curves corresponding to BLRC spectra with various normalized corner frequencies are shown in Figure 2-5. With this in mind, the DFT results obtained in the Image Processing Laboratory, Figures 2-6 through 2-8, were compared to the BLRC spectrum. The good agreement also supports the use of an RC image source spectrum model, if it is assumed that secondary bandlimiting is due to the presampling filter in the scanner.

B. THE OBSERVER

We only consider the human observer. Without too much conjecture, the human observer can be pictured as shown in Figure 2-9. An image is perceived by one of the two sensor modes, to be discussed below. The output of the sensor operation is then subjected to various feature and object extractors which operate on the sub-conscious level of the brain and are thus automatically performed by the human. The resulting features and objects are then passed on to the higher levels of the brain where scene interpretation occurs, also on the sub-conscious level. Where there is time and opportunity, the conscious level of the brain can perform intellectual processes to further refine the visual response.

Little is understood about the internal processes of the human observer. What is known is something of the physiology and performance of the sensor precesses. The sensor of the human visual perception system is the eye/optic nerve combination. It is well known that the first stages of this combination are a lens, followed by a field of photodetectors, followed by postprocessing. The light distribution formed by the lens of the living human eye on the retina has been measured and found to be the line spread function.

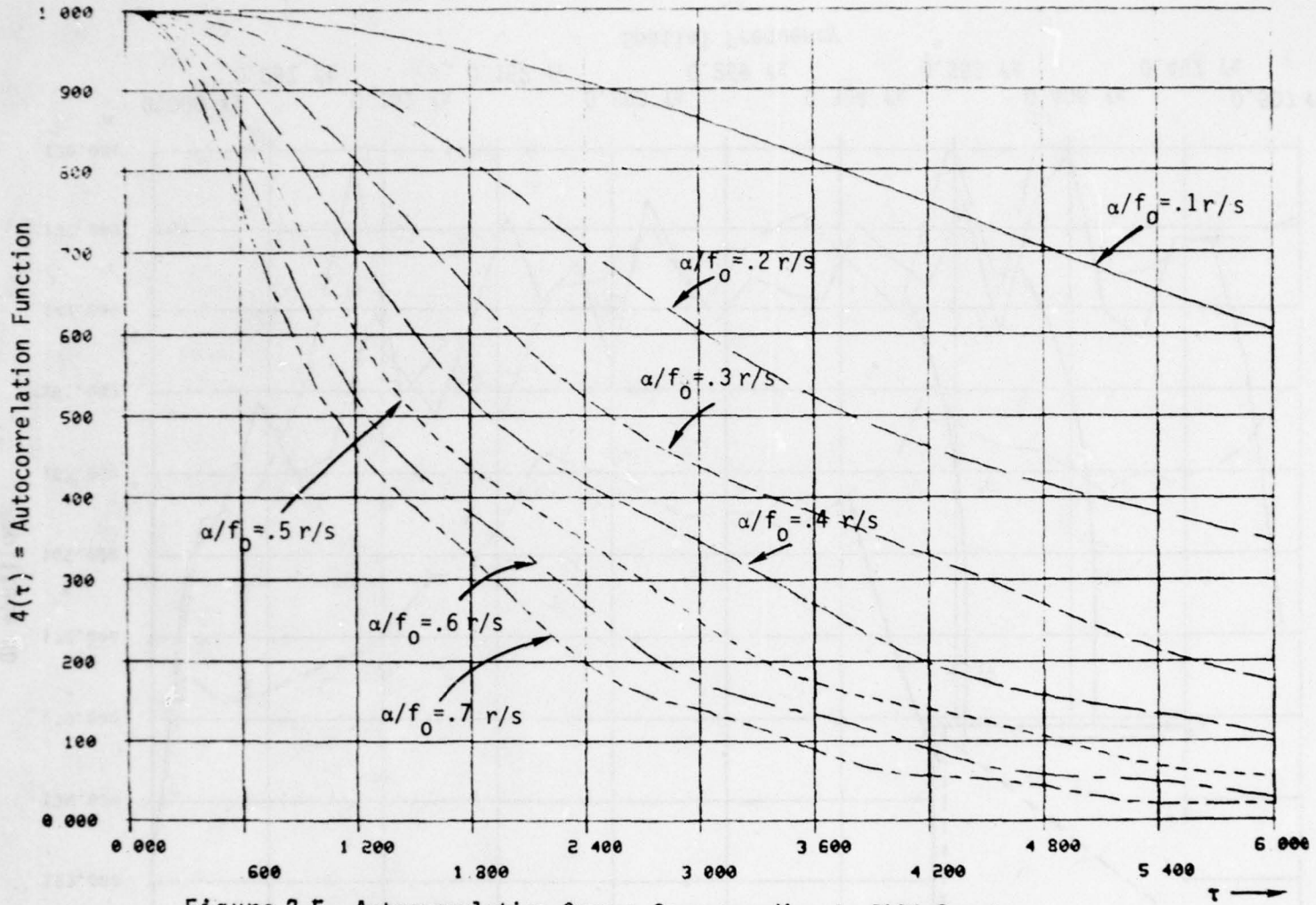


Figure 2-5. Autocorrelation Curves Corresponding to BLRC Spectra with Normalized Corner Frequency ω_c/ω_o as a Parameter

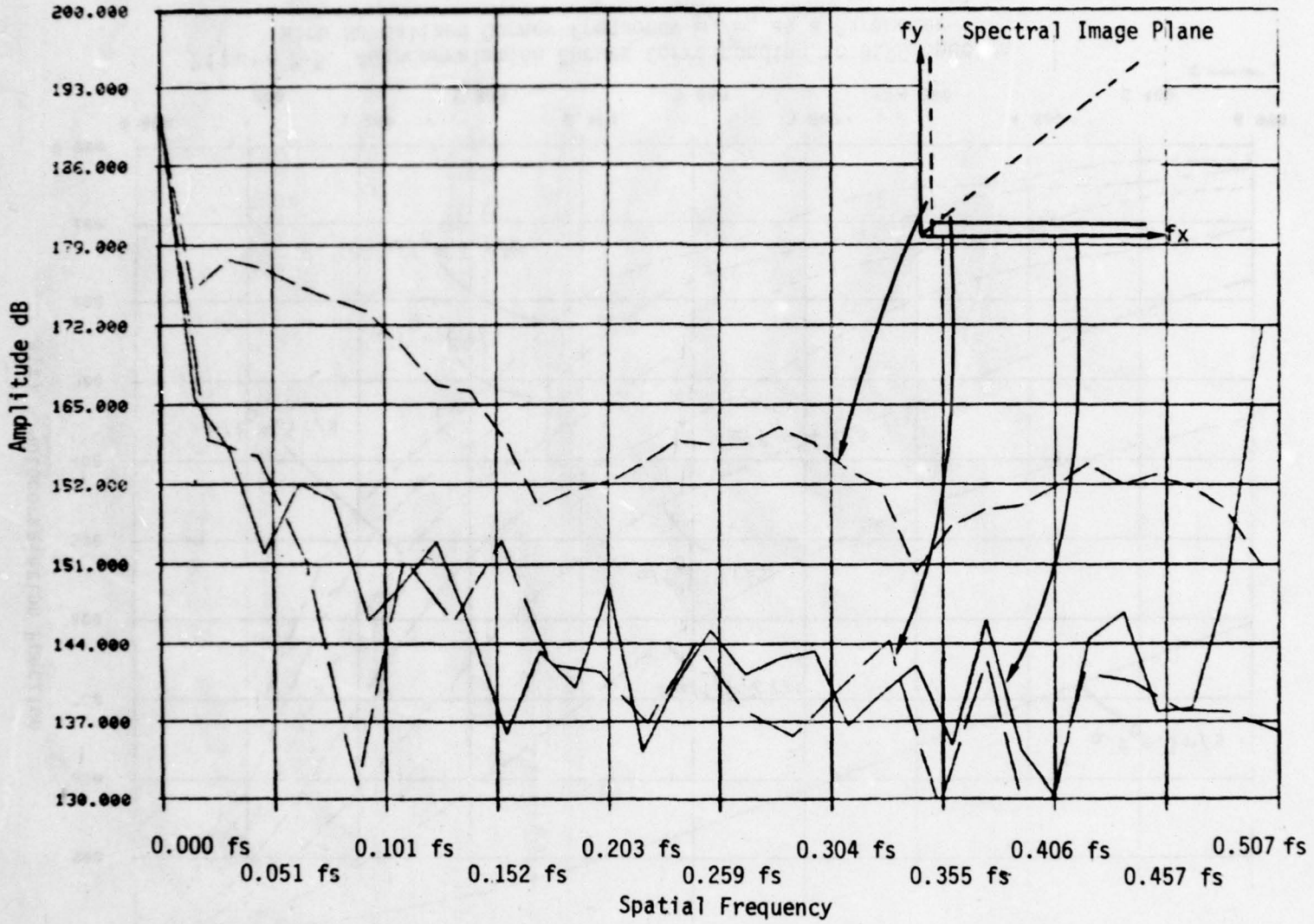


Figure 2-6. Spectrum of Low Resolution Vertical Digitized Photograph

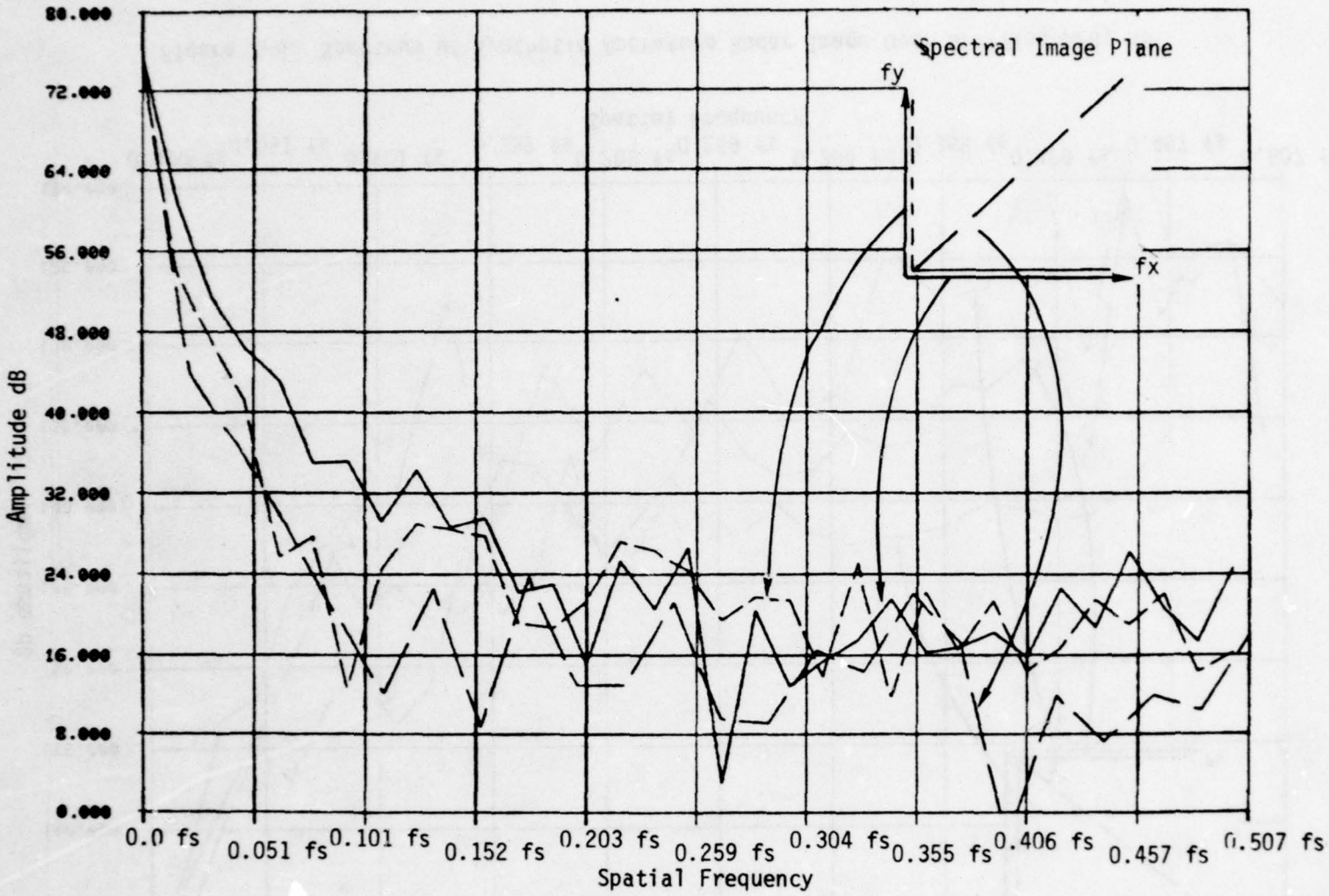


Figure 2-7. Spectrum of Infrared Image of Parked Image

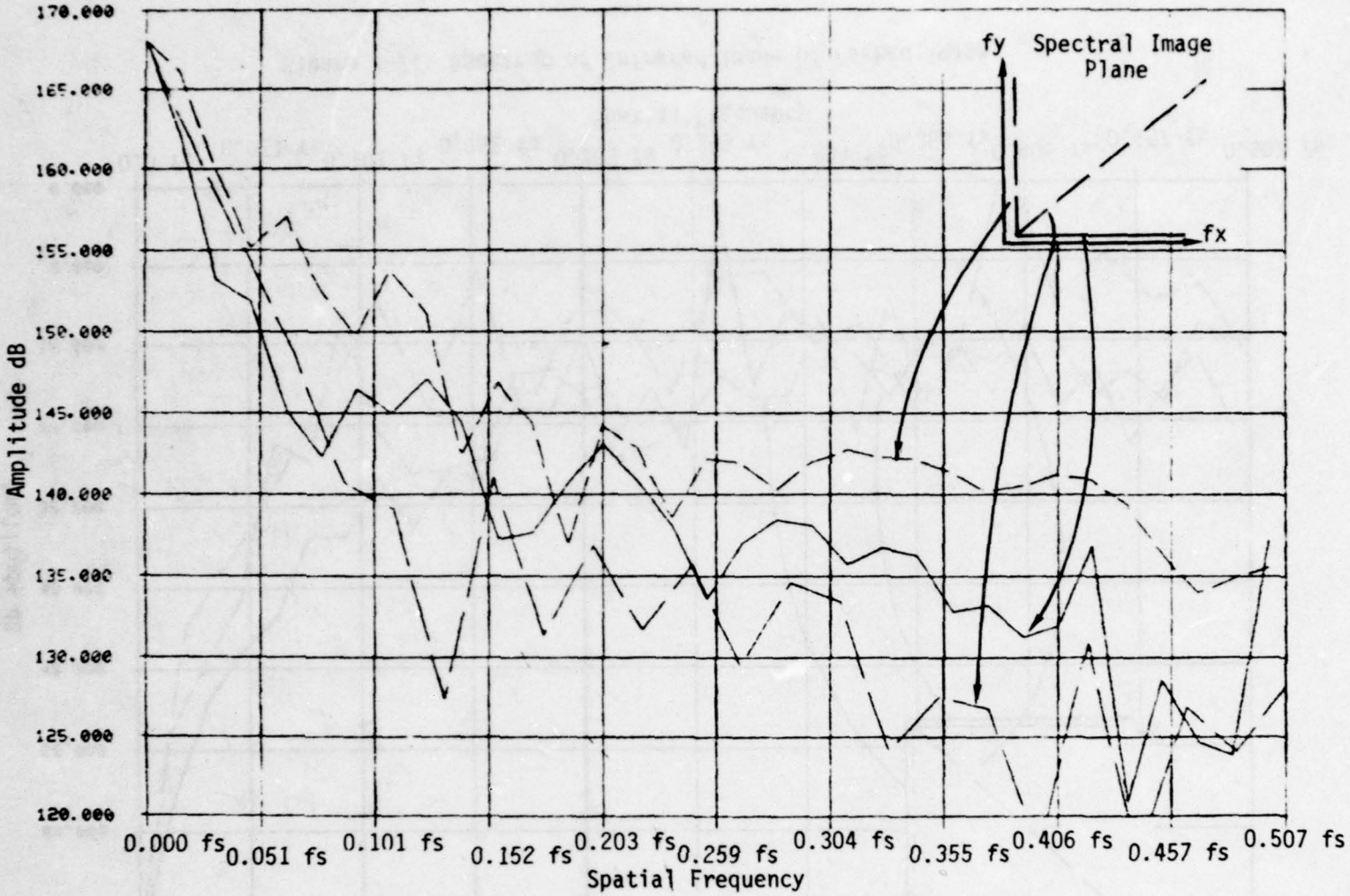


Figure 2-8. Spectrum of Synthetic Aperature Radar Image Over Griffiss AFB, NY

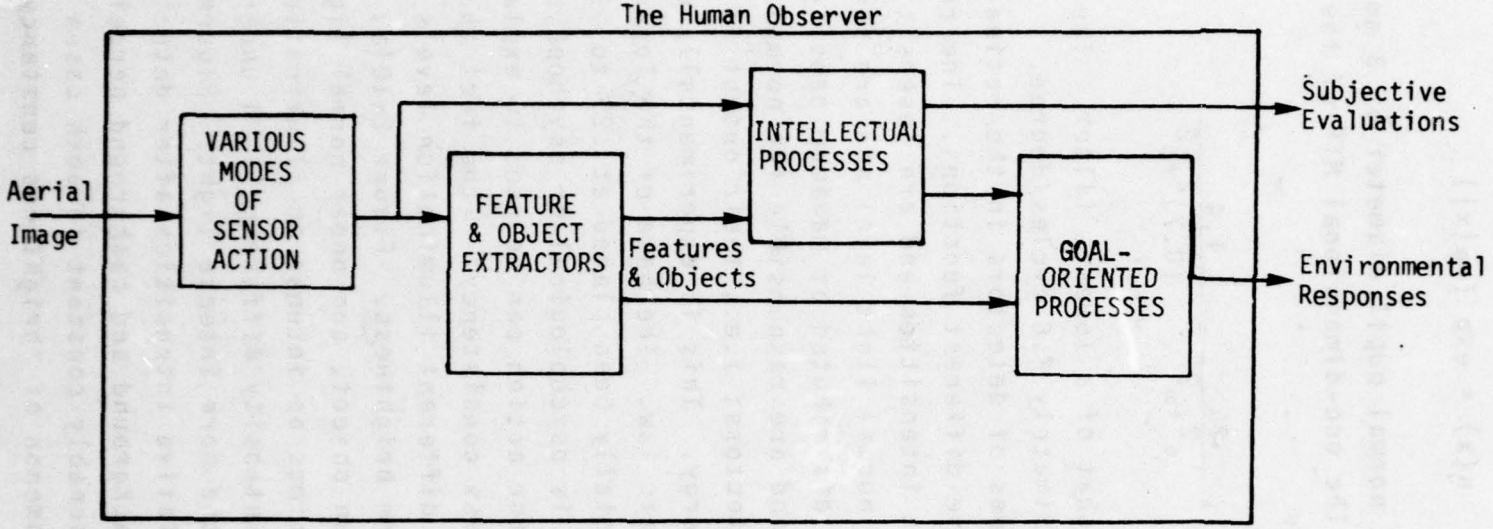


Figure 2-9. A Simplified Representation of the Human Observer

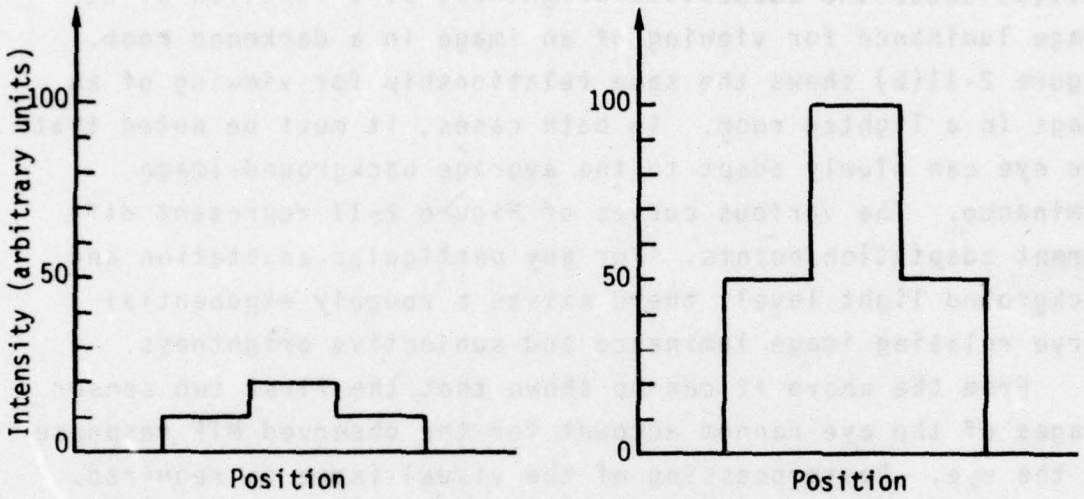
$$n(x) = \exp(-\alpha|x|)$$

For white light and a normal pupil diameter of 3 mm, α has a value of about 0.7. The one-dimensional MTF of the lens can thus be computed to be

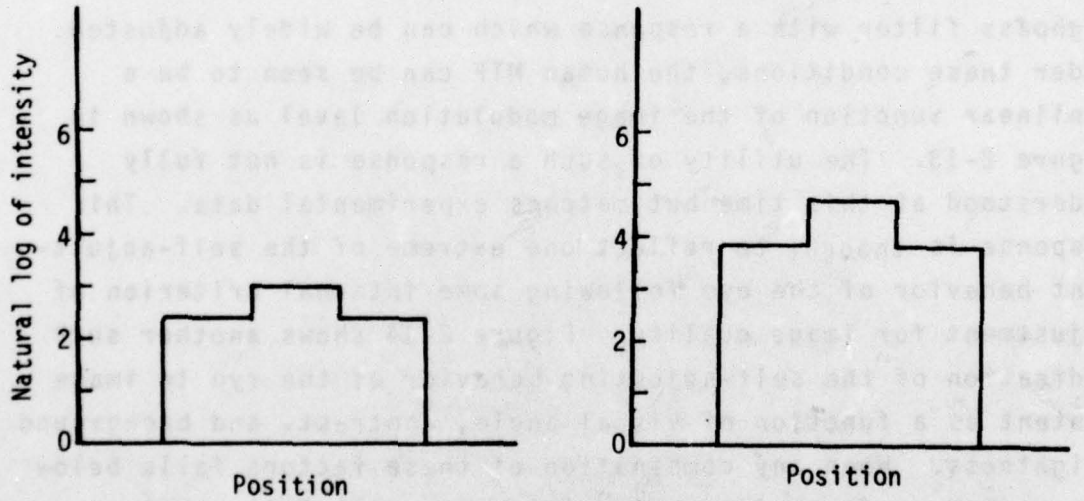
$$H(\omega) = \frac{2\alpha}{\alpha^2+\omega^2} = \frac{1.4}{(0.7)^2+\omega^2}$$

which is found to be that of a lowpass filter. The -3 dB point occurs at approximately 6.6 cycles/degree.

There are two types of detectors in the retina, rods and cones. These each have different functions. The rods function primarily at low light intensities and are insensitive to color. The cones function at normal light level and are sensitive to color. The cones are distributed at maximum density at the center of the retina and are responsible for normal vision. They are power-law detectors; i.e., their output is proportional to the input light energy. This is experimentally expressed as Fechner's logarithmic law. The base of the logarithmic function has experimentally been placed at .29 to .33 depending on whether the source is psychological or psychophysical data. The logarithmic detector action can be used to explain the phenomena of "brightness consistency" - the fact that the same object observed under different illumination levels appears to maintain a near uniform brightness. Figure 2-10(a) contains the intensity profile of an object, one under normal light level and the other under five times as intense an illumination. The object to background intensity difference is 1 under normal light and is 5 under the more intense light. Figure 2-10(b), however, shows the relative intensities after detection by the eye. The object to background and background perceived intensities now remain reasonably constant in both cases thereby illustrating the phenomenon of "brightness constancy."



(a) Actual Brightness



(b) Subjective Brightness

Figure 2-10. Intensity Profiles Illustrating "Brightness Constancy"

Obviously, however, the eye detection system is not an exact logarithmic function. Figure 2-11 is more exacting. Figure 2-11(a) shows the subjective brightness as a function of the image luminance for viewing of an image in a darkened room. Figure 2-11(b) shows the same relationship for viewing of an image in a lighted room. In both cases, it must be noted that the eye can slowly adapt to the average background-image luminance. The various curves of Figure 2-11 represent different adaptation points. For any particular adaptation and background light level, there exists a roughly exponential curve relating image luminance and subjective brightness.

From the above it can be shown that the first two sensor stages of the eye cannot account for the observed MTF response of the eye. Postprocessing of the visual image is required. Anatomically this can be modelled by the backward inhibitor network of Figure 2-12. This is one of four such model types proposed for neural networks. Assuming no self-inhibiting action and exponentially decreasing inhibitory interaction otherwise, this postprocessing stage can be shown to be a highpass filter with a response which can be widely adjusted. Under these conditions, the human MTF can be seen to be a nonlinear function of the image modulation level as shown in Figure 2-13. The utility of such a response is not fully understood at this time but matches experimental data. This response is thought to reflect one extreme of the self-adjustment behavior of the eye following some internal criterion of adjustment for image quality. Figure 2-14 shows another such indication of the self-adjusting behavior of the eye to image content as a function of visual angle, contrast, and background brightness. When any combination of these factors falls below the curved surface, image discrimination will fail, while a combination falling on a point above the surface permits seeing.

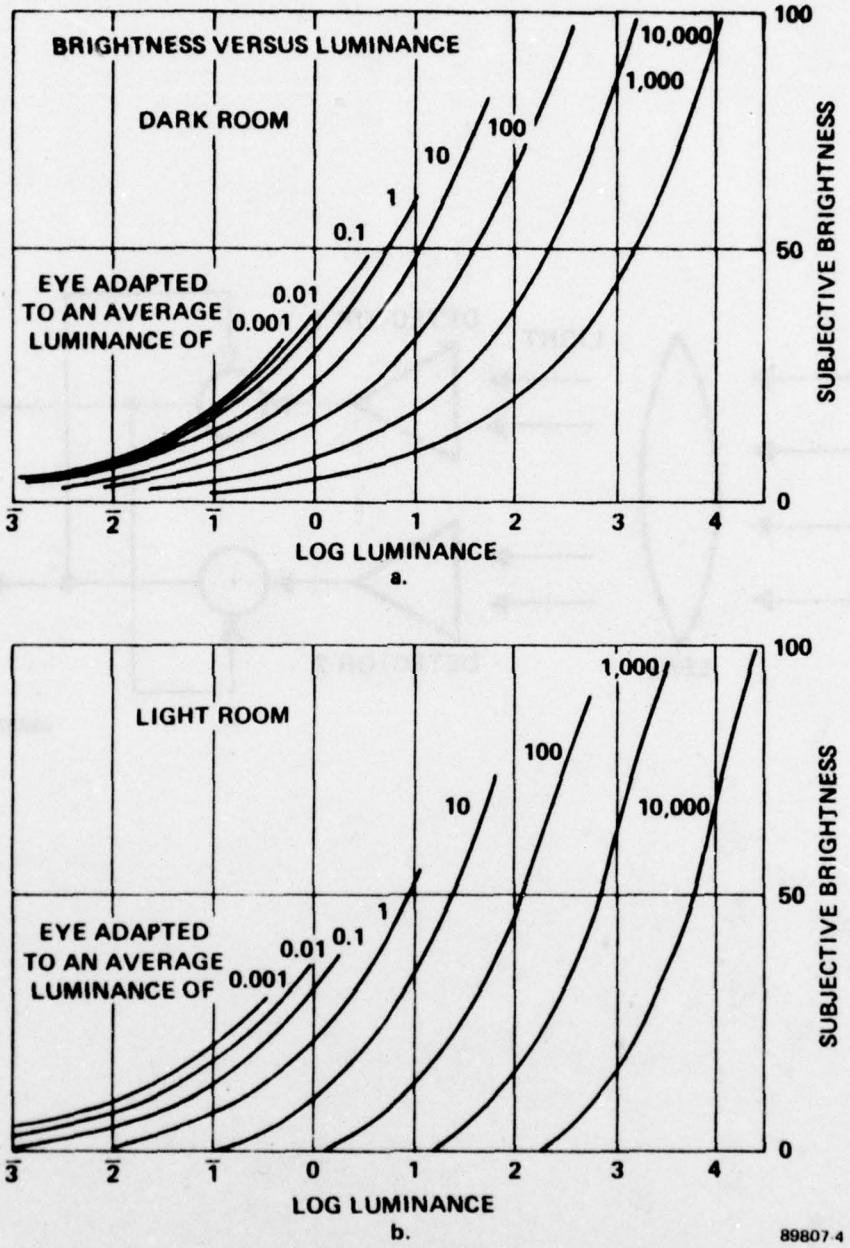


Figure 2-11. Subjective Brightness as a Function of Image Luminance

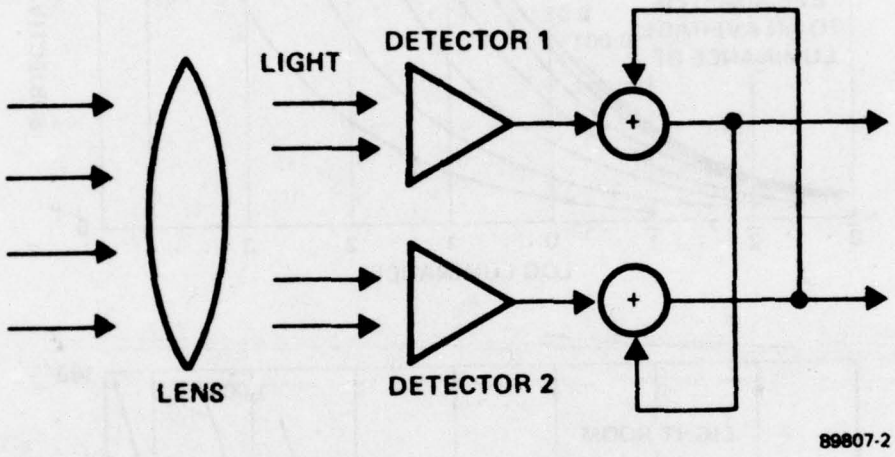


Figure 2-12. Backward Detector Inhibition Model

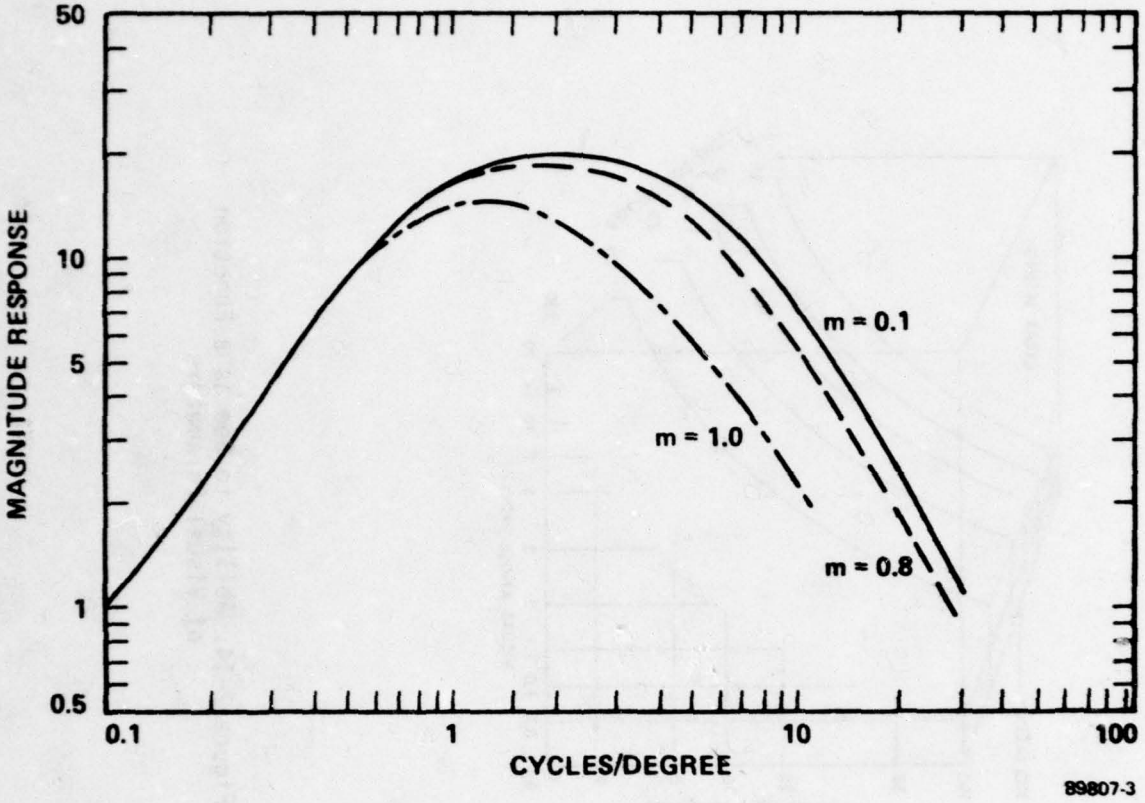


Figure 2-13. Overall Spatial Frequency Response for Several Values of Sinusoidal Modulation m

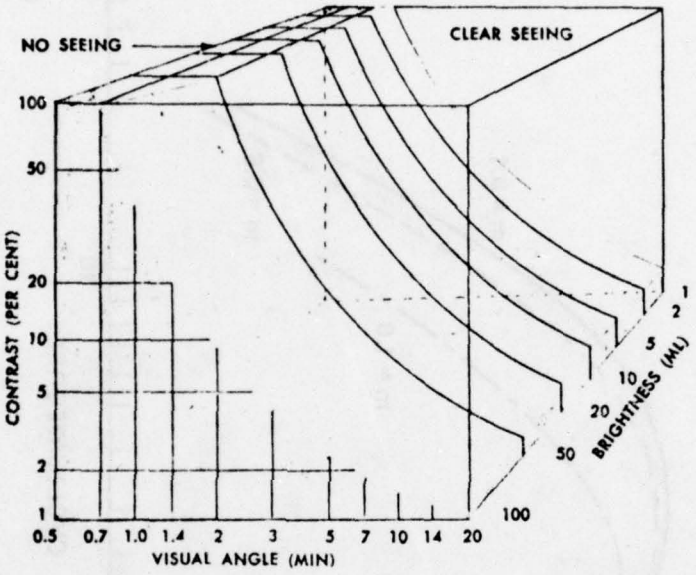


Figure 2-14. Ability to See as a Function of Visual Parameters

C. MAJOR COMPONENTS OF THE DIGITAL IMAGERY PROCESSING SUBSYSTEM

A Digital Imagery Processing Subsystem is composed of the elements shown in Figure 2-15. Generically, it consists of a conversion process which converts the aerial image into a digital representation. Once the digital image has been appropriately processed, it is converted back to an aerial image for viewing by the human observer.

It is most instructive to the purposes of the study to first view the process on an abstract level. Just as one can plot individual numbers on a graph or as positions in three-dimensional space, so can an entire image be thought of as occupying but a single point in an infinite dimension space. Thus image α and image β can occupy positions in this space as shown in Figure 2-16(a). The digital input conversion process partitions this space into regions such that if an input image lies in a particular region R, then the output of the digital image input conversion process is the code symbol R. In Figure 2-16(b) three such regions A, B, and C are shown. The symbols A, B, C thus are three separate digital images. Now if input images α and β are input to the digital input image conversion process, the digital images A and B would be respectively output.

The digital image processor most generally is a many to one mapping between digital images as shown in Figure 2-16(c). In the example shown, the digital images A and B are processed into the digital images 3 and 2 respectively.

The digital image output conversion process is then a mapping back into image space on a 1 to 1 basis, i.e., one digital image gives one point (one aerial image) in image space. This action is shown in Figure 2-16(d).

If the action of the entire digital image processing subsystem is sought, then the composite input conversion, digital processing mapping, and output conversion action must be determined. This is shown in Figure 2-16(e), the composite of the

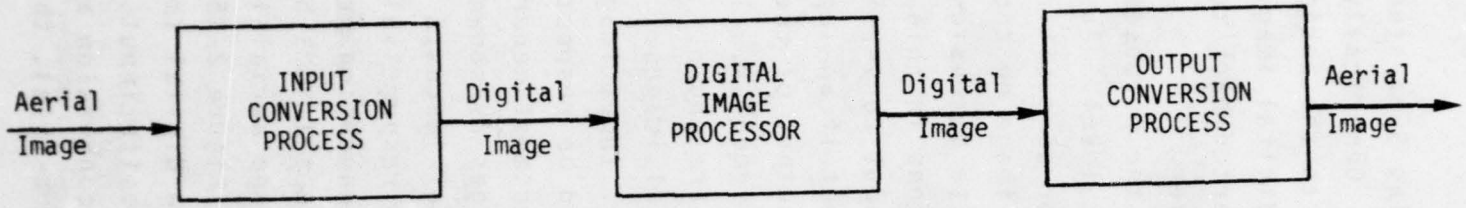
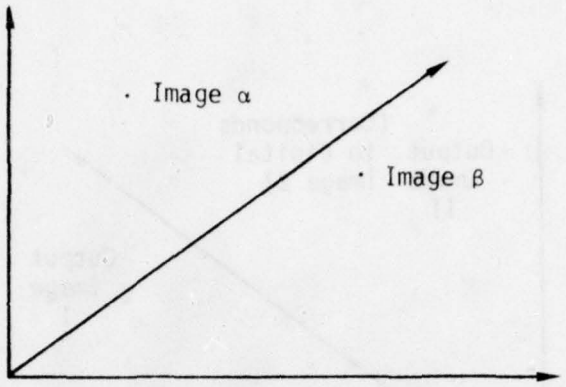
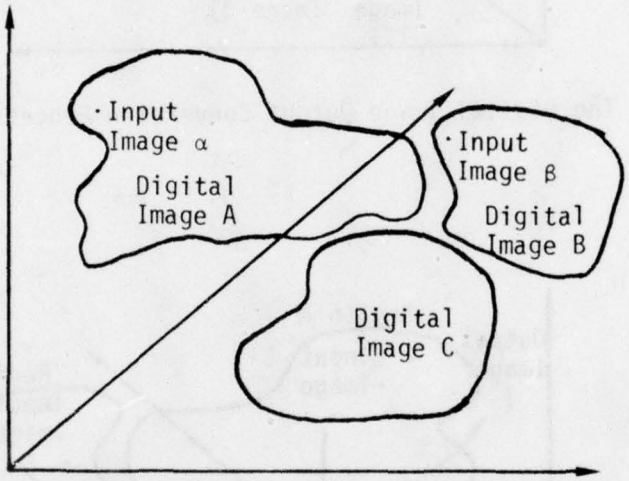


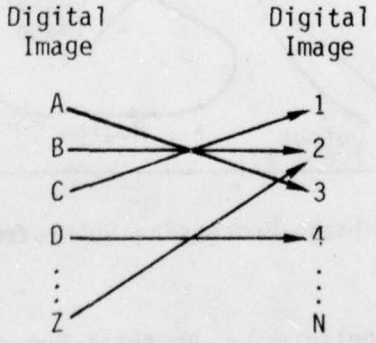
Figure 2-15. The Structure of the Digital Image Processing Subsystem



(a) Input Image Space

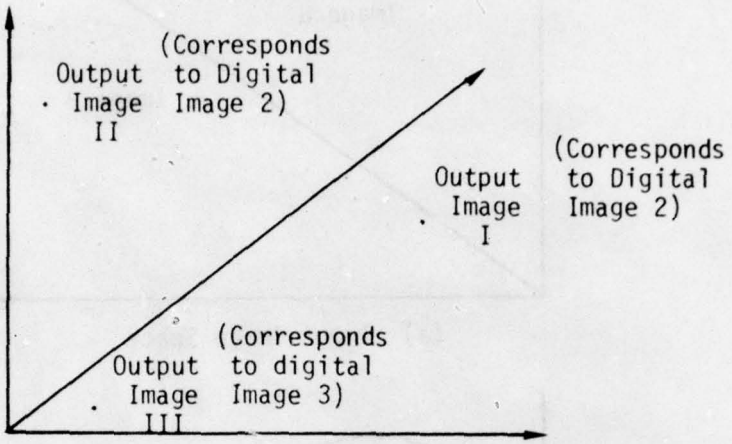


(b) The Digital Image Input Conversion Process

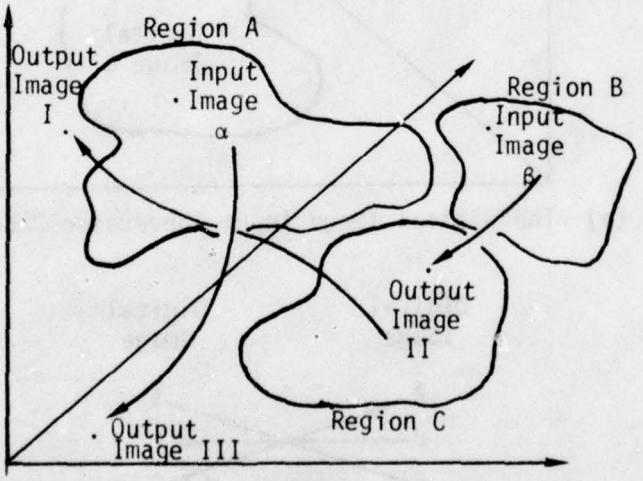


(c) The General Digital Image Processing Mapping

Figure 2-16. Abstract Representation of the Action Taken By A Digital Image Processing Subsystem



(d) The Digital Image Output Conversion Process



(e) The Composite Image Processing Subsystem Action

Figure 2-16 (Continued). Abstract Representation of the Action Taken By A Digital Image Processing Subsystem

actions of Figures 2-16(b), (c), and (d). Here it is seen that any input aerial image lying in Regions A, B, or C will result in output aerial images I, II, or III respectively. Thus if image α is input, image III will be output, or if image β is input, image II will be output.

From the above discussion three important conclusions emerge. First, in a digital image processing subsystem, many input images may result in the same output image, or conversely, any two specific input images may result in the same output image. Second, the output image need not bear any resemblance to its input image, or conversely, it may bear any resemblance to its input image. Finally, the response of the digital image subsystem to any image (such as a test image) in no way is necessarily indicative of its response to any other image.

While the above conclusions are true, current useful theoretical approaches to the digital image processing subsystem are more restrictive. These processes are discussed in Sections II-D and II-E. Current state-of-the-art hardware implementations are even more restrictive. These are considered separately in Section III.

D. THE DIGITAL IMAGE CONVERSION PROCESS

Since there are no digital imagery sources in nature and since the perceptual system of the human observer is ill-equipped to directly deal with the digital image once formed, there must exist conversion processes as shown in Figure 2-15. Current examples of hardware realizations of the input conversion process are CCD-TV, half-tone lithography, and laser beam scanners. Current examples of the hardware realizations of the output conversion process are digital CRT monitors, half-tone printers, and laser beam reproducers. Implementation specific data is contained in Section III. The utility of the present discussion is that it is more specific than that of the prior

section but is general enough to encompass the majority of future state-of-art developments.

At the usual theoretical level, a digital image can be taken as a finite collection of finite valued integers. Given this, an immediate relevant question arises; "Is it possible to develop digital image input and output conversion processes which will in all cases produce an output image identical to the input image?" The response is NO, since there are infinite numbers of possible input images but only a finite number of digital images. This succinct observation brings one rapidly to the crux of the matter - "With what quality does a given output image(s) approximate its input image(s)?" Since a general definition of image quality definition has not yet been agreed upon, the above question of image quality will be indirectly pursued.

In Figure 2-16(a), if image α is output when image α is input, then the image quality of the intervening processes can be said to be perfect for that image. If, however, an image is output which is sufficiently close to image α, then the image quality of the intervening processes should again be good. If, however, an image is output at a yet greater distance from image α in image space, then it is reasonable to assume that the image quality is not as good since the two images will be more dissimilar. Thus it is possible to loosely associate image quality with distance in image space, in that as the output image draws closer to the input image it is reasonable (but not strictly necessary) that the image quality of the output image should increase. It is possible therefore to replace the desire for digital conversion processes of high image quality by the desire to minimize the average distance between an input image and output image in image space. This average distance is widely referred to as the average mean square error of the output image relative to the input image. It is possible to show that the average mean square error can be made as

E. DIGITAL IMAGE PROCESSOR

The digital image processor (DIP) is a digitized version of the "Imagery Processing Subsystem" of Figure 2-2. Hence it is typically a specialized digital computer performing one or more algorithms on the digital data.

There are several different types of digital image processing in use today. One of the first uses was that of data compression where the DIP reduces the amount of digitized data needed to represent an image; typically the DIP would then include a TV camera, A/D converter, orthogonal transform algorithm, a communications channel, a receiver, detransformer, D/A converter and finally, a TV monitor.

Another common type of DIP is one used for image restoration. Here, the digital computer attempts to correct or compensate for the optical imperfections of the imagery processing subsystem. For example, the DIP may introduce an effective change in the MTF to compensate for the TV camera's MTF so that the visual high frequency content of the scene is more readily visible to a human observer.

Yet another type of DIP is that of image enhancement. This consists of performing operations on the image to make it appear more pleasing to the eye or increasing its utility to a human observer. To date, image enhancement consists mostly of ad hoc techniques, although the potential to incorporate knowledge of the human visual system appears to be good. One arbitrary example of image enhancement is given in Figure 2-17 for which the output is not necessarily a replica of the input but has certain desirable features enhanced.



(a) The input



(b) The output

Figure 2-17. Results of an Arbitrary Digital Image Processing Action

F. IMAGE EVALUATION

Evaluation of the changes effected by a digital processing subsystem can be accomplished by any of the three measurement methods of Figure 2-18. In contrasting the three methods it must be noted that the three methods use significantly different evaluation structures, and thus, the evaluation outputs can be expected to be quite different in content. The choice of evaluation technique will, therefore, be conditioned on the end use of the output evaluation.

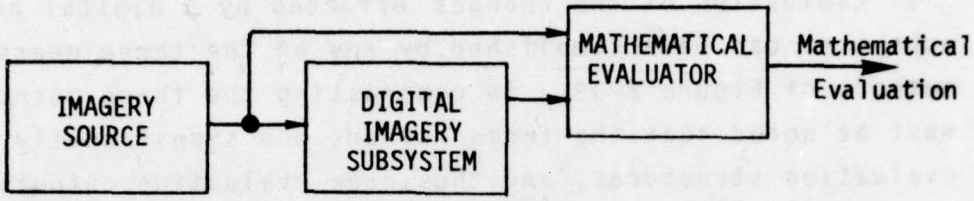
The mathematical approach is well suited to the measurement of system parameters against mathematically defined specifications such as

- Modulation Transfer Function
- Signal-to-Noise Ratio
- Gray Level Mapping
- Resolution
- Area Equivalent MTF
- Dynamic Range

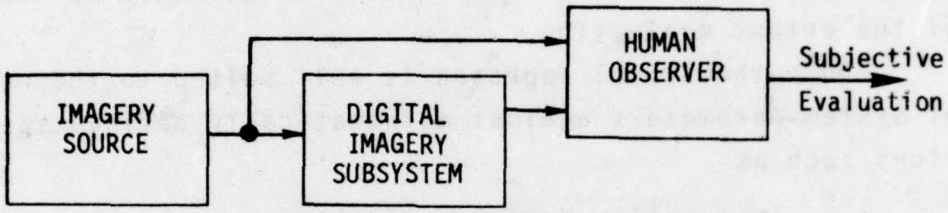
The subjective approach is well suited to the cataloging of human perceived changes engendered by the digital system such as

- Crispness
- Brightness
- Loss of Detail
- Appearance of Spurious Patterns
- Sparkle
- Contrast

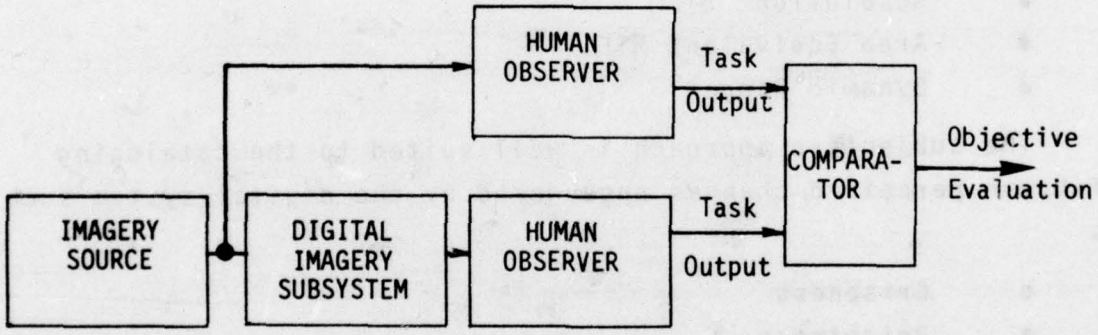
The objective approach is well suited to the determination of impairment or facilitation of the observer's reactions such as



(a) Mathematical Evaluation



(b) Subjective Evaluation



(c) Objective Evaluation

Figure 2-18. Evaluation of a Digital Imagery Subsystem

- Detection Time
- Accuracy of Recognition
- Mensuration Ability

G. IMAGE QUALITY

There exists no commonly accepted definition of image quality in the literature. In the case of interest here, i.e., the insertion of a digital imagery processing system into the natural imagery chain, image quality can reasonably be taken as the percentage measure of how well output images approximates their respective input images for the task at hand. The following problems arise, however:

- What is the appropriate measure of image quality?
- What is the set of input images to be considered?
- What is the task at hand?

An appropriate measure of image quality is not yet recognized in the literature. However, it is generally thought that the particular measure of average mean square error between input and output image is not appropriate. For the purposes of this report, and particularly Section IV, the measure is indirectly defined as the percentage utility of an output reconstructed digital image to the input image, as verbally expressed by a trained photointerpretator.

The set of input images to be considered is usually indirectly defined by examples or modelling such as performed in Section II-A. Section IV considers that the input image ensemble can be adequately specified by a few well chosen examples.

The task at hand is a critical question. It could range from artistic evaluation to target detection. In Section IV the task at hand is indirectly defined by asking the trained photointerpretator to assess the images based upon his experience in photointerpretation.

Although image quality has not and can not be definitized here, it is interesting to note what some of the desirable properties of a measure of image quality should be if it is to be mathematically useful and logically sound.

First, the condition of equality of image quality should be an equivalence relation. That is, the following should be obeyed:

(1) Symmetric Relationship

Any given output image should possess the same image quality relative to the input when compared with itself. This is patently true.

(2) Reflexive Relationship

If two output images A and B possess equal image quality, it should not matter that B is being compared to A or that A is being compared to B. This also is patently true.

(3) Transitive Relationship

If (1) two output images A and B possess equal image quality and (2) the two output images B and C possess equal image quality, then (3) A and C possess equal image quality. Many observers question if this is true. For instance, (1) if an output image A containing much noise seems to possess upon comparison with image B containing no noise but low dynamic range the same image quality, and (2) if image B seems to possess upon comparison with image C containing jitter the same image quality, then (3) it is <u>not necessarily apparent</u> that image A containing noise will appear to possess the same image quality as image C containing jitter when directly compared. This problem is experimentally addressed in Section IV.

The equivalence relation is basic to the formation of any mathematical measure. Should the equality of image quality not exist, there will be little means by which a body of image quality theory can emerge.

Second, images should be rankable in terms of image quality. That is, if the quality of image A appears better than that of B, and independently, the quality of B appears better than C, then when directly compared, A should also appear better than C. Obviously, if this does not hold, it will be impossible to obtain a measure of image quality. This condition is further considered in Section IV.

Third, image quality should ideally be a metric, i.e., the closer the output image is to the input image, the better should be the quality. One common example of a metric is the mean squared error (MSE) criterion. In some applications, this is likely not to be true since for instance, one can make an output image very similar to the input image except for a blackening of a very small area. The quality will drop precipitantly, however, if that blackened area happens to contain the target of interest but the MSE will be little affected if the blackened area originally contained the target of interest in a dark background.

SECTION III

SCANNERS AND REPRODUCERS

In this section, the theoretical and practical aspects of the scanning and reproducing of source images are considered.

The image degradations introduced by spatial sampling and reconstruction are discussed in Section III-A followed by a discussion of the image degradation due to quantizing noise in Section III-B. Finally, some of the practical aspects of image degradations introduced in the scanning and reproducing process are examined in Section III-C.

A. SPATIAL SAMPLING AND RECONSTRUCTION

Two fundamental operations are performed by the scanner in any digital imagery system: two-dimensional spatial sampling and quantizing each of the resulting analog values to a finite number of bits; i.e., a form of the general finite orthonormal approximation and digitization process, Section II-E. The result of these two operations is a digital representation of the source image that is discrete in both space and amplitude. The digitized image may be thought of as a two-dimensional matrix of sample values, in which each sample value is allowed to have one of a finite set of values. For convenience, the image is considered to be one-dimensional for the remainder of this section since the conclusions are readily extended to the two-dimensional case. In addition, some of the discussion is in in terms of time signals rather than spatial images. The correspondence between one-dimensional spatial images and time-signals is straightforward.

1. The Nyquist Sampling Theorem and Time-Limited Real Signals

The Nyquist Sampling Theorem states that any function f(t) containing frequencies no higher than W can be perfectly reconstructed from its samples taken $\frac{1}{2W}$ seconds apart. Signals which are sampled less frequently than $f_s=2W$ samples/second suffer a type of degradation called "foldover" or aliasing, in which high source frequency components masquerade as lower frequency components in the reconstruction process. A subtlety involved in any practical application of the Nyquist Sampling Theorem is due to the fact that any real-world signal of practical interest is finite in extent (time or space) and cannot therefore be truly bandlimited in the strict sense. This implies that the sampled signal cannot be reconstructed exactly for any finite sampling rate; however, the energy of the error signal can be made as small as desired by increasing the sampling rate. A result due to Landau and Pollak[3] quantifies the tradeoff between sampling rate and error signal energy as follows:

> if x(t) is time-limited to T seconds and the signal energy that falls outside the bandwidth B Hz is less than or equal to k times the total signal energy, then the energy of the error signal between x(t) and an approximation constructed using 2TB signal samples is less than 12 kE.

Using the results of reference[3], Slepian[4] has proposed meaningful definitions for bandlimited and time-limited signals using the notion of "distinguishability at level E."

One of the measures of image quality that is directly related to the spatial sampling rate is spatial resolution; another measure of image quality related to spatial sampling rate is the degree of aliasing degradation present. The relationships and tradeoffs among image bandwidth, image

resolution, sampling rate, and aliasing effects are classified in the following paragraphs.

2. Image Resolution and Aliasing

The original image to be transmitted possesses a continuous spectrum of spatial frequencies much as shown in Figure 3-1. When this image is (ideally) sampled at the scanner, the sampling process drastically modifies the original image spectrum as shown. The sampled spectrum is composed of an infinite number of original image spectra spaced at intervals f_s (the sampling rate) apart. When the transmitted sampled image is received at the recorder, it is desired to display not the sampled image itself, but a reconstruction of the original image. This is accomplished by trying to retrieve the spectrum of the original image by isolating the fundamental spectrum (crosshatched in Figure 3-1 and other figures) of the sampled image. This may be accomplished by placing the sampled image through the lowpass reconstruction filter shown in Figure 3-1 which "removes" all image data above spatial frequency $f_s/2$ to provide the reconstructed spectrum for display. Note that if the repeated spectra of the sampled image overlap as shown in Figure 3-1, then the isolation action of the reconstruction filter is imperfect and some spurious detail called aliasing, due solely to the sampling process, enters the displayed image. Since it does not visually relate to the basic image data this spurious detail is normally perceived as image noise degrading the quality of the display image.

A graphic example of the aliasing effect is shown in Figure 3-2, in which a sinusoid of linearly-increasing (with space) spatial frequency (a "chirp" waveform) which has also been sampled at a fixed frequency f_s is displayed on a recorder hardcopy output. In this figure, the abscissa is spatial location and since the source frequency is increasing with time, a spatial frequency can be identified with each spatial

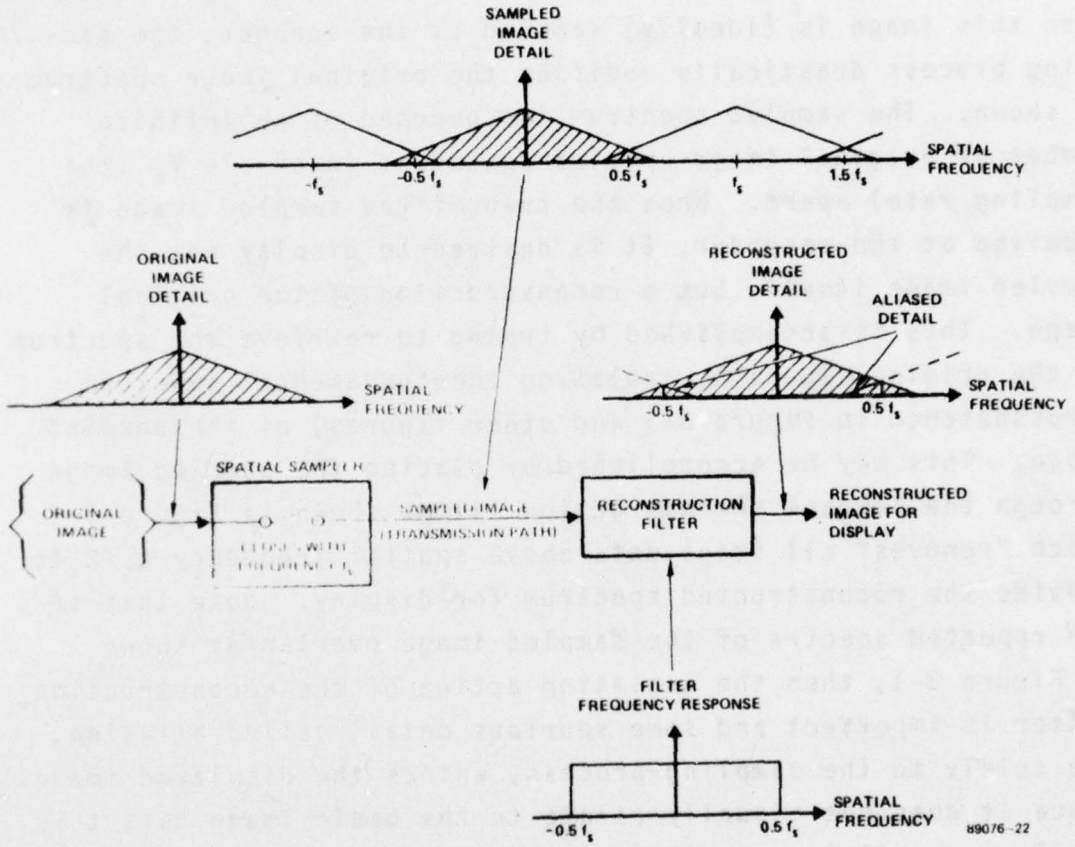
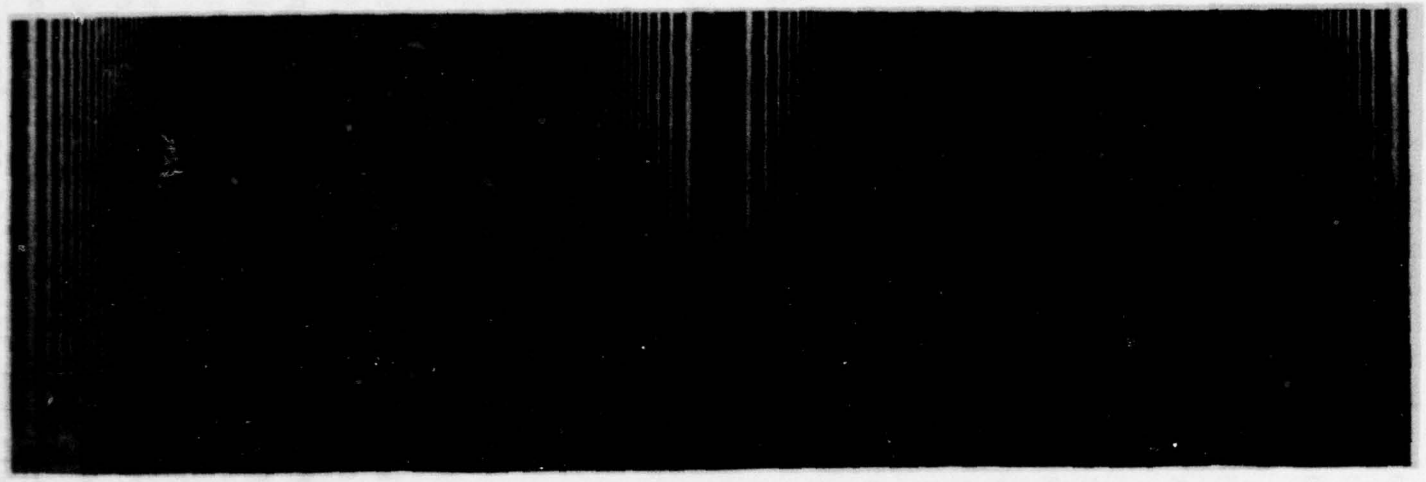


Figure 3-1. Sampled Imagery System with Aliasing

location on the abscissa. Because the MTF of the recorder attenuates all spatial frequencies greater than $f_s/2$, only the aliased frequency is visible on the recorder output. In Figure 3-2 the spatial frequency at spatial location x_o is zero. For source frequencies higher than $f_s/2$ (at x_1 in the figure), the MTF of the recorder attenuates the fundamental (principal alias) and passes the aliased frequency. At x_2, the source frequency is equal to f_s and the aliased frequency is zero while at x_4 the aliased component associated with $2f_s$ has zero frequency; the zero frequency display is evidenced as the three widest black stripes in the figure at x_0, x_2, and x_4. Although it is incidental to the discussion of aliasing, note the change in contrast along the vertical axis of Figure 3-2 which indicates that aliasing is not a function of contrast.

In general, there are only two ways theoretically to remove any spurious aliasing. The first is to move the spatial sampling frequency up to an f_s which is twice the spatial frequency content of the original image and to move the reconstruction filter lowpass cutoff to one-half that amount. The results are seen in Figure 3-3 for this case. Since the repeated copies of the original image spectrum within the sampled image do not now overlap, they can be correctly separated by the lowpass reconstruction filter without incurring any image degradation due to aliasing. The only problem with this approach is that is is counterproductive in terms of conserving image transmission bandwidth as it requires the transmission of more data due to the higher sampling rate. The second approach places a prefilter prior to the spatial sampler as shown in Figure 3-4 in order to "remove" all original image spatial frequencies higher than one-half the sampling frequency f_s. This prevents overlapping of the repeated copies of the prefiltered original image spectrum. Since these repeated copies do not overlap, they can now be correctly separated by the lowpass reconstruction filter without incurring any image



x_o x_1 x_2 x_3 x_4

$(fs/2)$ (fs) $(\frac{3fs}{2})$ $(2fs)$

(f_x=spatial frequency at x)

Spatial Location

Figure 3-2. Example of Aliasing

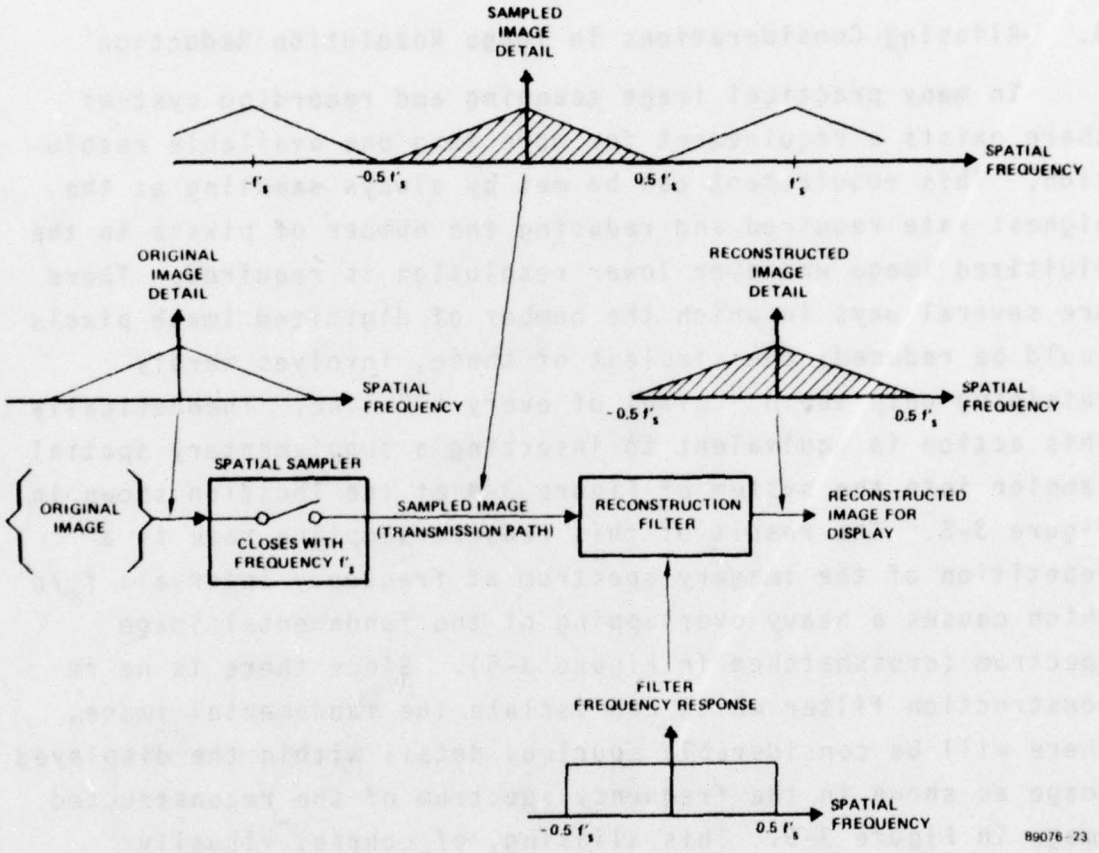


Figure 3-3. Sampled Imagery System, Sampling Frequency Adjusted to Prevent Aliasing

degradation due to aliasing. The net result has been to reduce the system resolution and eliminate aliasing degradation. As pictured in Figure 3-4, the final reconstructed image possesses none of the degradations of aliasing, although the resolution is poorer when compared to that of the original image.

3. Aliasing Considerations in Image Resolution Reduction

In many practical image scanning and recording systems there exists a requirement for more than one available resolution. This requirement can be met by always sampling at the highest rate required and reducing the number of pixels in the digitized image whenever lower resolution is required. There are several ways in which the number of digitized image pixels could be reduced; the simplest of these, involves merely retaining only the n^{th} pixel of every n^{th} line. Theoretically this action is equivalent to inserting a supplementary spatial sampler into the system of Figure 3-4 at the location shown in Figure 3-5. The result of this reduced sampling rate is a repetition of the imagery spectrum at frequency intervals f_s/n which causes a heavy overlapping of the fundamental image spectrum (crosshatched in Figure 3-5). Since there is no reconstruction filter which can isolate the fundamental image, there will be considerable spurious detail within the displayed image as shown in the frequency spectrum of the reconstructed image in Figure 3-5. This aliasing, of course, visually appears as noise-like detail degrading the image quality.

What modifications to this redundancy removal technique are appropriate in order to reduce the excessive aliasing effects incurred? From the sampling theory discussion of Figure 3-4, it is clear that an appropriate prefilter must be provided with a cutoff of $0.5\ f_s/n$ and that the reconstruction filter cutoff must also be decreased to $0.5\ f_s/n$.

If one now abandons the one-dimensional signal assumption and generalizes the results to a two-dimensional spatial image,

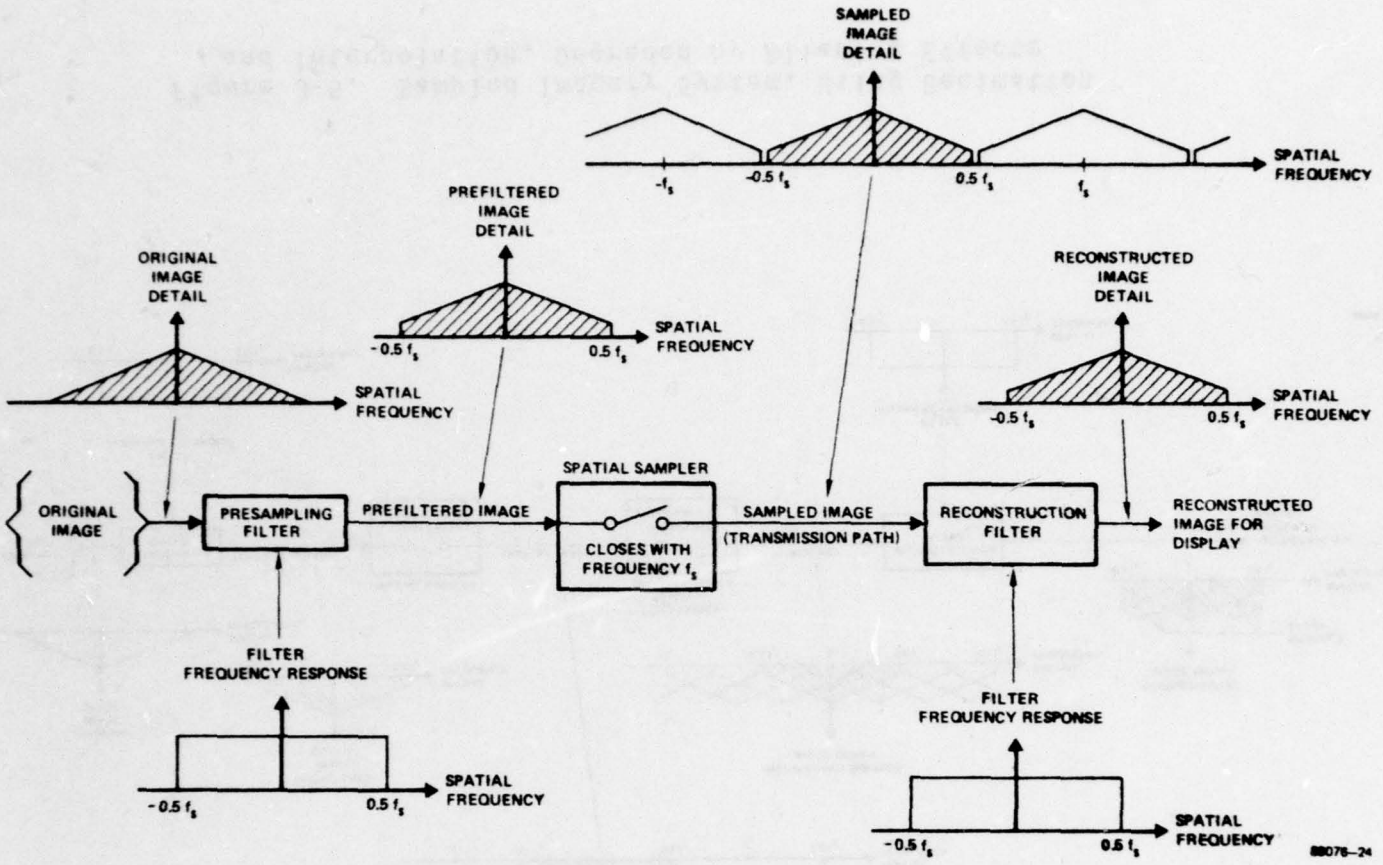


Figure 3-4. Sampled Imagery System, Prefiltered to Prevent Aliasing

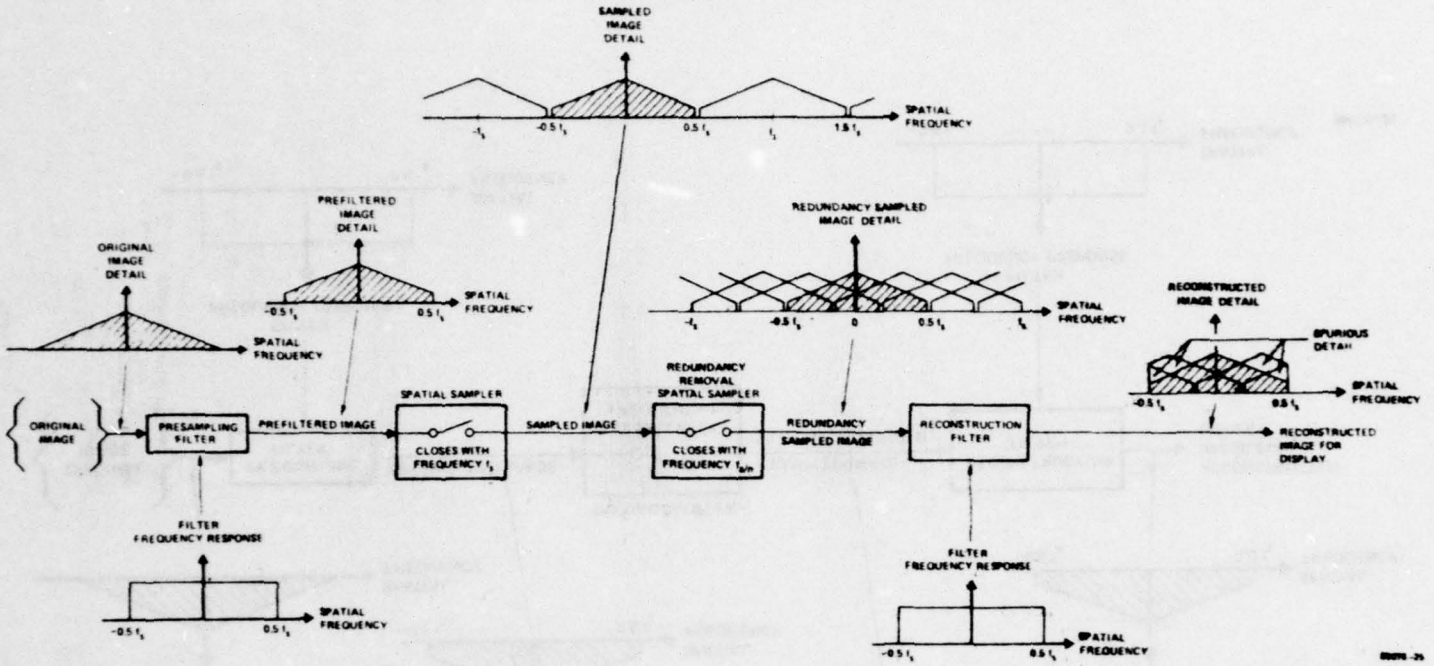


Figure 3-5. Sampled Imagery System, Using Decimation and Interpolation, Degraded by Aliasing Effects

it is clear that the "redundancy removal" filter function of Figure 3-5 must be a two-dimensional filter function. Implementing such a two-dimensional filter function requires enough memory to "sequentially assemble" the pixel values in a sufficiently large neighborhood of each image pixel as the image is point scanned. These neighboring pixel values are then properly weighted and summed to provide a single output value at each sampling instant.

The weighting function corresponding to the ideal lowpass filters shown in Figure 3-6 is a two-dimensional $\frac{\sin x}{x}$ function, which is infinite in extent. Truncated $\frac{\sin x}{x}$ weighting functions could be used to approximate the lowpass filter characteristic. As an example of the aliasing degradation that can be encountered in practical resolution reduction operations, assume that the weighting function (one-dimensional case) is uniform and encompasses a number of samples corresponding to twice the one-dimensional resolution reduction ratio, i.e., for a 4:1 resolution reduction, eight samples would be uniformly weighted.

The model for such a resolution reduction approach and corresponding spectra at key points are shown in Figure 3-7. In Figure 3-7, $h_1(t)$ is the digital decimating filter and $h_2(t)$ is the interpolating filter which includes the model for the analog interpolation process (D/A converter, sample-and-hold postfilter). Note the presence of aliasing between 0 and $f_s/8$ and the unwanted spectral components between $f_s/8$ anf $f_s/2$.

An alternative decimation approach that requires only one-fourth (for the two-dimensional case) of the computational complexity of that shown in Figure 3-7 involves using only four input samples rather than eight (see $h_1(t)$ of Figure 3-7) to obtain each "representative" pixel. The penalty for this reduced computation requirement is that the aliasing becomes more severe. The principal (desired) alias of $S_E(f)$ in Figure 3-7 is contaminated only by side lobes of the remaining

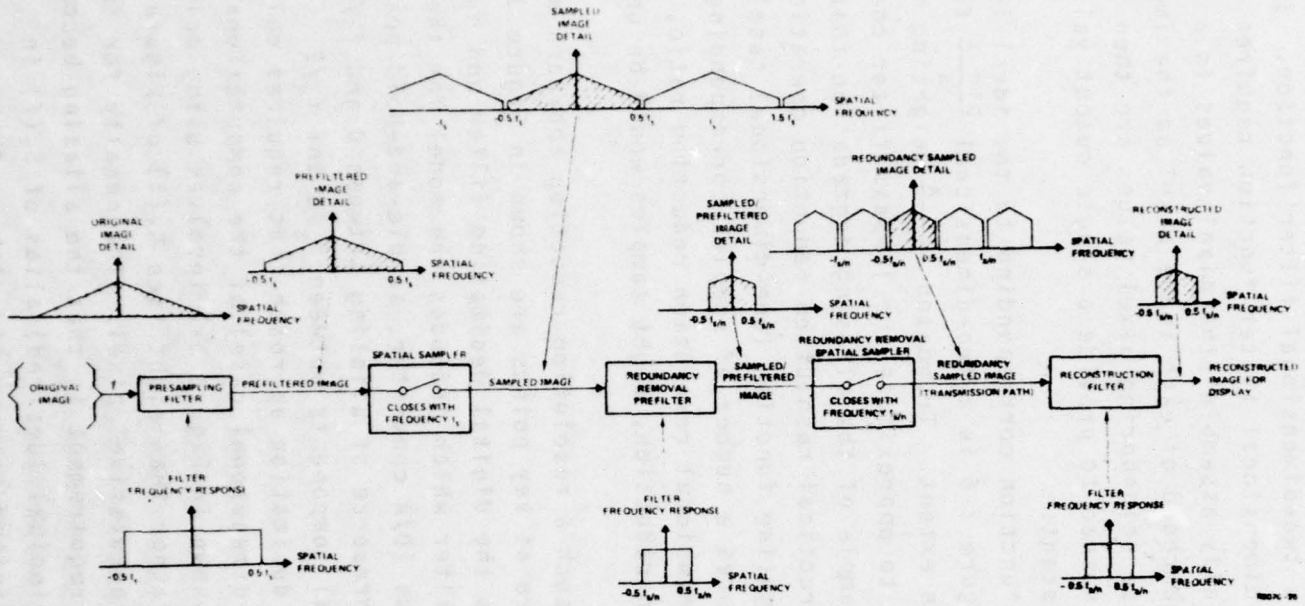


Figure 3-6. Sampled Imagery System Two-Dimensionally Filtered to Prevent Aliasing

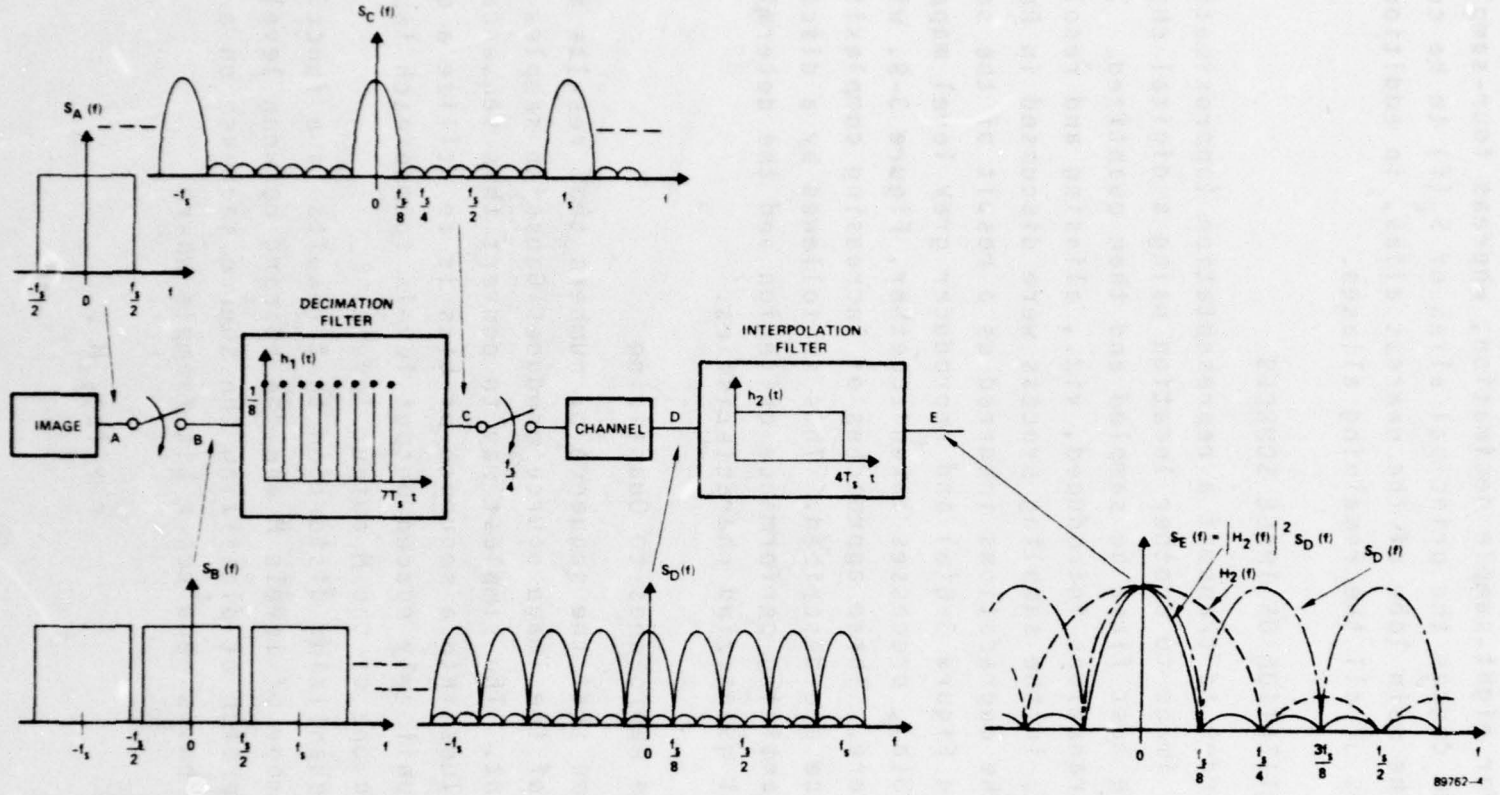


Figure 3-7. Nonideal Two-Dimensional Low-Pass Filtering Using Uniformly Weighted Input Values

aliases for eight-sample decimation, whereas four-sample decimation causes the principal alias of $S_E(f)$ to be contaminated by the main lobe of the nearest alias, in addition to the side lobes of all the remaining aliases.

B. QUANTIZATION OF IMAGE SOURCES

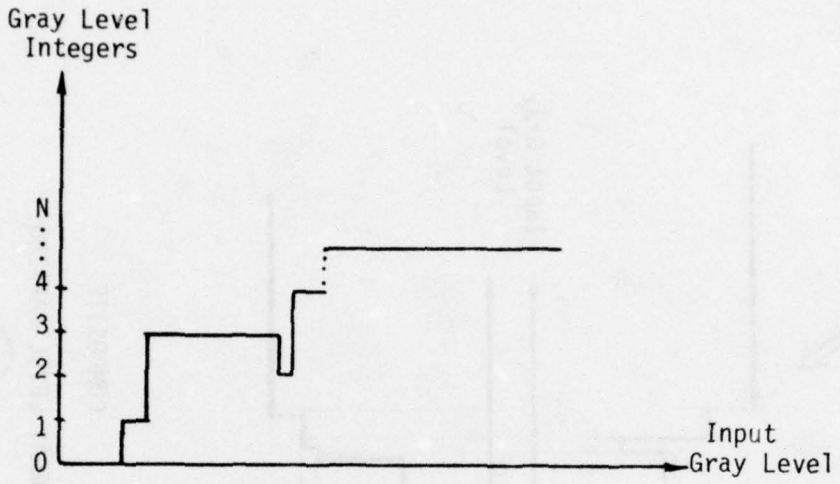
In order to transmit a representation (approximation) of an aerial image to another location using a digital channel, the source must first be sampled and then quantized. The image degradations introduced, viz., aliasing and resolution reduction, in the sampling process were discussed in Paragraph III-A. The degradations incurred as a result of the scanner quantizing Figure 3-8(a) and reproducer gray level mapping, Figure 3-8(b), processes taken together, Figure 3-9, will be treated here. Three approaches of increasing complexity and performance are described. This is followed by a discussion of the quantizing performance criterion and the determination of optimal quantizing characteristics.

1. Three Approaches to Quantizing

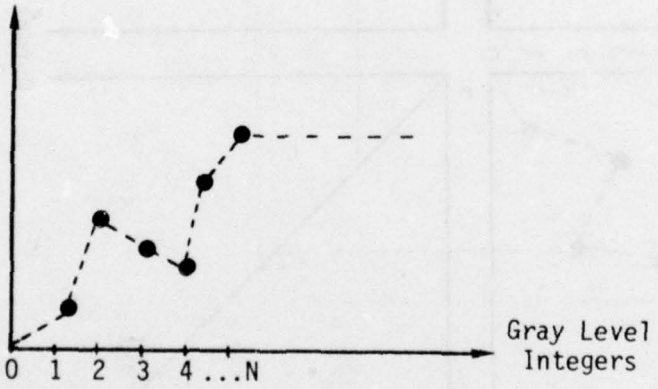
Assume that the sequence of numbers that results from the sampling of the image source produces Gaussian samples that are independent. The simplest way to convert this sequence of image sample values into a sequence of bits is to utilize a quantizer having M uniformly spaced output levels to map each input sample value into one of the M output levels.

The quantizing distortion that results is a function only of the number of levels M and the spacing between levels. This simple approach of digitizing the source sequence on a sample-by-sample basis requires r bits/sample where

$$r \geq \log_2 M .$$



(a) Scanner Gray Level Quantization



(b) Reproducer Gray Level Mapping

Figure 3-8. Scanner and Reproducer Gray Level Mappings

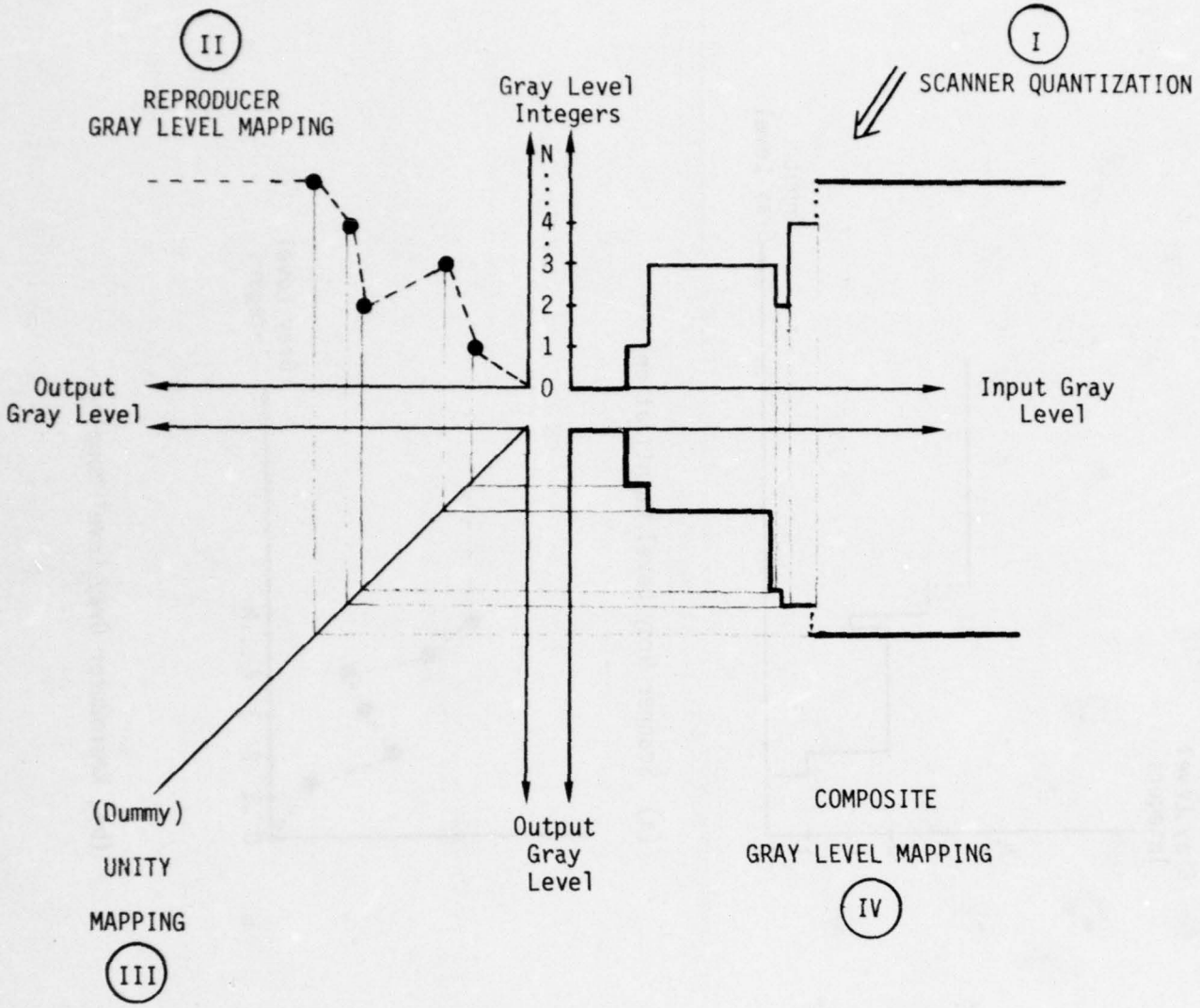


Figure 3-9. Development of the Composite Gray Level Mapping

A more complex quantizing approach treats the quantizer output as a M-ary source and assigns binary codewords to sequences or blocks of quantizer outputs. As the number of quantizer output symbols per block becomes large, the minimum number of bits/sample can approach $\log_2 M$, where M need not be an integer power of the base two. Note that the two approaches above yield an identical number of bits/sample in the special case $M=2^r$, integer = r.

The third and most complex of the three quantizing approaches takes advantage of the fact that a discrete-time Gaussian source will not have equiprobable outputs. For any source with a nonuniform amplitude probability density function, the M-level quantizer output will exhibit an entropy that is less than $\log_2 M$ bits/sample. The output of such a source quantizer can be entropy coded with a number of bits/sample that approaches the informational entropy of the quantizer output.

2. The Quantizing Performance Metric

The performance metric for quantizers is usually taken as the mean-squared error (MSE) between the quantizer input (source) and quantizer output. Although it is recognized that mean-squared error is an inadequate metric of subjective image quality, it is a useful measure of image quality in the sense that, if the MSE is made sufficiently small, the subjective image quality will be perceived as being "good" rather than "fair" or "poor". Whichever of the three quantizing approaches discussed is chosen for quantizing imagery, the quantizing characteristics can be specified so that the quantizing distortion (MSE) is its minimum possible value. All that is required is a knowledge of the amplitude probability density function p(x) of the source, which can be used to specify the quantizer threshold values x_i and representation values y_i by solving (numerically) the simultaneous equations

$$y_i = \int_{x_i}^{x_{i+1}} xp(x)dx \qquad i = 1,2 \ldots$$

and using

$$x_i = (y_i + y_{i-1})/2 \qquad i = 2,3 \ldots$$

It is clear from the first of these equations that the optimum representation level y_i is the centroid of the area of $p(x)$ between x_i and x_{i+1}.

3. Source Coding Subject to a Fidelity Criterion: Shannon's Rate-Distortion Theory

For all useful quantizing characteristics the magnitude of the MSE decreases as the number of bits/sample increases, i.e., the channel bit rate can be traded for quantizing distortion power ε^2.

The lower bound for this tradeoff is given by Shannon's [5] rate-distortion theory result

$$R(\text{bits/sample}) = 1/2 \log_2 (\sigma^2/\varepsilon^2)$$

where

$$\sigma^2 = \text{input signal variance}$$

and

$$\sigma^2/\varepsilon^2 = \text{signal-to-quantizing noise ratio .}$$

It is of interest to compare the performance of the three quantizing approaches described previously to the rate-distortion bound above. Figure 3-10 (taken from [6]) indicates that entropy coding of each uniformly-quantized image-source sample (see the HQ(v) curves) performs within 1/4 bit of the rate-distortion

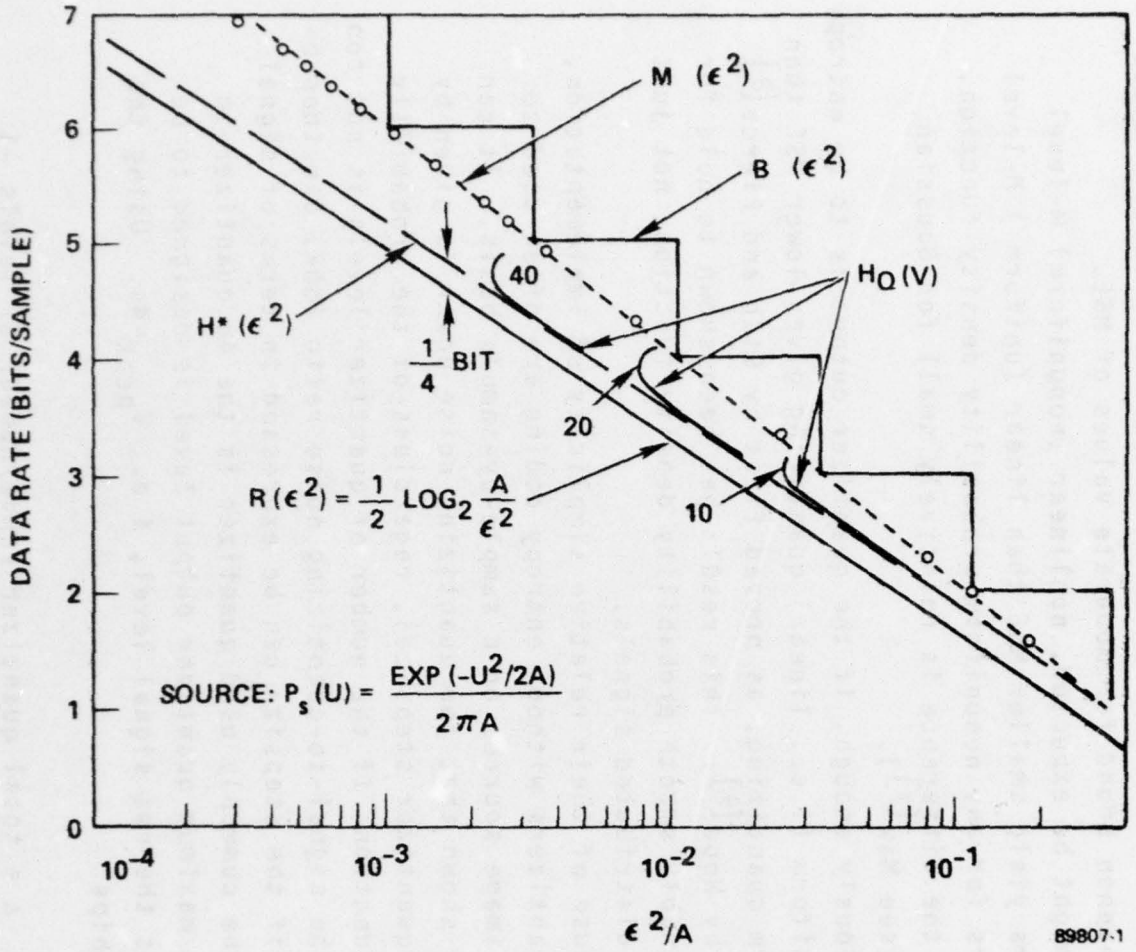


Figure 3-10. Data Rates Required to Send Uniform Quantizer Outputs to a Receiver as a Function of ϵ^2/A. Also Shown are Curves of Quantizer Output Entropy $H_Q(V)$ vs. ϵ^2/A as v_{max} is varied for M=10,20,40

bound. The curves in Figure 3-10 designated $M(\varepsilon^2)$ and $B(\varepsilon^2)$ refer to block coding and sample-to-sample quantizing, respectively, and show that even these relatively simple techniques exhibit rate-distortion performance that is reasonably close to the Shannon bound for moderate values of MSE.

As might be expected, nonlinear (nonuniform) M-level quantizers yield smaller MSE than linear (uniform) M-level quantizers for any nonuniform probability density function, although the difference is relatively small for Gaussian signals (see Max[7]).

Curiously enough, if the quantizer output is to be entropy coded, uniform (i.e., linear) quantizing gives lower MSE than nonuniform quantizing, as proved first by Gish and Pierce[8] and then by Wood[9]. This result has been shown to hold for any reasonably smooth probability density function, not just Gaussian distributed signals.

Because of their relative simplicity of implementation, linear quantizers without entropy coding are often used to digitize image sources on a sample-by-sample basis. It can be easily shown that the quantizing noise power is given by $\Delta^2/12$ (Δ=quantizer stepsize), regardless of the probability density function, if the number of quantizer levels is not too small. The signal-to-quantizing noise ratio (SNR) can then be obtained if the stepsize can be expressed in terms of signal power. One commonly used quantizer is the 4σ quantizer in which the maximum quantizer output level is designed to be four times the rms signal level; i.e., $V_{peak}=4\sigma$. Using the relationships

$$\Delta = \text{total quantizer range/number of levels } -1$$

$$\Delta = \frac{2V_{p\text{-}p}}{(2^{n-1})} \doteq \frac{8\sigma}{2^n}\ , \quad n = \frac{\#}{y} \text{ bits/sample}$$

and $$N_Q = \Delta^2/12$$

the resulting expression for SNR is

$$SNR = \sigma^2/N_Q = \frac{12(2^n)^2}{8^2}$$

or, in dB,

$$SNR\ (dB) = 10 \log SNR = (6n-7.27)\ dB$$

Of course, this expression is only accurate for signals whose rms value σ is one-fourth the maximum quantizer output level.

The corresponding derivation for full load sinusoidal signals yields

$$SNR(dB) = (6n+1.76)\ dB\ .$$

A problem encountered in practice is that real world signals are seldom truly stationary with respect to either signal power or amplitude probability density function. This fact results in suboptimum quantization. This effect can be ameliorated by designing a suboptimum logarithmic μ-law quantizer that performs well with a wide variety of probability density functions over a wide dynamic range of input power levels. The performance of μ-law quantizers is given [10] by

$$SNR\ (dB) = 20 \log \left(\frac{\sqrt{3}\ 2^n}{\log(1+\mu)} \right)\ dB$$

and for the commonly used μ=255 system, this reduces to

$$SNR(dB) = (6n-2.86)\ dB\ .$$

The rate distortion bound on SNR performance can be obtained from

$$n \frac{\text{bits}}{\text{sample}} = R(\varepsilon^2) = \tfrac{1}{2} \log_2 (\sigma^2/N_Q) = \tfrac{1}{2} \log_2(\text{SNR})$$

which implies

$$\text{SNR (dB)} = 10 \log_{10} (2^{2n}) = 6n(\text{dB}) .$$

Since one bit is equivalent to 6 dB, the 4σ quantizer and μ-law (μ=255) quantizer perform within 1.2 bits and 0.48 bit of the rate distortion bound, respectively.

C. PRACTICAL DIGITAL IMAGE DEGRADATION MECHANISMS

It has been shown above and in Section II-C that any digital image conversion process must introduce image degradations. It was also shown that theoretically, these degradations could be made as insignificant as desired.

In addition to any theoretical degradation incurred, there normally exists a large repertory of degradations encountered due to practical implementation considerations. For instance, any structural or parameter change from optimal will result in degradation. These changes can be due to noise, spurious signals, device limitations, design choice, the environment and component failures. In the most general state-of-the-art case, general orthonormal operation, the effects of these changes from optimality are blurred across the image. Thus the degradation will subjectively appear as a general worsening of image quality-generally with little specific to point to other than loss of resolution, contrast, and mudding of image detail.

In the case of spatially sampled orthonormal conversion, the effects of image processing system changes from optimality are much more distinct and differentiated than in the case of general orthonormal conversion. Since spatially sampled orthonormal conversion is used in the vast bulk of current state-of-the-art imagery scanners and recorders, it becomes important to

look more closely at their practical degradation effects. First, note that the orthonormal basis used is the impulse function. As a result, it will typically be found that any system change from optimality will affect only a very small region of the image. This is largely due to the fact that in this system any unit of data passing through the process contains information only about a corresponding local region of the image. If this data is perturbed by a system change, it is normally seen as a localized phenomenon (which may apply equally across the image). The eye of the observer, however, considers local imagery changes as imagery detail. Thus, those system changes which result in nonhomogeneous imagery degradation, i.e., localized changes, will be especially apparent.

In the case of digital scanners and reproducers, the following is a list of commonly encountered practical departures from theory, possible sources of the departure in terms of commonly encountered scanners and recorders, and the most likely perceived form of the resulting degradation.

Scanner

The Prefilter MTF Cutoff Frequency is Below Optimal

Possible Sources:

- System design
- The scanner optical path
- The scanner electronic circuits and filters

Perceived Degradations:

- Loss of fine detail, blurring (higher spatial frequencies)

The Prefilter MTF Cutoff Frequency is Above Optimal

Possible Sources:

- System design
- The scanner optical path

- The scanner electronic circuits and filters

Perceived Degradations:

- False low spatial frequency patterns instead of and at an angle to strong high spatial frequency image detail (such as waves at sea, plowed fields, shingled roofs, etc.)
- Periodic dropouts of thin lines at a slight angle to the scanning raster (such as seeing a dashed line where a power line is known to be present).
- Regular structure or detail on a boundary in the image known to be short and smooth
- General mottling of the image

<u>The Prefilter MTF Curve Shape Departs from Optimality</u>

Possible Sources:

- System design
- Optics
- Detector
- Preamplifier

Perceived Degradations:

- Decreased resolution (blurring)
- Ringing (appearance like ripples in water)
- Increased raster visibility
- Image too dark or too light

The Sampling Rate is Reduced Appreciably

Possible Sources:

- System design
- Electrical component failure in clocking circuit
- Operator error

Perceived Degradations:

- Loss of fine detail (above 1/2 the sampling rate)
- Image degenerates ultimately to a matrix of dots of varying intensity
- The effects (above) caused by the MTF going above optimal

The Sampling Rate is Systematically or Randomly Perturbed

Possible Sources:

- System design
- Electrical component failure in clocking circuit
- Mechanical scanning imperfections

Perceived Degradations:

- General mottling (for high spatial frequency perturbations)
- Image waviness or patterns in the image structure (for moderate spatial frequency perturbations)
- Geometric distortion accompanied by effects (above) caused by MTF cutoff going above and below optimal (for low spatial frequency perturbations).

The Spatial Sampling Structure Departs from Optimality

Possible Causes:

- System design
- Electrical component failure in sync circuit, line start circuit

Perceived Degradations:

- Effects (above) caused by MTF cutoff going above optimal-generally along one direction in the image, and simultaneously
- The effects (above) caused by MTF cutoff going below optimal-along some other direction in the image

The Digitizer Levels are All Chosen Too Low

Possible Causes:

- System design
- Preamplifier gain increased
- A/D malfunctioning
- Input image too light

Perceived Degradations:

- Total loss of detail in highlights

The Digitizer Levels are All Chosen Too High

Possible Causes:

- System design
- Preamplifier gain decreased
- A/D malfunctioning
- Input image too dark

Perceived Degradation:

- Total loss of detail in shadows

One or More Digitization Intervals is Enlarged

Possible Sources:

- System design
- Detector/preamplifier gain curve departs from optimality
- A/D malfunctioning

Perceived Degradations:

- False contouring seen in detail-less areas
- Portions of picture appear painted
- Loss of low contrast detail
- Apparent increase in image contrast

One or More of the Digitization Intervals is Randomly or Systematically Perturbed

Possible Sources:

- Mechanical vibrations
- Detector noise
- Preamplifier noise
- A/D malfunctioning

Perceived Degradations:

- Spot noise in the image
- General mottling
- Granularity

Reproducer

The Gray Level Mapping Levels are all Chosen Too Low

Possible Causes:

- System design
- Insufficient light output
- Insensitive output medium
- Amplifier gain too low

Perceived Degradations

- Image is too dark
- Cannot see shadow detail

The Gray Level Mapping Levels are all Chosen Too High

Possible Causes:

- System design
- Too intense a light output
- Too sensitive an output medium
- Amplifier gain too high

Perceived Degradations:

- Image is "washed out," flat
- Low contrast

One or More of the Gray Level Mapping Levels is Mischosen

Possible Causes:

- System design
- Amplifier/light modulator/output medium gain curve departs from optimality
- D/A malfunctioning

Perceived Degradations:

- False containing
- Masking of image detail
- Loss of contrast

One or More of the Gray Level Intervals is Randomly or Systematically Perturbed

Possible Sources:

- Mechanical vibration
- Light modulator noise
- Amplifier noise
- Channel noise
- A/D malfunctioning

Perceived Degradations:

- Spot noise in the image
- General mottling
- Scan pattern becomes visible
- Granularity

The Postfilter MTF Cutoff Frequency is Below Optimal

Possible Causes:

- System design
- The reproducer optical path
- The reproducer electronic filters

Perceived Degradations:

- Loss of fine detail, blurring

The Postfilter MTF Cutoff Frequency is Above Optimal

Possible Sources:

- System design
- The reproducer optical path
- The reproducer electronic circuits

Perceived Degradations:

- General mottling of the image
- The image raster will become more pronounced

- Object boundaries known to be smooth will become ragged

The Postfilter MTF Curve Departs from Optimality

Possible Sources:

- System design
- Optics
- Electronics
- Light modulator

Perceived Degradations:

- Decreased resolution (blurring)
- Ringing (appearance like ripples in water)
- Increased raster visibility
- Image too dark or light

The Reproduced Pixel Rate is Reduced Appreciably

Possible Sources:

- System design
- Electrical failure in clocking circuit
- Operator error

Perceived Degradation:

- Image will degenerate ultimately to a matrix of dots of varying intensity
- The effects (above) caused by the post-filter MTF going above optimal

The Reproduced Pixel Rate is Systematically or Randomly Perturbed

Possible Sources:

- System design
- Electrical failure in clocking circuit
- Mechanical scanning imperfections

Perceived Degradations:

- General mottling (for high spatial frequency perturbations)
- Image waviness or patterns across the image structure (for moderate spatial frequency perturbations)
- Geometric distortions caused by incorrect MTF of the postfilter

The Reproduced Pixel Structure Departs from Optimality

Possible Causes:

- System design
- Electrical failure in sync circuit or line start circuit

Perceived Degradations:

- Systematic jitter of image detail
- Incorrect postfilter MTF effects (above)

SECTION IV

SUBJECTIVE EFFECTS OF SELECTED DIGITAL DEGRADATIONS

Sections II and III consider the structural aspects of the imagery chain, methodology of evaluation and the definition and desirable features of a measure of image quality. These sections do not, however, directly consider the question of how sensitive and consistent the human observer's reaction is to various digital degradations likely to be encountered in practice. This is experimentally considered here.

Section IV-A discusses the test methodology, Section IV-B presents preliminary image comparative test sets for a variety of digital degradations and source imagery, and Section IV-C provides indications of the sensitivity of a trained photo-interpreter to various common digital degradation as well as the consistence of his observation.

The comparative test sets and corresponding indications of the photointerpreter's sensitivity to the various digital degradations should prove useful to a variety of hardware programs in the future.

A. TESTING

The testing procedure used was generally that of Figure 2-18(b), i.e., subjective evaluations were sought of all perceived digital effects.

In order to choose representative examples of the above imagery, a trained photointerpreter intimately familiar with the RADC Imagery Data Bank, Richard Petroski of Rome Research Corporation, was asked to make an appropriate selection. The following predigitized images were chosen for evaluation.

- B/W Vertical Photography (RC-8 camera) over Griffiss AFB, NY - approximately (1¼ ground ft.)^2 per pixel.
- B/W Vertical Photography (RC-8 camera) over Griffiss AFB, NY - approximately (8 ground ft.)^2 per pixel.
- Infrared image (sensor not identified) over Parked Aircraft.
- Synthetic Aperature Radar (UPD-4) over Griffiss AFB, NY.

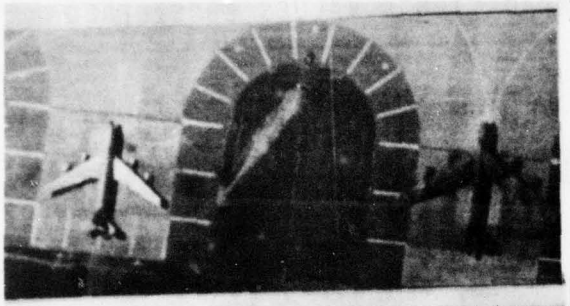
Representative 256x512 pixel samples of each image were chosen and used as the test reference (Figure 4-1). Each image was then subjected to controlled intensities of digital degradation in accordance with Table 1. Appendix A contains the documentation of the methodology and computer programming used. This methodology and programming has the unique feature of being easily extendable to include other digital effects including those encountered in a digital scanner.

The degraded images shown in Section IV-B were obtained in hardcopy and softcopy form. The hardcopy medium was 3-M's dry silver paper. The softcopy display was the Sony Color Digital TV at RADC.

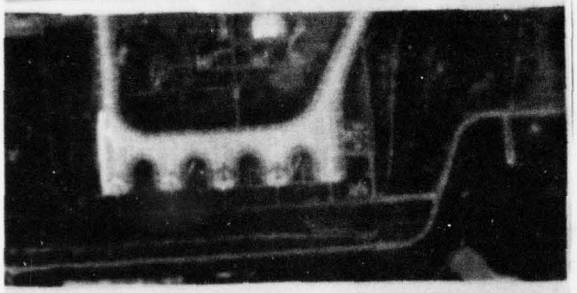
A trained photointerpreter, again Richard Petroski of Rome Research Corporation, was then given the directions contained in Table 2. The photointerpreter was permitted to select his working environment and use whatever aids he desired. The results of the above testing were collected and compiled. Results are given in Section IV-C and Appendix B.

B. PRELIMINARY IMAGE COMPARATIVE TEST SETS

The figures of this section contain high quality photographic reproductions of the series of hardcopy degraded imagery used in the experimental testing of this section.



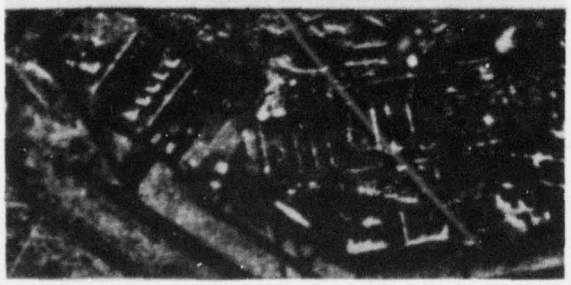
B/W vertical photography (RC-8 camera) over Griffiss AFB, NY - approximately (1-1/4 ground ft.)^2 per pixel.



B/W vertical photography (RC-8 camera) over Griffiss AFB, NY - approximately (8-3/4 ground ft.)^2 per pixel.



Infrared image (sensor not identified) over parked aircraft



Synthetic Aperture Radar (UPD-4) over Griffis AFB, NY

Figure 4-1. Master Digital Images

TABLE 1. LIST OF DIGITAL DEGRADATION & VALUES CONSIDERED

Additive Gaussian Spot Noise

Mean = 0

Standard Deviation = .3, .6, 1.22, 2.44, 4.88, 9.77, 19.52, 39.04% of the gray level dynamic range

Additive Gaussian Line Noise

Mean = 0

Standard Deviation = .3, .6, 1.22, 2.44, 4.88, 9.77, 19.52, 39.04% of the gray level dynamic range

Gaussian Line Jitter

Mean = 0

Standard Deviation = .05, .1, .2, .39, .78, 1.56, 3.13, 6.25 pixels

Quantization

No. of levels = 32, 16, 8, 4 gray levels

Sampling Reduction, High Aliasing

Reduction Size = 1/2, 1/3, 1/4, 1/5 of original

Sampling Reduction, Reduced Aliasing

Reduction Size = 1/2, 1/3, 1/4, 1/5 of original

TABLE 2. PHOTOINTERPRETATOR TEST INSTRUCTIONS

(1) Subjective Verbal Assessment of Image Quality

A. Look at each digitally perturbed image in reference to the original and define its percent utility to photointerpretive tasks.

100% utility - same as original

0% utility - of no use whatsoever

B. Note in words the nature and extent of interference to image quality relating to your percentile utility rating assigned.

(2) Determination of Isopreference Contours of Image Quality

Using selected images from one digitally perturbed series, match them to images of other series such that they visually seem to possess the same image quality.

(3) Crosscheck of the Transitiveness of Image Quality

Repeat Number (2) above.

(4) Specific Comparison of Aliased Imagery

For each image pair of digitally reduced spatially sampled images (high aliasing, low aliasing) determine which possess the higher image quality.

They are included as a key component of this report since via comparative techniques, they may be used to evaluate actual digital systems for similar degradations.

Figures 4-2 through 4-5 illustrate the effects of progressive digital degradation on a high resolution B/W vertical photograph, the top image of Figure 4-1.

Figures 4-6 through 4-11 illustrate the effects of progressive digital degradations on a low resolution B/W vertical photograph, the second image of Figure 4-1.

Figures 4-12 through 4-17 illustrate the effects of progressive digital degradations on an infrared image of parked aircraft, the third image of Figure 4-1.

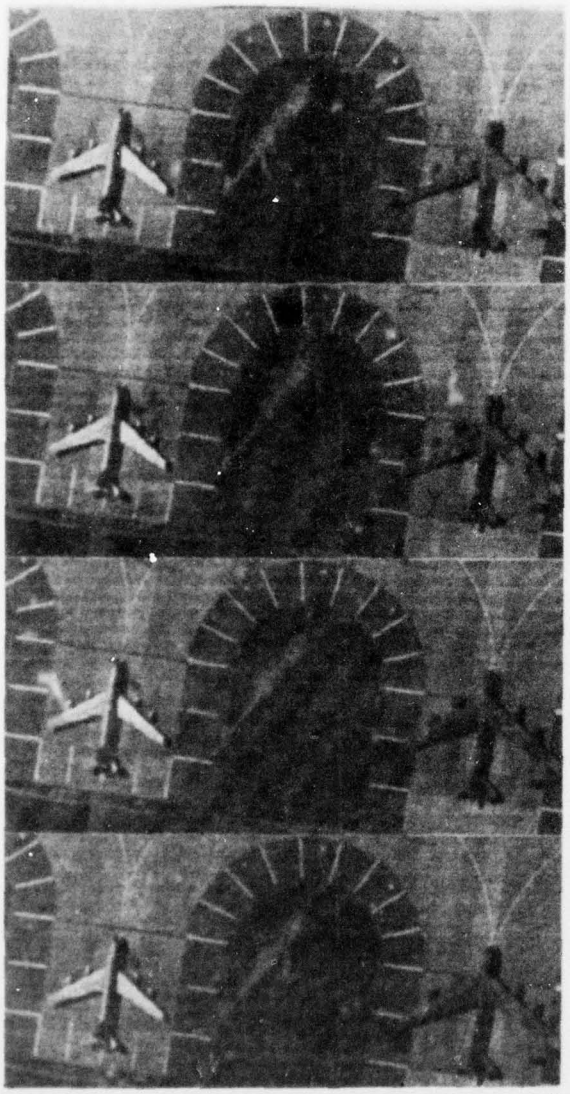
Finally Figures 4-18 through 4-23 illustrate the effects of progressive digital degradations on a synthetic aperature radar image, the bottom image of Figure 4-1.

C. RESULTS

The results of subjective photointerpretative evaluation of the preliminary test set of Section IV-B are given here.

The preliminary subjective image test set was evaluated according to the procedure of Section IV-A and Table 3. The results of the subjective hardcopy utility assessment of photointerpretative image content relative to the original digitized images are shown in Figures 4-25 through 4-29. The various absolute sensitivities recorded should be useful in comparative evaluations and the design of other imagery systems.

The figures, 4-24 through 4-29 show that the subjective image quality measure is a function of the form and degree of the digital degradation. The subjective image quality is also seen to be dependent upon the characteristics of the source image. The interdependency of the form and degree of digital degradation with the characteristics of the source image are found to be most complex and deserving of further study. No immediate correlation between the image spectrum of the original



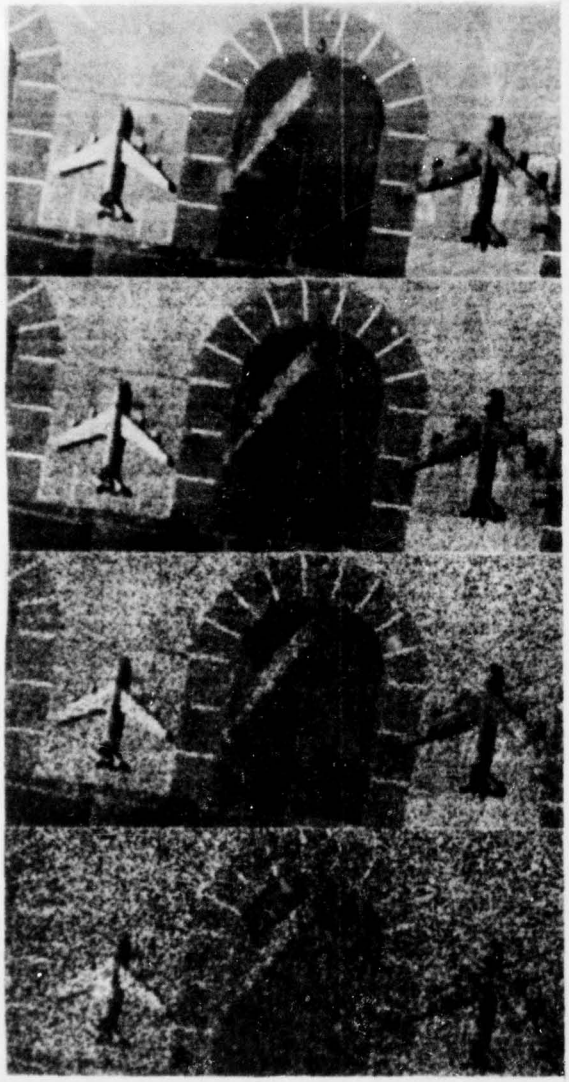
Standard deviation = .3%
of gray level range

Standard deviation = .6%
of gray level range

Standard deviation = 1.22%
of gray level range

Standard deviation = 2.44%
of gray level range

Figure 4-2. Additive Gaussian Spot Noise Applied to a High Resolution B/W Vertical Digitized Photograph



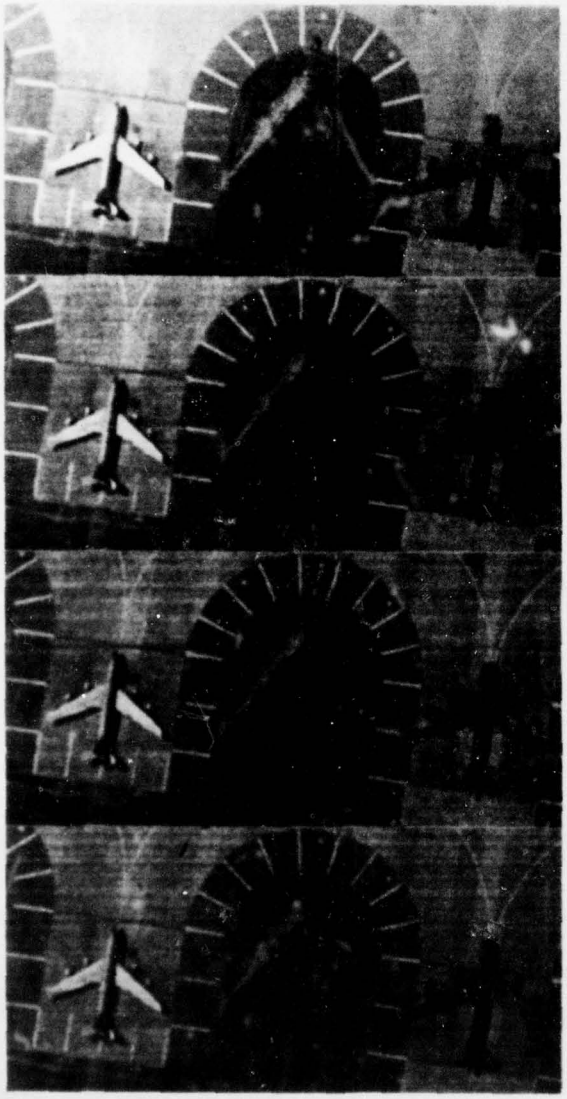
Standard deviation = 4.88%
of gray level range

Standard deviation = 9.77%
of gray level range

Standard deviation = 19.55%
of gray level range

Standard deviation = 39.04%
of gray level range

Figure 4-2 (Continued). Additive Gaussian Spot Noise Applied to a High Resolution B/W Vertical Digitized Photograph



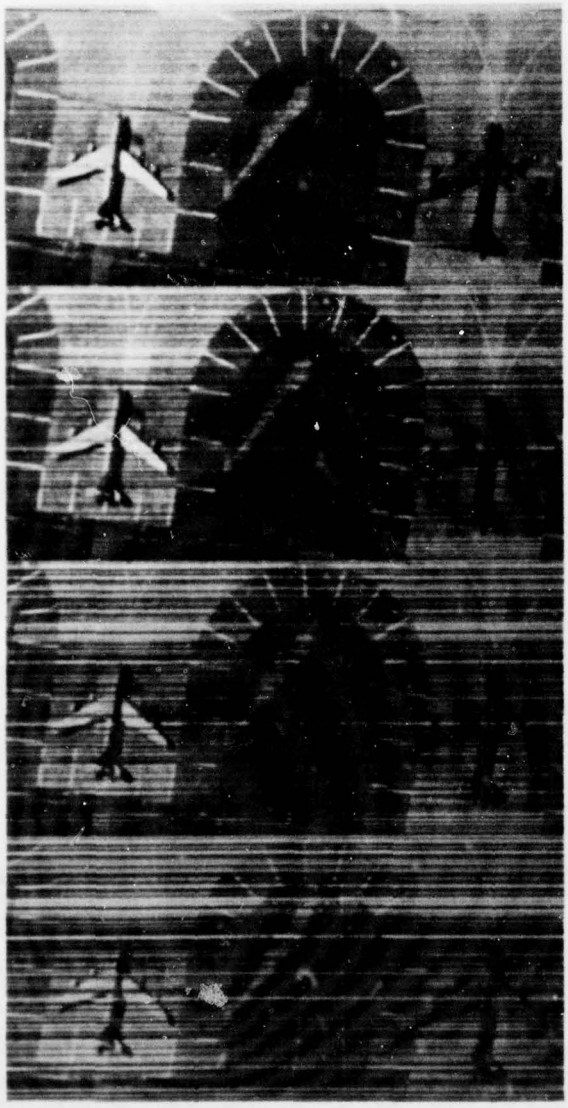
Standard deviation = .3%
of gray level range

Standard deviation = .6%
of gray level range

Standard deviation = 1.2%
of gray level range

Standard deviation = 2.44%
of gray level range

Figure 4-3. Additive Gaussian Line Noise Applied to a High Resolution B/W Vertical Digitized Photograph



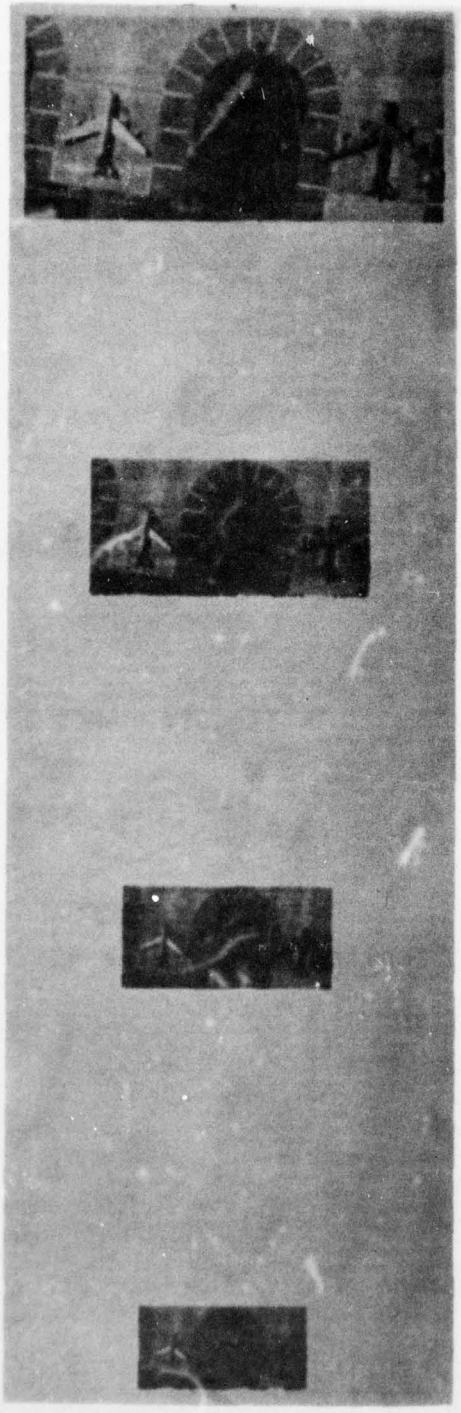
Standard deviation = 4.88%
of gray level range

Standard deviation = 9.77%
of gray level range

Standard deviation = 19.52%
of gray level range

Standard deviation = 39.04%
of gray level range

Figure 4-3 (Continued). Additive Gaussian Line Noise Applied to a High Resolution B/W Vertical Digitized Photograph



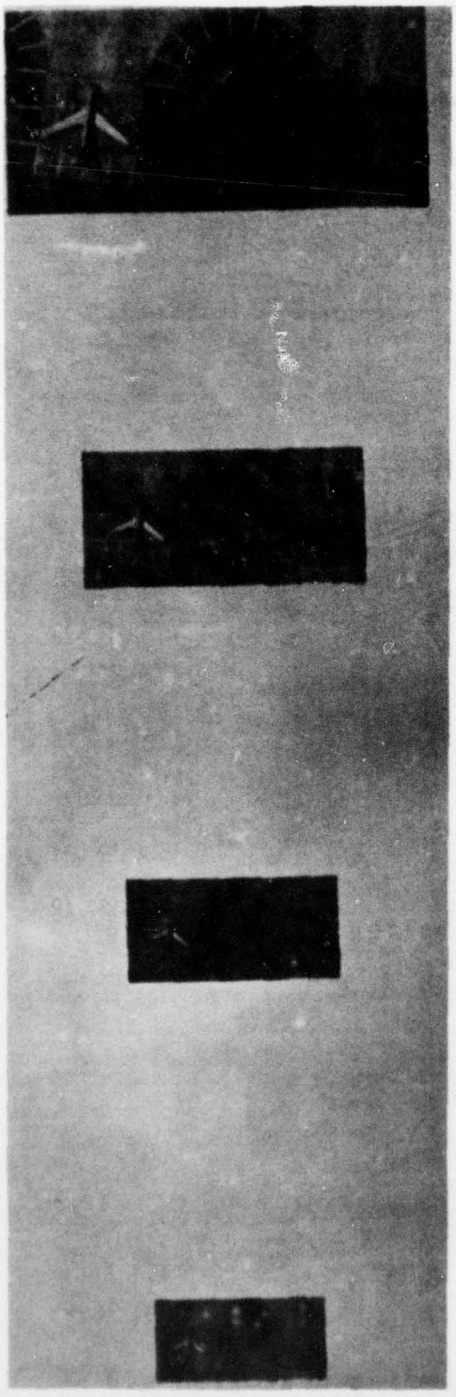
Sampling Reduction = 2

Sampling Reduction = 3

Sampling Reduction = 4

Sampling Reduction = 5

Figure 4-4. Varying the Sampling of a High Resolution B/W Vertical Digitized Photograph Under High Aliasing



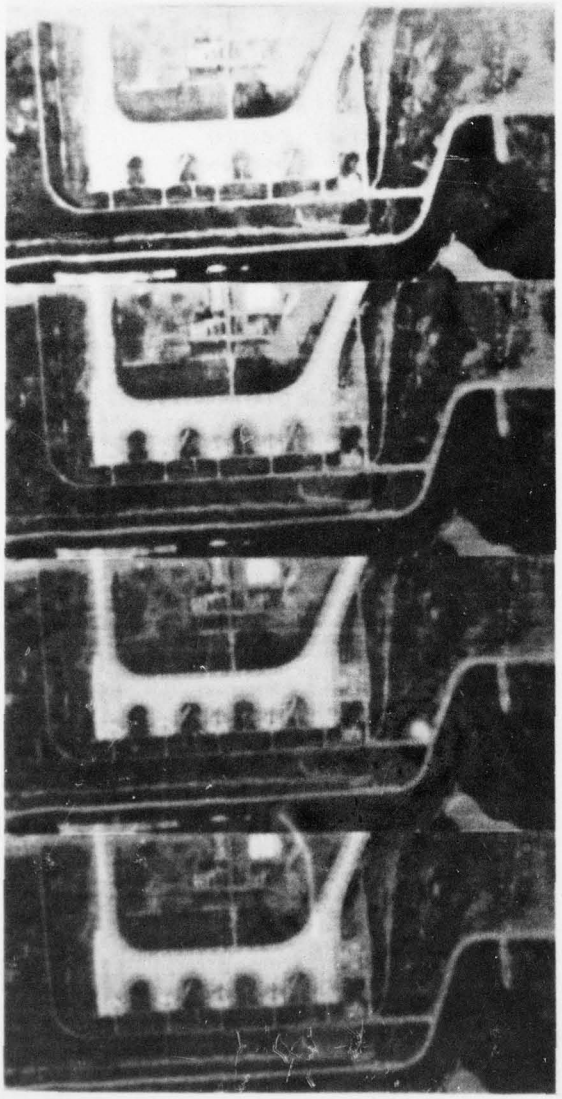
Sampling Reduction = 2

Sampling Reduction = 3

Sampling Reduction = 4

Sampling Reduction = 5

Figure 4-5. Varying the Sampling of a High Resolution B/W Vertical Digitized Photograph Under Reduced Aliasing



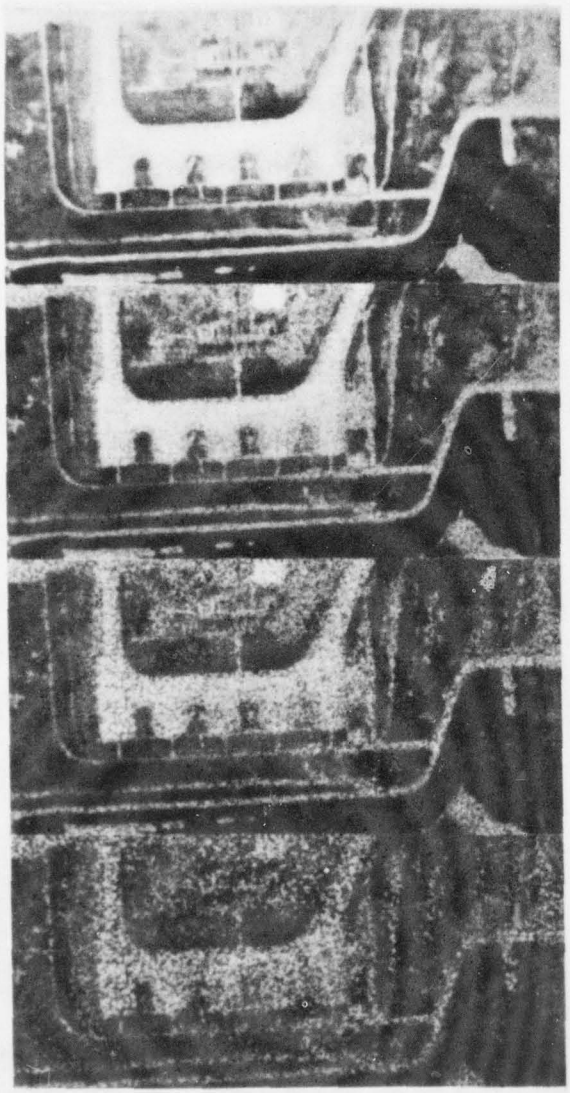
Standard deviation = .3%
of gray level range

Standard deviation = .6%
of gray level range

Standard deviation = 1.2%
of gray level range

Standard deviation = 2.44%
of gray level range

Figure 4-6. Additive Gaussian Spot Noise Applied to a Low Resolution B/W Vertical Digitized Photograph



Standard deviation = 4.88%
of gray level range

Standard deviation = 9.77%
of gray level range

Standard deviation = 19.52%
of gray level range

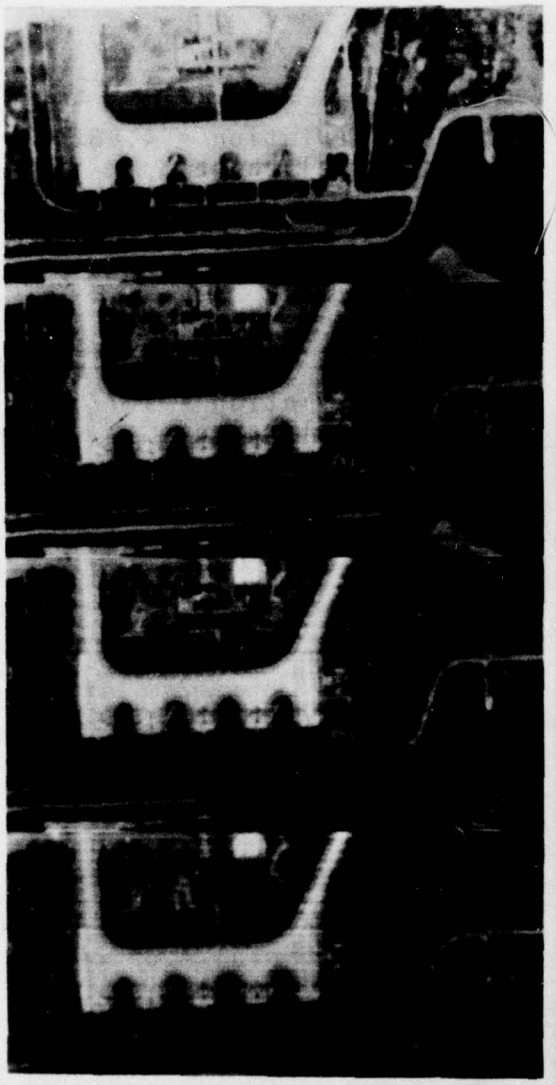
Standard deviation = 39.04%
of gray level range

Figure 4-6 (Continued). Additive Gaussian Spot Noise Applied to a Low Resolution B/W Vertical Digitized Photograph

AD-A049 798 HARRIS CORP MELBOURNE FLA ELECTRONIC SYSTEMS DIV F/G 9/4
DIGITAL IMAGERY TEST SET.(U)
NOV 77 R H COFER, A R MARTIN
UNCLASSIFIED RADC-TR-77-371 F30602-76-C-0296 NL

2 OF 3
AD A049798





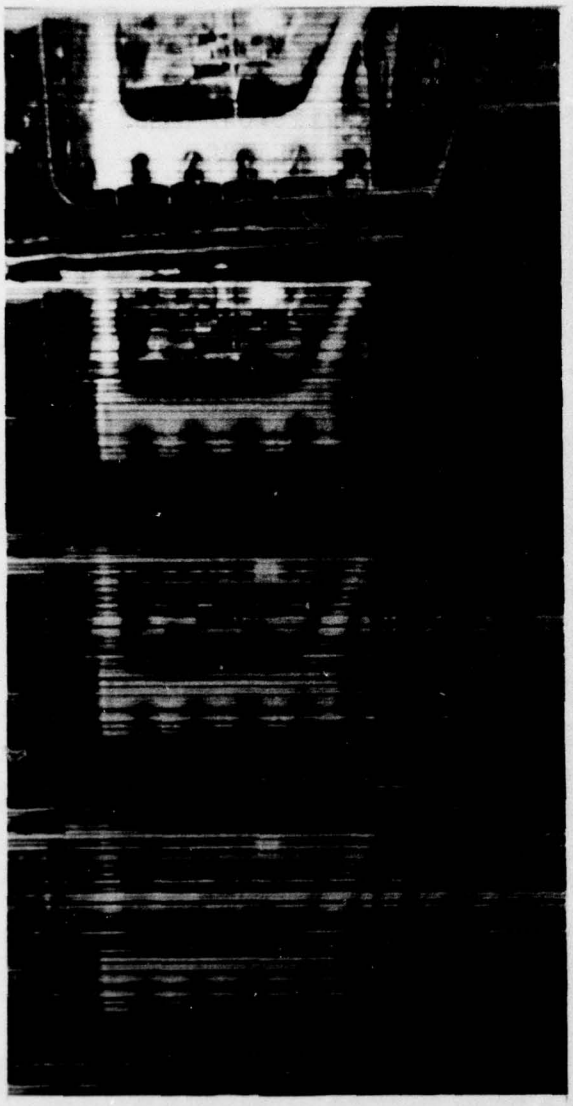
Standard deviation = .3%
of gray level range

Standard deviation = .6%
of gray level range

Standard deviation = 1.22%
of gray level range

Standard deviation = 2.44%
of gray level range

Figure 4-7. Additive Gaussian Line Noise Applied to a Low Resolution B/W Vertical Digitized Photograph



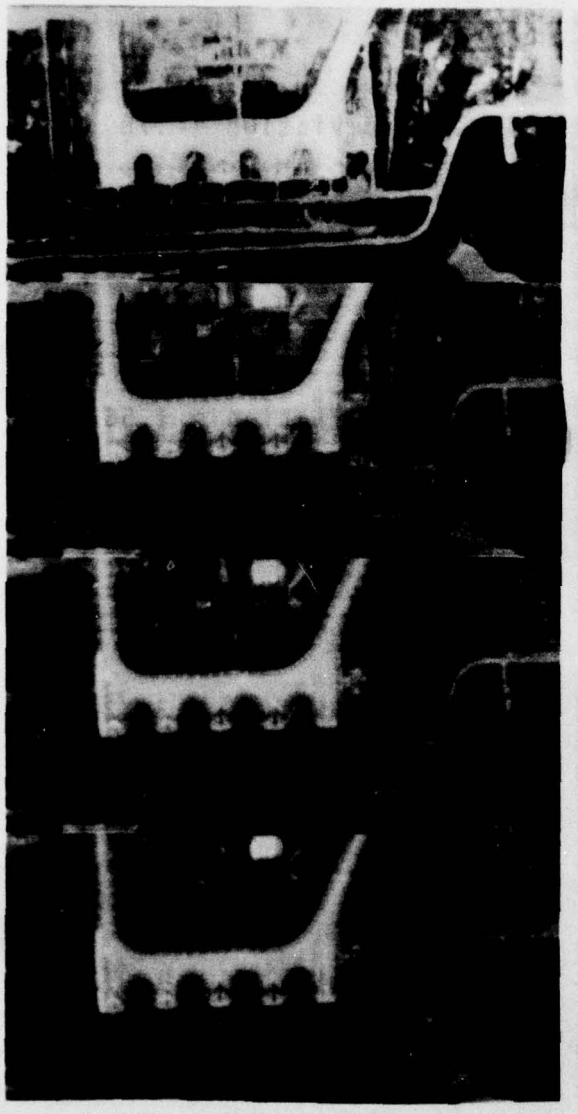
Standard deviation = 4.88%
of gray level range

Standard deviation = 9.77%
of gray level range

Standard deviation = 19.52%
of gray level range

Standard deviation = 39.04%
of gray level range

Figure 4-7 (Continued). Additive Gaussian Line Noise Applied to a Low Resolution B/W Vertical Digitized Photograph



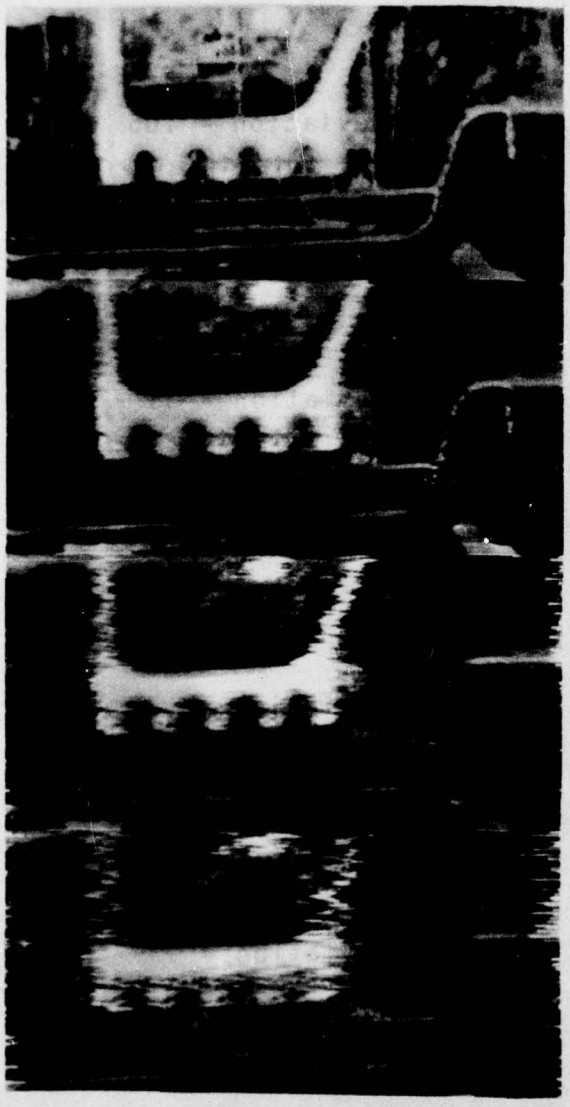
Standard deviation = .05 pixels

Standard deviation = .1 pixels

Standard deviation = .2 pixels

Standard deviation = .39 pixels

Figure 4-8. Gaussian Line Jitter Applied to a Low Resolution B/W Vertical Digitized Photograph



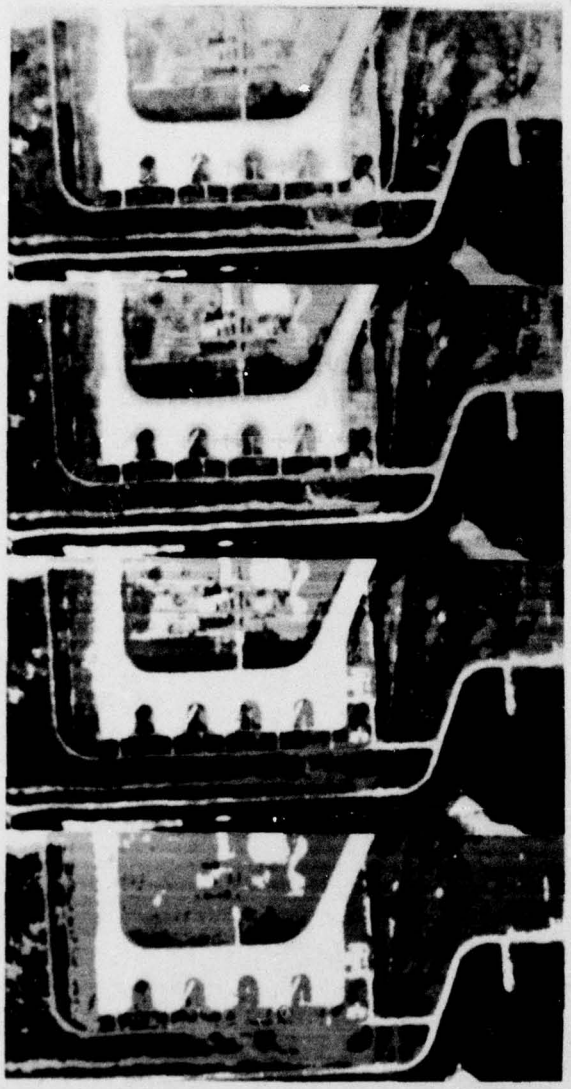
Standard deviation = .78 pixels

Standard deviation = 1.56 pixels

Standard deviation = 3.13 pixels

Standard deviation = 6.25 pixels

Figure 4-8 (Continued). Gaussian Line Jitter Applied to a Low Resolution B/W Vertical Digitized Photograph



Number of gray levels = 32

Number of gray levels = 16

Number of gray levels = 8

Number of gray levels = 4

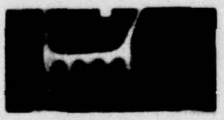
Figure 4-9. Varying the Quantization of a Low Resolution B/W Vertical Digital Photograph



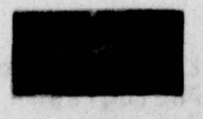
Sampling Reduction = 2



Sampling Reduction = 3



Sampling Reduction = 4



Sampling Reduction = 5

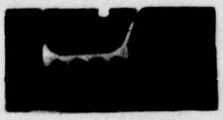
Figure 4-10. Varying the Sampling of a Low Resolution B/W Vertical Digitized Photograph Under High Aliasing



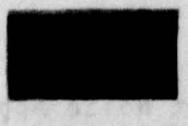
Sampling Reduction = 2



Sampling Reduction = 3



Sampling Reduction = 4



Sampling Reduction = 5

Figure 4-11. Varying the Sampling of a Low Resolution B/W Vertical Digitized Photograph Under Reduced Aliasing



Standard deviation = .3%
of gray level range

Standard deviation = .6%
of gray level range

Standard deviation = 1.22%
of gray level range

Standard deviation = 2.44%
of gray level range

Figure 4-12. Additive Gaussian Spot Noise Applied to an Infrared Image of Parked Aircraft



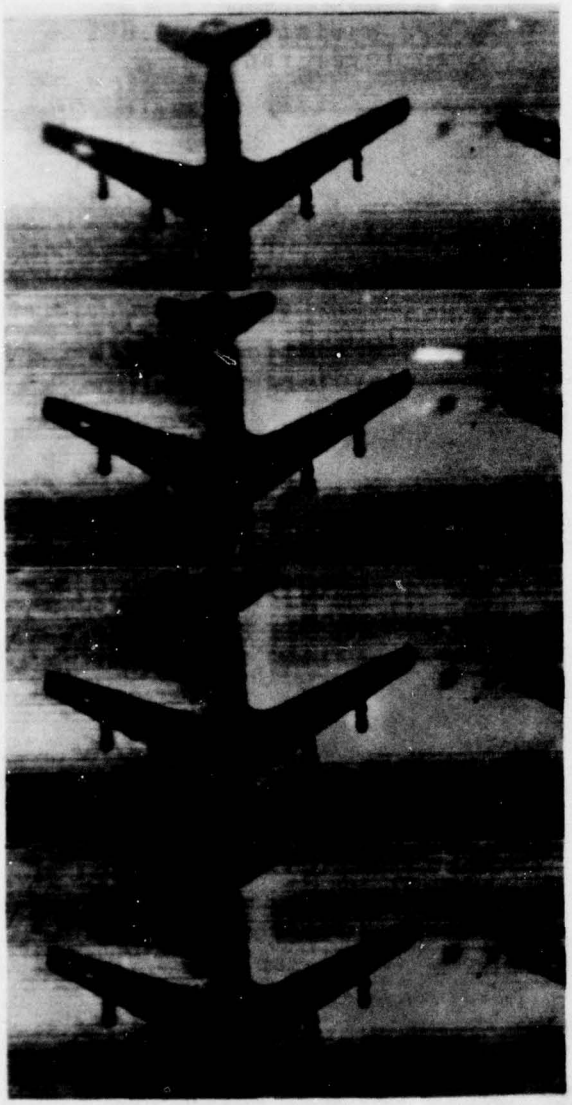
Standard deviation = 4.88%
of gray level range

Standard deviation = 9.77%
of gray level range

Standard deviation = 19.52%
of gray level range

Standard deviation = 39.04%
of gray level range

Figure 4-12 (Continued). Additive Gaussian Spot Noise Applied to an Infrared Image of Parked Aircraft



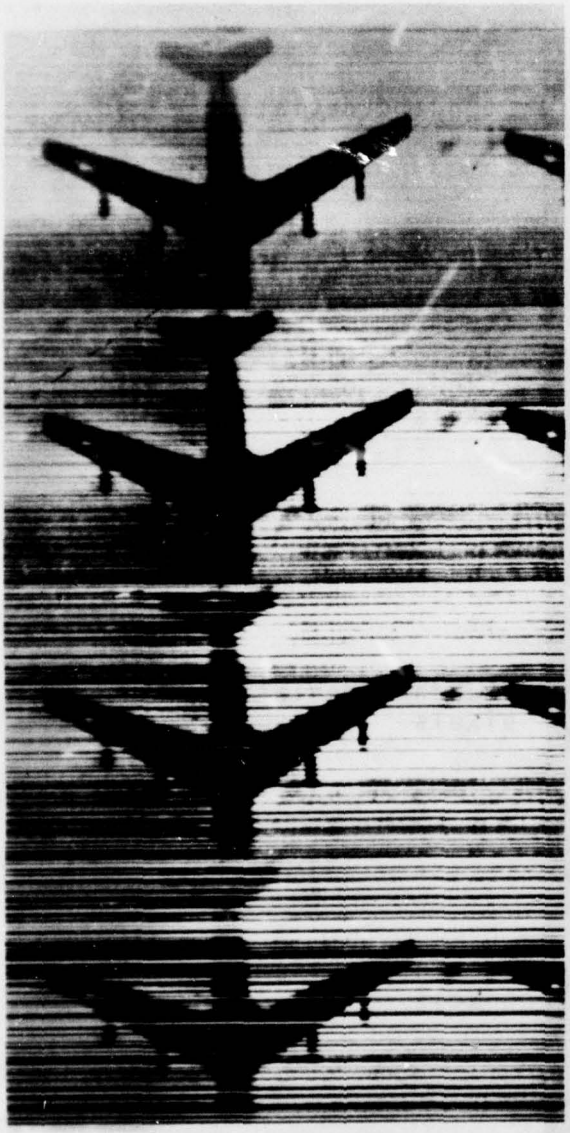
Standard deviation = .3%
of gray level range

Standard deviation = .6%
of gray level range

Standard deviation = 1.22%
of gray level range

Standard deviation = 2.44%
of gray level range

Figure 4-13. Additive Gaussian Line Noise Applied to an Infrared Image of Parked Aircraft



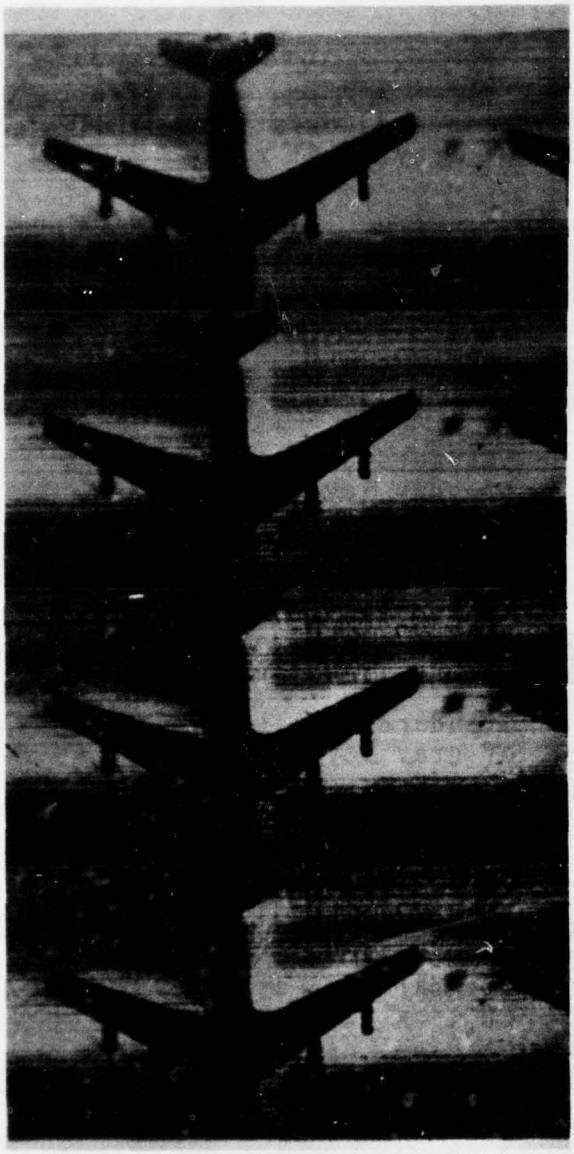
Standard deviation = 4.88%
of gray level range

Standard deviation = 9.77%
of gray level range

Standard deviation = 19.52%
of gray level range

Standard deviation = 39.04%
of gray level range

Figure 4-13 (Continued). Additive Gaussian Line Noise Applied to an Infrared Image of Parked Aircraft



Standard deviation = .05 pixels

Standard deviation = .1 pixels

Standard deviation = .2 pixels

Standard deviation = .39 pixels

Figure 4-14. Gaussian Line Jitter applied to an Infrared Image of Parked Aircraft



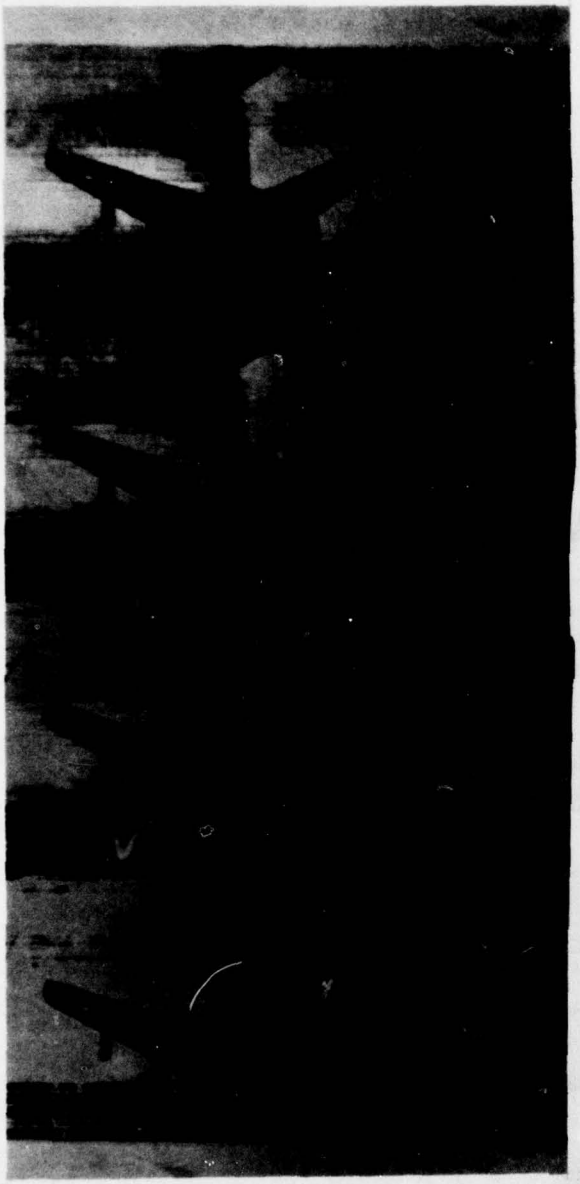
Standard deviation = .78 pixels

Standard deviation = 1.56 pixels

Standard deviation = 3.13 pixels

Standard deviation = 6.25 pixels

Figure 4-14 (Continued). Gaussian Line Jitter Applied to an Infrared Image of Parked Aircraft



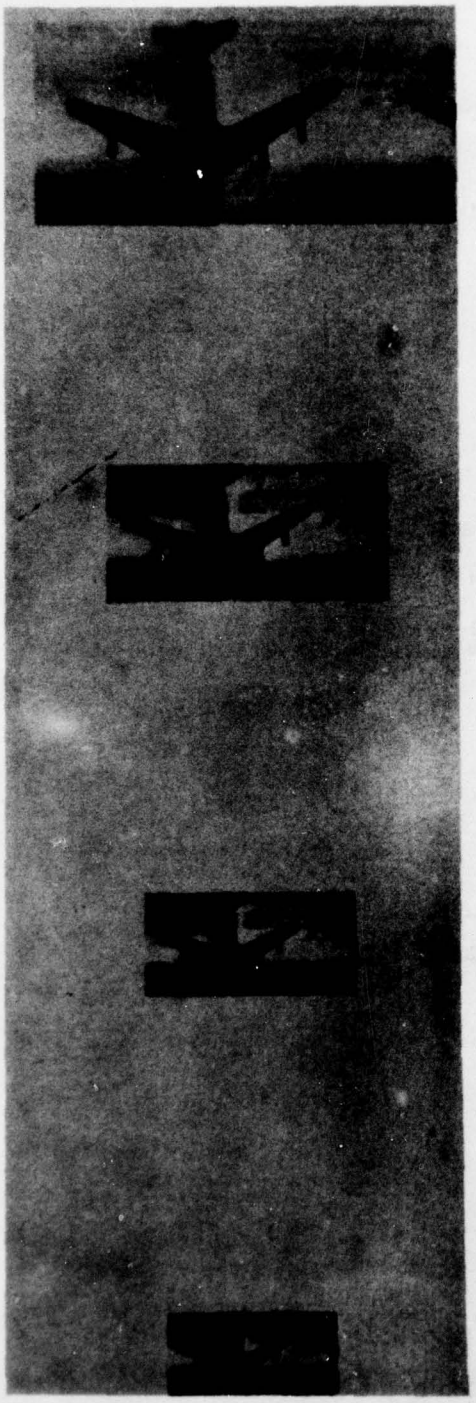
Number of gray levels = 32

Number of gray levels = 16

Number of gray levels = 8

Number of gray levels = 4

Figure 4-15. Varying the Quantization of an Infrared Image of Parked Aircraft



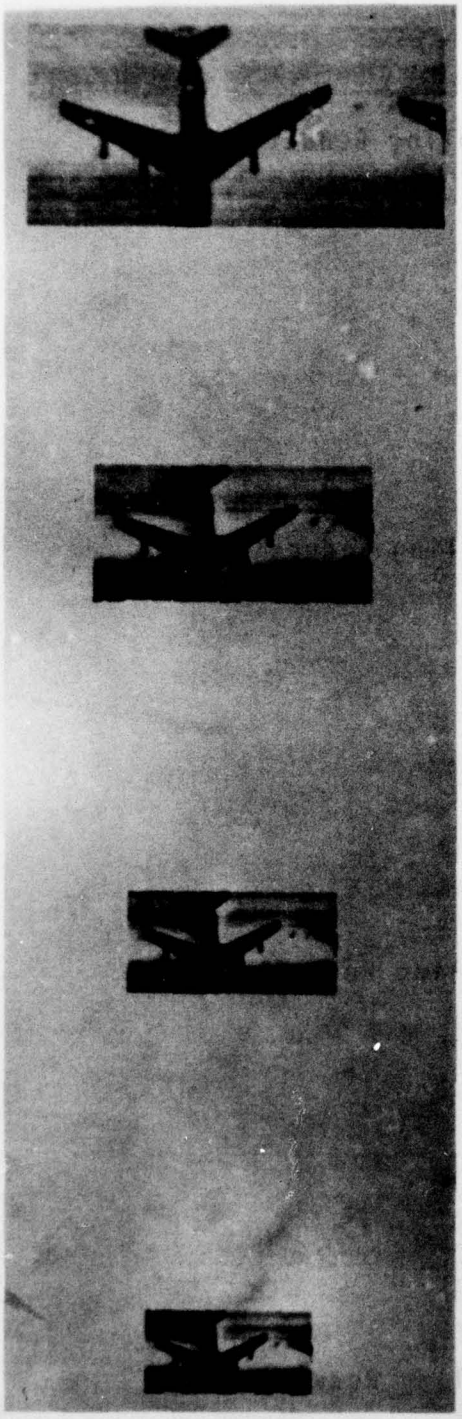
Sampling Reduction = 2

Sampling Reduction = 3

Sampling Reduction = 4

Sampling Reduction = 5

Figure 4-16. Varying the Sampling of an Infrared Image of Parked Aircraft Under High Aliasing



Sampling Reduction = 2

Sampling Reduction = 3

Sampling Reduction = 4

Sampling Reduction = 5

Figure 4-17. Varying the Sampling of an Infrared Image of Parked Aircraft Under Reduced Aliasing



Standard deviation = .3%
of gray level range

Standard deviation = .6%
of gray level range

Standard deviation = 1.22%
of gray level range

Standard deviation = 2.44%
of gray level range

Figure 4-18. Additive Gaussian Spot Noise Applied to a Synthetic Aperture Radar Image



Standard deviation = 4.88%
of gray level range

Standard deviation = 9.77%
of gray level range

Standard deviation = 19.52%
of gray level range

Standard deviation = 39.04%
of gray level range

Figure 4-18 (Continued). Additive Gaussian Spot Noise Applied to a Synthetic Aperture Radar Image



Standard deviation = .3%
of gray level range

Standard deviation = .6%
of gray level range

Standard deviation = 1.22%
of gray level range

Standard deviation = 2.44%
of gray level range

Figure 4-19. Additive Gaussian Line Noise Applied to a Synthetic Aperture Radar Image



Standard deviation = 4.88%
of gray level range

Standard deviation = 9.77%
of gray level range

Standard deviation = 19.52%
of gray level range

Standard deviation = 39.04%
of gray level range

Figure 4-19 (Continued). Additive Gaussian Line Noise Applied to a Synthetic Aperture Radar Image



Standard deviation = .05 pixels

Standard deviation = .1 pixels

Standard deviation = .2 pixels

Standard deviation = .39 pixels

Figure 4-20. Gaussian Line Jitter Applied to a Synthetic Aperture Radar Image



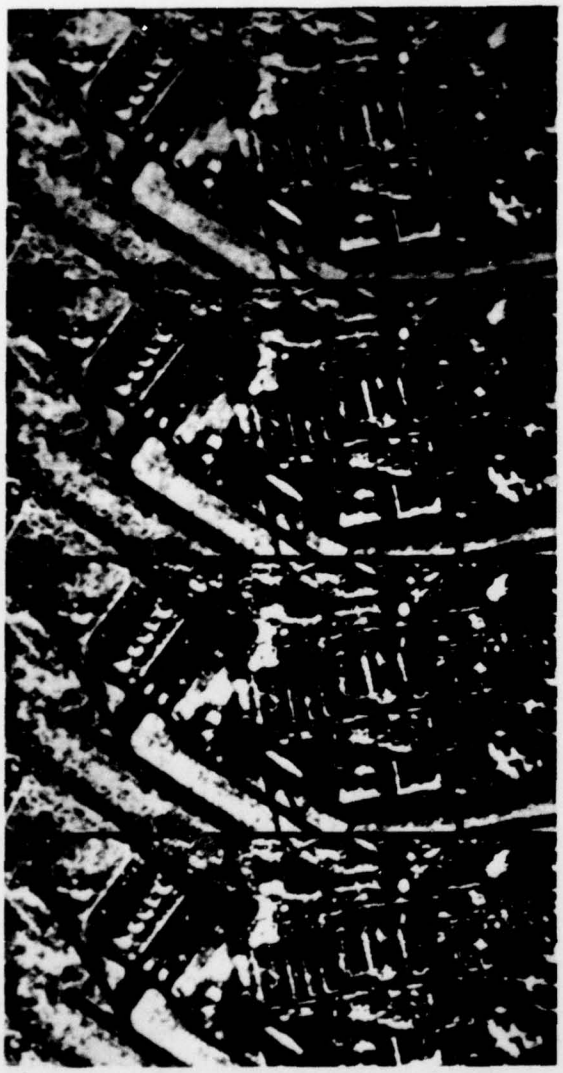
Standard deviation = .78 pixels

Standard deviation = 1.56 pixels

Standard deviation = 3.13 pixels

Standard deviation = 6.25 pixels

Figure 4-20 (Continued). Gaussian Line Jitter Applied to a Synthetic Aperture Radar Image



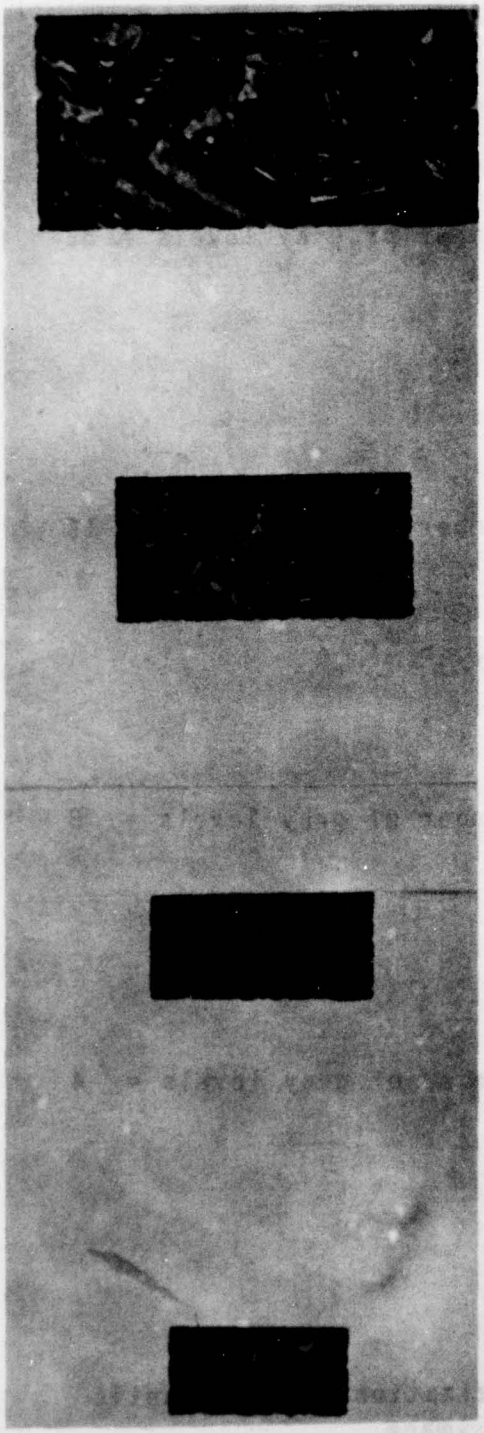
Number of gray levels = 32

Number of gray levels = 16

Number of gray levels = 8

Number of gray levels = 4

Figure 4-21. Varying the Quantization of a Synthetic Aperture Radar Image



Sampling Reduction = 2

Sampling Reduction = 3

Sampling Reduction = 4

Sampling Reduction = 5

Figure 4-22. Varying the Sampling of a Synthetic Aperture Radar Image Under High Aliasing

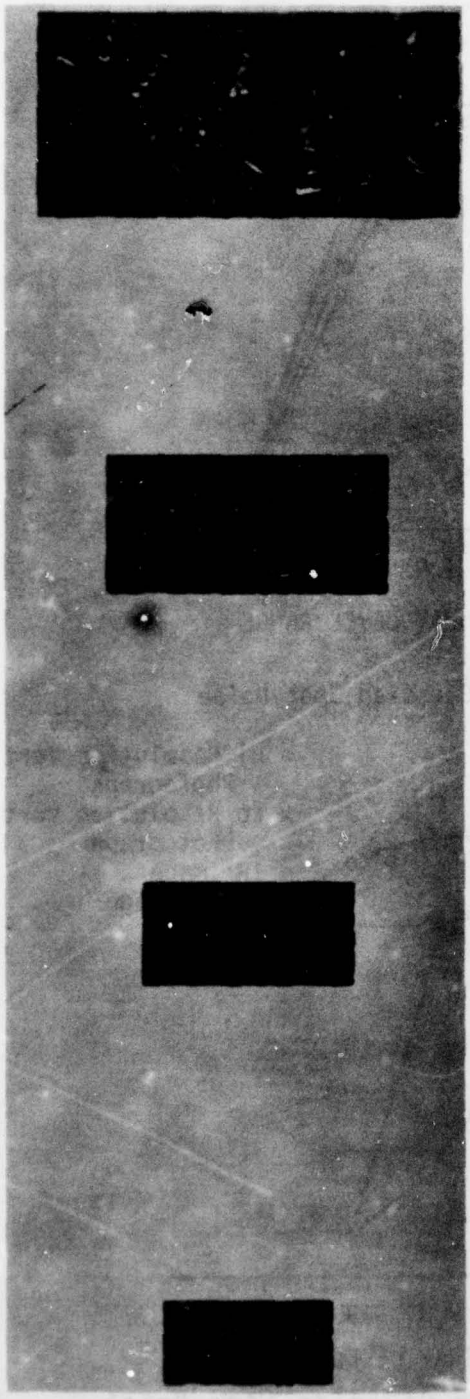


Figure 4-23. Varying the Sampling of a Synthetic Aperture Radar Image Under Reduced Aliasing

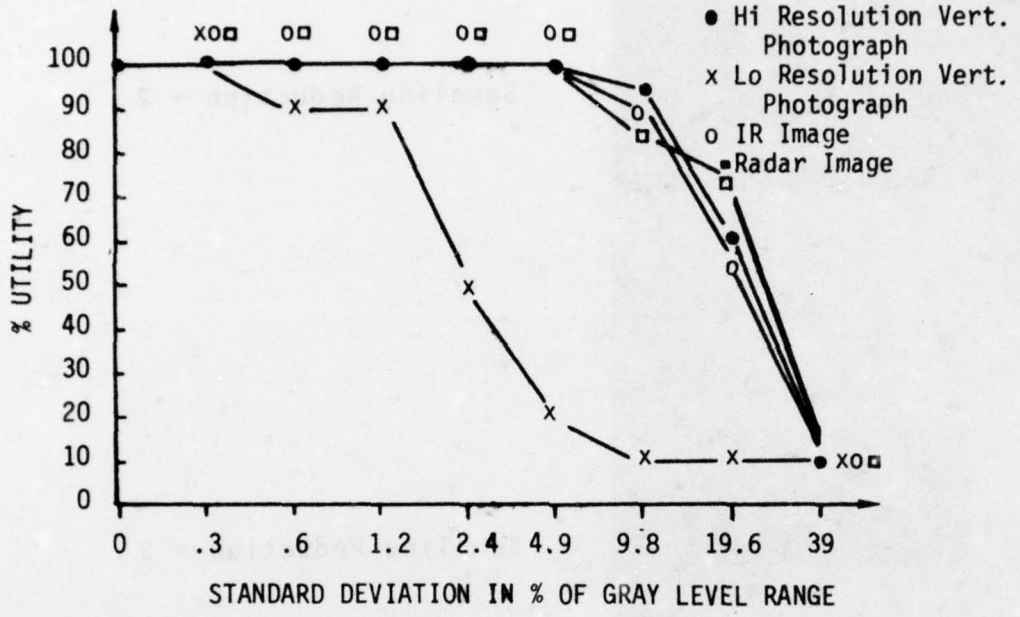


Figure 4-24. Effect of Additive Gaussian Spot Noise

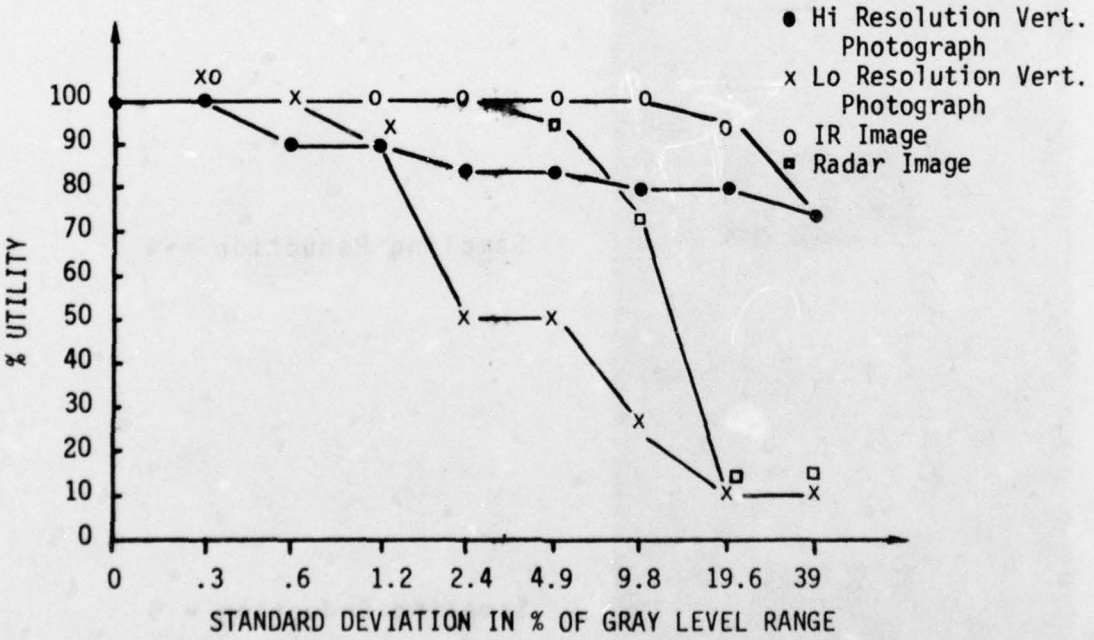


Figure 4-25. Effect of Additive Gaussian Line Noise

NOTE: the units of standard deviations correspond to the actual values chosen for the tests and provide an approximate logrithmic scale.

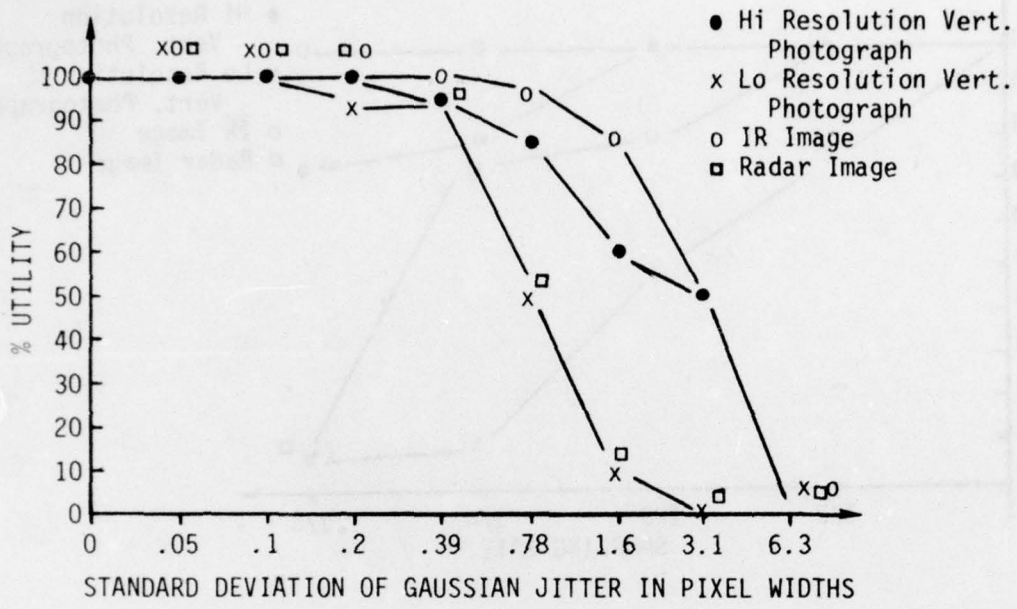


Figure 4-26. Effects of Jitter

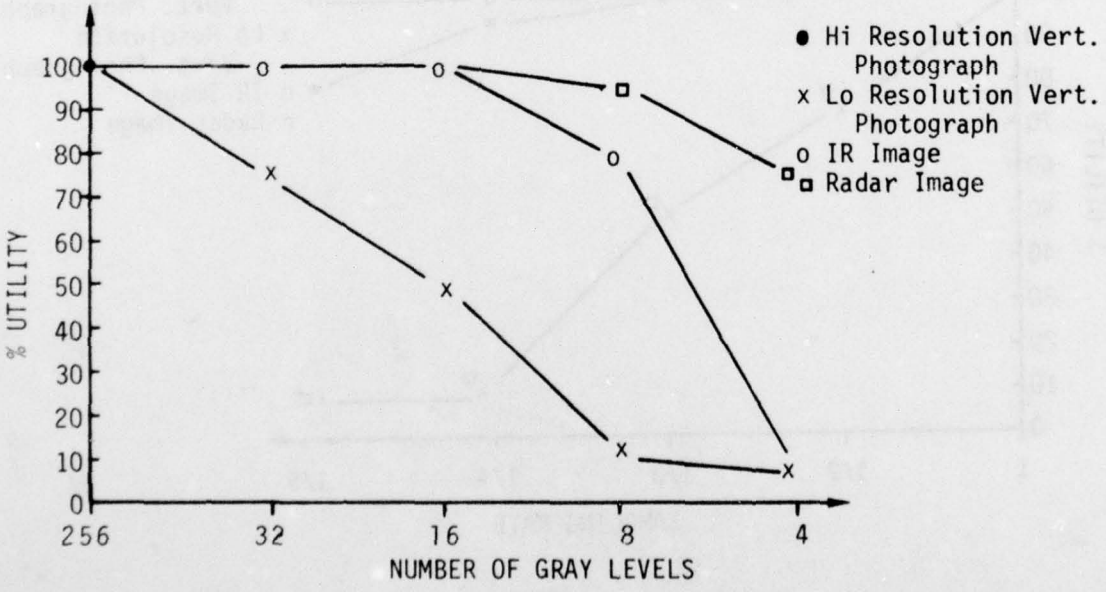


Figure 4-27. Effects of Number Gray Levels

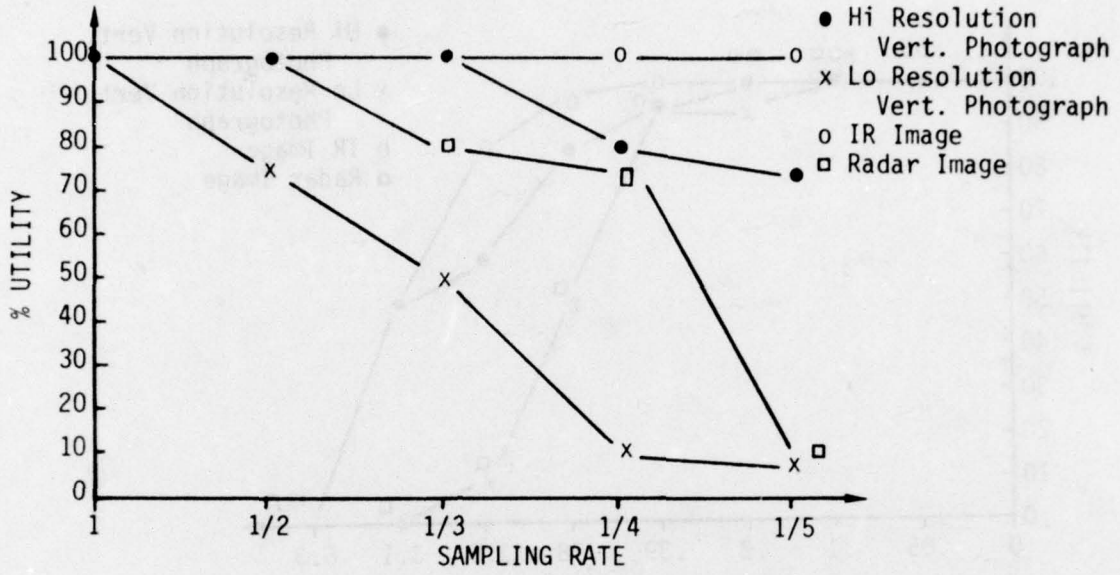


Figure 4-28. Effect of Sampling Rate, High Aliasing

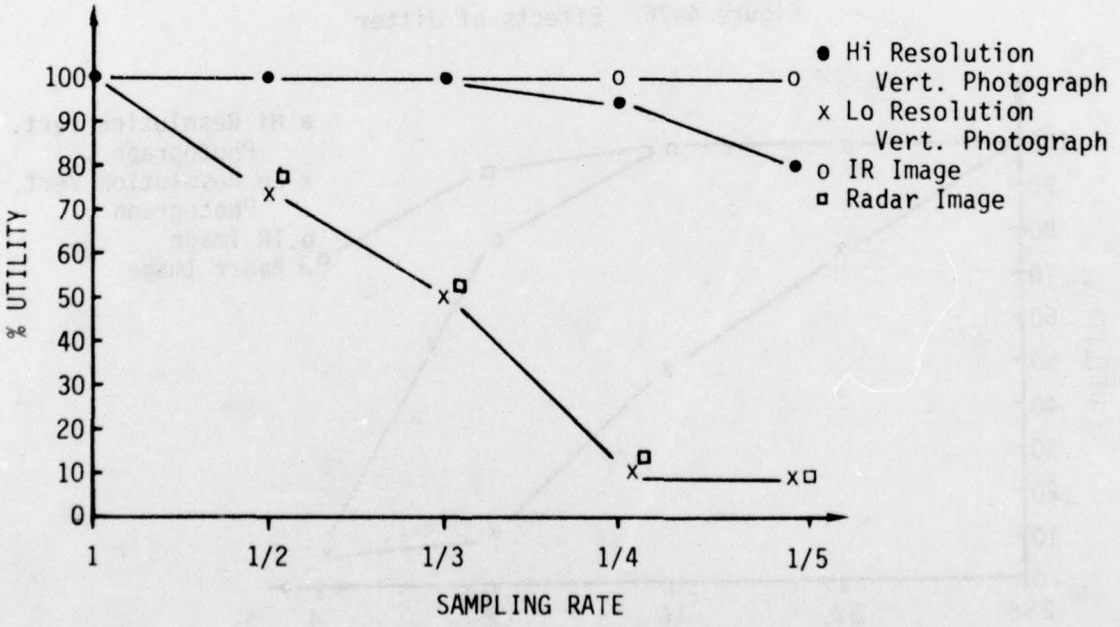


Figure 4-29. Effect of Sampling Rate, Low Aliasing

NOTE: The Photointerpreter was allowed use of a magnifying glass to compensate for the change in scale in these sampling rate tests.

TABLE 3. IMAGE EVALUATION FACTORS

1. Shape - Shape relates to the general configuration of an object depicted on the image scene. Although the shape of an object as seen from above is sometimes difficult to interpret, it often provides the most important clue to identification. Shape is often distorted on radar and infrared imagery because of such factors as spot size, pulse length, beamwidth and fold-over (radar), and temperature, spot size, and field of view (infrared). The aircraft attitude may introduce errors by pitch, roll, yaw, and improper altitude and velocity. These errors are common on all three general imagery types (photo, infrared, and radar). Distortions on the image scene may also be caused by digitizing the original data. When evaluating an image scene, the interpreter must consider shape distortion.

2. Size - Size relates to the dimensions, surface, and volume of an object depicted on the image scene. The size of one object can often be determined from its relative size to other objects. Where accurate dimensions are required, the scale of the digitized image must be calculated. The closeness of the object size on the digitized image to the actual object size will be the second factor considered when ranking an image scene by quality.

3. Surroundings - Surroundings refer to the spatial arrangement of objects and their relationship to natural objects (background). For example, a thermal electric power plant will have various target components (objects) surrounding it (such as a transformer yard, fuel supply, power line cuts) which will enable the interpreter to correctly identify the target by its surroundings. The location of the target also falls into the category of surroundings. When an image is degraded, certain of the target surroundings may not be identifiable. This will be the third criterion used when ranking an image scene. This category can also be referred to as the "minimum image concept" or "target skeleton concept." Here the interpreter must decide the minimum number of objects (target and surroundings) that must be identifiable to correctly determine the type of target present on the image scene.

TABLE 3. IMAGE EVALUATION FACTORS
(Continued)

4. Shade - Shade or tone refers to the brilliance with which light is reflected by an object. Without tone differences the shapes of objects could not be discerned on imagery. The overall image shade/tone quality will be determined during this fourth step of the evaluation.

5. Shadow - Shadow describes the condition wherein an intervening object prevents the direct sun rays from striking certain areas on the imagery. Shadows are important because their shapes are indicative of the profile views of objects, and can facilitate recognition, as in the case of a church steeple with the cross on the top, or a tall tower.

images, Figures 2-6 through 2-8, could be found with the curves of performance against degradation. This is thought to be due to the fact that the photointerpreter tends to concentrate on targets while the spectrum data is composed largely of background data.

Figures 4-30 through 4-33 show comparisons of subjective image utility as a function of display type. The results indicate, as expected, that hardcopy and softcopy utility is roughly comparable when the same image detail degradation and extent are shown on both outputs. There appears to be a slight bias toward preference of softcopy over hardcopy products. This bias may be a function of the testing procedure although the softcopy evaluations were held more than 30 days after the hardcopy evaluations due to the nonavailability of a softcopy display at Harris ESD during this time frame. The apparent preference of softcopy over hardcopy is probably due to the fact that both the softcopy and hardcopy curves for no noise start at 100% utility. This is probably not true: the basic utility of the noiseless hardcopy is probably better than the basic utility of the noiseless softcopy. Furthermore, as noise is introduced, the softcopy would be affected less than the hardcopy because the softcopy originally had more noise in the form of scan lines, phosphor noise on the screen, etc.

Other tests were held to indicate the repeatability and transitiveness (see Section II-G) of the photointerpreter's utility assessment. The repeatability was on the order of 80-90%. The utility assessment did seem to be transitive, thus the subjective utility assessment is an equivalence relation. As a result, it appears reasonable to talk of equal quality of two or more images even though they have been degraded by quite different mechanisms.

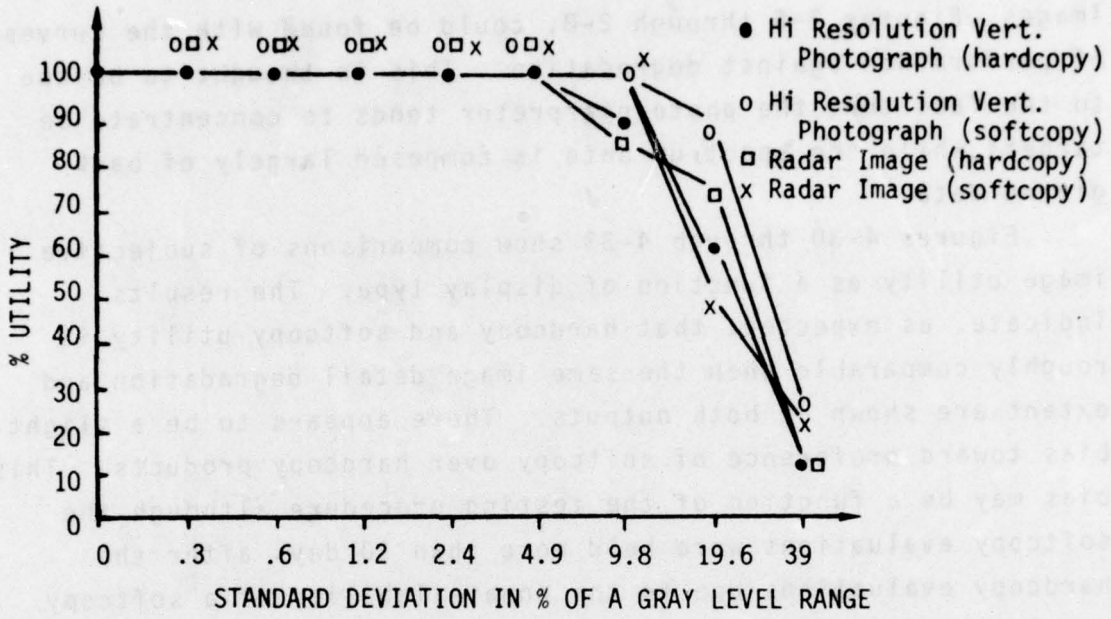


Figure 4-30 . Effect of Additive Gaussian Spot Noise (Hardcopy vs. Softcopy)

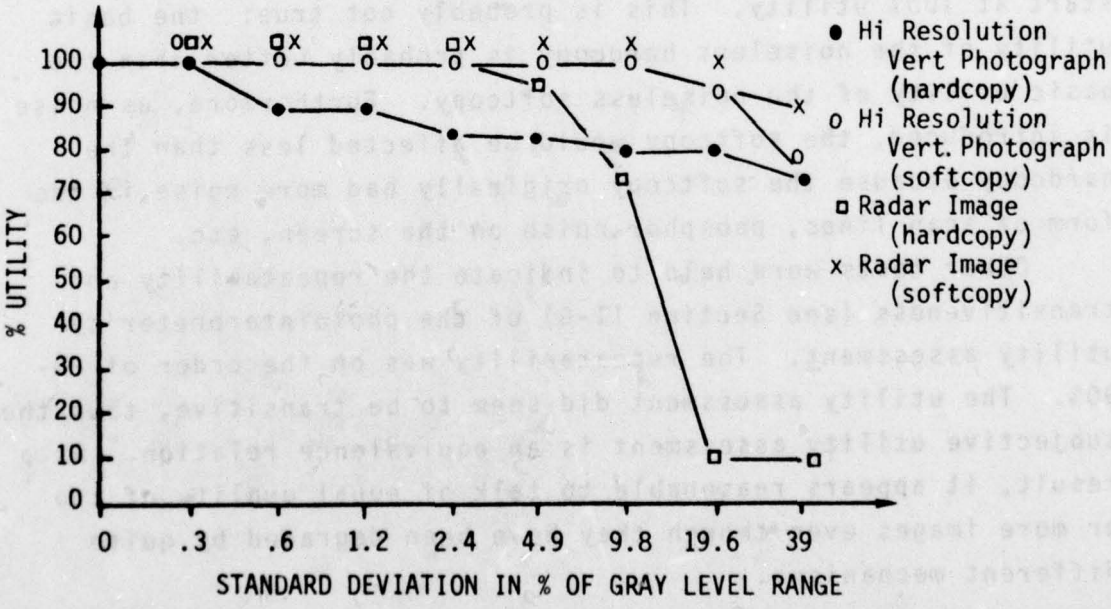


Figure 4-31. Effect of Additive Gaussian Line Noise (Hardcopy vs. Softcopy)

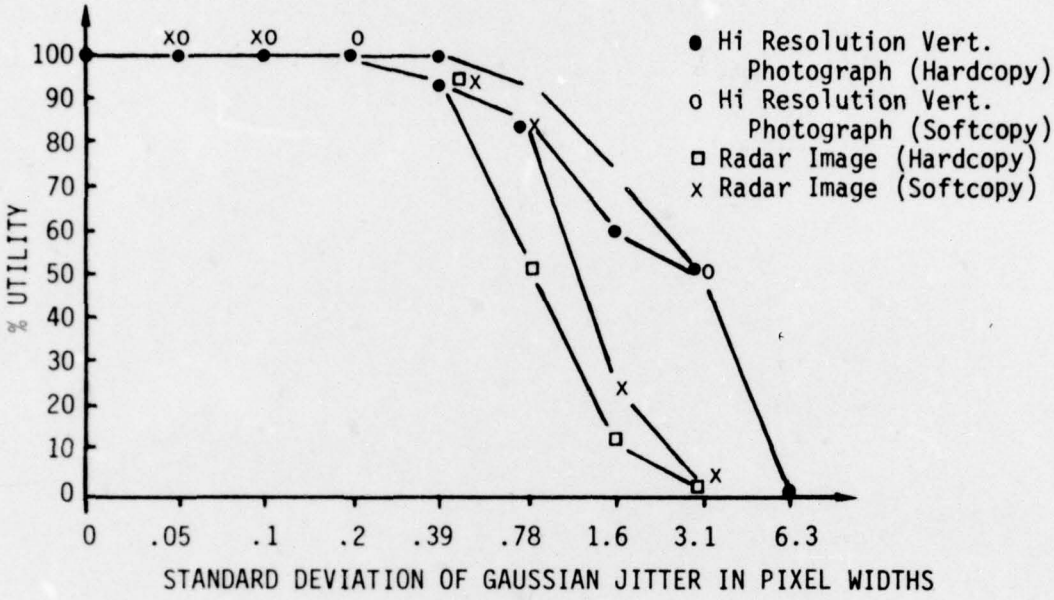


Figure 4-32. Effects of Jitter
(Hardcopy vs. Softcopy)

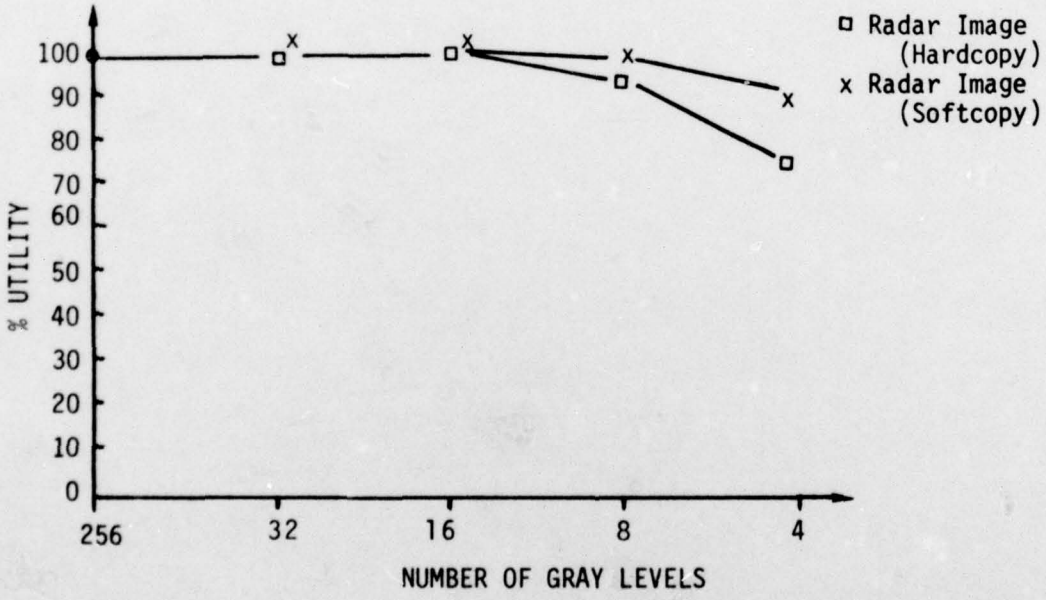


Figure 4-33. Effects of Number Gray Levels
(Hardcopy vs. Softcopy)

SECTION V

POSSIBLE DIGITAL IMAGE SYSTEM OBJECTIVE TEST PATTERNS

A set of test patterns will now be given which can be used to measure the various types of system degradations. Four basic types of image quality degradations of the imagery processing subsystem are proposed as criteria for the Test Set: (a) amplitude distortion, i.e., incorrectly representing the gray shade at a particular point in the image, (b) the system induced modulation transfer function (MTF), (c) geometric distortion, i.e., the "warping" of the output scene due to system geometric non-linearities, and (d) noise, which includes channel noise (bit errors), quantization noise, aliasing noise, etc.

This section provides simple visual methods of measuring the first three types of image degradations mentioned above.

A. MEASUREMENT OF SAMPLING RATE

The sampling rates of a digital imagery system can easily be measured through use of Moire' patterns. The following basis for a test procedure to determine the reproduction sampling rate is illustrative:

(1) Scan or reproduce a test image, Figure 5-1, consisting of vertical lines, with a density comparable to the scan density to be measured, and obtain a reproduced output.

(2) Lay the comparative test image consisting of radial lines emerging from the center, Figure 5-2, over the reproduced test image obtained from the above step.

Pattern frequency
1/2 sampling frequency

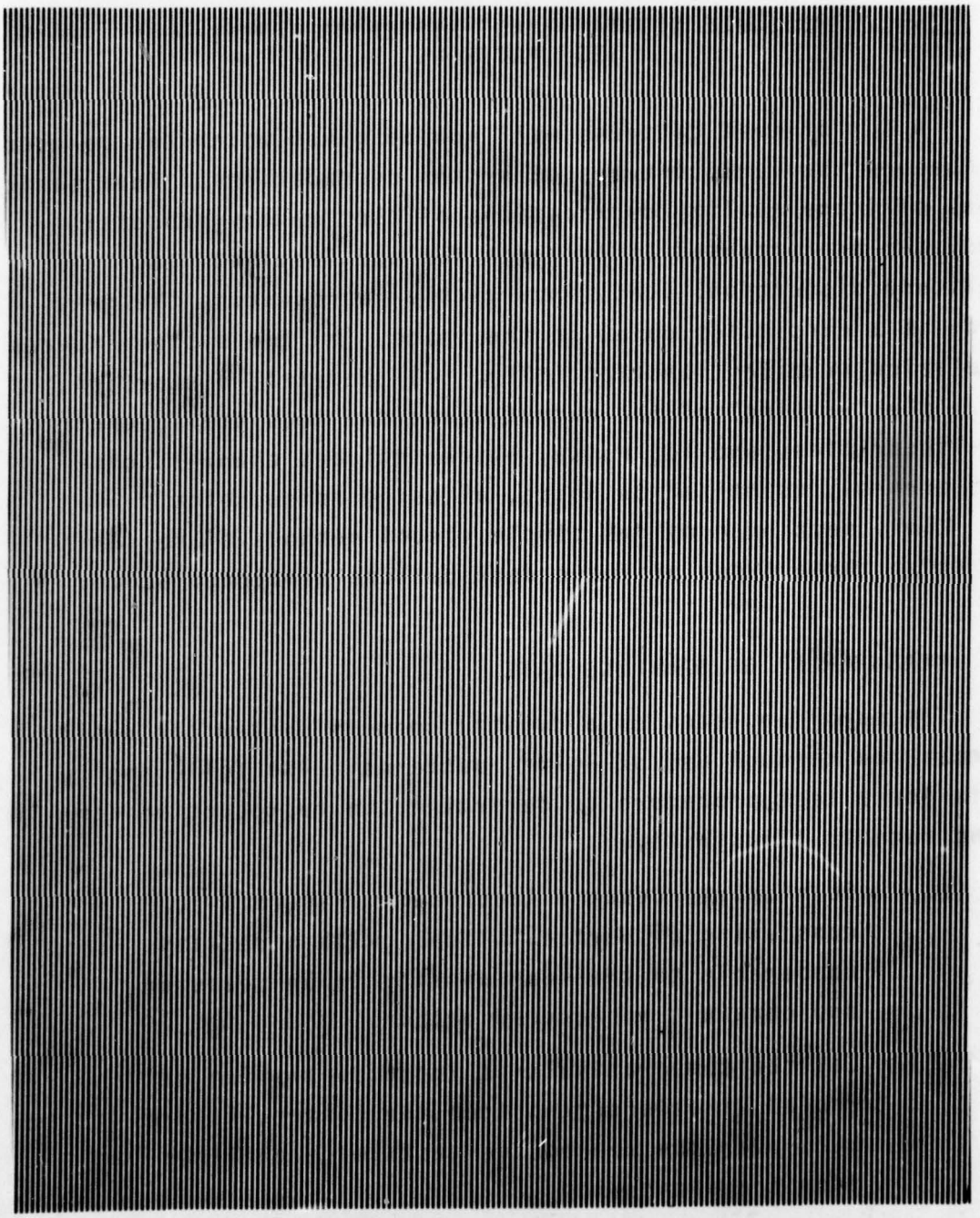


Figure 5-1. Input Sampling Rate Test Pattern

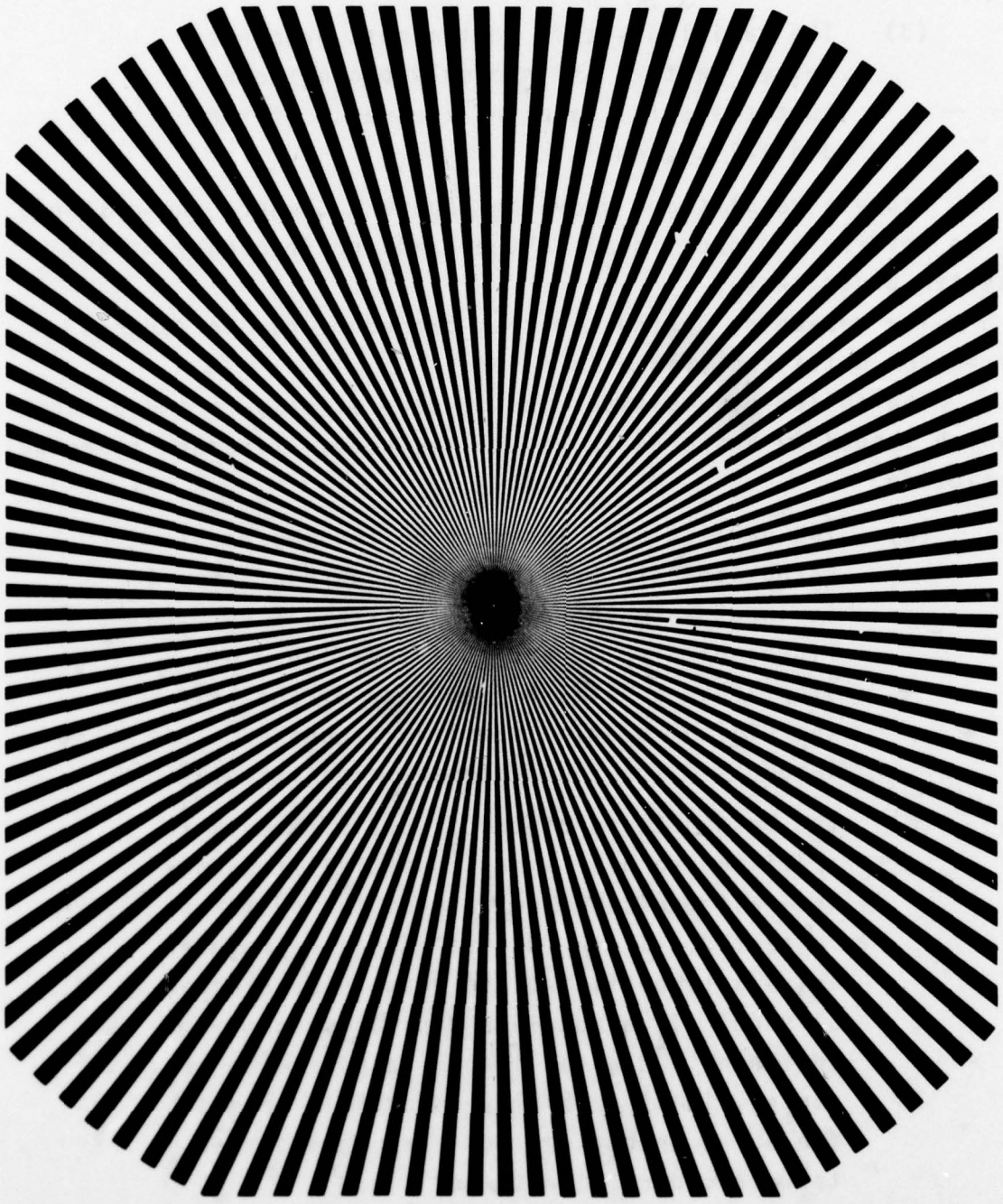


Figure 5-2. Comparative Sampling Rate

(3) The radial distance to the most prominent Moire' pattern is inversely proportional to the spatial sampling frequency of the digital system.

Example results are shown in Figure 5-3 where the distance c is inversely proportional to the sampling frequency of the system under test.

The reasoning behind the test procedure can be deduced from the details provided in Appendix C.

The following questions and considerations are among those which should be answered to reduce the above procedure to actual practice.

(a) Two particularly interesting and important things to note are that the figure of Step 1 is input into the digital system and not the figure of Step 2, and that the figure of Step 1 has a pattern frequency of one-half the digital spatial sampling frequency. See Appendix C for the necessary expanation.

(b) The test pattern of the figure of Step 1 is specified to have a basic spatial frequency one-half the sampling rate of the system to be tested. If the digital image reproducer only is to be tested, how can this be accomplished? If a complete digital system including a digital image scanner is to be tested, it is generally impossible to meet the above specification. How should the test procedure be altered?

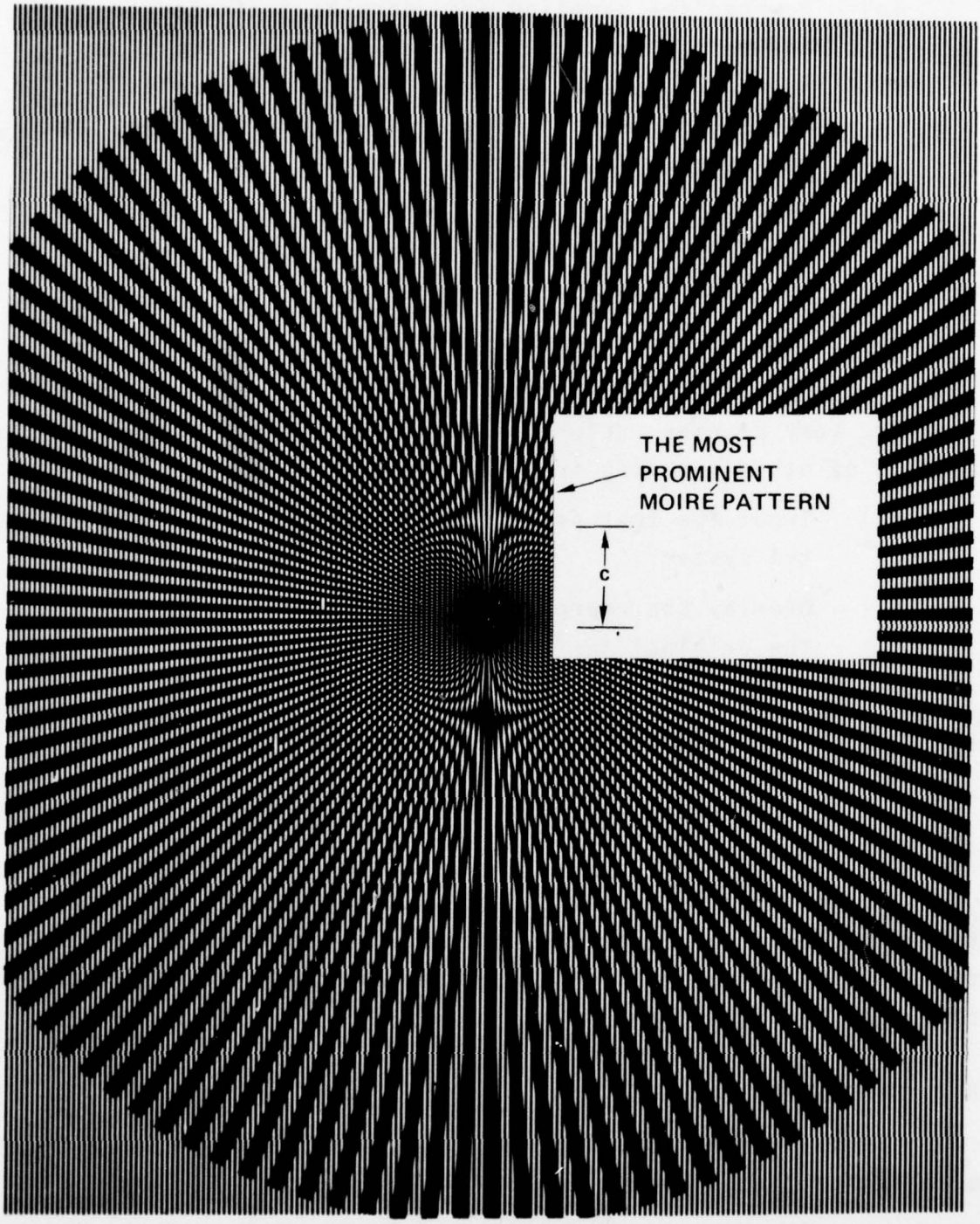


Figure 5-3. Example Results of Sampling Rate Test

(c) How can the sampling frequency be indicated on the comparison image of the figure of Step 2? A partial answer is to use concentric circles indicating the spatial frequency corresponding to the most significant Moire' pattern.

(d) Since the sampling can occur along more than one spatial axis simultaneously, how does the technique given above apply?

(e) How can the above procedure be altered to determine the scanner sampling rate?

Another, very precise, determination of the spatial sampling rate in lieu of other sampling irregularities follows:

(1) Input the test pattern of Figure 5-1 into the system.

(2) Overlay the reproduced test pattern with the original test pattern canted at a slight angle.

(3) The spacing between the Moire' patterns seen is proportional to the spatial reproduction rate of the system under test.

An illustrative example of the Moire' patterns to be obtained is shown in Figures 5-4 and 5-5. The slight bending of the patterns is a result of slight variations in the reproduction rate across the image.

B. MEASUREMENT OF MTF

MTF is a powerful and increasingly used guide to image quality for the following reasons:

- The MTF of multiply cascaded imagery system components can be easily combined into a system MTF.

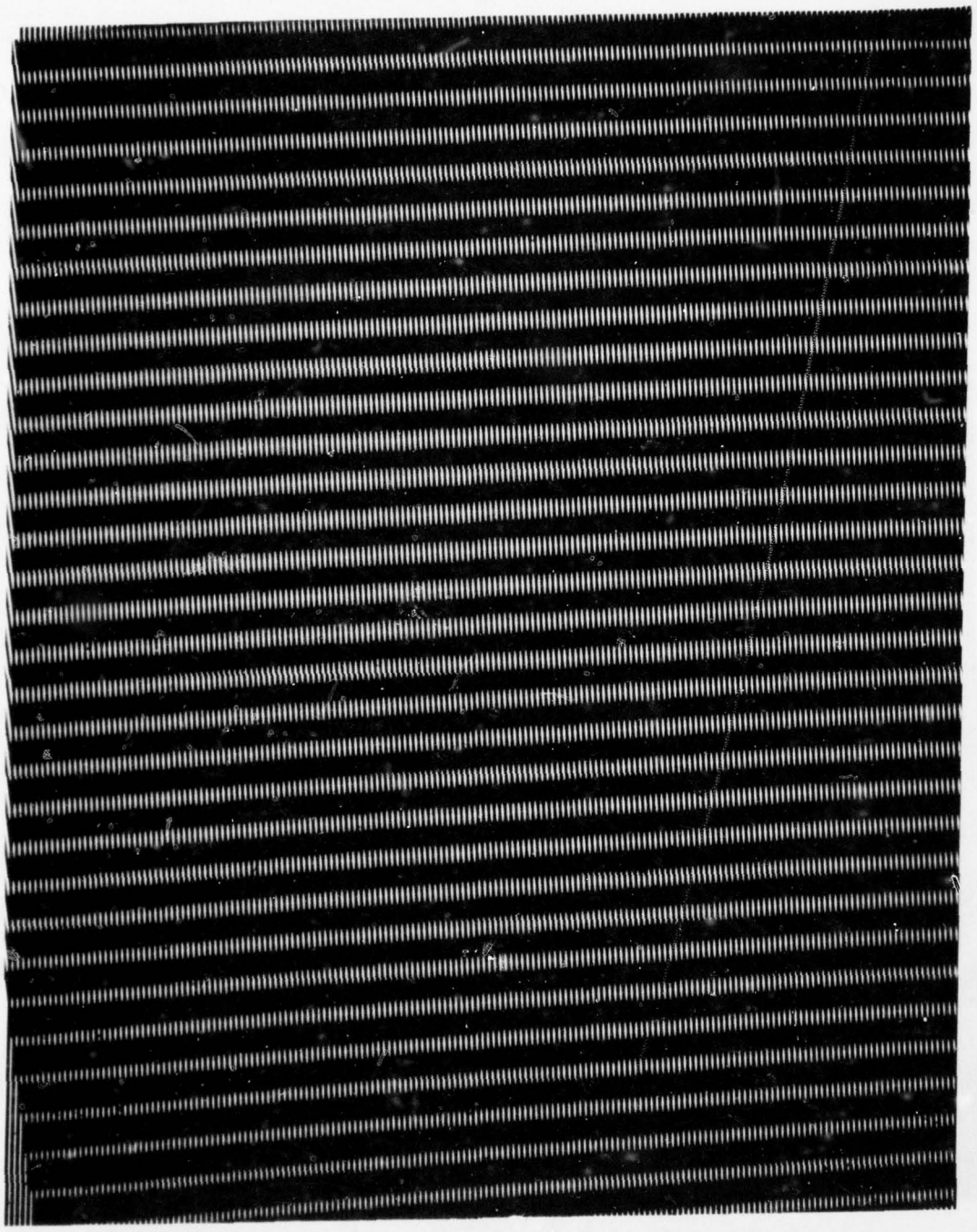


Figure 5-4. Determination of Spatial Sampling Reproduction Rate

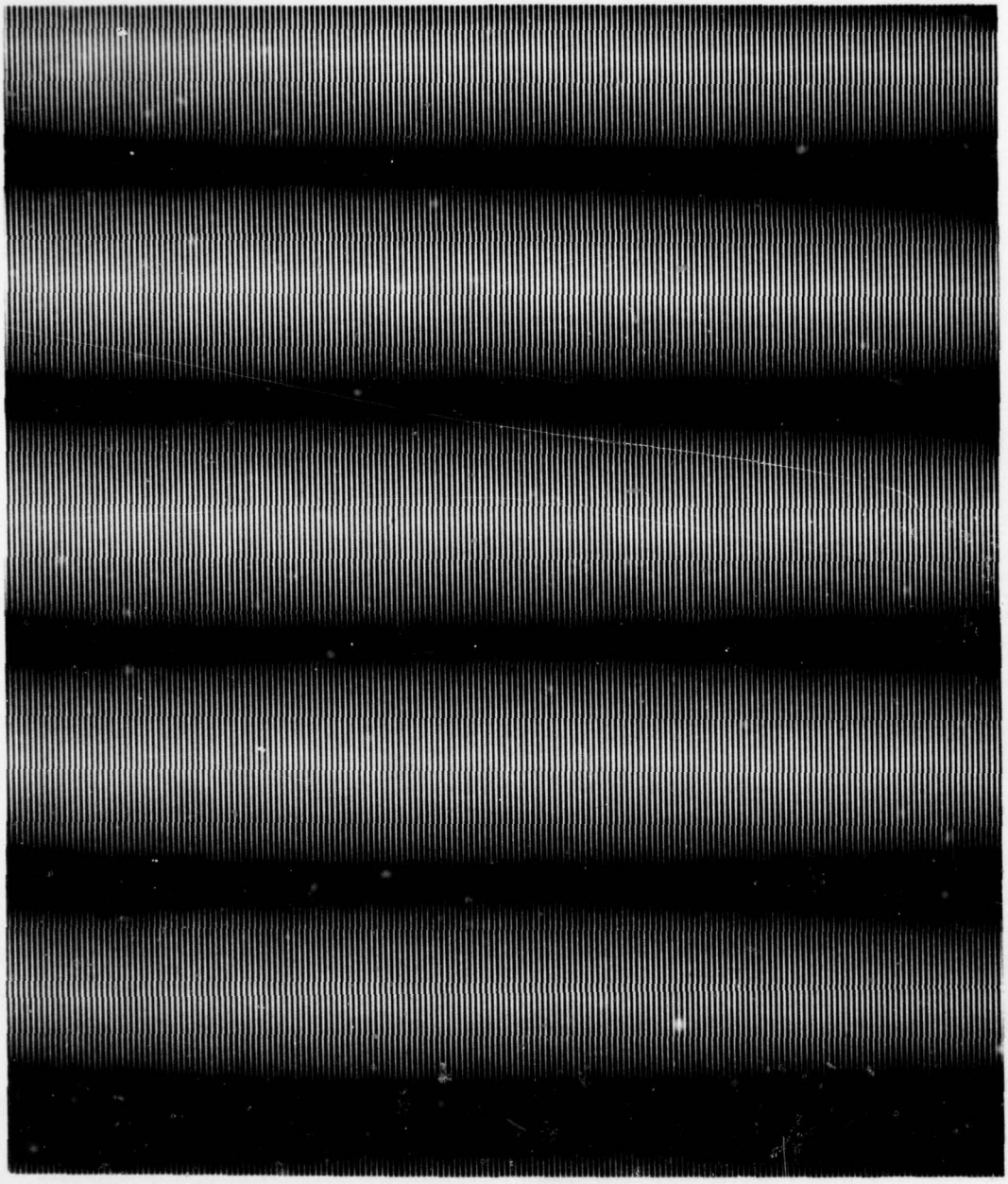


Figure 5-5. Precise Determination of Spatial Sampling Reproduction Rate

- The MTF can be converted into the "noise-equivalent passband" of the system, a parameter of particular interest in analysis of communications systems.
- The MTF is a guide to the capability of the system to image various sized imagery detail.

Considered here is a technique by which the system MTF can be measured. The technique is based upon a chirped spatial frequency procedure:

(1) Input a test image containing the luminance function given by

$$I(x,y) = 1 + y \sin x^2 \qquad (1)$$

where the coordinate system is so chosen that x corresponds with the horizontal frequency axis and y the vertical contrast axis.

(2) Take the resulting reproduced test image (an example is shown in Figure 5-6) and lay it down beside the original test image.

(3) Back up from both test images until it becomes possible to draw a curve in each separating the regions containing perceptual sine waves from those not perceptual. Call the curves a(x) and b(x) as shown in Figure 5-7.

(4) Derive the system MTF by plotting

$$MTF(x) = \frac{a(x)}{b(x)}$$

with results as shown in Figure 5-8.

The reasoning behind the procedure follows in Appendix E.

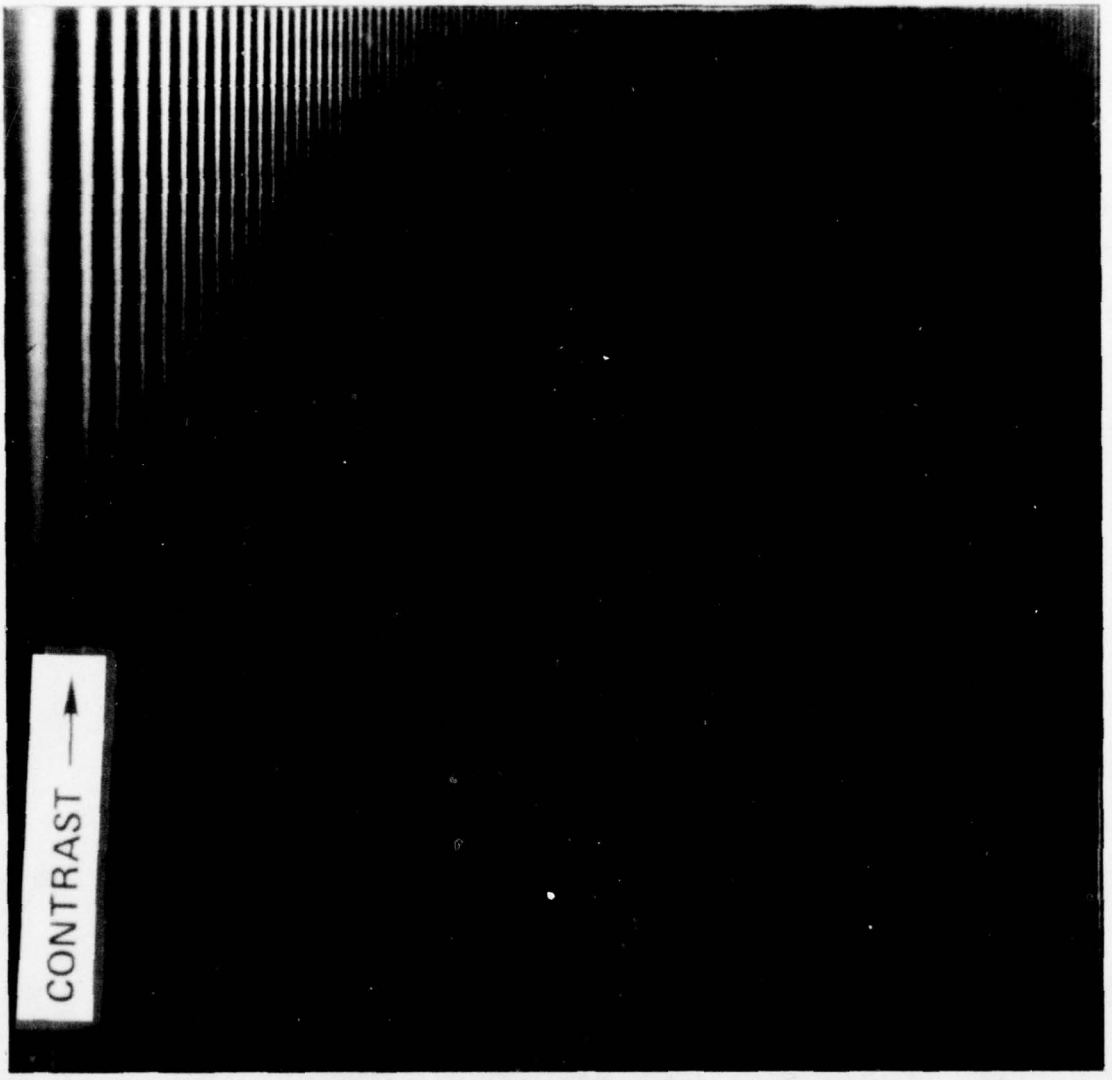


Figure 5-6. A Reproduced Chirped Test Image

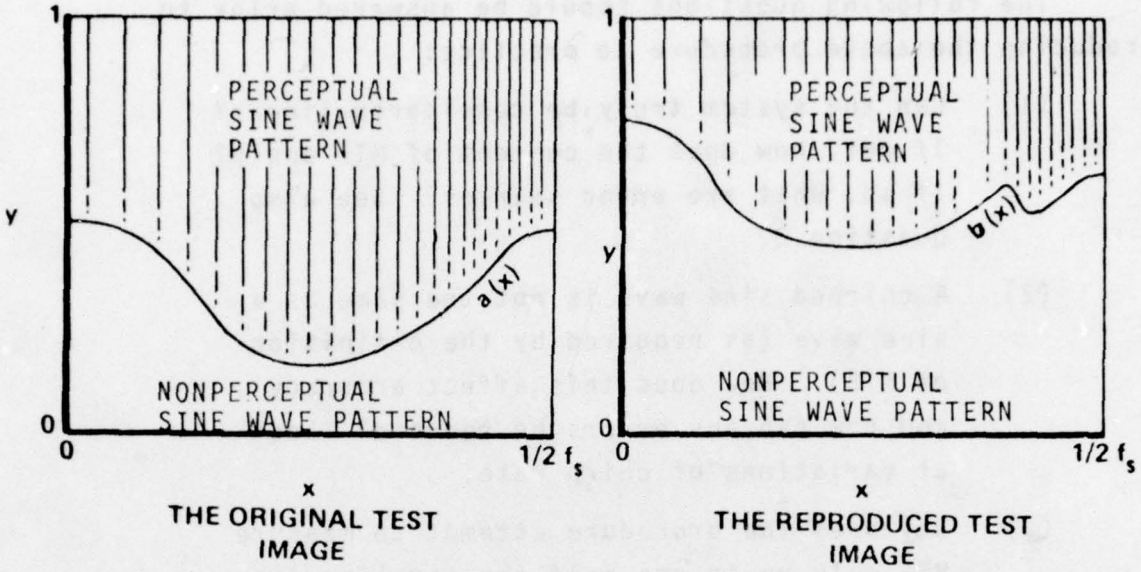


Figure 5-7. Comparison of Chirped Spatial Frequency Test Charts

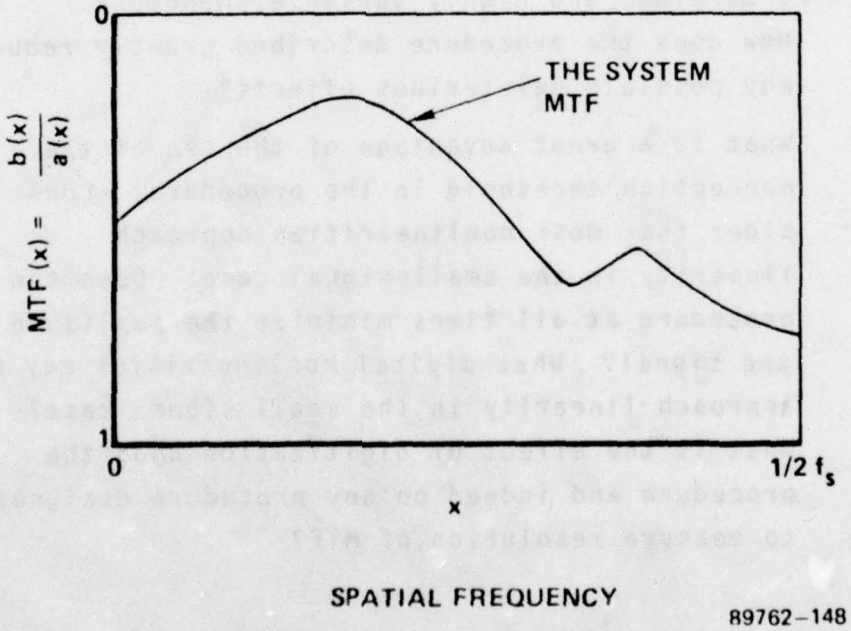


Figure 5-8. Example Derivations of MTF from the Chirped Spatial Frequency Test

The following questions should be answered prior to reducing the above procedure to practice:

(1) Can the system truly be considered linear? If not, how does the concept of MTF apply? If so, what are error sources? See also Question 2.

(2) A chirped sine wave is not the same as a sine wave (as required by the definition of MTF). How does this affect accuracy and how can any errors be reduced? Look at variations of chirp rate!

(3) Why does the procedure attempt to measure MTF only up to one half the sampling frequency of the system under test.

(4) Use of the perception threshold characteristics of the eye could be faulted as relying on a marginal and highly variable phenomena. How does the procedure described greatly reduce any possible deleterious effects?

(5) What is a great advantage of the use of the perception threshold in the procedure? Consider that most nonlinearities approach linearity in the small signal case! Does the procedure at all times minimize the amplitude of the signal? What digital nonlinearities may not approach linearity in the small signal case? What is the effect of digitization upon the procedure and indeed on any procedure designed to measure resolution of MTF?

(6) How could the division indicated in Step 5 be simplified to a manual rather than mental exercise? Consider a test signal in Equation (1)

$$I(x,y) = 1 + \log(y) \sin(x)^2$$

C. MEASUREMENT OF SAMPLING INHOMOGENEITIES

A common problem in digital sampling is the fact that the sampling rate often varies across the image with attendant effects. These inhomogeneities can easily be measured, in lieu of other sampling degradations, by the following procedure:

(1) Scan or reproduce the test image, Figure 5-9, consisting of horizontal lines and obtain a reproduced test image.

(2) Lay a slightly enlarged transparent copy of the test image, of Step 1, over the reproduced test image obtained above, canted at a slight angle.

(3) The Moire' pattern observed is a good approximation to the curve of the inhomogeneity of the scan rate.

As an example of the above procedure let Figure 5-10 be the reproduced image. Note that it has a scan nonhomogeneity which while present is difficult to fully quantify. Laying a slightly enlarged canted copy of the figure from Step 1 over Figure 5-10 gives the Figure 5-11.

Since the theory behind the appearance of this particular Moire' pattern is especially intriguing, it is further considered in Appendix D. It becomes apparent there, for instance, that theoretically (and in practice to a large degree) any degree of magnification of scanning inhomogeneities is possible.

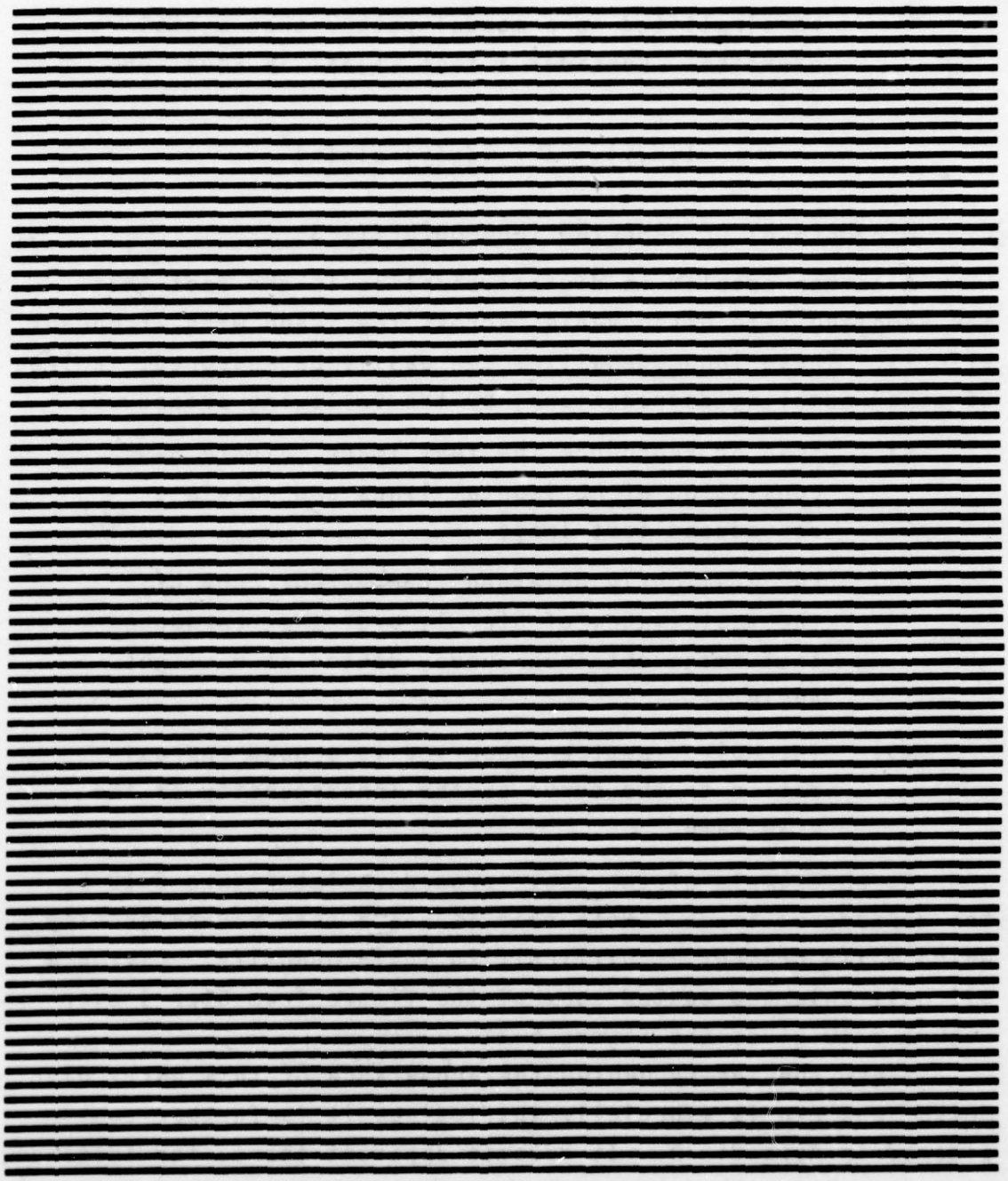


Figure 5-9. A Test Image for Scan Reproduction

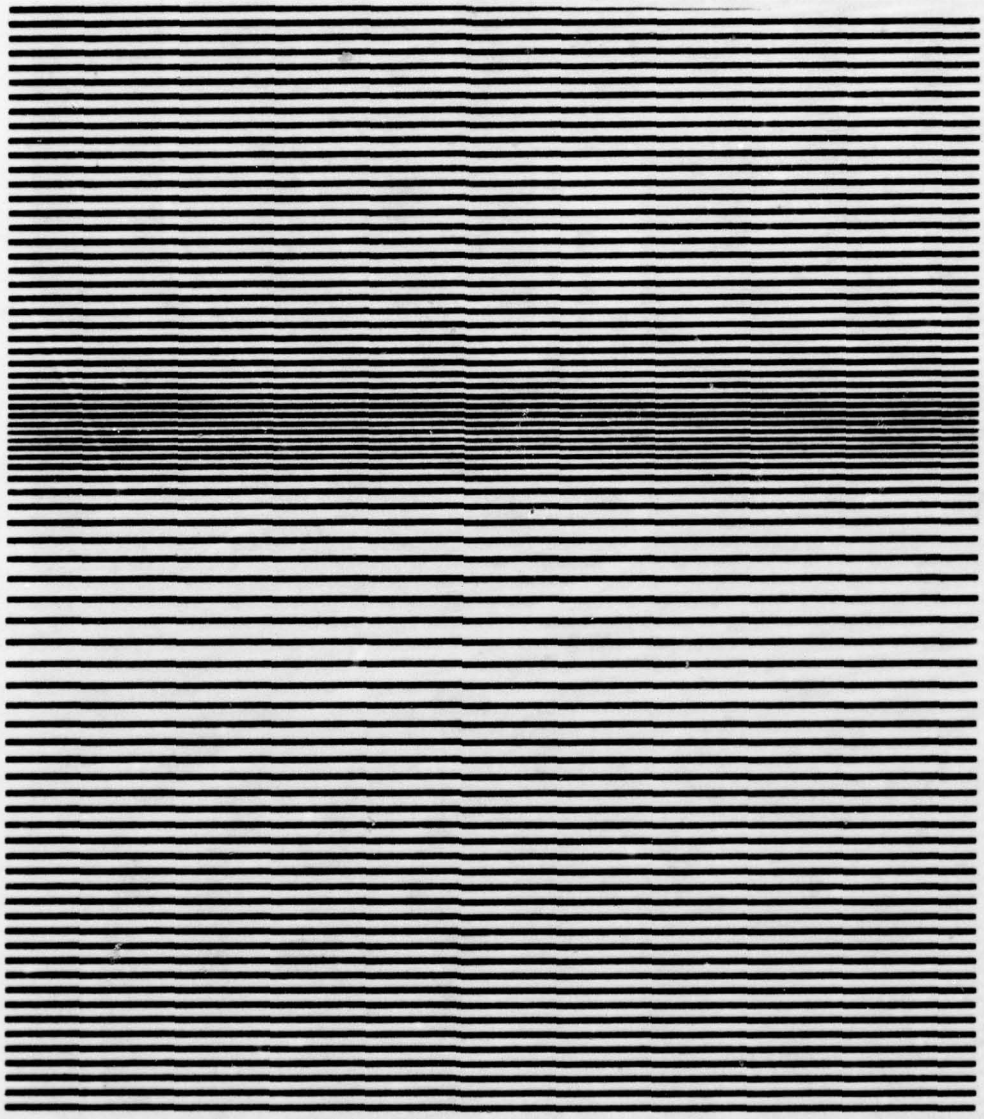


Figure 5-10. The Reproduced Version of Figure 5-9 With Scan Nonhomogeneity

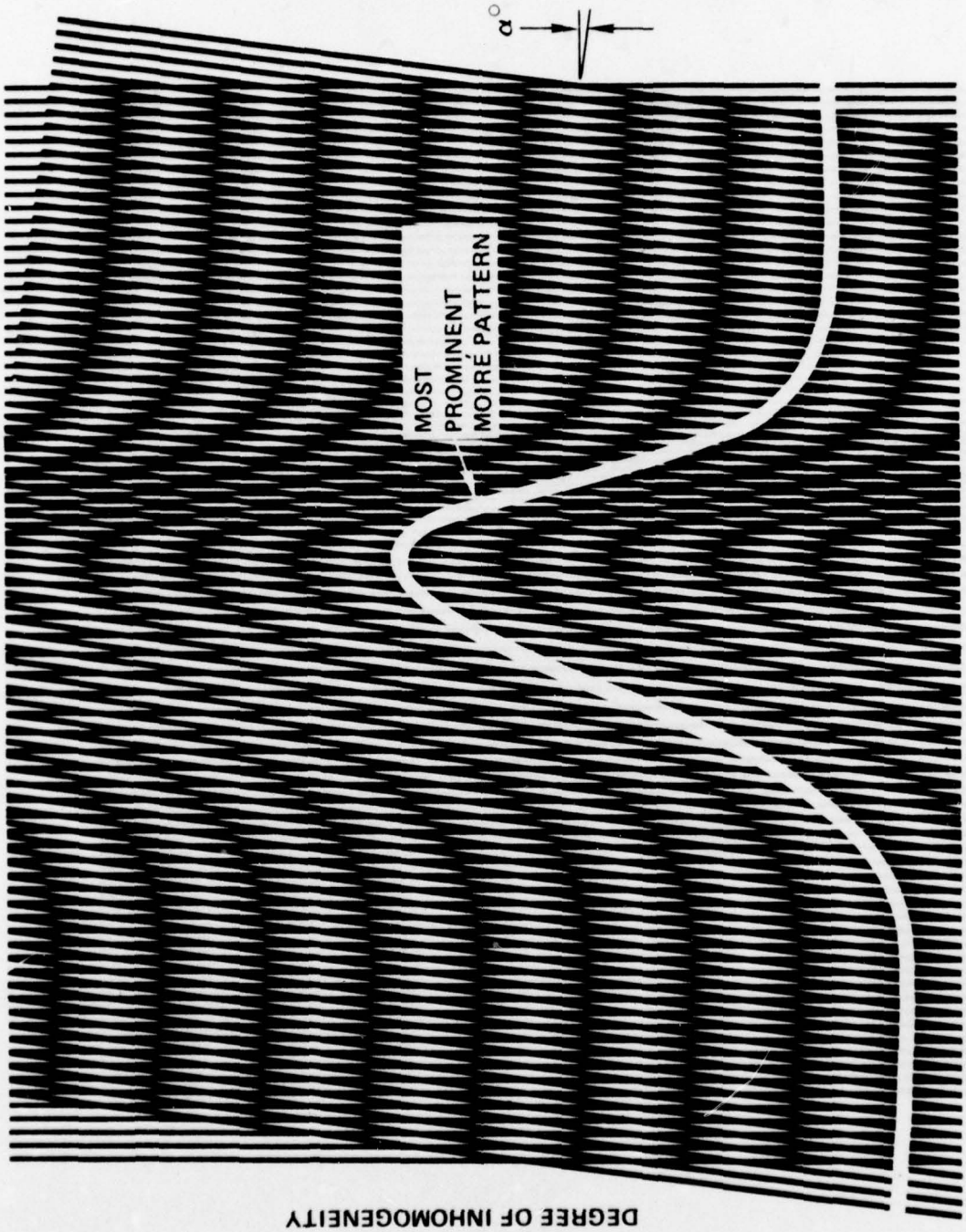


Figure 5-11. Example of Moire' Scan Nonlinearity

The following questions are among those which should be answered to reduce the above procedure to actual practice.

(1) How do other forms of digital sampling degradations affect the accuracy of the test?

(2) What are the second order effects of the approximation?

(3) What does "slightly enlarged" mean in the 2^{nd} step of the procedure (see Section V-E)?

(4) What is the effect of changing the angle α in Figure 5-11? (The first order effect is simple to obtain.)

D. MEASUREMENT OF REPRODUCER SAMPLING STRUCTURE

Some indication of the spot shape and placement structure of the reproducer can be obtained through the following procedure in lieu of a microscope:

(1) Reproduce the mathematical test pattern of Figure 5-12.

(2) Overlay the reproduced test pattern with a transparent copy of the test pattern at slight cant.

(3) The faint checkered pattern is a greatly amplified copy of the output image.

Figure 5-13 is a representative example of results possible with this method. In this case the Moire' pattern structure shows the microstructure of a 50% half-tone image.

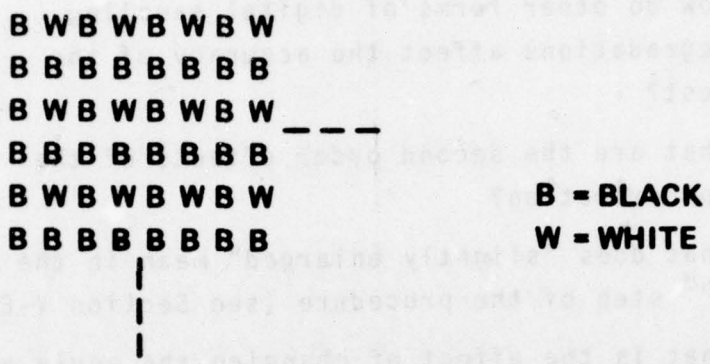


Figure 5-12. Mathematical Spot Test Image

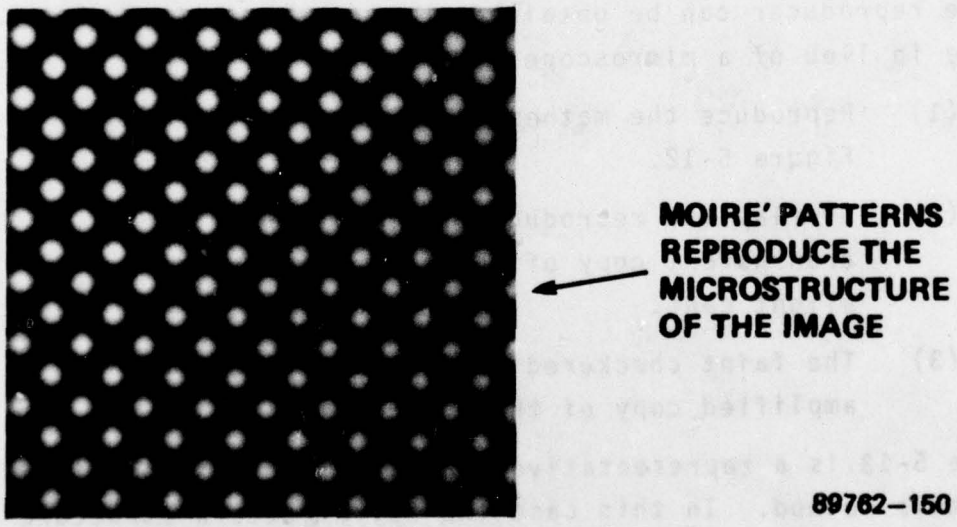


Figure 5-13. Example Results of Structural Determination

E. OBSERVATION OF SYSTEMATIC AND RANDOM IMAGE PERTURBATIONS

A very common form of digital degradation is the systematic or random perturbation of the image resulting in various superimposed image textures and patterns. While it is conceivable that these perturbations are functions of image content, the much more usual case is that the perturbation will be independent of the image detail and brightness. The most sensitive test for this case will be to input a flat (dc, no detail, gray) image of appreciable extent. Any observable detail within the output image will be due to degradation.

F. DETERMINATION OF THE IMAGERY SYSTEM GRAY-LEVEL MAPPING AND NUMBER OF LEVELS OF QUANTIZATION

A test image consisting of a continuous gray-level wedge is input to the scanner. The gray-levels of the output wedge in the reproduced image can be visually compared to the original image gray-level wedge in order to draw a curve of output to input gray levels. Ideally for maximum gray-level realism, this curve should be a straight 45^{o} positive slope line.

If the gray-level of the reproduced image wedge is composed of easily discernible gray-level steps, then the number of observable steps is equal to the number of observable quantization levels and of the potential for false contouring within an image.

A quick test for gray-level linearity of an image system is as follows:

(1) Input a gray-level wedge into the scanner

(2) Overlay the output gray-level wedge from the reproducer with a transparent copy of the original gray-level wedge. Turn this copy over as required to get an inverse gray-level wedge, i.e., decreasing density rather than increasing density.

(3) The resulting image area of the reproduced image overlaid with an inverted transparent copy of the original should be uniformly gray under strong light. Any deviation from uniformity will be an indication of system gray-level nonlinearity.

SECTION VI

RESULTS AND CONCLUSIONS

This study has taken an in-depth look at the problem of defining and measuring the image quality of a digital image processing system. We have taken two approaches in an attempt to measure image quality. The subjective method whereby a human observer judged the quality of degraded imagery in a subjective manner, and the objective method whereby mathematical or physical attributes of the imagery system were measured in an objective manner.

The subjective testing of imagery involved adding various types of commonly observed noise or degradations to four different types of images. The subjective "utility" of the degraded imagery was observed and tabulated. These results will enable a system designer to predict the performance of an imagery system for a number of common tasks when the system has been corrupted with various types of digital noise or degradations.

The objective method of measuring image degradations involved the conceptual measurement of the following type degradations:

- amplitude distortion,
- modulation transfer function,
- geometric distortion

The fourth type of degradation, classified as noise, was discussed in this report although no simplified objective test was included. The aliasing noise, discussed in Section III-A was exemplified by the chirp MTF test of Figure 5-6 although the quantitative measure was proposed for the MTF not aliasing

distortion. One of the recommendations for further work is the definition of the trade-offs in performance between the conflicting parameters of higher resolution and aliasing error; i.e., if the resolution of a digital imaging system is made to increase, then the aliasing error will also increase.

A model of imagery was developed using the Poisson distribution for the location of edges in imagery. This model generated a spectrum model which is in close agreement with empirically derived spectra for imagery.

A. SUBJECTIVE TESTS

The following four types of images were evaluated: (a) high resolution photograph, (b) low resolution photograph, (c) infrared image, (d) Synthetic Aperture Radar image. Each image was then subjected to varying amounts of spot noise, *line noise*, *line jitter*, *quantization* levels, as well as reduced sampling rates.

The results obtained suggest that

- The source image characteristics form strong contributing factors to the image quality of a digital image processing system.
- Subjective image quality is a more dominant image quality factor than objective image quality.
- The system parameters of the state-of-art scanners and reproducers can serve as dominant image quality factors.

B. OBJECTIVE TESTS

Several simple non-mechanized tests were developed, including the use of Moire' patterns, to measure the following objective parameters of a digital imagery system:

- Determination of Spatial Sampling Reproduction Rate
- Modulation Transfer Function Measurement
- Scan Nonhomogeneity
- Measurement of reproducer sampling structure

A simple method to measure the imagery system gray-level mapping and the number of levels of quantization were also developed. All of these objective tests are easy to implement and require no special measurement equipment.

C. CONCLUSIONS

The evaluation of digital image quality has lagged behind developments in the application of digital techniques to imaging systems. Surprisingly little is found in the open literature on digital imagery quality even the important considerations of MTF roll off versus aliasing errors. This preliminary investigation including both subjective and objective techniques forms a basis for the definition of a digital imagery test set.

The recommended test set criteria should include measurements in four categories of system performance: non-linear amplitude transfer characteristic, non-uniform MTF response (for frequencies up to one-half the Nyquist frequency), non-linear geometric response, and noise effects in general. These criteria have their roots in linear system theory so they should be good descriptors of digital image quality especially for the important class of applications for which

the desired output is a close replica or facsimile of the input source.

Digital imagery, based on its periodic or array structure, has interesting properties which provide simple tests for many, if not all, of the categories of system performance. In particular, Moire' patterns can provide powerful measurement techniques which exploit the array structure of the digital picture elements.

This initial study has provided the framework for a digital image test set with continuing efforts recommended for detailed specifications and construction of a test set. One development which was started in this effort and worth exploring further is the relationship between MTF response and aliased distortion. In addition, this study has generated computer programs for the subjective evaluation of digital degradations which would prove useful for simulating the performance of the sensor portion of the total digital imaging system

REFERENCES

[1] R. W. Cohen, I. Gorog, and C. R. Carlson, "Image Descriptors for Displays," Technical Report prepared for Office of Naval Research, Contract Number N00014-75-C-0184, NR-213-120, March 1975.

[2] J. B. O'Neal, Jr., "Delta Modulation Quantizing Noise Analytical and Computer Simulation Results for Gaussian and Television Input Signals," Bell Systems Technical Journal, January 1966, pp. 117-141.

[3] H. L. Landau and H. O. Pollak, "Prolate Spheroidal Wave Functions, Fourier Analysis and Uncertainty: III: The Dimensions of Space of Essentially Time- and Band-Limited Signals," Bell Systems Technical Journal, 41 (July 1962), pp. 1295-1336.

[4] Slepian, D., "On Bandwidth," Proceedings of the IEEE, Vol. 64, No. 3, March 1976.

[5] C. E. Shannon and W. Weaver, The Mathematical Theory of Communication, University of Illinois Press, Fifth Edition, 1972.

[6] T. J. Goblick and J. L. Holsinger, "Analog Source Digitization: A Comparison of Theory and Practice," IEEE Transactions on Information Theory, April 1967, pp. 323-326.

[7] J. Max, "Quantizing for Minimum Distortion," IEEE Transactions on Information Theory, March 1960, pp. 7-12.

[8] H. Gish and J. Pierce, "Asymptotically Efficient Quantizing," IEEE Transactions on Information Theory, September 1968, pp. 676-679.

[9] R. Wood, "On Optimum Quantization," IEEE Transactions on Information Theory, March 1969, pp. 248-252.

[10] P. F. Panter, Modulation, Noise and Spectral Analysis, McGraw-Hill, New York, 1965.

BIBLIOGRAPHY

DIGITAL IMAGE PROCESSING:

1. Pearson, D. E., Transmission and Display of Pictorial Information. Halsted Press, 1975.

2. Rosenfeld, Azriel and Kak, Avinach, C., Digital Picture Processing. Academic Press, 1976.

3. Scanlan, L. A., et. al., "Human Performance Evaluation Matrix Displays: Literature and Technology Review." AMRL-TR-76-39, Hughes Aircraft Co., Culver City, CA. June 1976.

4. Arguillo, Roger J., Sellner, Harvey R., and Stuller, John A., "Transfer Function Compensation of Sampled Imagery," IEEE Transactions on Computers, July 1972.

5. Ramirez, Robert W., "The Fast Fourier Transforms Errors are Predictable, Therefore Manageable." Electronics, June 13, 1974.

6. Proceedings of IEEE, August 1968.

7. Proceedings of IEEE, July 1972.

8. J. B. O'Neal, Jr., "Predictive Quantizing Systems (Differential Pulse Code Modulation) for the Transmission of Television Signals." The Bell Systems Technical Journal, Vol. XLV, No. 5, May-June 1966.

9. J. B. O'Neal, Jr. and T. Raj Natarajan. "Coding Isotropic Images." Research Paper.

10. M. Tasto and P. A. Wintz, "A Bound on the Rate-Distortion Function on Application to Images," IEEE Trans. on Information Theory. Vol. IT-18, No. 1, January 1972.

11. O'Neal, J. B., Jr., "A Bound on Signal-to-Quantizing Noise Ratio's for Digital Encoding Systems." Proceedings of the IEEE, Vol, 55, No. 3, March 1967.

12. Anil K. Jain and Edward Angel, "Image Restoration, Modelling and Reduction of Dimensionality," IEEE Transactions on Computers, Vol. C-23, No. 5, May 1974.

13. W. C. Adams, "The Effects of Zero-Order (Sample and Hold) Filters on Computer Simulation of BLWN and Other Signals." Memo 9330-WCA-040, Harris ESD, Melbourne, Florida.

14. Thomas S. Huang, James W. Burnett and Andrew G. Deczky, "The Importance of Phase in Image Processing Filters." IEEE Transactions on Acoustics, Speech, and Signal Processing, Vol. ASSP-23, No. 6, December 1975.

15. A. V. Oppenheim and D. H. Johnson, "Discrete Representation of Signals." Department of Elec. Eng. and Research Lab. of Electronics, MIT, Cambridge, MA.

16. A. M. Manders, "Sampling and Reconstruction of Pictures." University of Florida, GENESYS, Cape Canaveral, FL.

17. Harry C. Andrews, Computer Techniques in Image Processing, Academic Press, 1970.

MISCELLANEOUS:

1. Homer B. Tilton. "Design Tips-A 3-D Oscilloscope Display." Sperry Flight Systems Division, Phoenix, AZ.

2. Richard Gerdes, "Isometric Gray Scale Display." Optical Electronics, Tuscon, AZ.

3. Arthur P. Ginsburg, et. al., "Image Analysis Facility: An Interactive Digital Computer System." National Tech. Info. Service. U.S. Dept. of Commerce, AD-750-475, 23 May 1972.

4. Image Processing Research, University of Southern California Semiannual Technical Report Covering Research 1 March 1973 - 31 August 1973. ARPA Order No. 1706.

5. Image Processing Research, University of Southern California Semiannual Technical Report Covering Research 3 August 1971 - 29 February 1972. ARPA Order No. 1706.

6. Image Processing Research, University of Southern California Semiannual Technical Report Covering Research 1 March 1972 - 31 August 1972.

7. Abstracts of Invited Papers for the International Conference on Image Analysis and Evaluation. Journal of Applied Photographic Engineering, Vol. 2, Spring 1976.

8. North East Test Area, Rome Air Development Center (AFSC) Reconnaissance and Mapping Branch (IRR). Griffiss AFB, NY.

9. "Image Analysis and Modeling." Purdue University, RADC-TR-75-144 Technical Report. May 1975. Griffiss AFB, NY. (AD A011929)

10. Study of Image-Evaluation Techniques. Interim Engineering Report No. 9, 15 July-15 October 1964. ITEK Corp., Lexington, MA.

11. R. D. Kell, "Description of Experimental Television Transmitting Apparatus." Proceedings of the Institute of Radio Engineers, Vol. 21, No. 12.

12. M. Cole, G. L. Sturgess, T. Kelly and R. H. Heil, "The Image Analyzing Computer - A New Tool for Materials Evaluation." Harris ESD, Melbourne, FL.

DIGITAL FILTERING THEORY:

1. Julius T. Tou, Digital and Sampled-data Control Systems. McGraw-Hill Book Company, Inc., 1959.

2. Alan V. Oppenheimer and Schafer, Ronald W., Digital Signal Processing, Prentice-Hall Inc., 1975.

3. Donald Childers and Alan Durling, Digital Filtering and Signal Processing, West Publishing Company, 1975.

IMAGE DESCRIPTIONS:

1. IEEE Transactions on Information Theory, Vol. IT-20, No. 4, July 1974.

2. R. W. Cohen, I. Gorog, and C. R. Carlson, "Image Description for Displays." Technical Report RCA Laboratories, Princeton, NJ, March 1975.

3. R. W. Cohen, C. R. Carlson and G. S. Cody, "Image Descriptions for Displays." Technical Report RCA Laboratories, May 1976.

TV DISPLAY IMAGE QUALITY:

1. Perception of Displayed Information, Plenum Press, New York-London, 1973.

2. Electro-Optics Handbook, RCA, Commercial Engineering, Harrison, NJ, 1968.

3. "Image Quality in Sampled Data Systems," Paper P-741, Institute for Defense Analysis Science and Technical Division, August 1971.

4. "Image Quality and Face Recognition on Television Display," Human Factors, 1974, 16(3) 300-307.

5. Jim Wurtz, "Shedding Light on CRT Brightness, Electro-Optical Systems Design," Litton Industries, Electron Tube Division, San Carlos, CA.

6. "Objectives Performance Evaluation of Copy Generated by the Tactical Digital Facsimile (TDF) Validation Model AN/USC( )(V). Part 2: Random Bit Error Rate (BER) Material." 1 June 1976, Naval Electronics Lab. Center, San Diego, CA.

7. Carl F. Shelton, "Spatial Frequency Response of Flying-Spot Scanner Systems," A paper from the 11th SPIE Tech. Symposium, 22 August 1966, St. Louis, MO.

8. "A New Measure of Television Display Quality Relatable to Observer Performance." AMRL-TR-76-73, Aerospace Medical Research Lab, Wright-Patterson AFB, August 1976.

9. "An Experimental Evaluation of the Spot Wobble Method of Suppressing Raster Structure Visibility." AMRL-TR-75-63. Aerospace Medical Research Lab. Wright-Patterson AFB, November 1975.

10. "Human Factors Requirements for Electronic Displays Effects of S/N Ratio and TV Lines Over Target." Report A0217, Reconnaissance Lab, McDonnell Douglas Corp., January 1970.

PHOTOGRAPHIC IMAGE QUALITY:

1. Selected Readings in Image Evaluation, Waverly Press, Inc., 1976.

2. "Image Analysis and Evaluation," Technical Digest, July 19-23, 1976, Digest of Technical Papers, SPSE.

3. J. C. Dainty and R. Shaw, Image Science, Academic Press, 1974.

4. Arnold S. Weiss, "Optimizing Film Density Sensing." AIL Information Systems, A Cutler-Hammer Co., Los Angeles, CA.

5. T. L. Coluccia, S. MacLeod and J. J. Maier, "Effect of Image Contrast and Resolution on Photointerpreter Target Detection and Identification," Journal of the Optical Society of America, Vol. 59, No. 11, 1478-1481, November 1969.

IMAGE QUALITY OF VISUAL PERCEPTION:

1. Franc Grum, "Detector Intercomparison Results," Eastman Kodak, Rochester, NY, Joseph Cameron, NBS, Washington, DC.

2. A Primer on Spectroradiometry and Photometry, P. B. Watson, EG&G Inc., Salem, NC.

3. Frank A. Geldard, The Human Senses, John Wiley and Sons, Inc., 1953.

4. Albert Rose, Vision Human and Electronic, Plenum Press, 1910.

5. "Image Object and Illusion," Readings from Scientific American, May 1974.

IMAGE QUALITY TEST MATERIAL:

1. Test Procedure for Facsimile, IEEE No. 167, Std. 167-1966.

2. USAF Resolution Chart Data, Nomenclature and Specifications.

3. Television Test Charts, Sierra Scientific Corp., 2189 Leghorn St., Mountain View, CA.

4. SMPTE Test Materials for Motion Picture and Television. 1976-1977.

5. CONRAC, Contrast Ratio Calculator, Instrument/Controls Div., 330 Madison Ave., NY, NY 10017.

6. Index of EIA and JEDEC Standards and Engineering Publications, 1973 Revision, No. 2, EIA, 2001 Eye Street., N.W. Washington, DC.

PSYCHOPHYSICS:

1. "Experimental Evaluation of Optical Enhancement of Literal Visual Displays." ASD Technical Report 61-568, October 1961, Wright-Patterson AFB, Ohio.

2. Brainard, R. W., Lopez, L. J., and Ornstein, G. N., "Prediction of Image Interpretability by Psychophysical Judgements." North American Aviation Inc. NA65H-743, 1 September 1965.

3. "Performance of Photographic Interpreters as a Function of Time and Image Characteristics." RADC-TDR-63-313 Final Report, September 1964. RADC-Griffiss AFB, NY. (AD 608219)

4. "Specification and Maintenance of Interpreter Performance," RADC-TR-66-539 Final Report, October 1966, RADC, Griffiss AFB, NY.(AD 802122)

5. "Texture-Tone Study with Application to Digital Imagery," Technical Report 182-2. US Army Engineering Topographic Laboratories, Ft. Belvoir, VA, November 1971.

6. Williams, L. G., "Human Factors Studies of Reconnaissance Display Requirements." MH MPG Document R-RD6226, Honeywell Aeronautical Controls, January 4, 1962.

7. Zdenek D. Kalensky, "Changing Role of Image Interpretation," The Canadian Surveyor, Vol. 25, No. 4, September 1971.

BIBLIOGRAPHY (Continued)

8. G. Gnauck, "Photo-Interpretation (A Definition and Brief Analysis)." Inter-Office Communication, D9500-35-M. Harris ESD, Melbourne, FL.

9. Abraham H. Birnbaum, "Effect of Selected Photo-Characteristics on Detection and Identification." Symposium Photo Interpretation, Delft 1962.

10. Speech Quality Measurements, IEEE Transactions on Audio and Electroacoustics, September 1969.

APPENDIX A

DIGITAL IMAGERY TEST SET
PROGRAM DOCUMENTATION

APPENDIX A

DIGITAL IMAGERY TEST SET PROGRAM DOCUMENTATION

Software for evaluation of the Digital Imagery Test Set was developed in the Certified Processing Laboratory (CPL) at Harris ESD.

The hardware configuration of the CPL is shown in Figure A-1. Main hardware equipments in this configuration are:

- Datacraft 6024/5 CPU
  1.0 microsecond cycle time
  8-bit and 24-bit I/O channels, and ABC channels
- Core memory (64K, 24-bit words)
- Cartridge Disc System, 5.4 byte
- Digital Tape Units
  1 each (seven-track, 556/800 bits/inch)
  1 each (nine-track, 800 bits/inch)
- Punched card reader (300 cards/minute)
- Line Printer (200 lines/minute)
- Analog-to-Digital and Digital-to-Analog Converters (Harris ESD Design)
- Teletypewriter, ASR-33 Console Teletype
- Tektronix Model 4014/15 Graphics Terminal
- Tektronix Hard Copy Unit, Model 4631
- Harris ESD Imagery Terminal
- CONRAC CRT Display

An overall view of the DITS software processing system is shown in Figure A-2. The Digital Processing Subsystem and the Digital Display Subsystem are shown in Figure A-3 and A-4 respectively.

A digital tape with 6 image files was received from Pattern Analysis and Recognition Corp. Contents of the tape are listed in Table A-1. The data was digitized at 8 bits gray level per pixel.

Detailed descriptions, documentation and program listings of the software used to evaluate these images are contained in this Appendix. Section A contains program descriptions, Section B provides program listings, and Section C contains the program flowcharts.

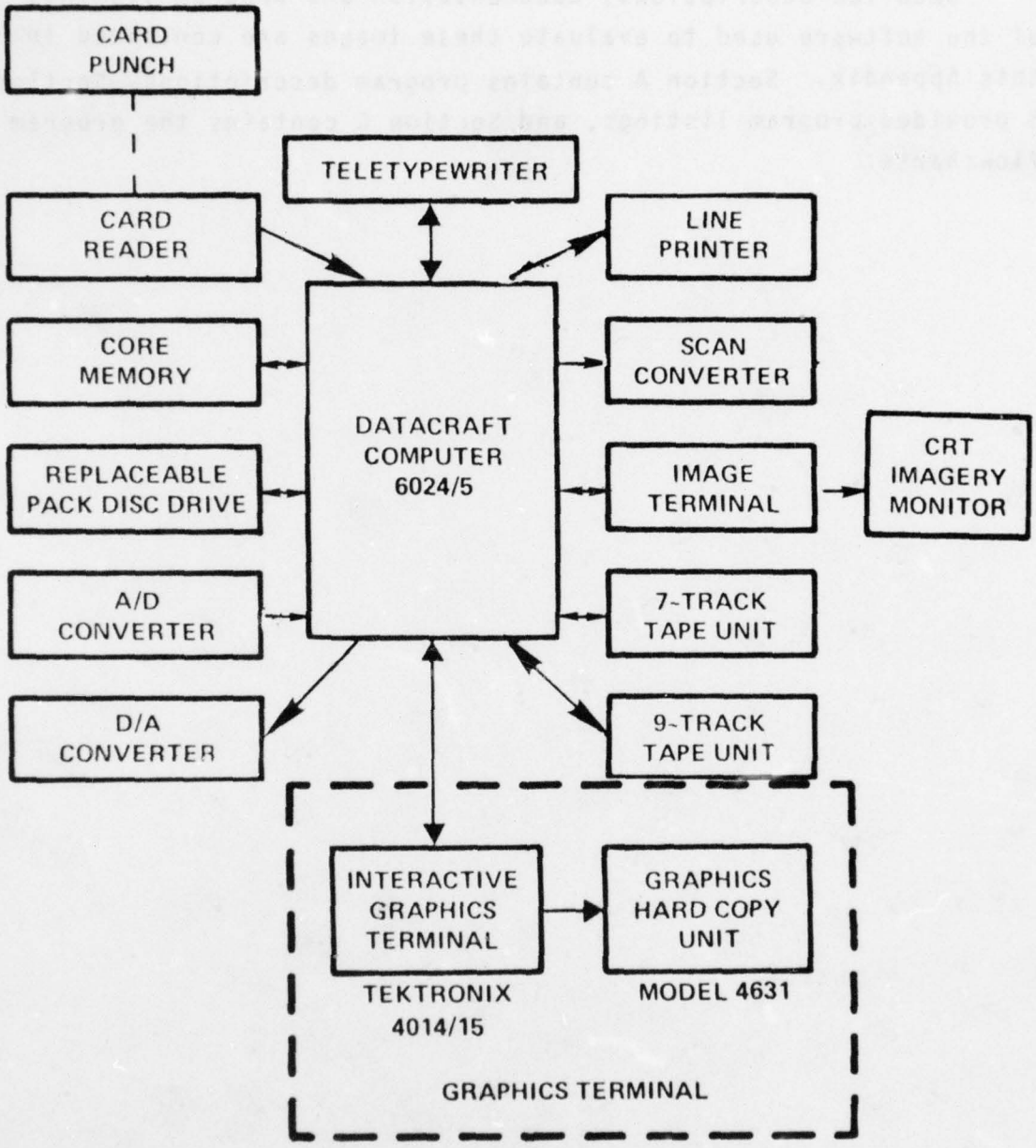


Figure A-1. CPL Hardware Configuration

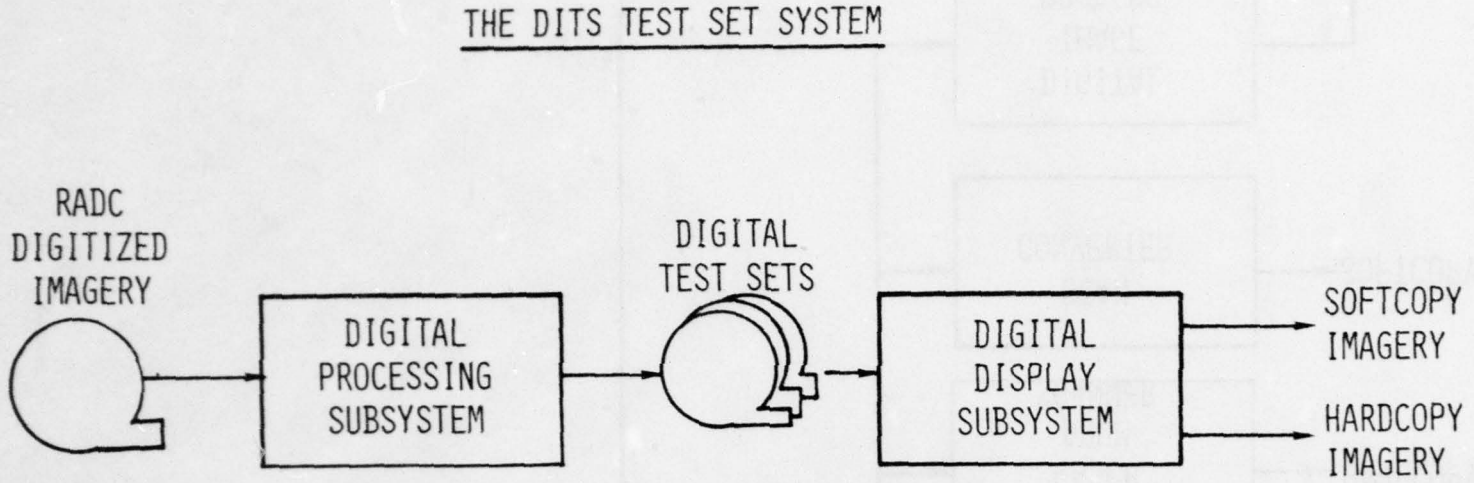


Figure A-2. The DITS Test Set System

Figure A-2

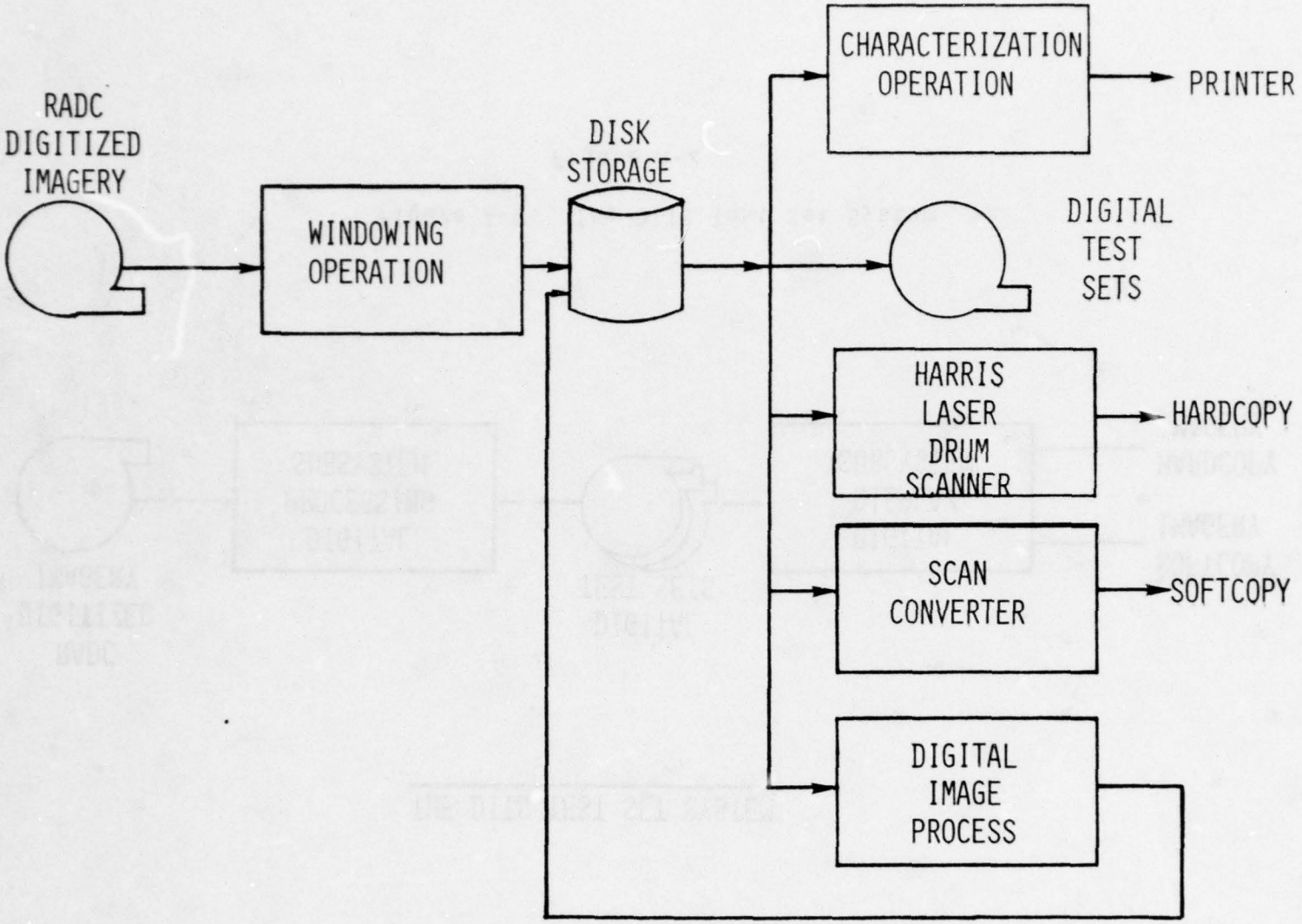


Figure A-3. The Digital Processing Subsystem

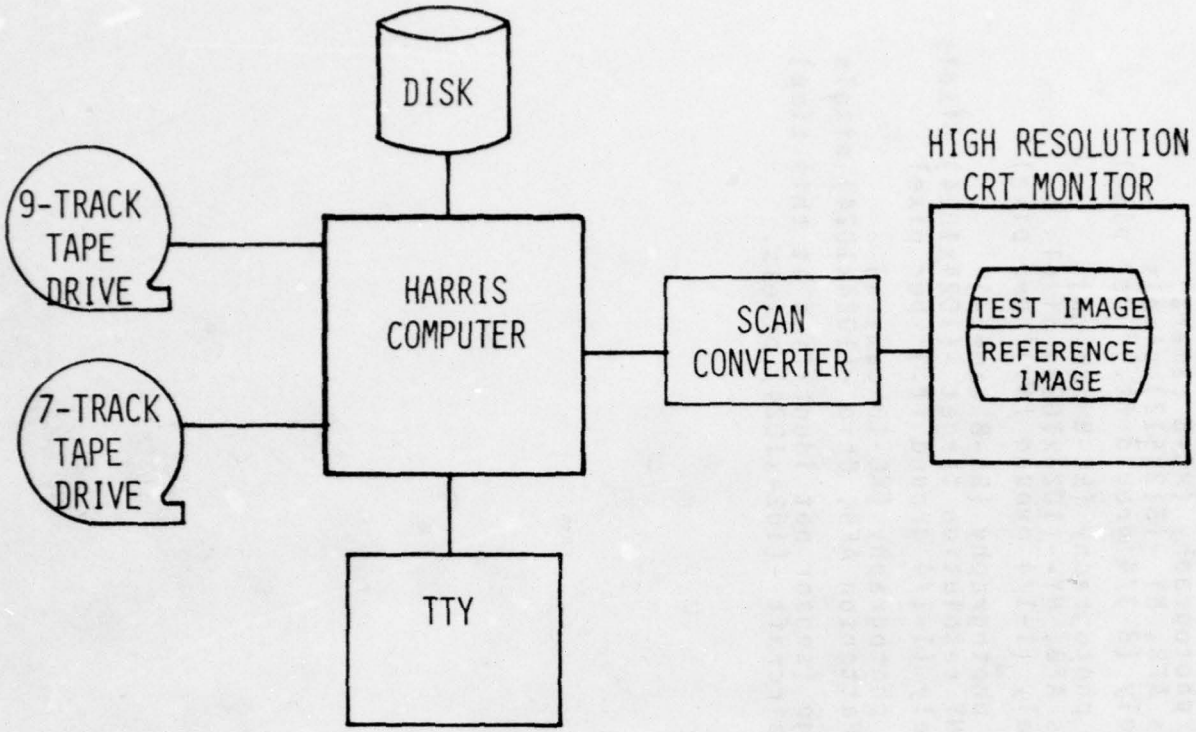


Figure A-4 The Digital Display Subsystem

TABLE A-1

1. Synthetic Aperature Radar (UPD-4)
   over Griffiss AFB, NY -(512x512) pixels
2. B/W vertical photography (RC-8 camera)
   over Griffiss AFB, NY -(512x512) pixels
   - approximately (8-3/4 ground ft.)^2 per pixel
3. B/W vertical photography (RC-8 camera)
   over Griffiss AFB, NY -(1023x1024) pixels
   - approximately (1-1/4 ground ft.)^2 per pixel
4. B/W vertical photography (RC-8 camera)
   over Floyd, NY resolution target -(1024x1024) pixels
   - approximately (1-1/4 ground ft.)^2 per pixel
5. B/W vertical photography (KC-1B camera)
   over Wright Patterson AFB, Ohio -(1024x1024) pixels
6. Infrared image (sensor not identified at this time)
   over parked aircraft -(1024x1024) pixels.

SECTION A

PROGRAM DESCRIPTIONS

PROGRAM NAME:	PARCON
PURPOSE:	Convert 8-bit packed data (32-bit word) to Harris 6024/5 8-bit data.
DESCRIPTION AND METHODS:	The digitized images received from PAR were 8-bit data packed 4 pixels/word. This data was converted for use on the Harris 6024/5 computer. An illustration of the difference in data formats, and the converted format used for actual processing is shown in Figure A-5.
INPUT VARIABLES:	ITI - Input tape device number ITO - Output tape device number NWR - Number of Words/Record NRF - Number of records/file ITF1 - Tape file number on Input Tape (99=End Program) ITF2 - Tape file number on output tape
PROGRAMMING LANGUAGE:	FORTRAN
PROGRAMMER:	G.R. CUTHBERT HARRIS ESD (305) 727-5284
COMPUTER	HARRIS 6024/5
OPERATING SYSTEM:	SERIES 6000 DISC OPERATING SYSTEM 61516-01 EXTENDED NON-SAU FORTRAN COMPILER REVISION LEVEL 24.083076

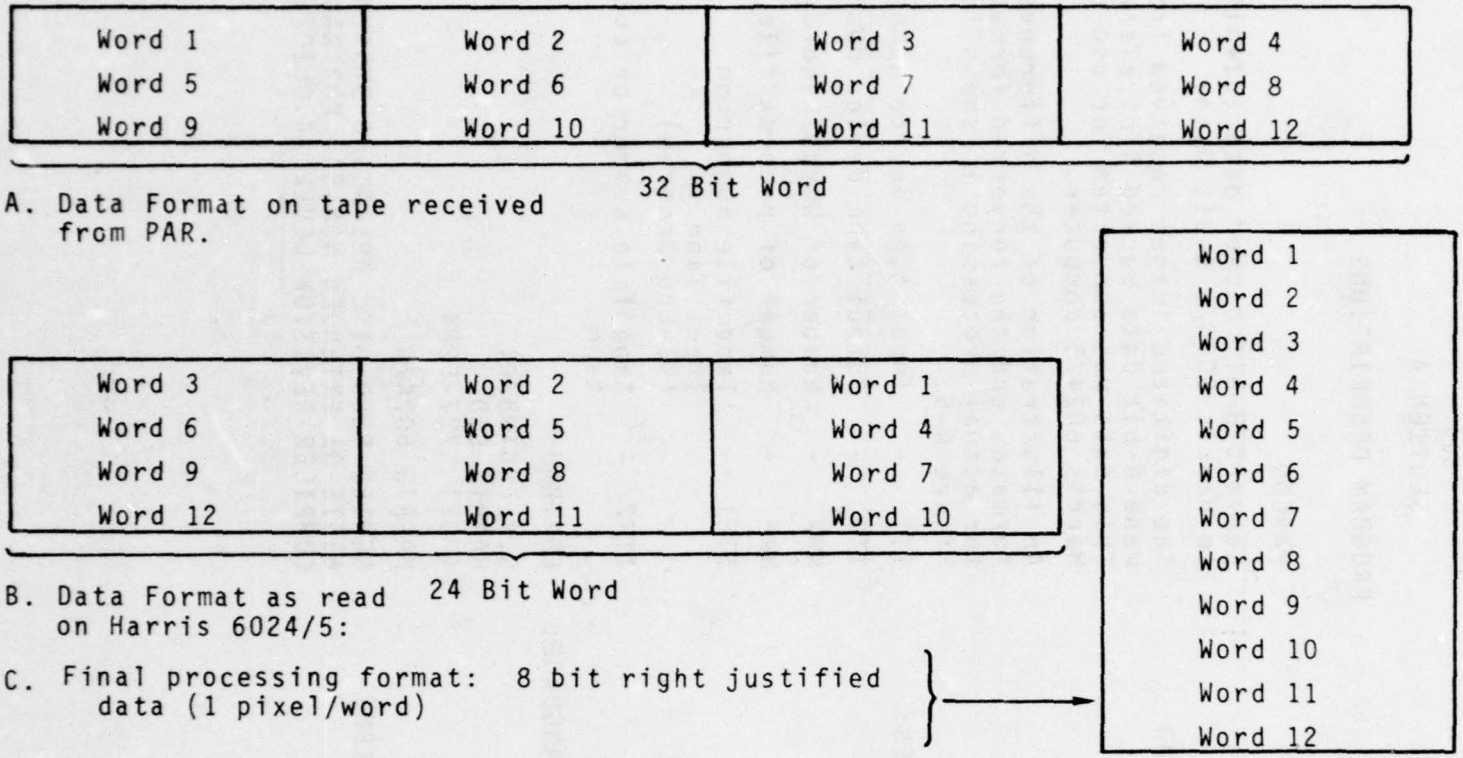


Figure A-5. Data Formats

PROGRAM: DITS MAIN

PURPOSE: This is a driver program used to execute one or a series of image processing subroutines. The subroutine processed is dependent upon the value of the variable ISUB as listed below:

ISUB	SUBROUTINE CALLED
1	TODWIN - Write a desired window to tape or disk
2	SPAXFM - Spatial frequency transform
3	GRALEV - Gray Level Histogram to TEKTRONIX
4	DUMMY - Not used at this time
5	DUMPSC - Dump a picture to the scanner
6	DUMPTV - Dump a picture to CONRAC
7	GNCOPY - Copy a picture from one device to another
8	GRAMAP - Gray Level Mapping
9	DUMMY - Not used at present time
10	JITTER - Introduce jitter into an image
11	GNOISE - Degrade with random Gaussian noise
12	DIGDEG - Digitization Degraded
13	HGHALS - Sampling degraded, high aliasing
14	REDALS - Sampling degraded,, reduced aliasing
99	END PROGRAM

DESCRIPTION AND METHOD: The program is modular in construction, and future routines can be incorporated with ease.

Format for input to all programs from cards is 8I10.

INPUT VARIABLES:	ISUB - Subroutine to be executed
PROGRAMMING LANGUAGE:	FORTRAN
PROGRAMMERS:	DR. R.H. COFER, G.R. CUTHBERT HARRIS ESD (305) 727-5284
COMPUTER:	Harris 6024/5
OPERATING SYSTEM:	Series 6000 DISC OPERATING SYSTEM 61516-01 EXTENDED NON-SAU FORTRAN COMPILER, REVISION LEVEL 24.083076

PROGRAM NAME:	TODWIN
PURPOSE:	Write a desired window from an image to a tape or disk file
DESCRIPTION AND METHODS:	Any subset of an image can be written to a new output file by specifying the line and pixel parameters of the desired window
INPUT VARIABLES:	M,N - Main picture size (M = no of lines) (N = no of pixels/line) MM - Location of first line in window NN - Location of first spot in window II - No. of lines to be transferred JJ - No. of spots/line to be transferred IDI- Input file number ITFI File no of input tape/disc ID2- Output file no ITF2 File no of output tape/disc
PROGRAMMING LANGUAGE:	FORTRAN
PROGRAMMER:	G.R. CUTHBERT HARRIS ESD (305) 727-5284
COMPUTER:	Harris 6024/5
OPERATING SYSTEM	Series 6000 DISC OPERATING SYSTEM 61516-01 EXTENDED NON-SAU FORTRAN COMPILER, REVISION LEVEL 24.083076

PROGRAM NAME:	GRALEV
PURPOSE:	Plot a histogram of image grey values on TEKTRONIX
DESCRIPTION AND METHODS:	Data is sequentially read from the input tape, the occurrences of grey values are counted, and the mean is computed. These results are then displayed on the TEKTRONIX CRT.
INPUT VARIABLES:	M,N Pictur. size (M = No of lines) (N = No of pixels/line)
PROGRAMMING LANGUAGE:	FORTRAN
PROGRAMMER:	G.R. CUTHBERT HARRIS ESD (305) 727-5284
COMPUTER:	HARRIS 6024/5
OPERATING SYSTEM:	Series 6000 DISC OPERATING SYSTEM 61516-01 EXTENDED NON-SAU FORTRAN COMPILER, REVISION LEVEL 24.083076

PROGRAM NAME:	SPAXFM
PURPOSE:	Output selected spatial transform values
DESCRIPTION AND METHODS:	A spatial transform is executed on selected pixels of an image using mathematics equivalent to a Fourier transform. Results are plotted on a TEKTRONIX CRT.
INPUT VARIABLES:	IU - Row number of pixel IV - Column number of pixel AMINR - Minimum value for X-axis plot AMAXR - Maximum value for X-axis plot AMINA - Minimum value for Y-axis plot AMAXA - Maximum value for Y-axis plot
PROGRAMMING LANGUAGE:	FORTRAN
PROGRAMMER:	DR. R.H. COFER, G.R. CUTHBERT HARRIS ESD (305) 727-5284
COMPUTER:	HARRIS 6024/5
OPERATING SYSTEM:	Series 6000 DISC OPERATING SYSTEM 61516-01 EXTENDED NON-SAU FORTRAN COMPILER, REVISION LEVEL 24.083076

PROGRAM NAME:	DUMMY
PURPOSE:	This is a dummy subroutine to allow for further expansion of the main program.
DESCRIPTION AND METHODS:	Establish a temporary subroutine by a call statement and an executable statement
INPUT VARIABLES:	None
PROGRAMMING LANGUAGE:	FORTRAN
PROGRAMMER:	DR. R.H. COFER, G.R. CUTHBERT HARRIS ESD (305) 727-5284
COMPUTER:	HARRIS 6024/5
OPERATING SYSTEM:	Series 6000 DISC OPERATING SYSTEM 61516-01 EXTENDED NON-SAU FORTRAN COMPILER, REVISION LEVEL 24.083076

PROGRAM NAME:	DUMPSC
PURPOSE:	Output an unpacked 6-bit picture to the scanner
DESCRIPTION AND METHODS:	8 bit data is converted to 6 bit data and read out to the scanner for a hardcopy
INPUT VARIABLES:	ID1 - Input device no. ITF1 - File no. on input tape II - No. of lines to be transferred JJ - No. of pixels/line to be transferred NFDPT- No. of first data point in a line to be transferred NBITS- No. of bits/pixel on input record (6 bits or 8 bits)
PROGRAMMING LANGUAGE:	FORTRAN
PROGRAMMER:	DR. R.H. COFER, G.R. CUTHBERT HARRIS ESD (305) 727-5284
COMPUTER:	HARRIS 6024/5
OPERATING SYSTEM:	Series 6000 DISC OPERATING SYSTEM 61516-01 EXTENDED NON-SAU FORTRAN COMPILER, REVISION LEVEL 24.083076

PROGRAM NAME:	DUMPTV
PURPOSE:	Dump a picture to the CONRAC CRT
DESCRIPTION AND METHODS:	This subroutine has not yet been implemented

PROGRAM NAME:	GNCOPY
PURPOSE:	Dump a picture from one device to another
DESCRIPTION AND METHODS:	A utility subroutine which gives the capability of transfer from disc/tape, tape/disc or tape/tape. Uses BUFFER IN, BUFFER OUT techniques
INPUT VARIABLES:	ID1 - Input device no. ITF1 - File no. on input device ID2 - Output device no. ITF2 - File no. on output device II - No. of records to be transferred JJ - No. of pixels/line to be transferred
PROGRAMMING LANGUAGE:	FORTRAN
PROGRAMMER:	DR. R.H. COFER, G.R. CUTHBERT HARRIS ESD (305) 727-5284
COMPUTER:	HARRIS 6024/5
OPERATING SYSTEM:	Series 6000 DISC OPERATING SYSTEM 61516-01 EXTENDED NON-SAU FORTRAN COMPILER, REVISION LEVEL 24.083076

PROGRAM NAME:	GRAMAP
PURPOSE:	Change grey level values as desired
DESCRIPTION AND METHODS:	Grey values are changed according to breakpoints and the new desired grey values input to the subroutine on data cards
INPUT VARIABLES	ID1 - Device no. for input picture ITF1 - File no. on input device ID2 - Device no. for output picture ITF2 - File no/ on output device IMAX - Total number of grey levels II - No/ of lines in picture JJ - No/ of pixels/line I1,I2 - Grey level mapping values I3 - Flag to stop reading I1,I2
PROGRAMMING LANGUAGE:	FORTRAN
PROGRAMMER:	DR. R.H. COFER, G.R. CUTHBERT HARRIS ESD (305) 727-5284
COMPUTER:	HARRIS 6024/5
OPERATING SYSTEM:	Series 6000 DISC OPERATING SYSTEM 61516-01 EXTENDED NON-SAU FORTRAN COMPILER, REVISION LEVEL 24.083076

PROGRAM NAME:	JITTER
PURPOSE:	Introduce random jitter to degrade a picture
DESCRIPTION AND METHODS:	Jitter is introduced at random points in an image through use of random number generator
INPUT VARIABLES:	ID1 - Device no. of the input picture ITF1 - File no. of input if tape ID2 - Device number of output picture ITF2 - File no. of output if tape II - No. of lines to be transferred JJ - No. of spots/line to be transferred ISD - Standard deviation IMN - Mean ISEED - Seed for GRN generator
PROGRAMMING LANGUAGE:	FORTRAN
PROGRAMMER:	G.R.CUTHBERT HARRIS ESD (305) 727-5284
COMPUTER:	HARRIS 6024/5
OPERATING SYSTEM:	Series 6000 DISC OPERATING SYSTEM 61516-01 EXTENDED NON-SAU FORTRAN COMPILER, REVISION LEVEL 24.083076

PROGRAM NAME:	GNOISE
PURPOSE:	Introduce Gaussian random noise into a picture
DESCRIPTION AND METHODS:	Gaussian noise is introduced into a picture through use a random number generator. The noise can be added to each pixel or by line.
INPUT VARIABLES:	ID1 - Device no. of input picture ITF1 - File no. of input if tape ID2 - Device no. of output picture ITF2 - File no. of output if tape II - No. of lines to be transferred JJ - No. of spot/line to be transferred IMAX - Maximum picture value ISD - Standard Deviation IMN - Specified mean ISEED - Seed for grn generator ISL = 0 - Add a different RV to each spot in picture = 1 - Add a Different RV to each line in picture
PROGRAMMING LANGUAGE:	FORTRAN
PROGRAMMER:	G.R. CUTHBERT HARRIS ESD (305) 727-5284
COMPUTER:	HARRIS 6024/5
OPERATING SYSTEM:	Series 6000 DISC OPERATING SYSTEM 61516-01 EXTENDED NON-SAU FORTRAN COMPILER, REVISION LEVEL 24.083076

PROGRAM NAME:	DIGDEG
PURPOSE:	Picture is degraded digitally
DESCRIPTION AND METHOD:	The number of bits/pixel is changed by shifting bits out according to values on input cards.
INPUT VARIABLES:	ID1 - Device no. of input picture ITF1 - File no. of input if tape ID2 - Device no. of output picture ITF2 - File no. of output if tape II - No. of lines in output picture JJ - No. of spots/line to be transferred NBIT - No. of bits to be shifted (right)
PROGRAMMING LANGUAGE:	FORTRAN
PROGRAMMER:	G.R. CUTHBERT HARRIS ESD (305) 727-5284
COMPUTER:	HARRIS 6024/5
OPERATING SYSTEM:	Series 6000 DISC OPERATING SYSTEM 61516-01 EXTENDED NON-SAU FORTRAN COMPILER, REVISION LEVEL 24.083076

PROGRAM NAME:	REDALS
PURPOSE:	Reduce a picture in size by low aliasing
DESCRIPTION AND METHODS:	Reduce the size of an image by operating on it in powers of two.
INPUT VARIABLES:	ID1 - Device no. of input picture ITF1 - File no. of input if tape ID2 - Device no. of output picture ITF2 - File no. of output if tape II - No. of lines to be transferred JJ - No. of spots/line to be transferred ISIZE - Power of 2 reductions in size IMAX - Maximum picture value
PROGRAMMING LANGUAGE:	FORTRAN
PROGRAMMER:	DR. R.H. COFER, G.R. CUTHBERT HARRIS ESD (305) 727-5284
COMPUTER:	HARRIS 6024/5
OPERATING SYSTEM:	Series 6000 DISC OPERATING SYSTEM 61516-01 EXTENDED NON-SAU FORTRAN COMPILER, REVISISON LEVEL 24.083076

PROGRAM NAME:	HGHALS
PURPOSE:	Reduce image using high aliasing
DESCRIPTION AND METHODS:	Reduce the size of an image by operating in powers of two
INPUT VARIABLES:	ID1 - Device no. of input picture IFT1 - File no. of input if tape ID2 - Device no. of output picture ITF2 - File no. of output if tape II - No. of lines to be transferred JJ - No. of spots/line to be transferred ISIZE - Power of 2 reductions in size IMAX - Maximum picture value
PROGRAMMING LANGUAGE:	FORTRAN
PROGRAMMER:	DR.R.H. COFER, G.R. CUTHBERT HARRIS ESD (305) 727-5284
COMPUTER:	HARRIS 6024/5
OPERATING SYSTEM:	Series 6000 DISC OPERATING SYSTEM 61516-01 EXTENDED NON-SAU FORTRAN COMPILER, REVISION LEVEL 24.083075

BEST AVAILABLE COPY

SECTION B

PROGRAM LISTINGS

```
      NAME PARCON
      DIMENSION IBUF1(344),IBUF2(1032)
      DATA ICR,ILP,ITTY/7,6,1/
C
C     CONVERT 8-BIT PACKED DATA (32-BIT WORD) TO
C     10 HARRIS 6024/5 8-BIT DATA (0 PIXEL/WORD
C                                  WORDS RIGHT JUSTIFIED
C
C     PROGRAMMER:                  GERI CUTHBERT
C     PROGRAM DATE:                2/24/76
C
C     VARIABLES USED:
C        ITI     - INPUT TAPE DEVICE
C        ITO     - OUTPUT TAPE DEVICE
C        NWR     - NO OF WORDS/RECORD
C        NRF     - NUMBER OF RECORDS/FILE
C        ITF1    - TAPE FILE NO ON INPUT TAPE (99 = PROGRAM END)
C        ITF2    - TAPE FILE NO ON OUTPUT TAPE
C
      READ(ICR,8000)ITI,ITO
   10 CONTINUE
      READ(ICR,8000)NRF,NWR,ITF1,ITF2
C     ADVANCE INPUT TAPE FILE IF NECESSARY
      IF(ITF1.EQ.99)GO TO 999
      IF(ITF1.EQ.1)GO TO 20
      DO 15 L=2,ITF1
   15 CALL ADF(111)
C     ADVANCE OUTPUT TAPE FILE IF NECESSARY
   20 IF(ITF2.EQ.1)GO TO 30
      DO 25 L=2,ITF2
   25 CALL ADF(ITO)
   30 CONTINUE
C     SET DEFAULT PICTURE SIZE TO 1024 (344 DC WORDS PACKED)
C     AND CHANGE IF NECESSARY
      IEND=344
      NREC=342
      IF(NWR.NE.1024)IEND=172
      IF(NWR.NE.1024)NREC=171
      DO 500 II=1,NRF
C     CLEAR OUT BOTH BUFFERS
      DO 35 L=1,344
   35 IBUF1(L)=0
```

BEST AVAILABLE COPY

```
      DO 38 L=1,1032
   38 IBUF2(L)=0
C
C     GET IN A BUFFER
      BUFFER IN(ITI,IBUF1,B,NREC,ISTAT)
   40 CALL STATUS(ITI)
      GO TO (40,50,50),ISTAT
C
C     PROCESS IN INCREMENTS OF 4 WORDS
   50 KK = -2
      DO 300 I=1,IEND,4
      DO 200 J=1,4
      KK=KK+3
      JJ=I+J-1
      IA=IBUF1(JJ).AND.'377
      IB=IBUF1(JJ).AND.'177400
      IC=IBUF1(JJ).AND.'77600000
      IBUF2(KK)=255-(IC.SHIFT.-16)
      IBUF2(KK+1)=255-(IB.SHIFT.-8)
      IBUF2(KK+2)=255-IA
  200 CONTINUE
  300 CONTINUE
C
C     BUFFER TWO CONTAINS OUTPUT DATA - PUT IT ON TAPE
      BUFFER OUT(ITO,IBUF2,B,NWR,ISTAT)
  230 CALL STATUS(ITO)
      GO TO (230,500,500),ISTAT
  500 CONTINUE
C
C     FILE FINISHED WRITE EOF
      END FILE ITO
C *** IF YOU WANT TO PROCESS THE NEXT FILE WITHOUT REWINDING
C *** THE TAPES AND ADVANCING THEM AGAIN, MAKE ITF1 & ITF2 = 1
      GO TO 10
  999 REWIND ITO
      CALL EXIT
 8000 FORMAT(8I10)
      END
```


BEST AVAILABLE COPY

```
      COMMON/IDATA/IBUF1(4096),IBUF2(4096)
      DATA ICR,ILP,ITTY/7,6,1/
C
C     PROGRAM PURPOSE:          THIS IS A DRIVER PROGRAM USED TO
C                               EXECUTE ONE OR A SERIES OF IMAGE
C                               PROCESSING SUBROUTINES.  THE
C                               SUBROUTINE PROCESSED IS DEPENDENT
C                               UPON THE VALUE OF THE VARIABLE ISUB
C                               AS LISTED BELOW:
C                    ISUB       SUBROUTINE CALLED
C                    ----       ---------- ------
C                       1       TODWIN-WRITE A DESIRED WINDOW
C                               TAPE TO DISK
C                       2       SPAXFM - SPATIAL FREQUENCY TRANSFORM
C                       3       GRALEV - GRAY LEVEL HISTO
C                               TO TEKTRONIX
C                       4       DUMMY  - NOT USED AT PRESENT TIME
C                       5       DUMPSC - DUMP PICTURE TO
C                               SCANNER (6-BIT)
C                       6       DUMPTV - DUMP PICTURE TO TV
C                       7       GNCOPY - COPY A PICTURE FROM ONE
C                               DEVICE TO ANOTHER
C                       8       GRAMAP - GRAY LEVEL MAPPING
C                       9       DUMMY  - NOT USED AT PRESENT TIME
C                      10       JITTER - JITTER
C                      11       GNOISE - DEGRADE WITH RANDOM
C                               GAUSSIAN NOISE
C                      12       DIGDEG - DIGITIZATION DEGRADED
C                      13       HGRALS - SAMPLING DEGRADED -
C                               HIGH ALIASING
C                      14       REDALS - SAMPLING DEGRADED -
C                               REDUCED ALIASING
C                      99                - END PROGRAM
C
C     PROGRAM DATE:             2/19/77
C     PROGRAMMERS:              GERI CUTHBERT/ DR R.H. COFER
C
C
C     NOTE:   ALL  SUBROUTINES WILL BE RESPONSIBLE FOR READING
C     DATA REQUIRED, REWINDING DEVICES, AND WRITING EOF'S.
C
C          FORMAT FOR INPUT FROM CARDS IS A10
```

BEST AVAILABLE COPY

```
C       DETERMINE WHICH SUBROUTINE TO EXECUTE
   10 CONTINUE
      READ(ICR,8000)ISUB
      IF(ISUB.EQ.99)GO TO 9999
      GO TO (100,200,300,400,500,600,700,800,900,1000,
     1       1100,1200,1300,1400),ISUB
C
C       EXECUTE SUBROUTINE TODWIN - WRITE WINDOW SEGMENT
  100 CONTINUE
C
C       SUBROUTINE VARIABLES READ IN TODWIN - 8I10 FORMAT
C          M,N     - MAIN PICTURE SIZE(M=NO OF LINES,
C                    N=NO OF SPOTS/LINE)
C          MM      - LOCATION OF FIRST LINE IN WINDOW
C          NN      - LOCATION OF FIRST DESIRED SPOT IN MM
C          II      - NO OF LINES TO BE TRANSFERRED
C          JJ      - NO OF SPOT/LINE TO BE TRANSFERRED
C          ID1     - INPUT FILE NUMBER
C          ITF1    - FILE NO OF INPUT IF TAPE
C          ID2     - OUTPUT FILE NO
C          ITF2    FILE NO OF OUTPUT IF TAPE
C
C       READ(ICR,8000)M,N,MM,NN,II,JJ
C       READ(ICR,8000) ID1,ITF1,ID2,ITF2
C
        CALL TODWIN
        GO TO 10
C
  200 CONTINUE
C
C       EXECUTE SUBROUTINE SPAXFM - COMPUTE THE SPATIAL TRANSFORM
C
C          IF1     - INPUT FILE NUMBER
C          ID2     - DISK FILE OF WINDOWED AREA
C          IRS     - START ROW OF THE WINDOW
C          N       - SIZE OF WINDOW (MUST BE SQUARE)
        CALL TODWIN
C       READ IN THE NECESSARY VARIABLES
        READ(ICR,8000)ID2,N
        CALL SPAXFM(ID2,N)
        GO TO 10
C
```

BEST AVAILABLE COPY

```
C      EXECUTE  GRLEV2 - GRAY LEVEL HISTO TO TEKTRONICS
C
  300 CONTINUE
C      EXECUTE GRALEV- PLOT HISTOGRAM OF GRAY VALUES
       CALL GRALEV
       GO TO 10
C
C      EXECUTE SUBROUTINE          - SPECTRAL FREQ XFRM
  400 CALL DUMMY
       GO TO 10
  500 CONTINUE
C
C      EXECUTE SUBROUTINE DUMPSC - DUMP PICTURE TO SCANNER(6-BITS)
C      SUBROUTINE VARIABLES READ IN DUMPSC
C         ID1     - DISK FILE NUMBER
C         ITF1    - FILE NO OF INPUT IF TAPE
C         II      - NO OF LINES TO BE TRANSFERRED
C         JJ      - NO OF SPOT/LINE TO BE TRANSFERRED
C         NFDPT   - 1ST DATA POINT TO BE TRANSFERRED
C         NBITS   - NUMBER OF BITS/PIXEL(8-BIT DATA OR 6-BIT DATA)
C
C      READ(ICR,8000) ID1,ITF1,II,JJ,NFDPT,NBITS
C
       CALL DUMPSC
       GO TO 10
C
C      EXECUTE SUBROUTINE DUMPTV - DUMP PICTURE TO TV

  600 CALL DUMMY
       GO TO 10
C
  700 CONTINUE
C
C      EXECUTE SUBROUTINE GNCOPY - COPY A PICTURE FROM
C                                  ONE DEVICE TO ANOTHER
C      SUBROUTINE VARIABLES READ IN GNCOPY
C         ID1     - INPUT DEVICE NUMBER
C         ITF1    - FILE NO OF INPUT IF TAPE
C         ID2     - OUTPUT DEVICE NUMBER
C         ITF2    FILE NO OF OUTPUT IF TAPE
C         II      - NO OF LINES TO BE TRANSFERRED
C         JJ      - NO OF SPOT/LINE TO BE TRANSFERRED
```

BEST AVAILABLE COPY

```
C
C     READ(ICR,8000)ID1,ITF1,ID2,ITF2,II,JJ
C
      CALL GNCOPY
      GO TO 10
C
  800 CONTINUE
C     EXECUTE SUBROUTINE GRAMAP - GRAY LEVEL MAPPING
C     VARIABLES TO BE READ IN BY GRAMAP
C        ID1     - DEVICE NO OF INPUT PICTURE
C        ITF1    - FILE NO OF INPUT IF TAPE
C        ID2     - DEVICE NO OF OUTPUT PICTURE
C        ITF2    FILE NO OF OUTPUT IF TAPE
C        IMAX    - MAXIMUM PICTURE VALUE
C        II      NO OF LINES TO BE TRANSFERRED
C        JJ      - NO OF SPOTS/LINE TO BE TRANSFERRED
C
C     READ(ICR,8000)ID1,ITF1,ID2,ITF2,IMAX,II,JJ
C
      CALL GRAMAP
      GO TO 10
C
C     EXECUTE SUBROUTINE LININT - LINE INTENSITY DEGRADATION
  900 CALL DUMMY
      GO TO 10
C
C     EXECUTE SUBROUTINE JITTER - JITTER
 1000 CONTINUE
C     VARIABLES TO BE READIN IN BY JITTER
C        ID1     - DEVICE NO OF THE INPUT PICTURE
C        ITF1    - FILE NO OF INPUT IF TAPE
C        ID2     - DEVICE NUMBER OF OUTPUT PICTURE
C        ITF2    FILE NO OF OUTPUT IF TAPE
C        II      - NO OF LINES TO BE TRANSFERRED
C        JJ      - NO OF SPOTS/LINE TO BE TRANSFERRED
C        ISD     - STANDARD DEVIATION
C        IMN     - MEAN
C        ISEED   - SEED FOR GRN GENERATOR
C
C     READ(ICR,8000)ID1,ITF1,ID2,ITF2,II,JJ
C     READ(ICR,8000)ISD,IMN,ISEED
C
```

BEST AVAILABLE COPY

AD-A049 798 HARRIS CORP MELBOURNE FLA ELECTRONIC SYSTEMS DIV F/G 9/4
DIGITAL IMAGERY TEST SET.(U)
NOV 77 R H COFER, A R MARTIN

UNCLASSIFIED RADC-TR-77-371 F30602-76-C-0296 NL

3 OF 3
AD A049798



END
DATE FILMED
3-78
DDC

```
      CALL JITTER
      GO TO 10
 1100 CONTINUE
C     EXECUTE SUBROUTINE GNOISE - DEGRADE WITH RANDOM  GAUSSIAN
C     NOISE
C     SUBROUTINE VARIABLES READ IN GNOISE
C        ID1     - DEVICE NO OF INPUT PICTURE
C        ITF1    - FILE NO OF INPUT IF TAPE
C        ID2     - DEVICE NO OF OUTPUT PICTURE
C        ITF2    FILE NO OF OUTPUT IF TAPE
C        II      - NO OF LINES TO BE TRANSFERRED
C        JJ      - NO OF SPOT/LINE TO BE TRANSFERRED
C        IMAX    - MAXIMUM PICTURE VALUE
C        ISD     - STANDARD DEVIATION
C        IMN     - SPECIFIED MEAN
C        ISEED   - SEED FOR GRN GENERATOR
C        ISL     = 0 - ADD A DIFFERENT RV TO EACH SPOT IN PICTURE
C                = 1 - ADD A DIFFERENT RV TO EACH LINE IN PICTURE
C
C     READ(ICR,8000)ID1,ITF1,ID2,ITF2,II,JJ
C     READ(ICR,8000)IMAX,ISD,IMN,ISEED,ISL
C
      CALL GNOISE
      GO TO 10
 1200 CONTINUE
C     EXECUTE SUBROUTINE DIGDEG - DIGITIZATION DEGRADED
C
C     VARIABLES READ IN DIGDEG
C        ID1     - DEVICE NO OF INPUT PICTURE
C        ITF1    - FILE NO OF INPUT IF TAPE
C        ID2     - DEVICE NO OF OUTPUT PICTURE
C        ITF2    FILE NO OF OUTPUT IF TAPE
C        II      NO OF LINES TO BE TRANSFERRED
C        JJ      - NO OF SPOTS/LINE TO BE TRANSFERRED
C        NBIT    - NO OF BITS TO SHIF (CANNOT BE 0)
C
C     READ(ICR,8000)ID1,ITF1,ID2,ITF2,II,JJ,NBIT
C
      CALL DIGDEG
      GO TO 10
 1300 CONTINUE
C     EXECUTE SUBROUTINE HGHALS - SAMPLING DEGRADED HIGH ALAIS-
      ING
```

BEST AVAILABLE COPY

```
C      VARIABLES READ IN HGHALS
C         ID1     - DEVICE NO OF INPUT PICTURE
C         ITF1    - FILE NO OF INPUT IF TAPE
C         ID2     - DEVICE NO OF OUTPUT PICTURE
C         ITF2    FILE NO OF OUTPUT IF TAPE
C         II      NO OF LINES TO BE TRANSFERRED
C         JJ      - NO OF SPOTS/LINE TO BE TRANSFERRED
C         ISIZE   - POWER OF 2 REDUCTIONS IN SIZE
C
C      READ(ICR,8000)ID1,ITF1,ID2,ITF2,II,JJ,ISIZE
C
       CALL HGHALS
       GO TO 10
 1400  CONTINUE
C      EXECUTE SUBROUTINE REDALS - SAMPLING DEGRADED
C                                  REDUCED ALIASING
       CALL REDALS
       GO TO 10
C
C      END PROGRAM
 9999  CONTINUE
       CALL EXIT
 8000  FORMAT(8I10)
       END
```

BEST AVAILABLE COPY

```
      SUBROUTINE TODWIN
      COMMON/IDATA/IBUF1(4096),IBUF2(4096)
      DATA ICR,ILP,ITTY/7,6,1/
C
C     SUBROUTINE PURPOSE:     WRITE A DESIRED WINDOW SEGMENT FROM
C                             TAPE TO DISK
C
C     INITIALIZE IBUF1 AND IBUF2
      DO 10 K=1,4096
      IBUF1(K)=0
   10 IBUF2(K)=0
C
C
C     READ IN NECESSARY VARIABLES
C        M,N     - MAIN PICTURE SIZE(M=NO OF LINES,
C                    N=NO OF SPOTS/LINE)
C        MM      - LOCATION OF FIRST LINE IN WINDOW
C        NN      - LOCATION OF FIRST DESIRED SPOT IN MM
C        II      - NO OF LINES TO BE TRANSFERRED
C        JJ      - NO OF SPOT/LINE TO BE TRANSFERRED
C        ID1     - INPUT FILE NUMBER
C        ITF1    - FILE NO OF INPUT IF TAPE
C        ID2     - OUTPUT FILE NO
C        ITF2    FILE NO OF OUTPUT IF TAPE
      READ(ICR,8000)M,N,MM,NN,II,JJ
      READ(ICR,8000) ID1,ITF1,ID2,ITF2
      REWIND ID1
      REWIND ID2
C     SET THE VALUES OF IWORD AND ILINE
      IWORD=(NN+JJ)-1
      ILINE =(MM+II)-1
C
C     ADVANCE TO CORRECT FILE NO  IF NECESSARY
      IF(ITF1.LE.1)GO TO 3
      DO 1 K=2,ITF1
    1 CALL ADF(ID1)
    3 CONTINUE
      IF(ITF2.LE.1)GO TO 5
      DO 4 K=2,ITF2
    4 CALL ADF(ID2)
    5 CONTINUE
C     ADVANCE TO FIRST LINE IN WINDOW
```

BEST AVAILABLE COPY

```
      IF(MM.EQ.1)GO TO 70
      IADV=MM-1
      DO 65 K=1,IADV
      BUFFER IN(ID1,IBUF1,B,N,ISTAT)
   50 CALL STATUS(ID1)
      GO TO (50,65,60),ISTAT
   60 WRITE(ITTY,9010)
      STOP
   65 CONTINUE
   70 CONTINUE
C     READ IN WINDOW AND WRITE TO DISK
      DO 100 I=MM,ILINE
      BUFFER IN(ID1,IBUF1,B,N,ISTAT)
   80 CALL STATUS(ID1)
      GO TO (80,85,90),ISTAT
   90 WRITE(ITTY,9020)
      STOP
   85 CONTINUE
C
C     CHECK TO SEE IF THE WHOLE LINE SHOULD GO TO THE DISK
      IF(IWORD.EQ.N)GO TO 300
C
C     TRANSFER THE NECESSARY WORDS TO IBUF2
      KK=0
      DO 200 K=NN,IWORD
      KK=KK+1
  200 IBUF2(KK)=IBUF1(K)
C
C     WRITE THIS BUFFER TO THE DISK
      BUFFER OUT(ID2,IBUF2,B,JJ,ISTAT)
  210 CALL STATUS(ID2)
      GO TO (210,220,220),ISTAT
  220 GO TO 100
C
C     WRITE THE WHOLE LINE TO THE DISK
  300 BUFFER OUT(ID2,IBUF1,B,N,ISTAT)
  240 CALL STATUS(ID2)
      GO TO(240,100,100),ISTAT
  100 CONTINUE
C
C     DATA TRANSFER SHOULD BE COMPLETE
      END FILE ID2
      REWIND ID1
      REWIND ID2
      RETURN
 8000 FORMAT(8I10)
 9010 FORMAT(1X,'EOF ENCOUNTERED IN ADVANCING TO WINDOW')
 9020 FORMAT(1X,'EOF ENCOUNTERED DURING WINDOW PROCESSING')
      END
```


BEST AVAILABLE COPY

```
      SUBROUTINE SPAXFM(ID2,N)
C     OUTPUT SAMPLE SPATIAL TRANSFORM VALUES
      COMMON/IDATA/IBUF1(4096),IBUF2(4096)
      DIMENSION IU(512),IV(512),A(512),P(512),R(512)
      DATA IYES/3HYES/
C
C        IU      - ROW NUMBER
C        IV      - COLUMN NUMBER
C        R       - SQRT(IU**2+IV**2)--(VALUES FOR X-AXIS PLOT)
C        A       - AMPLITUDE VALUES
C        P       - PHASE VALUES
C        ID2     - DISK FILE OF PICTURE
C
      PI=3.14159265
C
C     READ IN X MIN AND MAX
C     READ IN Y MIN AND MAX -IN DB)
      READ(7,50)AMINR,AMAXR,AMINA,AMAXA
   50 FORMAT(4F10.3)
      NRUN=0
  100 CONTINUE
      NS=0
      NRUN=NRUN+1
C     READ IN SPATIAL SAMPLING FREQUENCY LOCATIONS
    1 READ(7,2) IUD,IVD,IFLAG
    2 FORMAT(2I5,11)
      NS=NS+1
      A(NS)=0.
      P(NS)=0.
      IU(NS)=IUD
      IV(NS)=IVD
      R(NS)=SQRT(FLOAT(IUD)**2+FLOAT(IVD)**2)
      IF(IFLAG.EQ.1) GO TO 3
      GO TO 1
C
C     START THE TRANSFORM PROCESS
    3 CONST=-6.2831853/FLOAT(N)
C     DO THE ROWS FIRST FOR MINIMAL DISK ACCESS
      REWIND ID2
      DO 4 IX1=1,N
      IX=IX1-1
      BUFFER IN(ID2,IBUF1,B,N,ISTAT)
```

BEST AVAILABLE COPY

```
   29  CALL STATUS(ID2)
       GO TO (20,25,25),ISTAT
   25 CONTINUE
C      DO THE COLUMNS NEXT FOR MINIMAL DISK ACCESS
       DO 4 IY1=1,N
       IY=IY1-1
C      GET THE SPOTS VALUE
       VAL=FLOAT(IBUF1(IY1))
       VAL=1.1**VAL
C      ADD IN EFFECT AT EACH SAMPLE SPATIAL FREQUENCY
       DO 4 K=1,NS
       ARG=CONST*FLOAT(IX*IU(K)+IY*IV(K))
C      TEMPORARLY STORE REAL PART IN P, IMAG PART IN A
       A(K)=A(K)-VAL*SIN(ARG)
       P(K)=P(K)+VAL*COS(ARG)
    4 CONTINUE
C
C      DO FINAL PROCESSING
       DO 5 K=1,NS
       A(K)=A(K)/FLOAT(N)**2
       P(K)=P(K)/FLOAT(N)**2
       ABSOLU =10.*ALOG10(A(K)**2+P(K)**2)
       P(K)=ATAN2(A(K),P(K))
       A(K)=ABSOLU
    5 CONTINUE
      WRITE(6,6)
    6 FORMAT(' SAMPLE#,U,V,AMPLITUDE, PHASE')
      DO 7 I=1,NS
      ANG=P(1)*57.29578
    7 WRITE(6,8) I,IU (1),IV (1),A(1),ANG
    8 FORMAT(1X,3I10,2 (3X,E15.8))
      CALL PLOTIT(NRUN,NS,R(1),A(1),0.0,0.0,0.0,0.0,10.0,10.0)
      IF(NRUN.LT.3)GO TO 100
      CALL HDCOPY
      RETURN
      END
```

BEST AVAILABLE COPY

```
      SUBROUTINE GRALEV
      COMMON /IDATA/IBUF1(4096),IBUF2(4096)
      DIMENSION IGRA(256),AX(256),AY(256)
      DATA ICR,ILP,ITK /7,6,21/
C
C     SUBROUTINE PURPOSE: PLOT A PICTURE HISTOGRAM ON TEKTRONIX
C     VARIABLES:
C        M,N     - PICTURE SIZE (M=NO OF LINES,N=NO OF SPOTS)
C        ID1     - INPUT FILE
C
      READ(ICR,8000)ID1,M,N
 8000 FORMAT(8I10)
C
C     INITIALIZE IGRA BUFFER
      DO 10 I=1,256
   10 IGRA(I)=0
      ASUM =0.0
      ADIV=FLOAT(M)*FLOAT(N)
C
C     GET IN DATA, COUNT GRAY VALUES
C     ACCUMULATE SUM FOR MEAN CALCULATION
      DO 50 I=1,M
      BUFFER IN(ID1,IBUF1,6,N,ISTAT)
   20 CALL STATUS(ID1)
      GO TO (20,30,30),ISTAT
   30 DO 40 J=1,N
      VAL =IBUF1(J)-128
      ASUM=ASUM+VAL
      IV=IBUF1(J)
   40 IGRA(IV)=IGRA(IV)+1
   50 CONTINUE
C
C     COMPUTE MEAN
      ASUM=(ASUM/ADIV)+128.
C
C     SET UP THE TEKTRONIX HISTO
      DO 60 I=1,256
      AX(I)=FLOAT(I-1)
   60 AY(I)=FLOAT(IGRA(I))
      WRITE(6,9900)(AX(I),AY(I),I=1,256)
      WRITE(6,9900)ASUM
 9900 FORMAT(8(2X,F10.3))
```

BEST AVAILABLE COPY

```
      CALL INITT(960)
      CALL BINITT
      CALL TERM (1,1024)
      CALL NPTS(256)
C
C     GET THE MIN & MAX FOR THE Y-AXIS
      YMIN = 10000.0
      YMAX= -10000.0
      CALL MNMX(AY,YMIN,YMAX)
      CALL DLIMX(0.0,255.0)
      CALL DLIMY(YMIN,YMAX)
      CALL VBARST(8,5,3)
      CALL CHECK(AX,AY)
      CALL DSPLAY(AX,AY)
C
C     WRITE OUT THE MEAN
      CALL PNTABS(60,30)
      CALL ANMODE
      WRITE(ITK,9020)ASUM
 9020 FORMAT(1H+,'MEAN = ',F10.4)
C
C     GET A HARDCOPY
      CALL TINPUT(IC)
      CALL FINITT(0,0)
      RETURN
      END



      SUBROUTINE DUMMY
C     DUMMY SUB
      X=1
      RETURN
      END
```

BEST AVAILABLE COPY

```
      SUBROUTINE DUMPSC
      COMMON/IDATA/IBUF1(4096),IBUF2(4096)
      DATA ICR,ILP,ITTY/7,6,1/
C
C     SUBROUTINE PURPOSE      OUTPUT AN UPACKED 6-BIT
C                             PICUTRE TO SCANNER
C
C     READ IN NECESSARY VARIABLES
C        ID1     - DISK FILE NUMBER
C        ITF1    - FILE NO OF INPUT IF TAPE
C        II      - NO OF LINES TO BE TRANSFERRED
C        JJ      - NO OF SPOT/LINE TO BE TRANSFERRED
C        NFDPT   - 1ST DATA POINT TO BE TRANSFERRED
C        NBITS   - NUMBER OF BITS/PIXEL
C
      READ(ICR,8000) ID1,ITF1,II,JJ,NFDPT,NBITS
C     ADVANCE TO CORRECT FILE NO  IF NECESSARY
      IF(ITF1.LE.1)GO TO 3
      DO 1 K=2,ITF1
    1 CALL ADF(ID1)
    3 CONTINUE
      DO 100 I=1,II
C     GET THE DATA FROM THE DISK
C
      BUFFER IN(ID1,IBUF1,8,JJ,ISTAT)
   20 CALL STATUS(ID1)
      GO TO (20,30,30),ISTAT
C
C     CHECK FOR 6-BIT OR 8-BIT DATA
   30 CONTINUE
      IF(NBITS.EQ.8)CALL SIXBIT(JJ)
      CALL OTSCAN(IBUF1,NFDPT,JJ,IERR)
      IF(IERR.NE.0)WRITE(ITTY,9000)IERR
  100 CONTINUE
C
C     PICTURE SHOULD BE PROCESSED
      WRITE(ITTY,9010)
      RETURN
 8000 FORMAT(8I10)
 9000 FORMAT(1X,'ERROR IN OUTPUT TO SCANNER',I5)
 9010 FORMAT(1X,'PICTURE PROCESSED')
      END
```

BEST AVAILABLE COPY

```
      SUBROUTINE SIXBIT(JJ)
      COMMON /IDATA/ IBUF1(4096),IBUF2(4096)
      DATA ICR,ILP,ITTY/7,6,1/
C
C     SUBROUTINE PURPOSE:     CONVERT 8 BIT DATA TO 6 BIT DATA BY
C                             REMOVING TWO LSB (SHIFT RIGHT 2)
C
C        JJ      - NO OF PIXELS/LINE
      DO 10 I=1,JJ
   10 IBUF1(I)=IBUF1(I).SHIFT.-2
      RETURN
      END
```

BEST AVAILABLE COPY

```
      SUBROUTINE GNCOPY
      COMMON /IDATA/IBUF1(4096),IBUF2(4096)
      DATA ICR,ILP,ITTY/7,6,1/
C     SUBROUTINE PURPOSE:    DUMP A PICTURE FROM ONE DEVICE
C                            TO ANOTHER
C                                 (DISK TO DISK)  (DISK TO TAPE)
C                                 (TAPE TO TAPE)  (TAPE TO DISK)
C
C     READ IN NECESSARY VARIABLES:
C        ID1     - INPUT DEVICE NUMBER
C        ITF1    - FILE NO OF INPUT IF TAPE
C        ID2     - OUTPUT DEVICE NUMBER
C        ITF2    FILE NO OF OUTPUT IF TAPE
C        II      - NO OF LINES TO BE TRANSFERRED
C        JJ      - NO OF SPOT/LINE TO BE TRANSFERRED
C
      READ(ICR,8000)ID1,ITF1,ID2,ITF2,II,JJ
C
C     REWIND THE DEVICES
      REWIND ID1
C
C     ADVANCE TO CORRECT FILE NO  IF NECESSARY
      IF(ITF1.LE.1)GO TO 3
      DO 1 K=2,ITF1
    1 CALL ADF(ID1)
    3 CONTINUE
      IF(ITF2.LE.1)GO TO 5
      DO 4 K=2,ITF2
    4 CALL ADF(ID2)
    5 CONTINUE
      DO 100 I=1,II
C     GET THE INPUT DATA
      BUFFER IN(ID1,IBUF1,B,JJ,ISTAT)
   20 CALL STATUS(ID1)
      GO TO(20,30,30),ISTAT
   30 CONTINUE
C     WRITE THE DATA TO THE OUTPUT DEVICE
      BUFFER OUT(ID2,IBUF1,B,JJ,ISTAT)
   50 CALL STATUS(ID2)
      GO TO (50,60,60),ISTAT
   60 CONTINUE
  100 CONTINUE
C     DATA TRANSFER SHOULD BE COMPLETE
      END FILE ID2
      REWIND ID1
      WRITE(ITTY,9000)
      RETURN
 9000 FORMAT(1X,'COPY COMPLETED')
 8000 FORMAT(8I10)
      END
```


BEST AVAILABLE COPY

```
      SUBROUTINE GRAMAP
      COMMON/IDATA/IBUF1(4096),IBUF2(4096)
      DIMENSION IN(100),IO(100),IOUT(1000)
      DATA ICR,ILP,ITY/7,6,1/
C     PURPOSE--TO REMAP THE GRAY LEVEL OF A WINDOW
C     VARIABLES TO BE READ IN BY GRAMAP
C        ID1     - DEVICE NO OF INPUT PICTURE
C        ITF1    - FILE NO OF INPUT IF TAPE
C        ID2     - DEVICE NO OF OUTPUT PICTURE
C        ITF2    FILE NO OF OUTPUT IF TAPE
C        IMAX    - MAXIMUM PICTURE VALUE
C        II      - NO OF LINES TO BE TRANSFERRED
C        JJ      - NO OF SPOTS/LINE TO BE TRANSFERRED
C     SET UP INTERNAL DIMENSIONING LIMITS
      MAXBPS=100
      MAXPTS=1000
C     READ IN USUAL VARIABLES
      READ(ICR,8000)ID1,ITF1,ID2,ITF2,IMAX,II,JJ
      IMAX=IMAX+1
C     NOTE THAT IMAX HERE REFERS TO THE TOTAL NUMBER
C     OF GRAY LEVELS
C
C     REWIND THE DEVICES
      REWIND ID1
C     ADVANCE TO CORRECT FILE NO  IF NECESSARY
      IF(ITF1.LE.1)GO TO 3
      DO 1 K=2,ITF1
    1 CALL ADF(ID1)
    3 CONTINUE
      IF(ITF2.LE.1)GO TO 5
      DO 4 K=2,ITF2
    4 CALL ADF(ID2)
    5 CONTINUE
C     READ IN BREAK POINTS OF MAPPING FUNCTION
      DO 21  IBP=1,MAXBPS
      READ(ICR,8000) I1,I2,I3
      IF(I3.NE.0) GO TO 41
      IN(IBP)=I1+1
   21 IO(IBP)=I2
      WRITE(ITY,31)
   31 FORMAT(' READ IN TOO MANY GRAY-LEVEL MAPPING BREAKPTS-
     1STOPPING')
      STOP
```


BEST AVAILABLE COPY

```
   41 IF(IMAX.LE.MAXPTS) GO TO 6
      WRITE(ITY,51)
   51 FORMAT(' NOT ENOUGH MEMORY FOR GRAY LEVEL MAPPING-STOPPING'
      STOP
    6 IBP=IBP-2
      DO 9 I=1,IMAX
      DO 7 J=1,IBP
    7 IF(I.GE.IN(J).AND.I.LE.IN(J+1)) GO TO 11
      WRITE(ITY,8)
    8 FORMAT(' THE GRAY LEVEL SPECIFICATION IS WRONG-STOPPING')
      STOP
   11 CONTINUE
      X=              FLOAT((IO(J+1)-IO(J))*(I-IN(J)))/FLOAT
     * (IN(J+1)-IN(J))
      IF(X.GE.0) IOUT(I)=IFIX(X+.5+IO(J))
      IF(X.LT.0) IOUT(I)=IFIX(X+.499+IO(J))
    9 CONTINUE
C     PERFORM THE MAPPING
      DO 100 I=1,II
      BUFFER IN(ID1,IBUF1,B,JJ,ISTAT)
   20 CALL STATUS(ID1)
      GO TO(20,30,30),ISTAT
   30 CONTINUE
      DO 40 J=1,JJ
      IV=IBUF1(J)+1
   40 IBUF2(J)=IOUT(IV)
C     WRITE OUT THE MAPPED PICTURE
      BUFFER OUT(ID2,IBUF2,B,JJ,ISTAT)
   50 CALL STATUS(ID2)
      GO TO (50,100,100),ISTAT
  100 CONTINUE
C     CLOSE FILES
      END FILE ID2
      REWIND ID1

      RETURN
 8000 FORMAT(8I10)
      END
```

BEST AVAILABLE COPY

```
      SUBROUTINE JITTER
      COMMON /ILDATA/IBUF1(4096),IBUF2(4096)
      DATA ICR,ILP,ITTY/7,6,1/
C
C     SUBROUTINE PURPOSE - CREATE RANDOM LINE JITTER
C     SUBROUTINE VARIABLES
C        ID1     - DEVICE NO OF THE INPUT PICTURE
C        ITF1    - FILE NO OF INPUT IF TAPE
C        ID2     - DEVICE NUMBER OF OUTPUT PICTURE
C        ITF2    FILE NO OF OUTPUT IF TAPE
C        II      - NO OF LINES TO BE TRANSFERRED
C        JJ      - NO OF SPOTS/LINE TO BE TRANSFERRED
C        ISD - STANDARD DEVIATION
C        IMN     - MEAN
C        ISEED   - SEED FOR GRN GENERATOR
C
C     INTIALIZE IBUF1
      DO 10 I=1,4096
   10 IBUF1(I)=0
C
C     READ IN THE VARIABLES
      READ(ICR,8000)ID1,ITF1,ID2,ITF2,II,JJ
      READ(ICR,8000)ISD,IMN,ISEED
C
C     CONVERT MEAN & STD DEV TO FLOATING POINT
      SD=FLOAT(ISD)/1000.
      XMEAN = FLOAT(IMN)
C     REWIND THE DEVICES
      REWIND ID1
C     ADVANCE TO CORRECT FILE NO  IF NECESSARY
      IF(ITF1.LE.1)GO TO 3
      DO 1 K=2,ITF1
    1 CALL ADF(ID1)
    3 CONTINUE
      IF(ITF2.LE.1)GO TO 5
      DO 4 K=2,ITF2
    4 CALL ADF(ID2)
    5 CONTINUE
C     OPERATE ON THE PICTURE
      DO 100 I=1,II
C
      GET THE INPUT LINE
```

BEST AVAILABLE COPY

```
      BUFFER IN(ID1,IBUF1,B,JJ,ISTAT)
   20 CALL STATUS(ID1)
      GO TO (20,25,25),ISTAT
C     GET A GAUSSIAN RV AND SET IJITT
   25 CALL RNORM(SAMP,ISEED,SD,XMEAN)
      IJITT=IFIX(SAMP+0.5)
C
C     CLEAR THE OUTPUT LINE TO ZERO
      DO 30 J=1,JJ
   30 IBUF2(J)=0
      IF(IABS(IJITT).GE.JJ)GO TO 90
C     PUT IN THE JITTER
      IF(IJITT.GE.0)GO TO 50
      IJ=IABS(IJITT)+1
      J1=0
      DO 40 J=IJ,JJ
      J1=J1+1
   40 IBUF2(J1)=IBUF1(J)
      GO TO 90
   50 CONTINUE
      IJ=IJITT+1
      J1=0
      DO 60 J=IJ,JJ
      J1=J1+1
   60 IBUF2(J)=IBUF1(J1)
   90 CONTINUE
C
C     PUT OUT THE LINE
      BUFFER OUT(ID2,IBUF2,B,JJ,ISTAT)
   70 CALL STATUS(ID2)
      GO TO (70,100,100),ISTAT
  100 CONTINUE
      END FILE ID2
      REWIND ID1
      RETURN
 8000 FORMAT(8I10)
      END
```

BEST AVAILABLE COPY

```
      SUBROUTINE GNOISE
      COMMON /IDATA/IBUF1(4096),IBUF2(4096)
      DATA ICR,ILP,ITTY/7,6,1/
C
C     SUBROUTINE VARIABLES READ IN GNOISE
C        ID1     - DEVICE NO OF INPUT PICTURE
C        ITF1    - FILE NO OF INPUT IF TAPE
C        ID2     - DEVICE NO OF OUTPUT PICTURE
C        ITF2    - FILE NO OF OUTPUT IF TAPE
C        II      - NO OF LINES TO BE TRANSFERRED
C        JJ      - NO OF SPOT/LINE TO BE TRANSFERRED
C        IMAX    - MAXIMUM PICTURE VALUE
C        ISD     - STANDARD DEVIATION
C        IMN     - SPECIFIED MEAN
C        ISEED   - SEED FOR GRN GENERATOR
C        ISL     = 0 - ADD A DIFFERENT RV TO EACH SPOT IN PICTURE
C                = 1 - ADD A DIFFERENT RV TO EACH LINE IN PICTURE
C
C     INITIALIZE IBUF1 & IBUF2
      DO 10 I=1,4096
      IBUF1(I)=0
   10 IBUF2(I)=0
C
C     READ IN THE VARIABLES
      READ(ICR,8000)ID1,ITF1,ID2,ITF2,II,JJ
      READ(ICR,8000)IMAX,ISD,IMN,ISEED,ISL
C
C     CONVERT MEAN  AND STD DEV TO FLOATING POINT
      SD=FLOAT(ISD)/1000.
      XMEAN=FLOAT(IMN)
C     REWIND THE INPUT AND OUTPUT DEVICES
      REWIND ID1
C     ADVANCE TO CORRECT FILE NO  IF NECESSARY
      IF(ITF1.LE.1)GO TO 3
      DO 1 K=2,ITF1
    1 CALL ADF(ID1)
    3 CONTINUE
      IF(ITF2.LE.1)GO TO 5
      DO 4 K=2,ITF2
    4 CALL ADF(ID2)
    5 CONTINUE
C     OPERATE ON THE PICTURE
      DO 100 I=1,II
C     IF ADDING RV TO THE LINE, GET THE RV
      IF(ISL.EQ.1)CALL RNORM(SAMP,ISEED,SD,XMEAN)
      BUFFER IN(ID1,IBUF1,0,JJ,ISTAT)
   20 CALL STATUS(ID1)
      GO TO (20,30,30),ISTAT
   30 CONTINUE
```


BEST AVAILABLE COPY

```
      DO 50 J=1,JJ
C     IF ADDING RV TO EACH SPOT, GET THE RV
      IF(ISL.EQ.0)CALL RNORM(SAMP,ISEED,SD,XMEAN)
C     ADD IN THE NOISE
      IBUF2(J)=IFIX(FLOAT(IBUF1(J))+SAMP+0.5)
      IF(IBUF2(J).LT.0)IBUF2(J)=0
      IF(IBUF2(J).GT.IMAX)IBUF2(J)=IMAX
   50 CONTINUE
C
C     WRITE OUT THE NOISY PICTURE
      L=L+1
      BUFFER OUT(ID2,IBUF2,6,JJ,ISTAT)
   60 CALL STATUS(ID2)
      GO TO (60,70,70),ISTAT
   70 CONTINUE
      CALL RNORM(SAMP,ISEED,SD,XMEAN)
      CALL RNORM(SAMP,ISEED,SD,XMEAN)
      CALL RNORM(SAMP,ISEED,SD,XMEAN)
  100 CONTINUE
C
C     REWIND THE DEVICES
      END FILE ID2
      REWIND ID1
      RETURN
 8000 FORMAT(8I10)
      END
```

BEST AVAILABLE COPY

```
      SUBROUTINE DIGDEG
      COMMON/IDATA/IBUF1(4096),IBUF2(4096)
      DATA ICR,ILP,ITY/7,6,1/
C     SUBROUTINE PURPOSE - DEGRADE BY RECODING DIGITIZATION
C     VARIABLES READ IN DIGDEG
C        ID1     - DEVICE NO OF INPUT PICTURE
C        ITF1    - FILE NO OF INPUT IF TAPE
C        ID2     - DEVICE NO OF OUTPUT PICTURE
C        ITF2    - FILE NO OF OUTPUT IF TAPE
C        II      - NO OF LINES IN INPUT PICTURE
C        JJ      - NO OF SPOTS/LINE TO BE TRANSFERRED
C        NBIT    - NO OF BITS TO BE SHIFTED (RIGHT)
C     READ IN THE NECESSARY VARIABLES
      READ(ICR,8000)ID1,ITF1,ID2,ITF2,II,JJ,NBIT
      IF(NBIT.EQ.0)WRITE(ITY,9000)NBIT
      IF(NBIT.GT.7)WRITE(ITY,9000)NBIT
C
C     REWIND THE DEVICES
      REWIND ID1
C     ADVANCE TO CORRECT FILE NO  IF NECESSARY
      IF(ITF1.LE.1)GO TO 3
      DO 1 K=2,ITF1
    1 CALL ADF(ID1)
    3 CONTINUE
      IF(ITF2.LE.1)GO TO 5
      DO 4 K=2,ITF2
    4 CALL ADF(ID2)
    5 CONTINUE
C
C     DEGRADE THE PICTURE
      ID1V=2**NBIT
      DO 100 I=1,II
      BUFFER IN (ID1,IBUF1,3,JJ,ISTAT)
   20 CALL STATUS(ID1)
      GO TO (20,30,30),ISTAT
   30 CONTINUE
C
C     DEGRADE THE SPOT BY SHIFTING
C     TO ACCOMPLISH THE SHIFT DIVIDE BY 2**NBIT
      DO 40 J=1,JJ
   40 IBUF2(J)=IBUF1(J)/ID1V*ID1V
C
```

BEST AVAILABLE COPY

```
C       WRITE OUT THE NEW BUFFER
        BUFFER OUT(ID2,IBUF2,3,JJ,ISTAT)
   50   CALL STATUS(ID2)
        GO TO(60,100,100),ISTAT
  100   CONTINUE
C
C       CLOSE OUT THE FILES
        END FILE ID2
        REWIND ID1
        RETURN
 8000   FORMAT(8I10)
 9000   FORMAT(1X,'SHIFT VALUE WRONG, NII=',I5)
        END
```

BEST AVAILABLE COPY

```
      SUBROUTINE REDALS
      COMMON/IDATA/IBUF1(4096),IBUF2(4096)
      DATA ICR,ILP/7,6/
C     SUBROUTINE VARIABLES USED IN REDALS
C        ID1    - DEVICE NO OF INPUT PICTURE
C        ITF1   - FILE NO OF INPUT IF TAPE
C        ID2    - DEVICE NO OF OUTPUT PICTURE
C        ITF2   FILE NO OF OUTPUT IF TAPE
C        II     - NO OF LINES TO TRANSFERRED
C        JJ     - NO OF SPOTS/LINE TO BE TRANSFERRED
C        ISIZE  - POWER OF 2 REDUCTIONS IN SIZE
C        IMAX   - MAXIMUM PICTURE VALUE


C     INITALIZE IBUF1 & IBUF2
      DO 10 I=1,4096
      IBUF1(I)=0
   10 IBUF2(I)=0
C
C     READ IN THE VARIABLES
      READ(ICR,8000)ID1,ITF1,ID2,ITF2,II,JJ,ISIZE

      IF(ISIZE.LE.0)RETURN
C     GET THE CORRECT ROW AND COLUMN OFFSETS
      IROW=IFIX(FLOAT(II)*(1.-    1.    /FLOAT(ISIZE))/2.)-1
      ICOL=IFIX(FLOAT(JJ)*(1.-      1. /FLOAT(ISIZE))/2.)-1
      ISZ=ISIZE**2
C     REWIND THE INPUT AND OUTPUT DEVICES
      REWIND ID1
C     ADVANCE TO CORRECT FILE NO  IF NECESSARY
      IF(ITF1.LE.1)GO TO 3
      DO 1 K=2,ITF1
    1 CALL ADF(ID1)
    3 CONTINUE
      IF(ITF2.LE.1)GO TO 5
      DO 4 K=2,ITF2
    4 CALL ADF(ID2)
    5 CONTINUE
C
C     OPERATE ON THE PICTURE
C
C     INSERT THE TOP BORDER
      L=1
      DO 102 I=1,IROW
      L=L+1
      BUFFER OUT(ID2,IBUF2,8,JJ,ISTAT)
  103 CALL STATUS(ID2)
      GO TO (103,102,102),ISTAT
```


BEST AVAILABLE COPY

```
  102 CONTINUE
      DO 100 I=1,II,ISIZE
      DO 132 I3=1,JJ
  132 IBUF2(I3)=0
      DO 107 I111=1,ISIZE
      BUFFER IN(ID1,IBUF1,B,JJ,ISTAT)
   20 CALL STATUS(ID1)
      GO TO (20,30,30),ISTAT
   30 CONTINUE
      K=ICOL
      DO 143 I3=1,JJ,ISIZE
      K=K+1
      I3MAX=I3+ISIZE-1
      DO 143 I4=I3,I3MAX
  143 IBUF2(K)=IBUF2(K)+IBUF1(I4)
  107 CONTINUE
      L=L+1
      K=ICOL
      DO 144 IS=1,JJ,ISIZE
      K=K+1
  144 IBUF2(K)=IBUF2(K)/ISZ
C
C     WRITE OUT THE NOISY PICTURE
      BUFFER OUT(ID2,IBUF2,B,JJ,ISTAT)
   60 CALL STATUS(ID2)
      GO TO (60,70,70),ISTAT
   70 CONTINUE
  100 CONTINUE
C
C     INSERT THE BOTTOM BORDER
      DO 104 I=1,JJ
  104 IBUF2(I)=0
      DO 105 I=L,II
      BUFFER OUT(ID2,IBUF2,B,JJ,ISTAT)
  106 CALL STATUS(ID2)
      GO TO (106,105,105),ISTAT
  105 CONTINUE
C
C     REWIND THE DEVICES
      END FILE ID2
      REWIND ID1
      RETURN
 8000 FORMAT(8I10)
      END
```

```
      SUBROUTINE HGHALS
      COMMON/IDATA/IBUF1(4096),IBUF2(4096)
      DATA ICR,ILP/7,6/
C     SUBROUTINE VARIABLES USED IN HGHALS
C        ID1    - DEVICE NO OF INPUT PICTURE
C        ITF1   - FILE NO OF INPUT IF TAPE
C        ID2    - DEVICE NO OF OUTPUT PICTURE
C        ITF2   FILE NO OF OUTPUT IF TAPE
C        II     - NO OF LINES TO TRANSFERRED
C        JJ     - NO OF SPOTS/LINE TO BE TRANSFERRED
C        ISIZE - POWER OF 2 REDUCTIONS IN SIZE
C        IMAX   - MAXIMUM PICTURE VALUE


C     INTIALIZE IBUF1 & IBUF2
      DO 10 I=1,4096
      IBUF1(I)=0
   10 IBUF2(I)=0
C
C     READ IN THE VARIABLES
      READ(ICR,8000)ID1,ITF1,ID2,ITF2,II,JJ,ISIZE

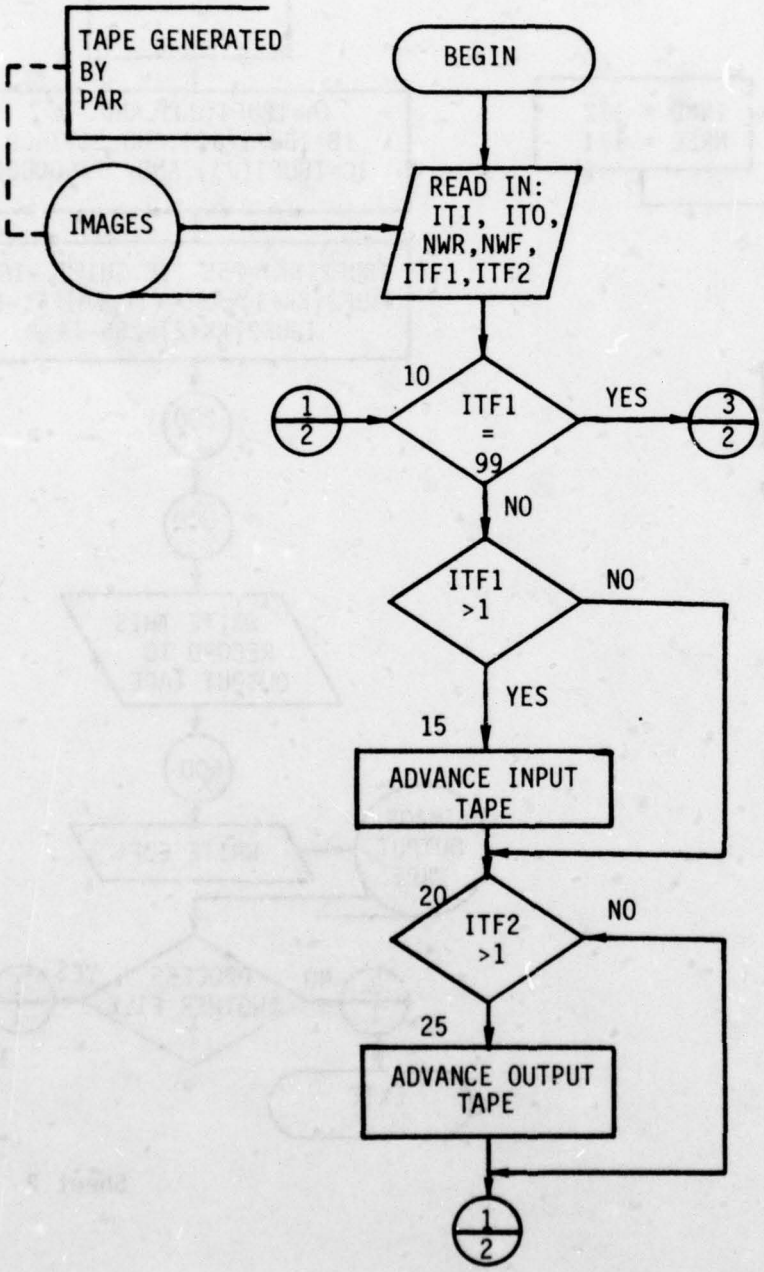
      IF(ISIZE.LE.0)RETURN
C     GET THE CORRECT ROW AND COLUMN OFFSETS
      IROW=IFIX(FLOAT(II)*(1.-    1.    /FLOAT(ISIZE))/2.)-1
      ICOL=IFIX(FLOAT(JJ)*(1.-      1. /FLOAT(ISIZE))/2.)-1
C     REWIND THE INPUT AND OUTPUT DEVICES
      REWIND ID1
C     ADVANCE TO CORRECT FILE NO  IF NECESSARY
      IF(ITF1.LE.1)GO TO 3
      DO 1 K=2,ITF1
    1 CALL ADF(ID1)
    3 CONTINUE
      IF(ITF2.LE.1)GO TO 5
      DO 4 K=2,ITF2
    4 CALL ADF(ID2)
    5 CONTINUE
C
C     OPERATE ON THE PICTURE
C
C     INSERT THE TOP BORDER
      L=1
      DO 102 I=1,IROW
      L=L+1
      BUFFER OUT(ID2,IBUF2,B,JJ,ISTAT)
  103 CALL STATUS(ID2)
      GO TO (103,102,102),ISTAT
  102 CONTINUE
      DO 100 I=1,II,ISIZE
      DO 107 I111=1,ISIZE
```

```
      BUFFER IN(ID1,IBUF1,B,JJ,ISTAT)
   20 CALL STATUS(ID1)
      GO TO (20,30,30),ISTAT
   30 CONTINUE
  107 CONTINUE
      K=ICOL
      DO 50 J=1,JJ,ISIZE
C     SAMPLE THE IMAGE
      K=K+1
      IBUF2(K)=IBUF1(J)
   50 CONTINUE
      L=L+1
C
C     WRITE OUT THE NOISY PICTURE
      BUFFER OUT(ID2,IBUF2,B,JJ,ISTAT)
   60 CALL STATUS(ID2)
      GO TO (60,70,70),ISTAT
   70 CONTINUE
  100 CONTINUE
C
C     INSERT THE BOTTOM BORDER
      DO 104 I=1,JJ
  104 IBUF2(I)=0
      DO 105 I=L,II
      BUFFER OUT(ID2,IBUF2,B,JJ,ISTAT)
  106 CALL STATUS(ID2)
      GO TO (106,105,105),ISTAT
  105 CONTINUE
C
C     REWIND THE DEVICES
      END FILE ID2
      REWIND ID1
      RETURN
 8000 FORMAT(8I10)
      END
```

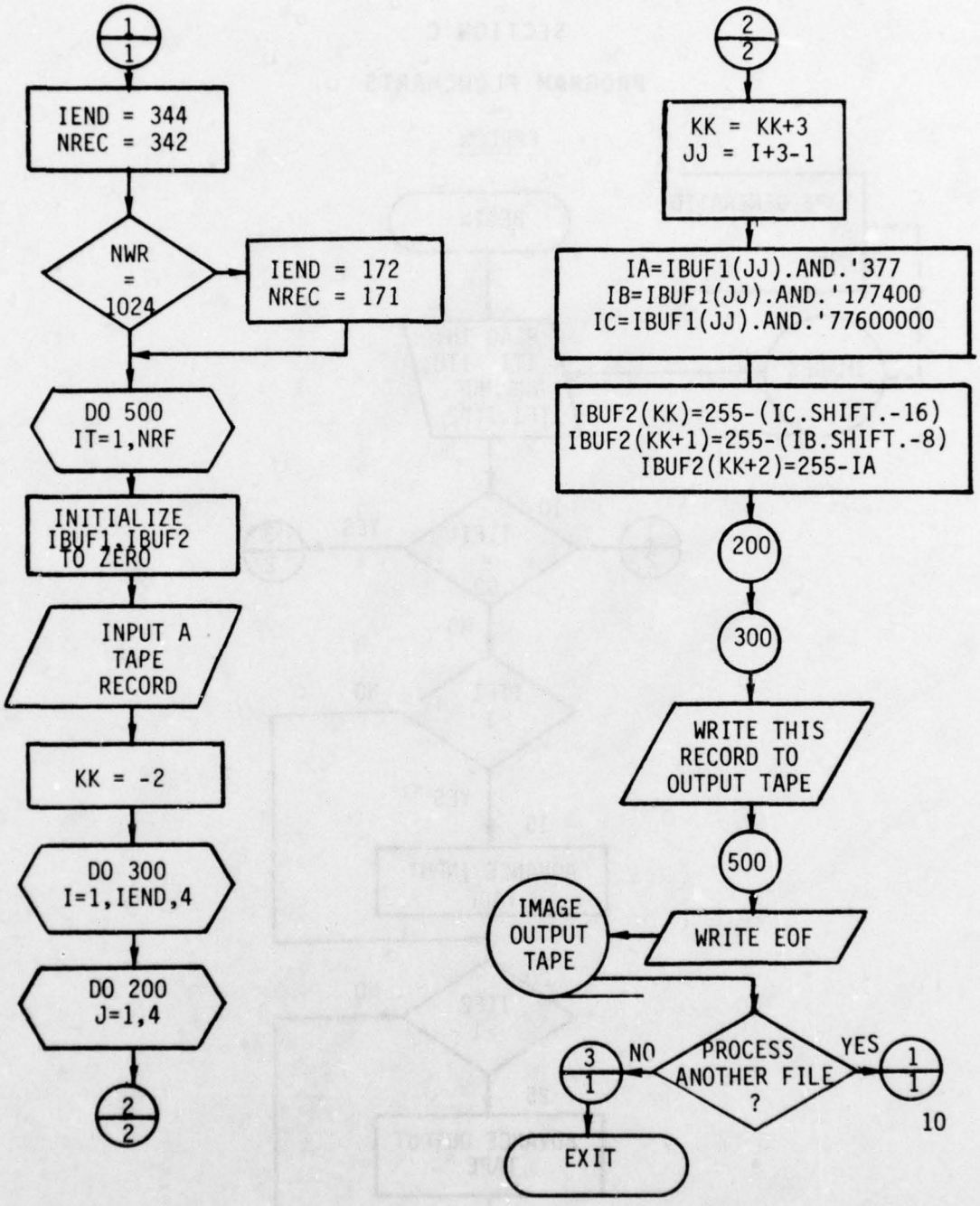
SECTION C

PROGRAM FLOWCHARTS

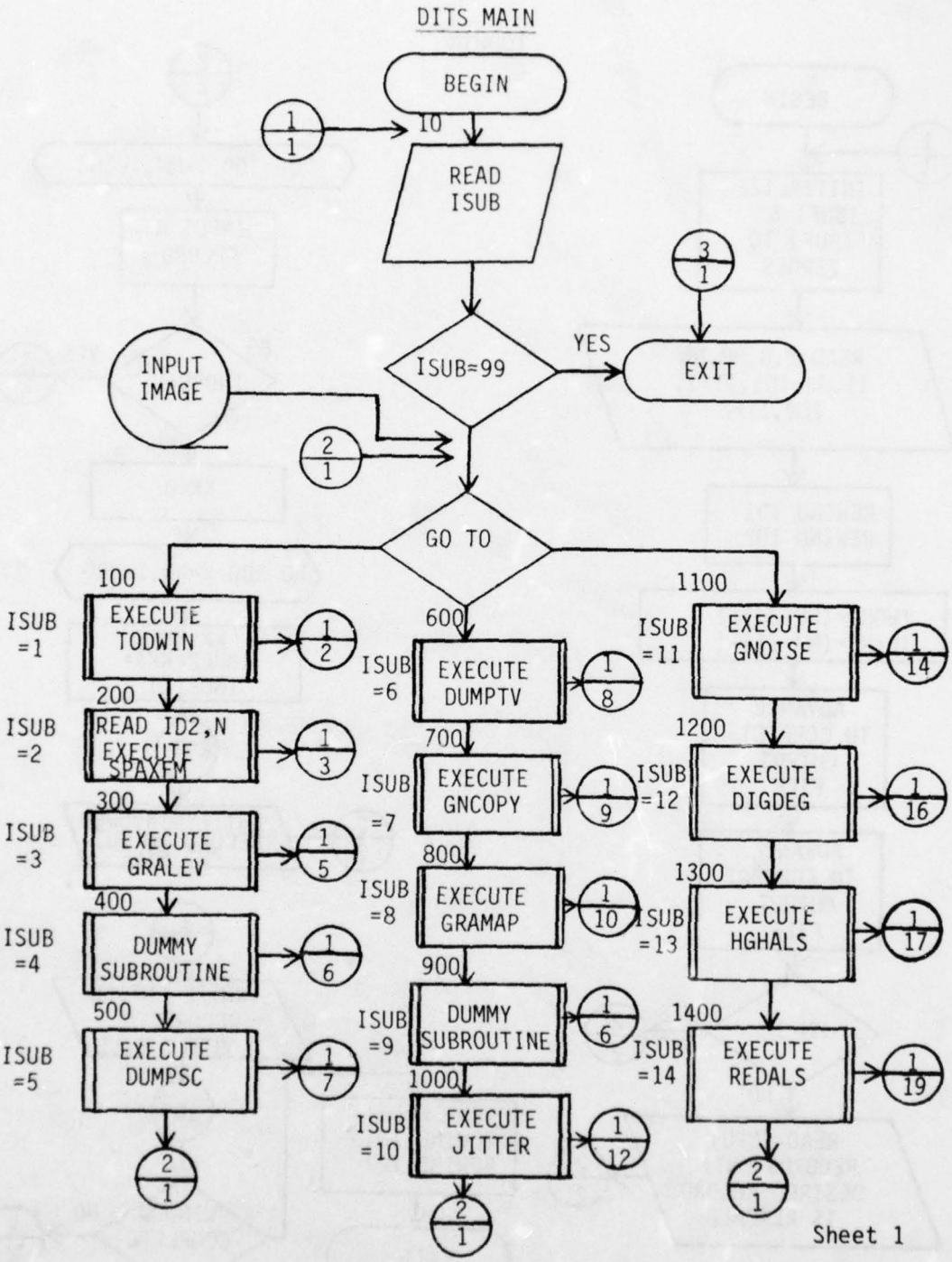
PARCON



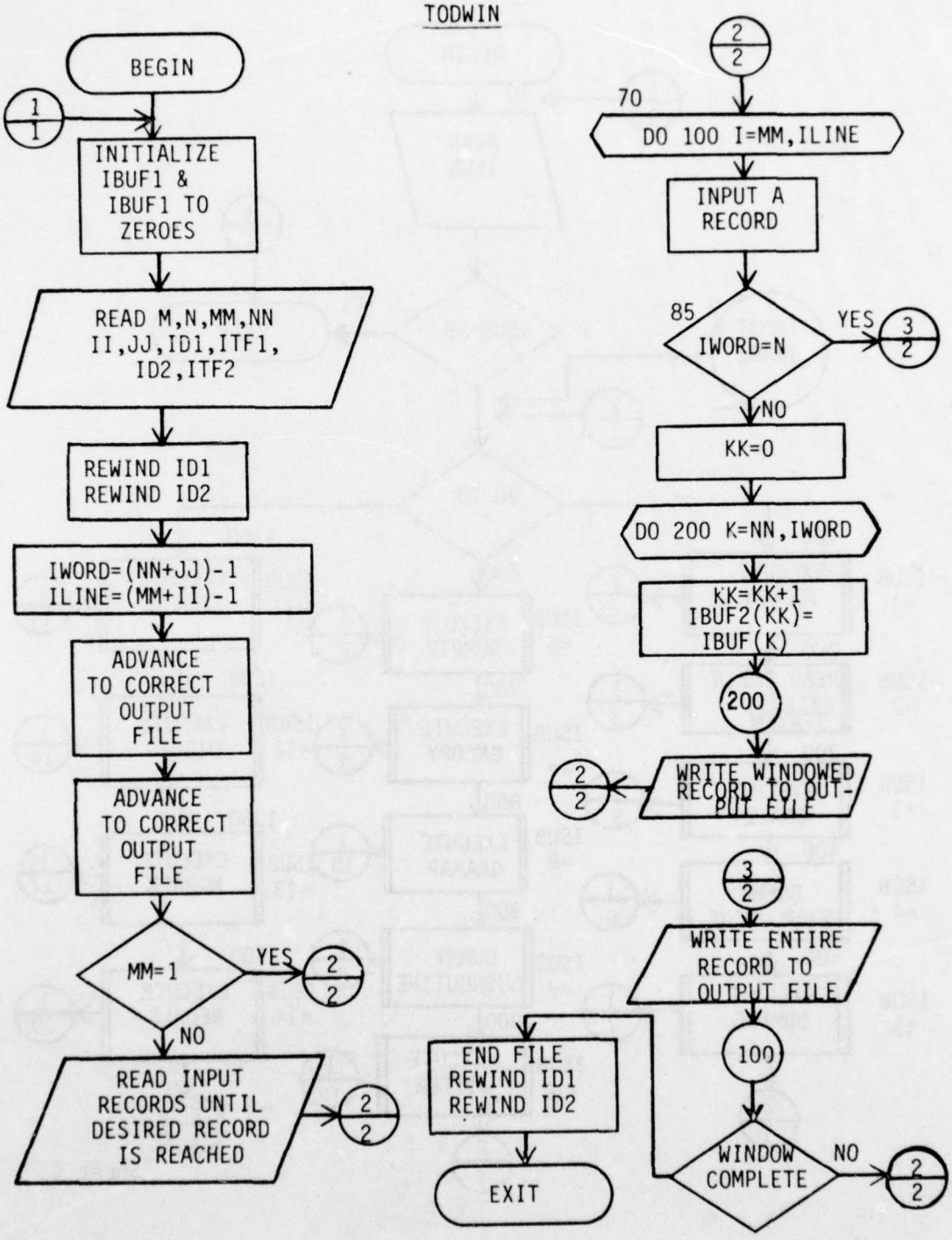
Sheet 1


1/1
IEND = 344
NREC = 342
NWR = 1024
IEND = 172
NREC = 171
DO 500 IT=1,NRF
INITIALIZE IBUF1,IBUF2 TO ZERO
INPUT A TAPE RECORD
KK = -2
DO 300 I=1,IEND,4
DO 200 J=1,4
2/2
2/2
KK = KK+3
JJ = I+3-1
IA=IBUF1(JJ).AND.'377
IB=IBUF1(JJ).AND.'177400
IC=IBUF1(JJ).AND.'77600000
IBUF2(KK)=255-(IC.SHIFT.-16)
IBUF2(KK+1)=255-(IB.SHIFT.-8)
IBUF2(KK+2)=255-IA
200
300
WRITE THIS RECORD TO OUTPUT TAPE
500
WRITE EOF
IMAGE OUTPUT TAPE
PROCESS ANOTHER FILE ?
NO
YES
3/1
1/1
10
EXIT

Sheet 2

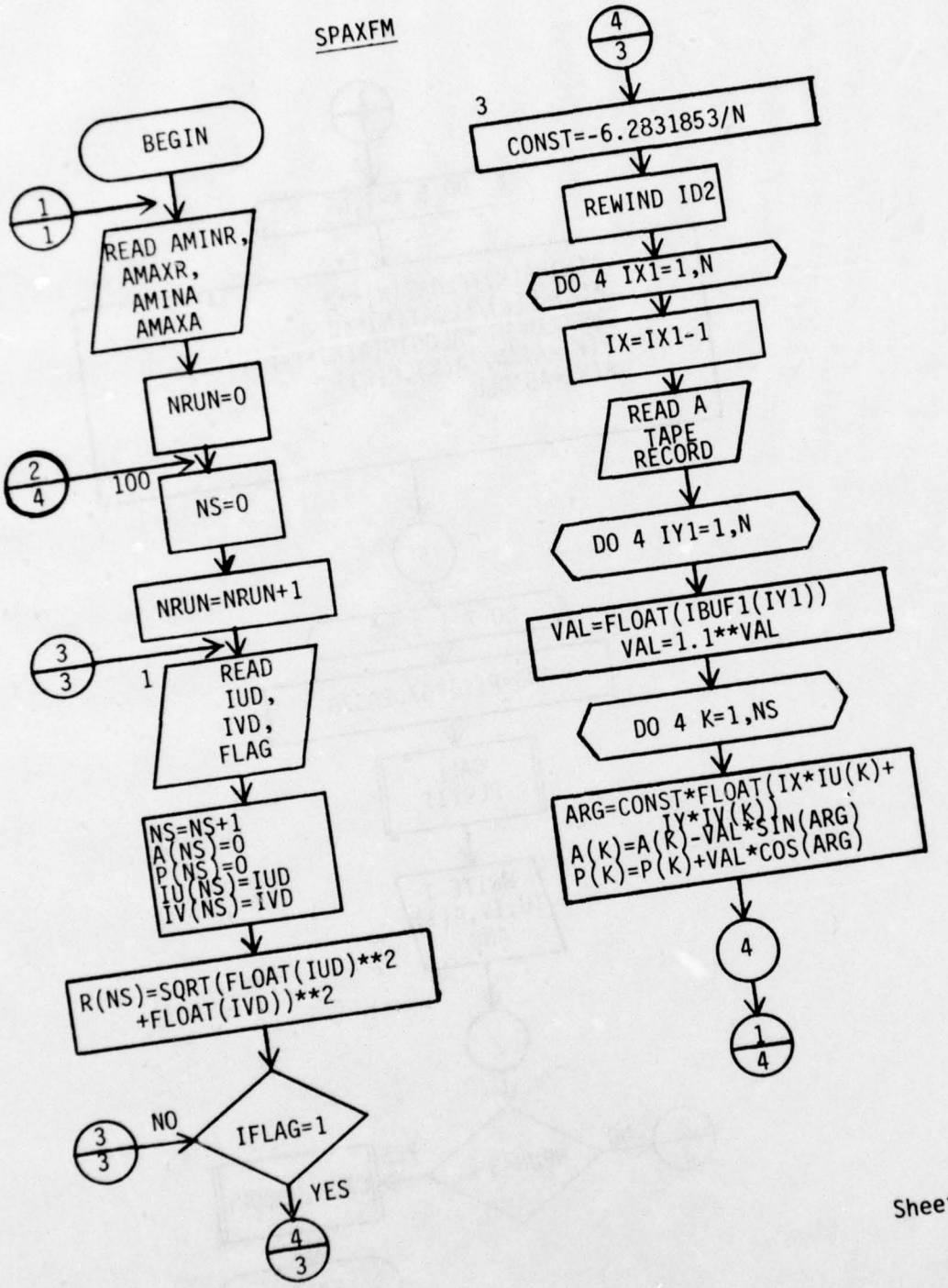

DITS MAIN
BEGIN
10
READ ISUB
ISUB=99
YES
EXIT
INPUT IMAGE
GO TO
100
ISUB =1
EXECUTE TODWIN
200
ISUB =2
READ ID2,N EXECUTE SPAXEM
300
ISUB =3
EXECUTE GRALEV
400
ISUB =4
DUMMY SUBROUTINE
500
ISUB =5
EXECUTE DUMPSC
600
ISUB =6
EXECUTE DUMPTV
700
ISUB =7
EXECUTE GNCOPY
800
ISUB =8
EXECUTE GRAMAP
900
ISUB =9
DUMMY SUBROUTINE
1000
ISUB =10
EXECUTE JITTER
1100
ISUB =11
EXECUTE GNOISE
1200
ISUB =12
EXECUTE DIGDEG
1300
ISUB =13
EXECUTE HGHALS
1400
ISUB =14
EXECUTE REDALS
Sheet 1

TODWIN

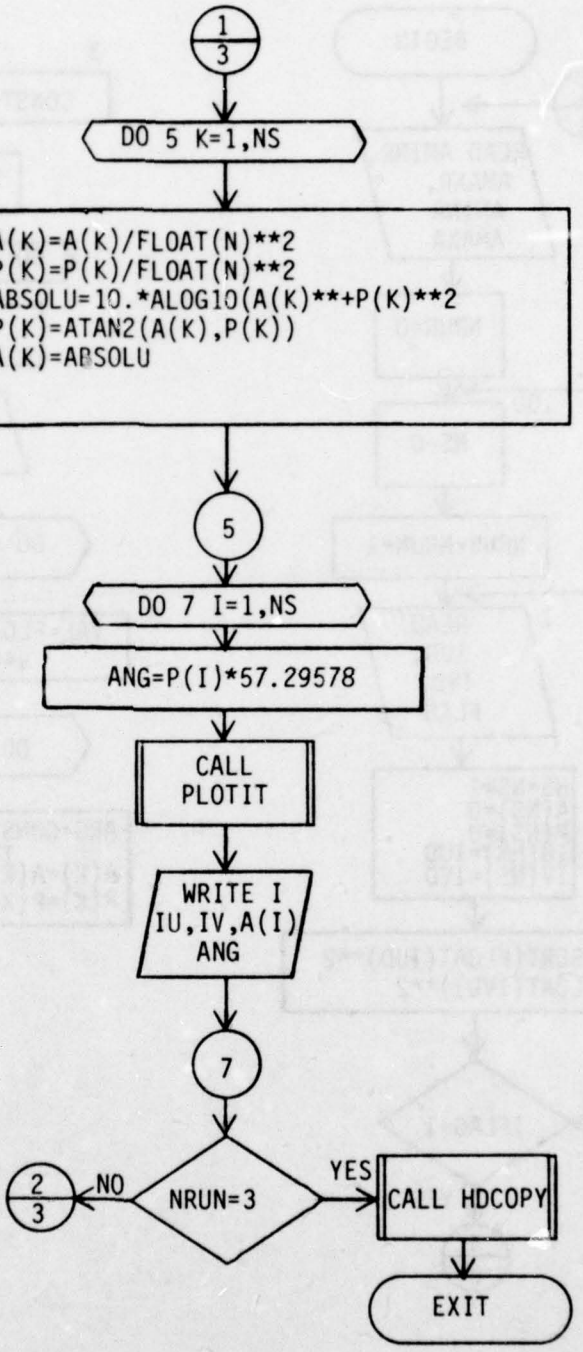


Sheet 2

SPAXFM

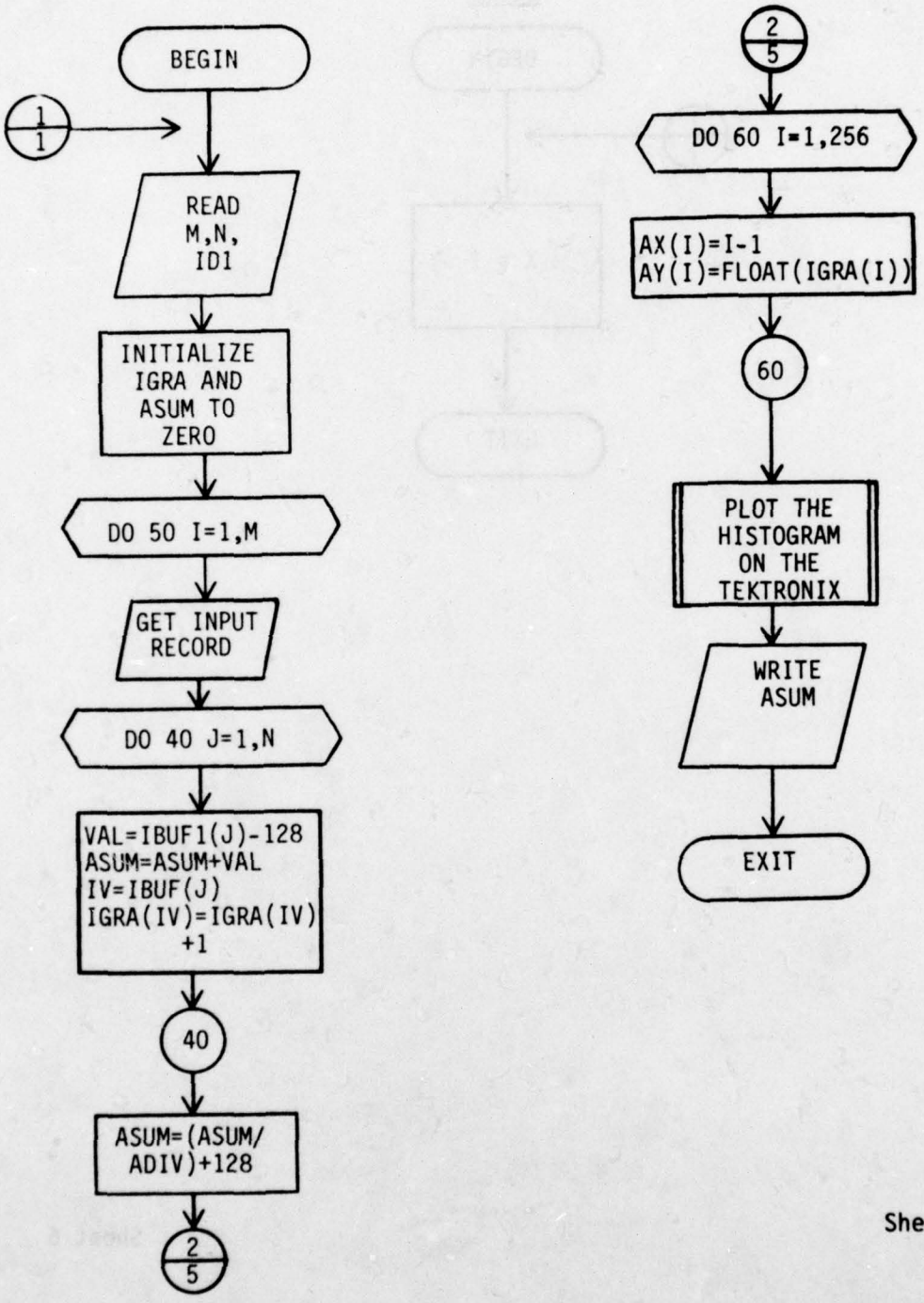


Sheet 3

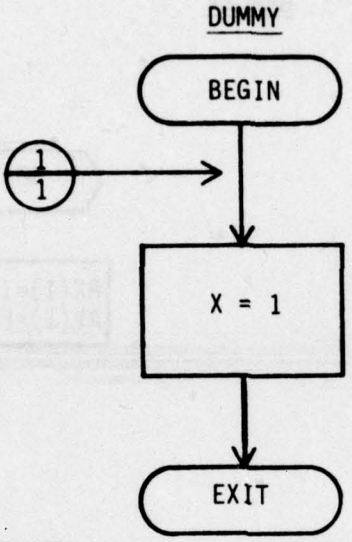

1/3
DO 5 K=1,NS
A(K)=A(K)/FLOAT(N)**2
P(K)=P(K)/FLOAT(N)**2
ABSOLU=10.*ALOG10(A(K)**+P(K)**2
P(K)=ATAN2(A(K),P(K))
A(K)=ABSOLU
5
DO 7 I=1,NS
ANG=P(I)*57.29578
CALL PLOTIT
WRITE I IU,IV,A(I) ANG
7
2/3
NO
NRUN=3
YES
CALL HDCOPY
EXIT

Sheet 4

GRALEV

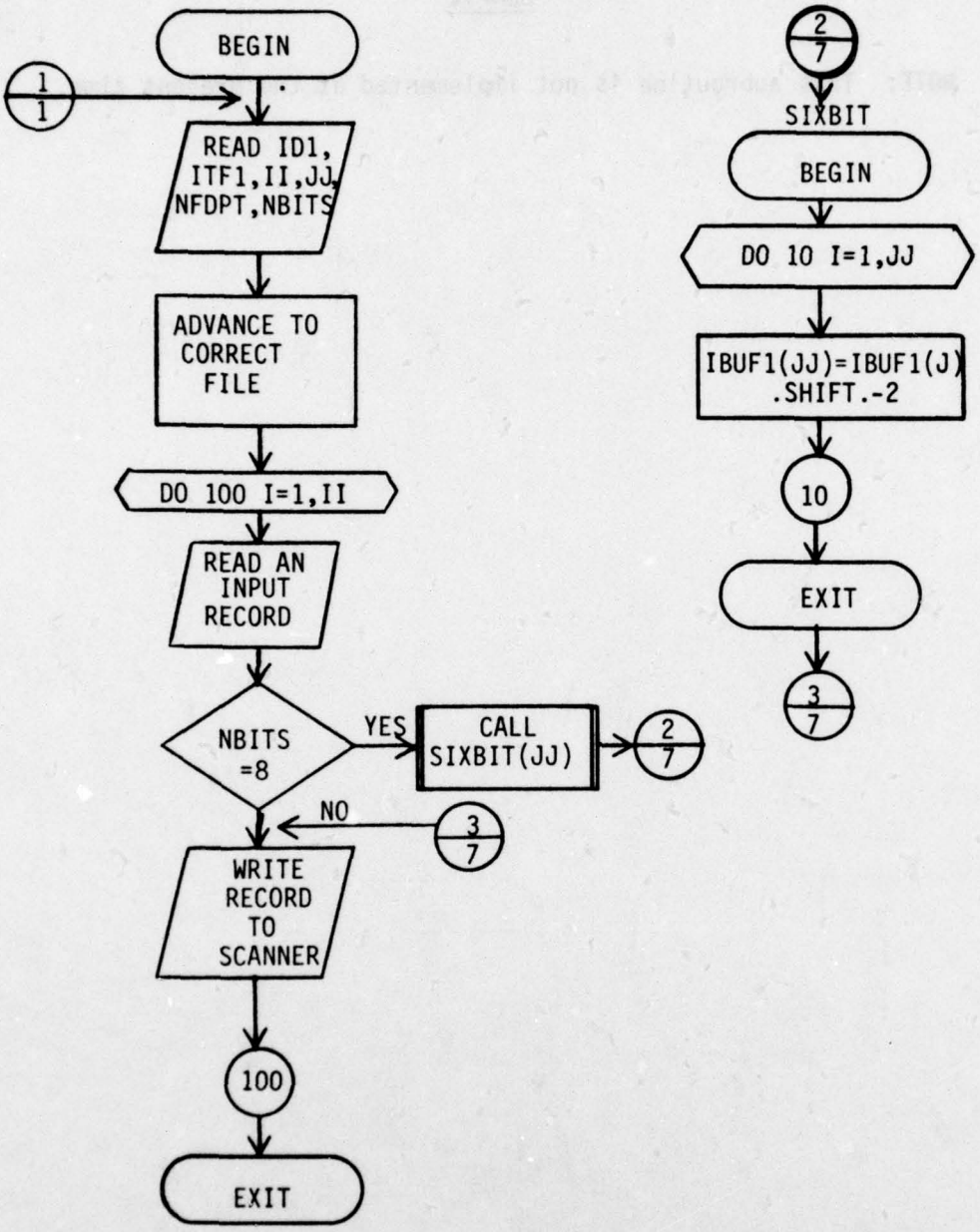


Sheet 5



Sheet 6

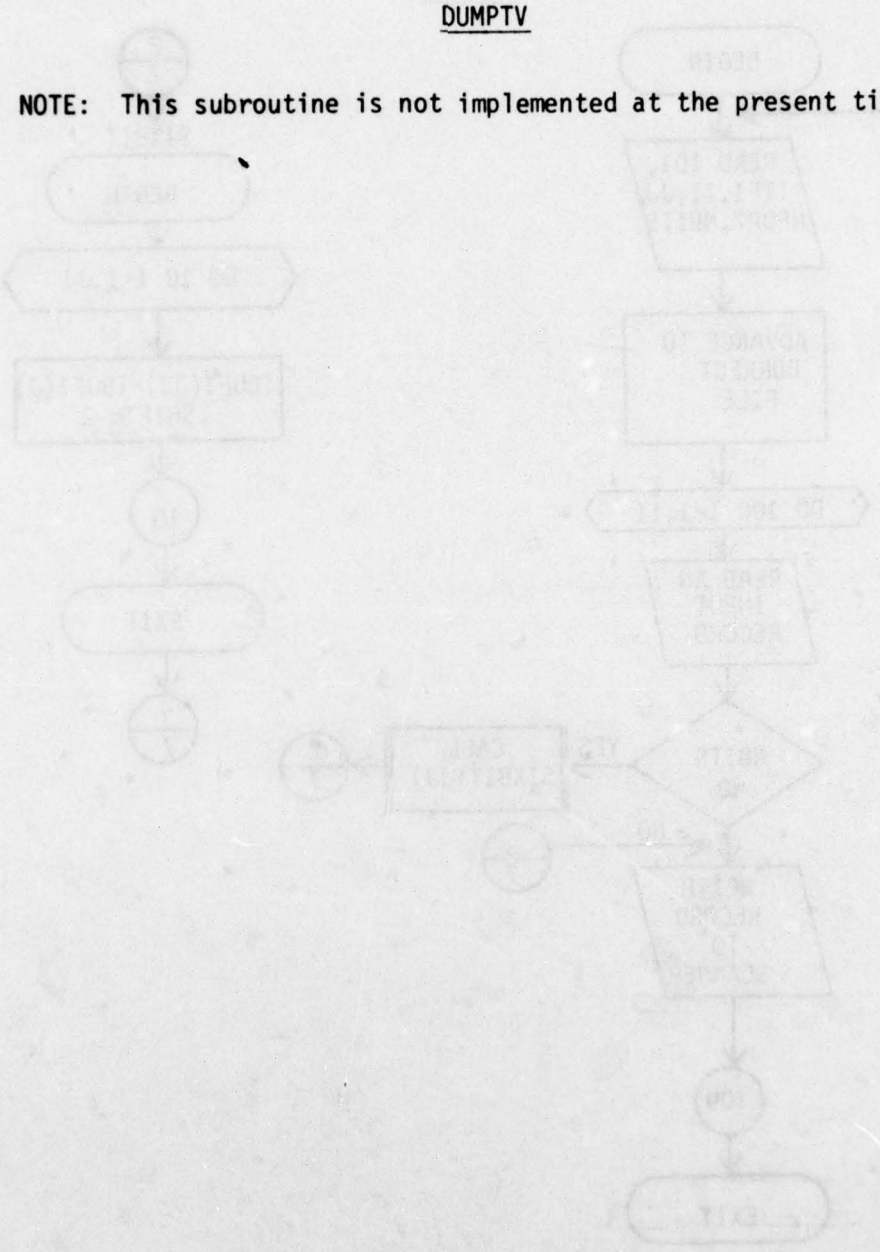
DUMPSC



Sheet 7

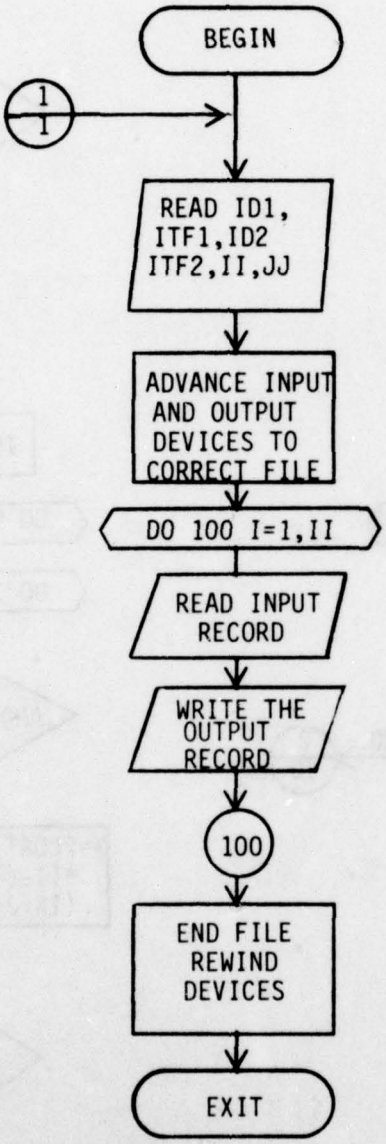
DUMPTV

NOTE: This subroutine is not implemented at the present time.

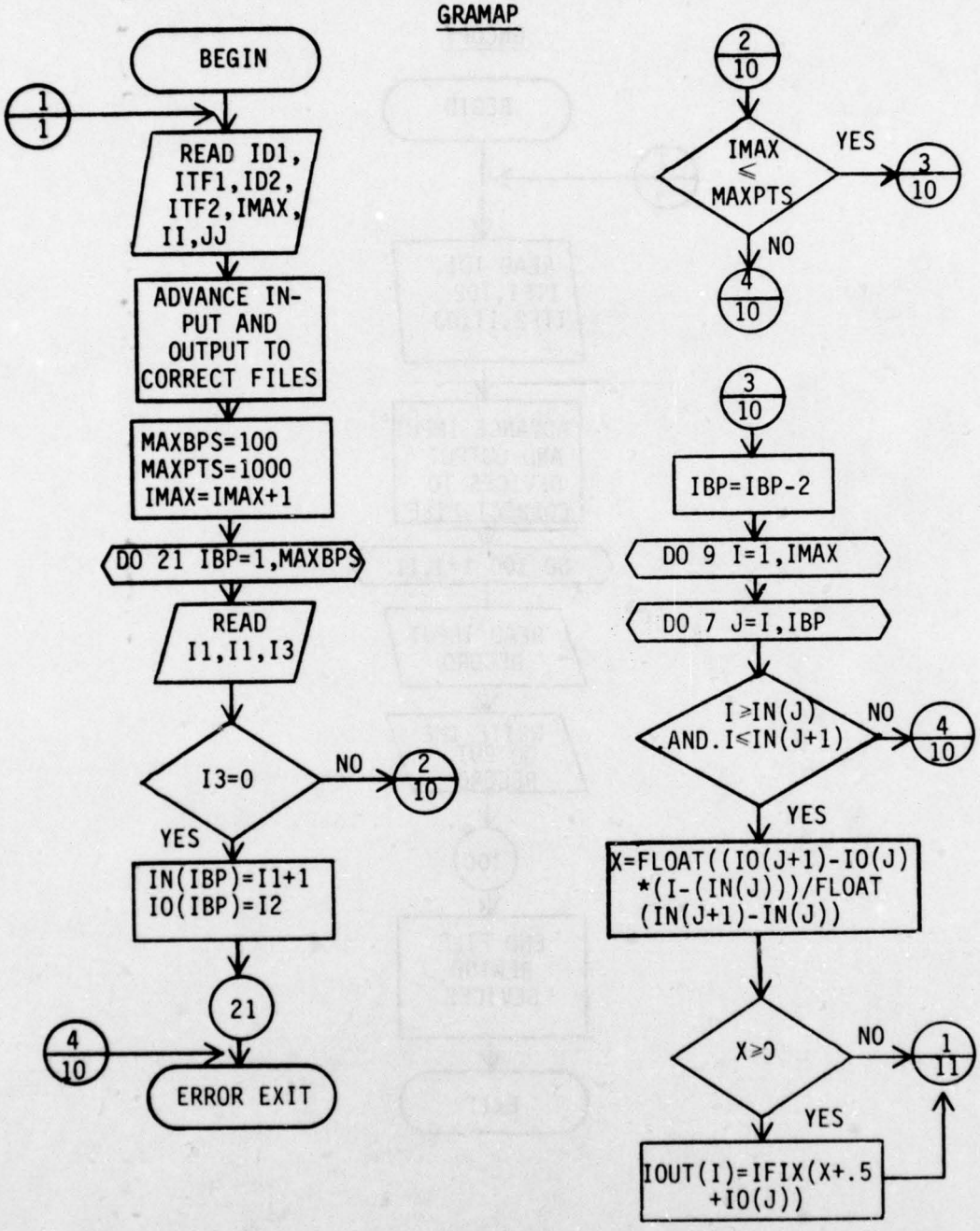


Sheet 8

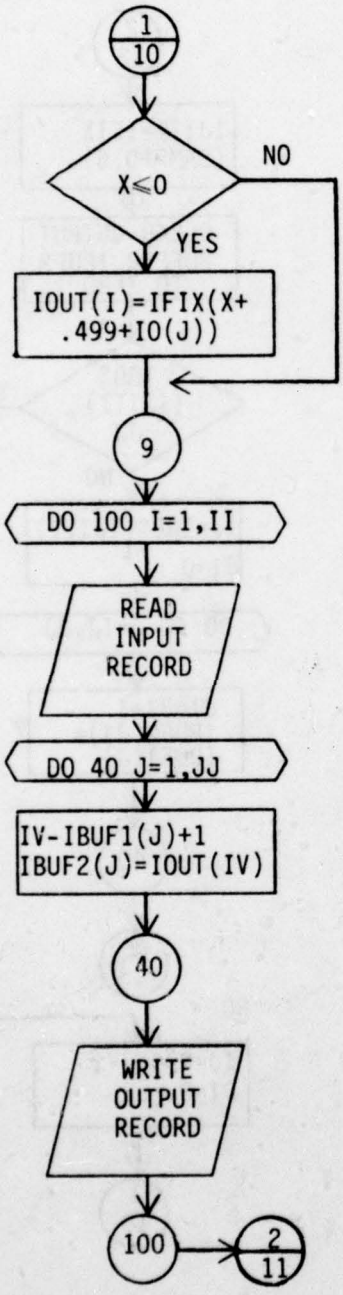
GNCOPY

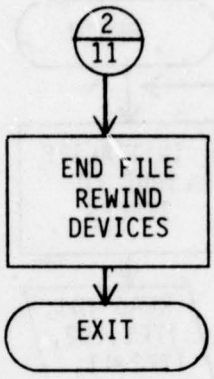


Sheet 9


GRAMAP
BEGIN
1/1
READ ID1, ITF1, ID2, ITF2, IMAX, II, JJ
ADVANCE INPUT AND OUTPUT TO CORRECT FILES
MAXBPS=100
MAXPTS=1000
IMAX=IMAX+1
DO 21 IBP=1,MAXBPS
READ I1,I1,I3
I3=0
NO
2/10
YES
IN(IBP)=I1+1
IO(IBP)=I2
21
4/10
ERROR EXIT
2/10
IMAX ≤ MAXPTS
YES
3/10
NO
4/10
3/10
IBP=IBP-2
DO 9 I=1,IMAX
DO 7 J=I,IBP
I≥IN(J) .AND. I≤IN(J+1)
NO
4/10
YES
X=FLOAT((IO(J+1)-IO(J) *(I-(IN(J)))/FLOAT (IN(J+1)-IN(J))
X≥0
NO
1/11
YES
IOUT(I)=IFIX(X+.5 +IO(J))

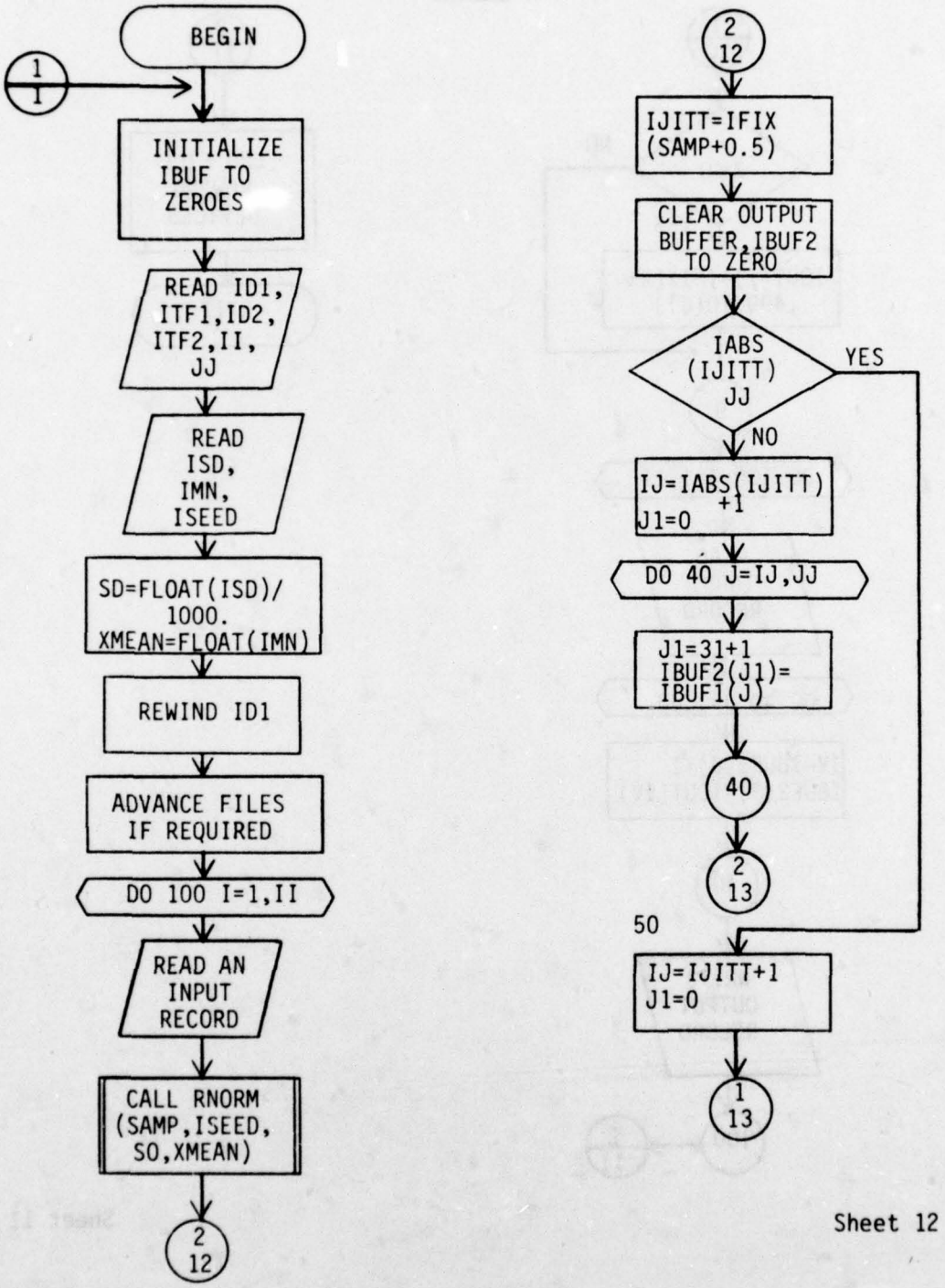
Sheet 10


1
10
X≤0
NO
YES
IOUT(I)=IFIX(X+
.499+IO(J))
9
DO 100 I=1,II
READ
INPUT
RECORD
DO 40 J=1,JJ
IV-IBUF1(J)+1
IBUF2(J)=IOUT(IV)
40
WRITE
OUTPUT
RECORD
100
2
11

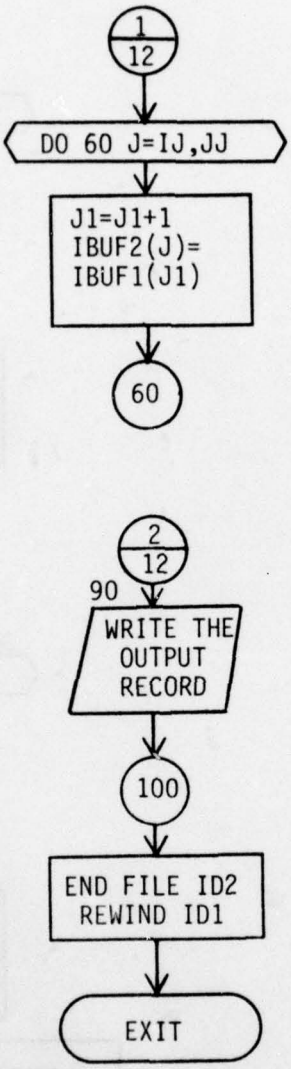

2
11
END FILE
REWIND
DEVICES
EXIT

Sheet 11

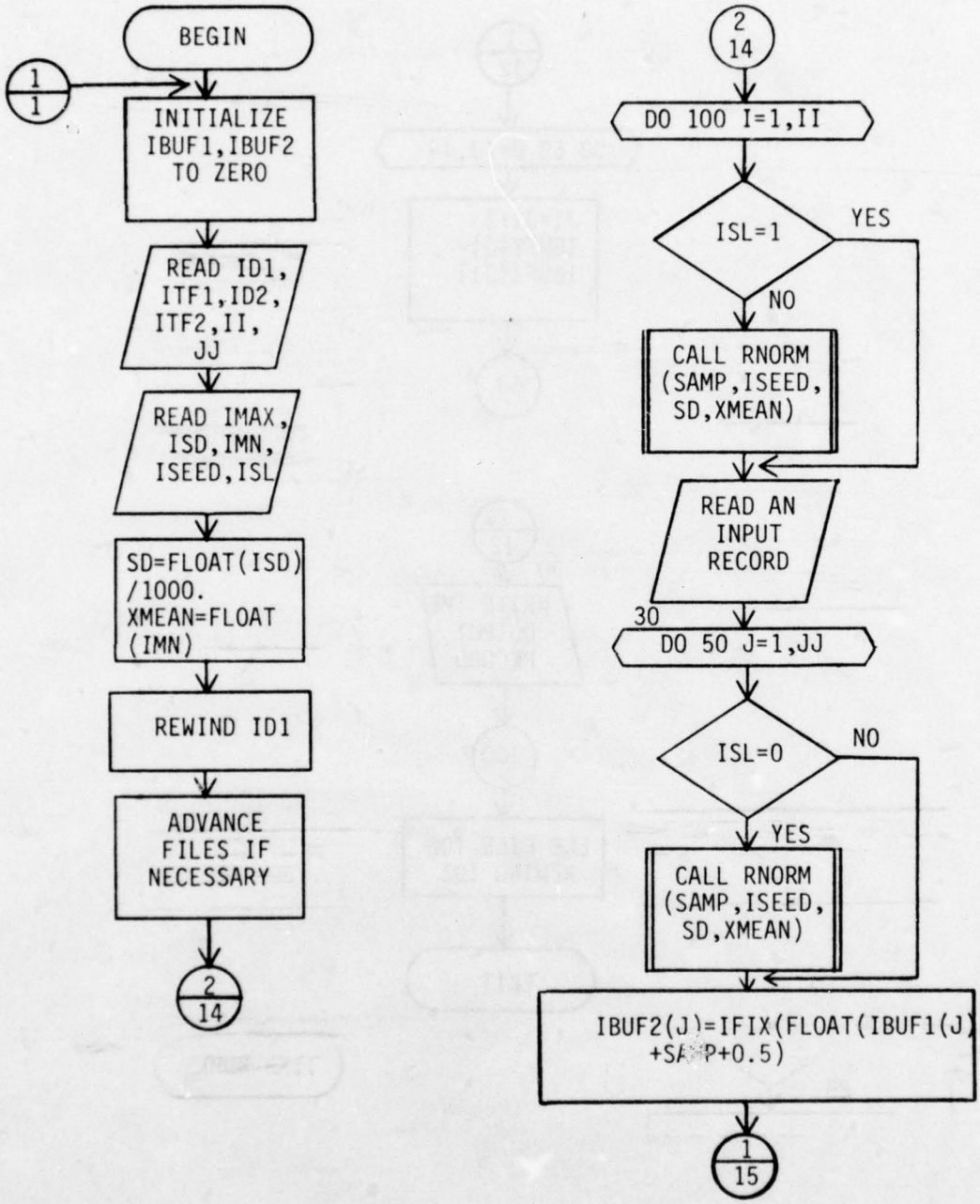
JITTER



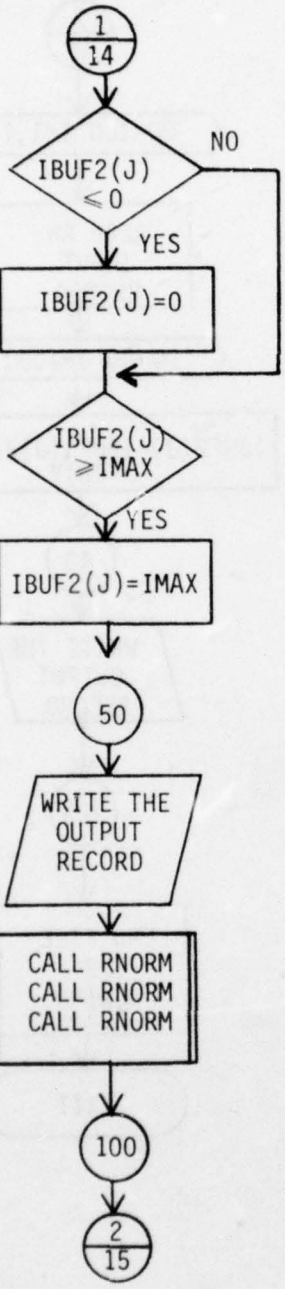
Sheet 12

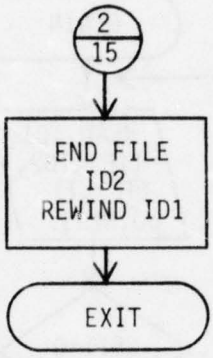

1
12
DO 60 J=IJ,JJ
J1=J1+1
IBUF2(J)=
IBUF1(J1)
60
2
12
90
WRITE THE
OUTPUT
RECORD
100
END FILE ID2
REWIND ID1
EXIT

Sheet 13


BEGIN
1
1
INITIALIZE IBUF1,IBUF2 TO ZERO
READ ID1, ITF1,ID2, ITF2,II, JJ
READ IMAX, ISD,IMN, ISEED,ISL
SD=FLOAT(ISD) /1000. XMEAN=FLOAT (IMN)
REWIND ID1
ADVANCE FILES IF NECESSARY
2
14
2
14
DO 100 I=1,II
ISL=1
YES
NO
CALL RNORM (SAMP,ISEED, SD,XMEAN)
READ AN INPUT RECORD
30
DO 50 J=1,JJ
ISL=0
NO
YES
CALL RNORM (SAMP,ISEED, SD,XMEAN)
IBUF2(J)=IFIX(FLOAT(IBUF1(J)
+SAMP+0.5)
1
15

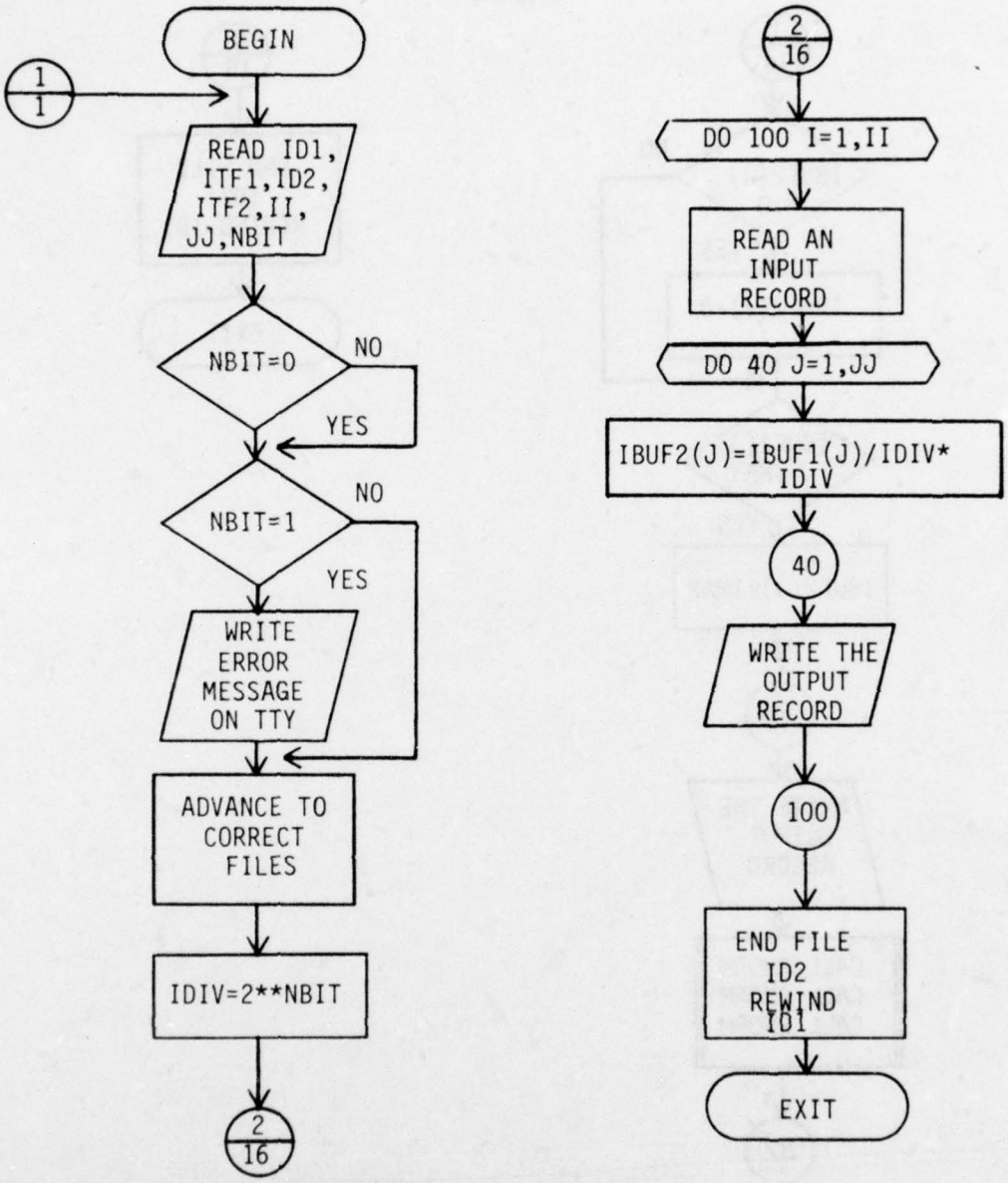
Sheet 14


1
14
IBUF2(J)
≤0
NO
YES
IBUF2(J)=0
IBUF2(J)
≥IMAX
YES
IBUF2(J)=IMAX
50
WRITE THE
OUTPUT
RECORD
CALL RNORM
CALL RNORM
CALL RNORM
100
2
15


2
15
END FILE
ID2
REWIND ID1
EXIT

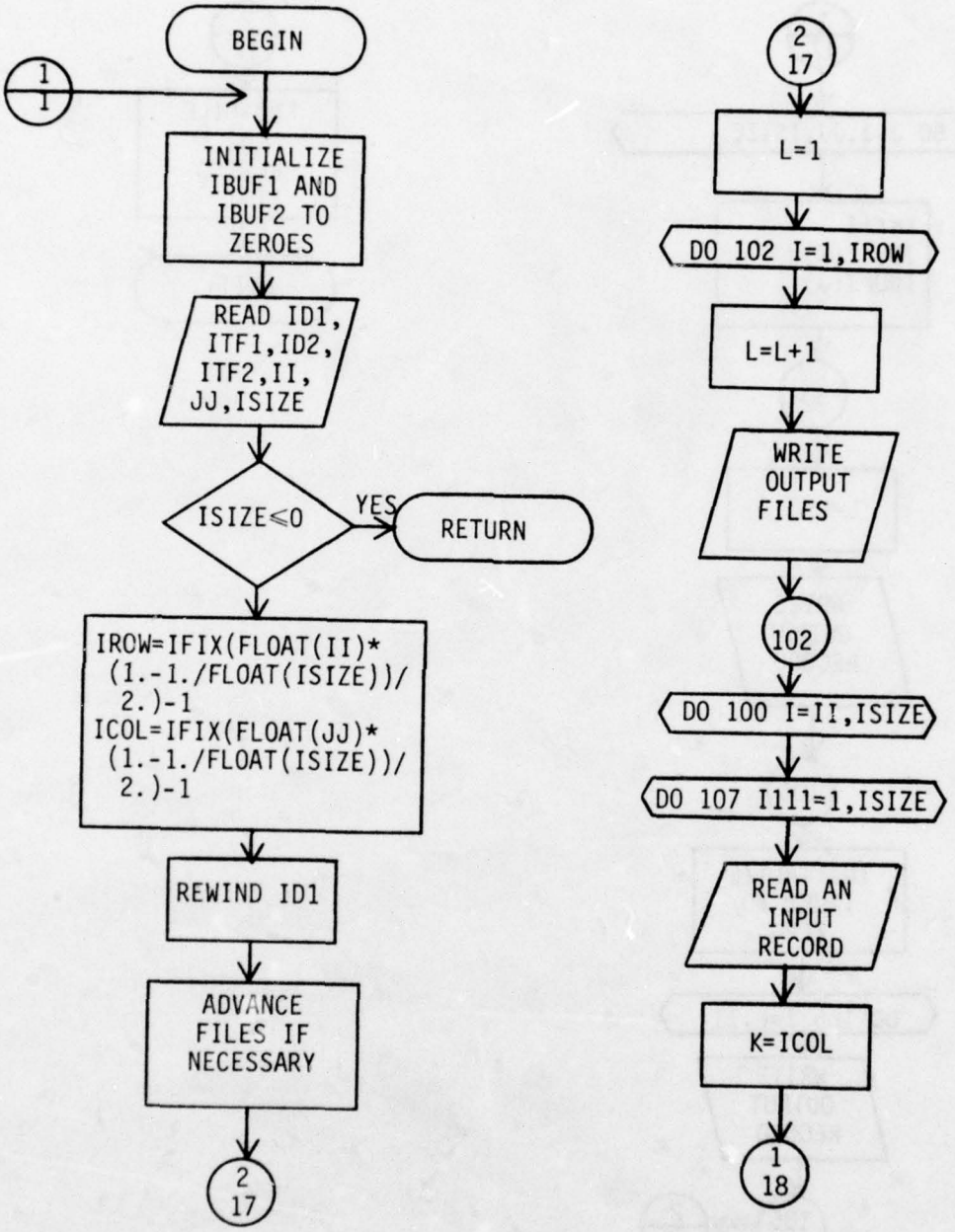
Sheet 15

DIGDEG

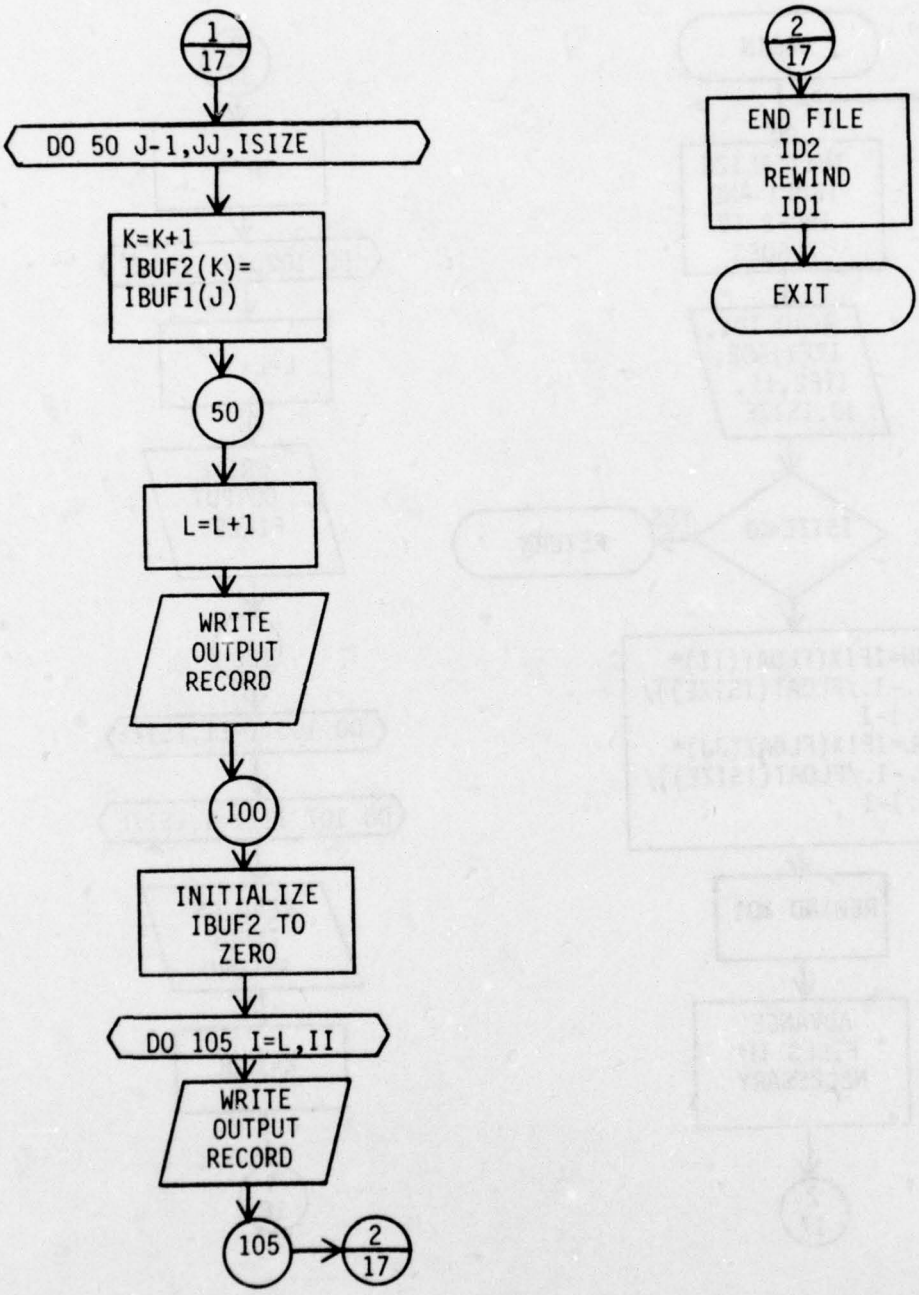


Sheet 16

HGHALS

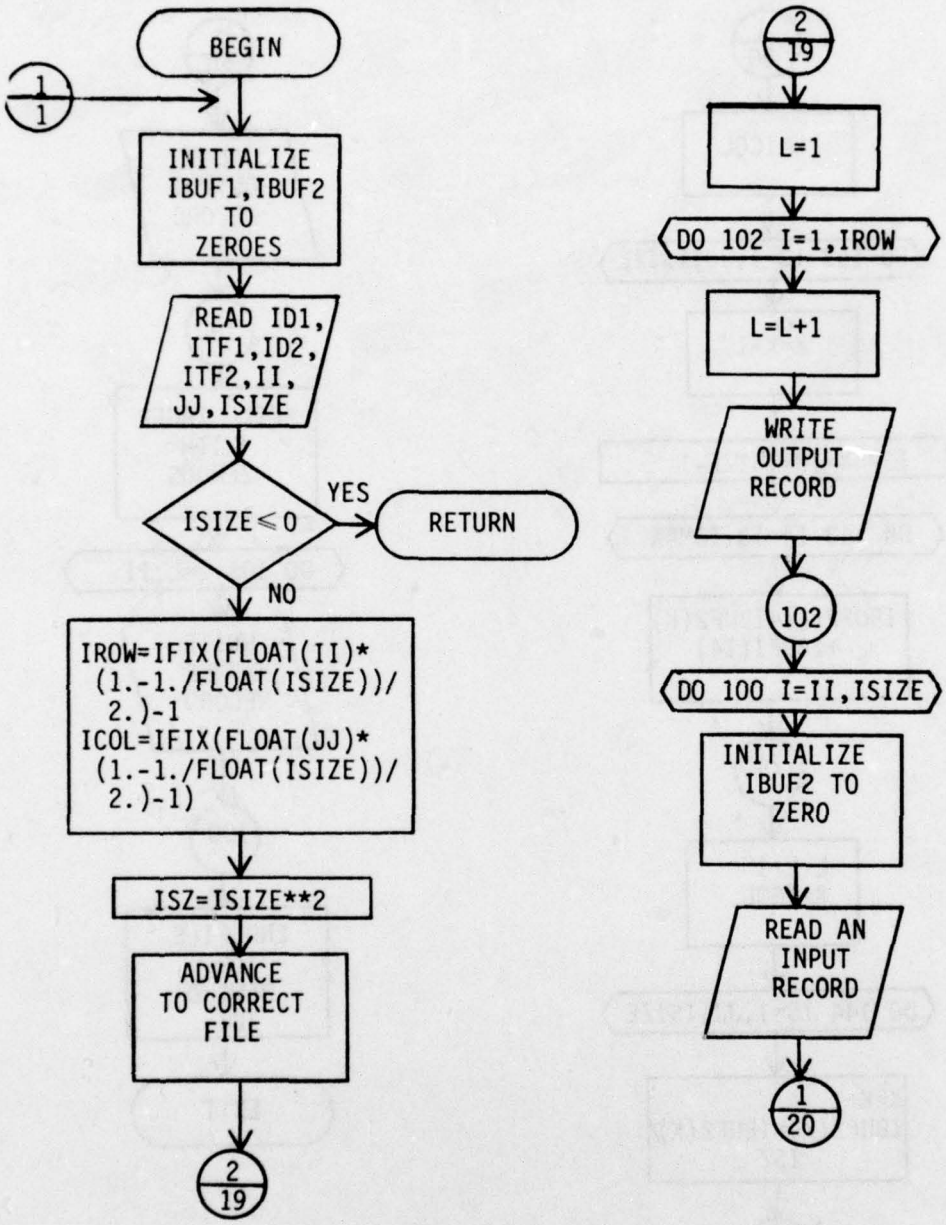


Sheet 17

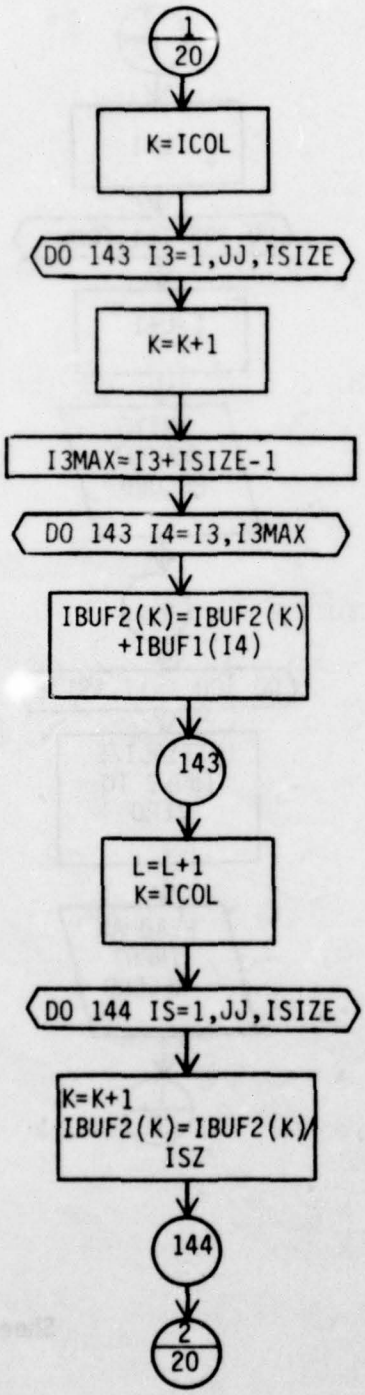

1/17
DO 50 J-1,JJ,ISIZE
K=K+1
IBUF2(K)=
IBUF1(J)
50
L=L+1
WRITE
OUTPUT
RECORD
100
INITIALIZE
IBUF2 TO
ZERO
DO 105 I=L,II
WRITE
OUTPUT
RECORD
105
2/17
2/17
END FILE
ID2
REWIND
ID1
EXIT

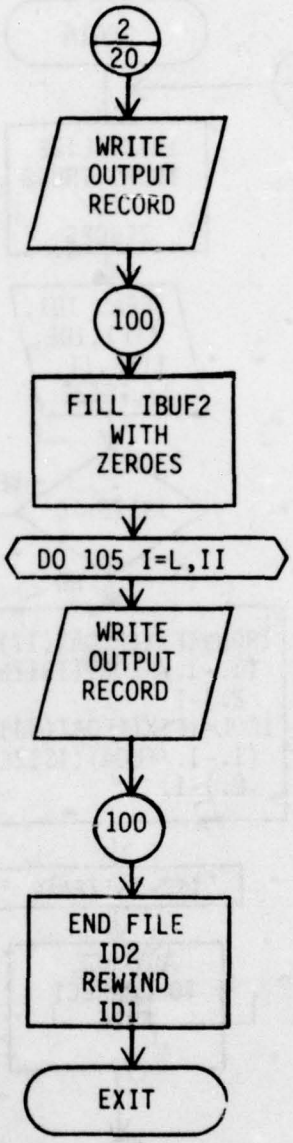
Sheet 18

REDALS



Sheet 19


1
20
K=ICOL
DO 143 I3=1,JJ,ISIZE
K=K+1
I3MAX=I3+ISIZE-1
DO 143 I4=I3,I3MAX
IBUF2(K)=IBUF2(K)
+IBUF1(I4)
143
L=L+1
K=ICOL
DO 144 IS=1,JJ,ISIZE
K=K+1
IBUF2(K)=IBUF2(K)/
ISZ
144
2
20


2
20
WRITE
OUTPUT
RECORD
100
FILL IBUF2
WITH
ZEROES
DO 105 I=L,II
WRITE
OUTPUT
RECORD
100
END FILE
ID2
REWIND
ID1
EXIT

Sheet 20

APPENDIX B

SUBJECTIVE EFFECTS OF SELECTED DIGITAL DEGRADATIONS

APPENDIX B

SUBJECTIVE EFFECTS OF SELECTED DIGITAL DEGRADATIONS

Section IV-B gives a preliminary subjective image test set. In asking a trained photointerpretator to evaluate the effects of the various digital degradations selected, the prominent response was verbal. These verbal comments, recorded in Tables B-1 through B-23, are indicative of the subjective effects noted.

TABLE B-1. ADDITIVE GAUSSIAN SPOT NOISE APPLIED TO A HIGH RESOLUTION B/W VERTICAL DIGITIZED PHOTOGRAPH

Standard Deviation = .3% of Gray Level Range

Good detail, good shadows

Standard Deviation = .6% of Gray Level Range

Good detail, good shadows

Standard Deviation = 1.2% of Gray Level Range

Good detail, good shadows

Standard Deviation = 2.4% of Gray Level Range

Some loss in detail of KC-135 tail section, probably caused by graininess.

NOTE: Loss of tonal differences between B-52 (painted A/C) and background may cause the interpreter some difficulty.

Shadow detail is good on all image scenes.

Standard Deviation = 4.88 of Gray Level Range

Graininess causes some loss detail along edges of targets. Tonal difference between B-52 and portion of it's background appears to be enhanced by this graininess.

TABLE B-1. ADDITIVE GAUSSIAN SPOT NOISE APPLIED TO A HIGH RESOLUTION B/W VERTICAL DIGITIZED PHOTOGRAPH (Continued)

Standard Deviation = 9.77% of Gray Level Range

Detail of tail sections on both aircraft affected by graininess. There is a loss in target background tone that is caused by this "salt and pepper-like" appearance. Detail of left tip of KC-135 wing completely lost. Mensuration would be difficult.

Standard Deviation = 19.52% of Gray Level Range

Detail on KC-135 only apparent on right wing, portion of left wing and fuselage. Detail of B-52 is completely lost under magnification. Loss of background detail caused by the "salt and pepper-like" appearance. Accurate target mensuration would be impossible.

Standard Deviation = 39.04% of Gray Level Range

Almost complete loss of detail under magnification.

TABLE B-2. ADDITIVE GAUSSIAN LINE NOISE APPLIED TO A HIGH RESOLUTION B/W VERTICAL DIGITIZED PHOTOGRAPH

Standard Deviation = .3% of Gray Level Range

Edges as sharp as original, good shadow, good tonal differences.

Standard Deviation = .6% of Gray Level Range

Tone differences not as great on KC-135, primarily between nose of A/C and fuselage.

B-52 fuselage blending in with hard stand parking ramp - poor tonal differences causing lack of target detail. Overall mesh effect.

Standard Deviation = 1.2% of Gray Level Range

Shadow detail not as sharp as on original image - difference in image tone on KC-135 not as great as on original image.

Standard Deviation = 2.44% of Gray Level Range

Many "noise lines" across target causes some "break-up" of image and loss of detail.

Loss of target detail due to absence of tonal differences between B-52 and hard stand.

Standard Deviation = 4.88% of Gray Level Range

Noise apparent on overall image scene, horizontal "noise lines" break-up target, especially left edge of KC-135 wing - mensuration of wing-span would prove difficult - same applies to B-52, left edge of wing almost lost due to lack of target and background tonal

TABLE B-2. ADDITIVE GAUSSIAN LINE NOISE APPLIED TO A HIGH RESOLUTION B/W VERTICAL DIGITIZED PHOTOGRAPH (Continued)

differences and noise. Poor detail in tail section of B-52 because of noise and lack of tonal differences.

Standard Deviation = 8.77% of Gray Level Range

Excessive noise breaks-up target - causing lack of detail - wide "noise-bands" very disturbing. Almost complete lack of detail in left wing edge of B-52 and tail section.

Standard Deviation = 19.55% of Gray Level Range

"Wide black and white noise bands" breaks-up target detail. Target mensuration would be extremely difficult if not impossible.

Standard Deviation = 39. % of Gray Level Range

Noise level causes greater loss of image detail than image scene above.

NOTE: Adequate shadow detail is present on each image scene.

TABLE B-3. GAUSSIAN LINE JITTER APPLIED TO A HIGH RESOLUTION B/W VERTICAL DIGITIZED PHOTOGRAPH

Standard Deviation = .05 Pixels

Standard Deviation = .1 Pixels

Standard Deviation = .2 Pixels

Edges not as sharp as on other images.

Standard Deviation = .39 Pixels

Excessive "jitter" causing "break-up" in edges of target and target shadow. Detail of KC-135 tail-section almost completely lost.

Detail of back section of fuselage and tail section of B-52 almost completely lost.

This "jitter" is quite apparent on vertical painted lines on hard stand.

Standard Deviation = .78 Pixels

Excessive jitter breaking up target and target shadow - Detail lost on nose section and back part of fuselage and tail of B-52.

Standard Deviation = 1.56 Pixels

No target detail apparent - except on back edge of KC-135 wings and back edge of B-52's left wing. Greater loss of detail apparent on painted B-52 vs silver (painted KC-135).

TABLE B-3. GAUSSIAN LINE JITTER APPLIED TO A HIGH RESOLUTION B/W VERTICAL DIGITIZED PHOTOGRAPH (Continued)

Standard Deviation = 3.13 Pixels

Detail of B-52 completely lost. Edges of KC-135 broken-up to the point where all target detail is lost except in wing sections.

Standard Deviation = 6.25 Pixels

100% loss of target detail and shadow - shape is still apparent.

NOTE: Shape of target remains apparent on each image scene, particularly when no magnification is used. There is poor contrast between target and target background making accurate interpretation difficult.

TABLE B-4. VARYING THE SAMPLING OF A HIGH RESOLUTION B/W VERTICAL DIGITIZED PHOTOGRAPH UNDER HIGH ALIASING

Sampling Reduction = 2

Some loss of detail in nose section (radar) of B-52.

Sampling Reduction = 3

Some loss of detail in tail section of KC-135 and nose of B-52.

Sampling Reduction = 4

Loss of detail in nose section, tail section and engines of KC-135 - overall target image lacks sharpness. Much of B-52 (especially right wing tip) "blends-into" target background. Target image lacks sharpness.

Sampling Reduction = 5

Edge of left wing KC-135 very "choppy". Engines on that wing not very apparent - very little detail in tail section of aircraft. Target shadow and background tone differences are not as good as on original image scene. Poor detail in B-52. Target tends to blend in with background.

TABLE B-5. VARYING THE SAMPLING OF A HIGH RESOLUTION B/W VERTICAL DIGITIZED PHOTOGRAPH UNDER REDUCED ALIASING

Sampling Reduction = 2

Good detail, good shadow, good tonal differences between target and background.

Sampling Reduction = 3

Overall image (especially KC-135 appears a bit fuzzy)

Sampling Reduction = 4

Targets do not appear sharp, loss of detail in nose sections and tail sections of A/C. Wing-tips of B-52 tend to "blend-in" with background.

Sampling Reduction = 5

Targets lack overall sharpness, much detail lost. Right engine of KC-135 not apparent under magnification. Right wing of B-52 blending in with background.

TABLE B-6. ADDITIVE GAUSSIAN SPOT NOISE APPLIED TO A LOW RESOLUTION B/W VERTICAL DIGITIZED PHOTOGRAPH

Standard Deviation = .3% of Gray Level Range

Standard Deviation = .6% of Gray Level Range

Some detail is lost in targets. Second aircraft from the left appears to be a "delta wing" aircraft, rather than a swept wing.

Standard Deviation = 1.22% of Gray Level Range

Standard Deviation = 2.44% of Gray Level Range

Very "spotty" - loss of edge detail because of spottiness. Target background (aircraft parking area) tone affected by "salt and pepper-like" interference taking away from the target itself, by "blending-in" with the target.

Standard Deviation = 4.88% of Gray Level Range

Aircraft are still detectable, however, they are not identifiable. Edges of hard stand lack any detail or sharpness. Area between third and fourth hard stand appears to contain an aircraft (false alarm).

Standard Deviation = 9.77% of Gray Level Range

Spot noise effects entire image scene. "False alarm" detected still apparent. Target can still be interpreted as an A/C parking area.

TABLE B-6. ADDITIVE GAUSSIAN SPOT NOISE
APPLIED TO A LOW RESOLUTION
B/W VERTICAL DIGITIZED PHOTOGRAPH (Continued)

Standard Deviation = 19.51% of Gray Level Range

Area can still be interpreted as an A/C parking area. No other information can be obtained from this scene.

Standard Deviation = 39.04% of Gray Level Range

Target area not identifiable.

TABLE B-7. ADDITIVE GAUSSIAN LINE NOISE APPLIED TO A LOW RESOLUTION B/W VERTICAL DIGITIZED PHOTOGRAPH

Standard Deviation = .3% of Gray Level Range

Standard Deviation = .6% of Gray Level Range

Standard Deviation = 1.22% of Gray Level Range

Line noise effecting (distorting) shape of the two A/C on the third and fourth hard stand.

Standard Deviation = 2.44% of Gray Level Range

Line noise effecting shape of all parked aircraft.

Standard Deviation = 4.88% of Gray Level Range

Aircraft are still identifiable.

Standard Deviation = 9.77% of Gray Level Range

Aircraft are detectable; however, the "wide-bands" or line noise is "breaking-up" the target and making interpretation difficult.

Standard Deviation = 19.52% of Gray Level Range

All aircraft are detectable. None are identifiable.

Standard Deviation = 39.04% of Gray Level Range

It is still apparent that the target is an aircraft parking area. Two aircraft are detectable, but not identifiable.

TABLE B-8. GAUSSIAN LINE JITTER APPLIED TO A LOW RESOLUTION B/W VERTICAL DIGITIZED PHOTOGRAPH

Standard Deviation = .05 Pixels

Standard Deviation = .1 Pixels

Standard Deviation = .2 Pixels

Edges of fourth aircraft from the left are broken.

Standard Deviation = .39 Pixels

Standard Deviation = .78 Pixels

Aircraft shape distorted by "jitter". Edges of taxi-ways and hard stands are also distorted.

Standard Deviation = 1.56 Pixels

Hard stand still identifiable. Aircraft can be detected.

Standard Deviation = 3.13 Pixels

Hard stand still identifiable. Aircraft can be detected.

Standard Deviation = 6.25 Pixels

Target not identifiable.

TABLE B-9. VARYING THE QUANTIZATION OF A LOW RESOLUTION B/W VERTICAL DIGITIZED PHOTOGRAPH

Number of Gray Levels = 32

Poor contrast between target and target background make identification difficult. All four aircraft are detectable, however,

Number of Gray Levels = 16

Many of the target components "blend into" their background. Identification of the aircraft not possible. They are detectable.

Number of Gray Levels = 8

Aircraft not detectable. Target can be identified as an aircraft parking ramp.

Number of Gray Levels = 4

No detail in image; however, the overall shape of the target area might allow an interpreter to make an accurate interpretation.

TABLE B-10. VARYING THE SAMPLING OF A LOW RESOLUTION B/W VERTICAL DIGITIZED PHOTOGRAPH UNDER HIGH ALIASING

Sampling Reduction = 2

Target area is identifiable, and aircraft are detectable.

Sampling Reduction = 3

Target area is identifiable, and aircraft are detectable.

Sampling Reduction = 4

Target area is identifiable. Loss of detail does not allow for the detection of the aircraft.

Sampling Reduction = 5

No detail in image. Shape of A/C parking area is still apparent.

TABLE B-11. VARYING THE SAMPLING OF A LOW RESOLUTION B/W VERTICAL DIGITIZED PHOTOGRAPH UNDER REDUCED ALIASING

Sampling Reduction = 2

Target area identifiable. Aircraft are still detectable.

Sampling Reduction = 3

Target area identifiable. Two aircraft detectable.

Sampling Reduction = 4

Target area identifiable. Aircraft are not detectable.

Sampling Reduction = 5

Parking area still maintains shape. No target detail apparent. No A/C detectable.

TABLE B-12. ADDITIVE GAUSSIAN SPOT NOISE APPLIED TO AN INFRARED IMAGE OF PARKED AIRCRAFT

Standard Deviation = 3% of Gray Level Range

Edges broken, detail remains.

Standard Deviation = .6% of Gray Level Range

Edges broken, detail remains.

Standard Deviation = 1.22% of Gray Level Range

Edges broken, detail remains.

Standard Deviation = 2.44% of Gray Level Range

Edges broken, detail remains.

Standard Deviation = 4.88% of Gray Level Range

Edges not sharp, some loss in detail especially on boom (located rear of tail section) and tail section itself.

Standard Deviation = 9.77% of Gray Level Range

"Salt and pepper" effect takes away from target sharpness and detail. The right-rear portion of the fuselage blends in with the background because of "spotty" effect. Tip of right wing appears to be rounded rather than straight and sharp.

Standard Deviation = 19.52% of Gray Level Range

Greater "spotty" or "salt and pepper-like" effects cause loss of target detail and edge sharpness. Boom completely lost under magnification. Right wing-tip

TABLE B-12. ADDITIVE GAUSSIAN SPOT NOISE APPLIED TO AN INFRARED IMAGE OF PARKED AIRCRAFT (Continued)

appears to be rounded. Much of target blends into the background when viewed under magnification.

Standard Deviation = 39.04% of Gray Level Range

Loss of all target detail under magnification. Image appears almost like a half-tone newspaper picture.

TABLE B-13. ADDITIVE GAUSSIAN LINE NOISE
APPLIED TO AN INFRARED IMAGE OF PARKED AIRCRAFT

Standard Deviation = .3% of Gray Level Range

Standard Deviation = .6% of Gray Level Range

Standard Deviation = 1.22% of Gray Level Range

Standard Deviation = 2.44% of Gray Level Range

Standard Deviation = 4.88% of Gray Level Range

Some loss of detail on in-board engine, right wing. Edges of target very "choppy" due to wide-bands or lines.

Standard Deviation = 9.77% of Gray Level Range

Some loss of detail on in-board engine, right wing. Edges of target very "choppy" due to wide bands or lines.

Standard Deviation = 19.52% of Gray Level Range

Some loss of detail on in-board engine right wing. Edges of target very "choppy" due to wide bands or lines. More loss of detail due to wide bands or lines. Refueling boom almost completely lost under magnification.

Standard Deviation = 39.04% of Gray Level Range

Rear section of fuselage lost because of "banding" and lines. Boom completely lost under magnification.

TABLE B-14. GAUSSIAN LINE JITTER APPLIED TO AN INFRARED IMAGE OF PARKED AIRCRAFT

Standard Deviation = .05 Pixels

Standard Deviation = .1 Pixels

Standard Deviation = .2 Pixels

Standard Deviation = .39 Pixels

Standard Deviation = .78 Pixels

Target edges "broken" by jitter. This is apparent on all target components except the rear edge of the right wing.

Standard Deviation = 1.56 Pixels

Lack of detail caused by "broken" edges.

Standard Deviation = 3.13 Pixels

Target lacking detail. No edge sharpness at all. Complete loss of target components, i.e., engines, boom.

Standard Deviation = 6.25 Pixels

Complete loss of target detail. Shape could be interpreted as a "thermal shadow."

TABLE B-15. VARYING THE QUANTIZATION OF AN INFRARED IMAGE OF PARKED AIRCRAFT

Number of Gray Levels = 32

Number of Gray Levels = 16

Light gray border along edge of target. This does not effect the detail too badly.

Number of Gray Levels = 8

Gray border along edges of target distort the detail. Engines on right wing appear to be separated from the wing. Boom located in tail section is lost. Shape of rear portion of fuselage is distorted.

Number of Gray Levels = 4

Step-like edges in tail section of A/C. Target lacks detail in general. Front portion of fuselage blends in with background ("smearing effect").

TABLE B-16. VARYING THE SAMPLING OF AN INFRARED IMAGE OF PARKED AIRCRAFT UNDER HIGH ALIASING

Sampling Reduction = 2

Poorer target - background contrast than other three images, especially in tail section.

Sampling Reduction = 3

Better contrast. Good tone differences between target and target background.

Sampling Reduction = 4

Good tone differences between target and target background.

Sampling Reduction = 5

Good tone differences between target and target background.

TABLE B-17. VARYING THE SAMPLING OF AN INFRARED IMAGE OF PARKED AIRCRAFT UNDER REDUCED ALIASING

Sampling Reduction = 2

Poorer target - background contrast than other three image scenes, especially in tail section of A/C.

Sampling Reduction = 3

Good target/background contrast; better detail.

Sampling Reduction = 4

Good target/background contrast; better detail.

Sampling Reduction = 5

Some detail lost in boom section of aircraft. Good target/background contrast.

TABLE B-18. ADDITIVE GAUSSIAN SPOT NOISE APPLIED TO A SYNTHETIC APERATURE RADAR IMAGE

Standard Deviation = .3% of Gray Level Range

Standard Deviation = .6% of Gray Level Range

Standard Deviation = 1.22% of Gray Level Range

Standard Deviation = 2.44% of Gray Level Range

Very little (if any) change was noted between these four image scenes and the original image.

Standard Deviation = 4.88% of Gray Level Range

Image appears slightly grainy.

Standard Deviation = 9.77% of Gray Level Range

Shape of aircraft on parking ramp distorted, graininess increased causing some loss of background detail and target sharpness.

Standard Deviation = 19.52% of Gray Level Range

Detail lost, especially in hanger area. Aircraft shape distorted. Change in run-way construction material (on over-run, not as apparent as it is on original).

Standard Deviation = 39.04% of Gray Level Range

Detail almost completely lost in hanger area closest to hard stand. Shape of aircraft distorted beyond recognition. Complete loss of background detail, road not as apparent as in the other three image scenes due to "salt and pepper" (spotty) effects.

TABLE B-19. ADDITIVE GAUSSIAN LINE NOISE APPLIED TO A SYNTHETIC APERATURE RADAR IMAGE

Standard Deviation = .3% of Gray Level Range

Standard Deviation = .6% of Gray Level Range

Some distortion in shape of aircraft noted.

Standard Deviation = 1.22% of Gray Level Range

Some distortion in shape of aircraft noted.

Standard Deviation = 2.44% of Gray Level Range

Some distortion in shape of aircraft noted.

Standard Deviation = 4.88% of Gray Level Range

Lines "breaking-up" edges of hard stand, taxi-ways and hangers. Parked A/C distorted.

Standard Deviation = 9.77% of Gray Level Range

Lines more prominent. Hangers to right of hard stand may be interpreted as separate building rather than one long building because of the line noise. Detail in parked aircraft lost.

Standard Deviation = 19.55% of Gray Level Range

The only thing that an interpreter can say about this image scene is that it is an airfield and aircraft parking area. The edges of the hard stand are still recognizable.

TABLE B-19. ADDITIVE GAUSSIAN LINE NOISE APPLIED TO A SYNTHETIC APERATURE RADAR IMAGE (Continued)

Standard Deviation = 39.04% of Gray Level Range

Line noise makes any detail interpretation impossible. Targets are "broken-up" by the noise. The scene can, however, be recognized as an airfield and aircraft parking area. The hangers located in the vicinity of the parking area (hard stand) are no longer apparent.

TABLE B-20. GAUSSIAN LINE JITTER APPLIED TO A SYNTHETIC APERATURE RADAR IMAGE

Standard Deviation = .05 Pixels

Standard Deviation = .1 Pixels

Standard Deviation = .2 Pixels

Standard Deviation = .39 Pixels

Edges of run-way and taxi-ways appear "choppy" because of jitter.

Imagery is still useful to the interpreter.

Standard Deviation = .78 Pixels

Target shapes are distorted due to jitter. Straight lines appear extremely "choppy."

Standard Deviation = 1.56 Pixels

The target scene can be recognized as an airfield; however, all detail is lost. Parked A/C is no longer detectable and the hangers are no longer recognizable.

Standard Deviation = 3.13 Pixels

The runway can still be detected; however, I believe that is true only because I am familiar with the image scene.

Standard Deviation = 6.25 Pixels

Same as above.

TABLE B-21. VARYING THE QUANTIZATION OF A SYNTHETIC APERATURE RADAR IMAGE

Number of Gray Levels = 32

Number of Gray Levels = 16

Number of Gray Levels = 8

"Gray-like, blotchy appearance" takes away from target detail. This is especially true in hanger area to the right of the A/C parking area. In addition, much background detail is lost by this "blotchiness."

Number of Gray Levels = 4

Same as above.

TABLE B-22. VARYING THE SAMPLING OF A SYNTHETIC APERATURE RADAR IMAGE UNDER HIGH ALIASING

Sampling Reduction = 2

Sampling Reduction = 3

Parked A/C no longer detectable. Some loss of detail in overall scene.

Sampling Reduction = 4

Parked A/C not detectable. Great loss of detail in overall scene.

Sampling Reduction = 5

Parked A/C and hangers not detectable. Target scene can be recognized as an airfield. The digitization caused a "false-alarm" situation. The aircraft might be interpreted as a parked A/C.

TABLE B-23. VARYING THE SAMPLING OF A SYNTHETIC APERATURE RADAR IMAGE UNDER REDUCED ALIASING

Sampling Reduction = 2

Parked aircraft not detectable. Poor contrast between targets and background causing loss of detail in overall image scene.

Sampling Reduction = 3

Parked aircraft not detectable. Poor contrast between targets and background causing loss of detail in overall image scene.

Sampling Reduction = 4

Loss of contrast and overall sharpness causes loss of detail in any targets that may be present in the image scene.

Sampling Reduction = 5

The target scene can be recognized as an airfield; however, all detail is lost.

APPENDIX C

INTERPRETATION OF MOIRE' PATTERN FORMATION AS A DIGITAL SAMPLING PROCESS

APPENDIX C

INTERPRETATION OF MOIRE' PATTERN AS A DIGITAL SAMPLING PROCESS

Moire' patterns are those shimmering patterns seen in everyday life when looking through layers of screen mesh, folds of silk, or even parallel bridge railings. Since these Moire' patterns are exceptionally sensitive to displacements, their use has been abstracted for use in science to detect optical flatness, crystalline inhomogeneities, stress, faint signals, etc.

At its conceptual simplist, the Moire' pattern is formed by viewing one periodic structure through another periodic structure. Such an example was shown previously in Figure 5-4.

The formation of the Moire' pattern is best understood in terms of the spatial frequency representation of a digital sampling process. Figure C-1 is the spatial frequency representation of the test image, Figure 5-1. The test image is actually composed of square waves and thus possesses an infinite number of harmonics. For simplicity and with no serious results we ignore the harmonics in this discussion. Now remember that the test image was seen by viewing through its slightly rotated self, Figure C-2, giving Figure 5-4. Thus the transparent rotated copy of the test image forms a spatial sampler of the nature discussed in Section III-A. The resulting sampling action is one-dimensional. This implies that the spatial frequency spectrum will be replicated throughout the spatial frequency plane with the origin moved to each of the points ϕ_i as shown in Figure C-3. The results of the replication are seen in Figure C-4, the spatial frequency representation of Figure 5-4.

From Figure C-5, the MTF response of the human visual system, it is apparent that certain spatial frequencies are more prominent to the human than others. By moving the image of

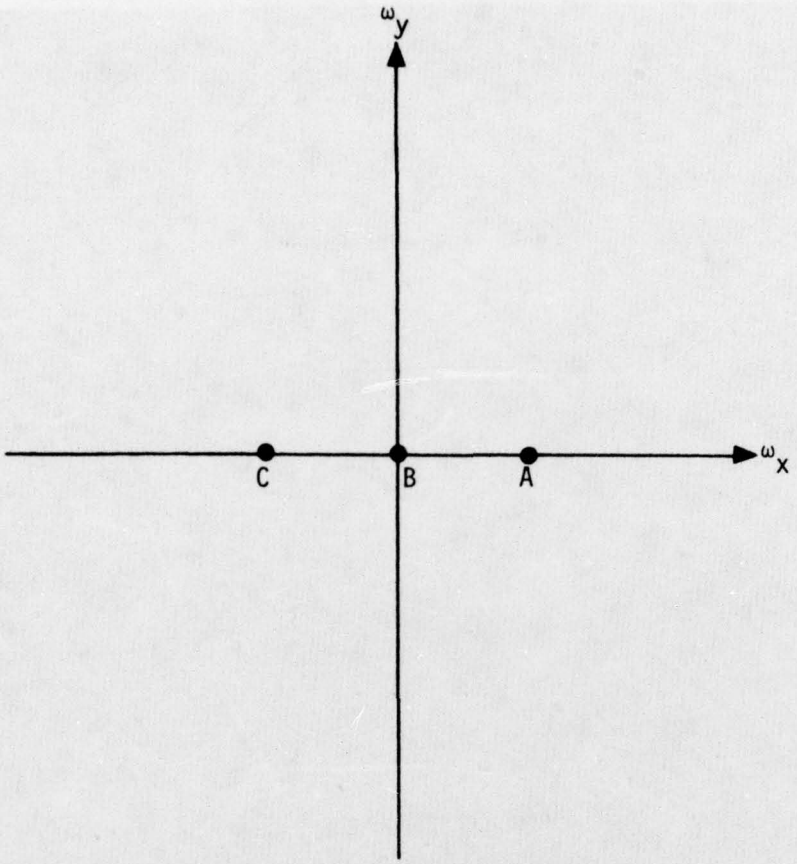


Figure C-1. The Spatial Frequency Representation of the Image of Figure 5-1

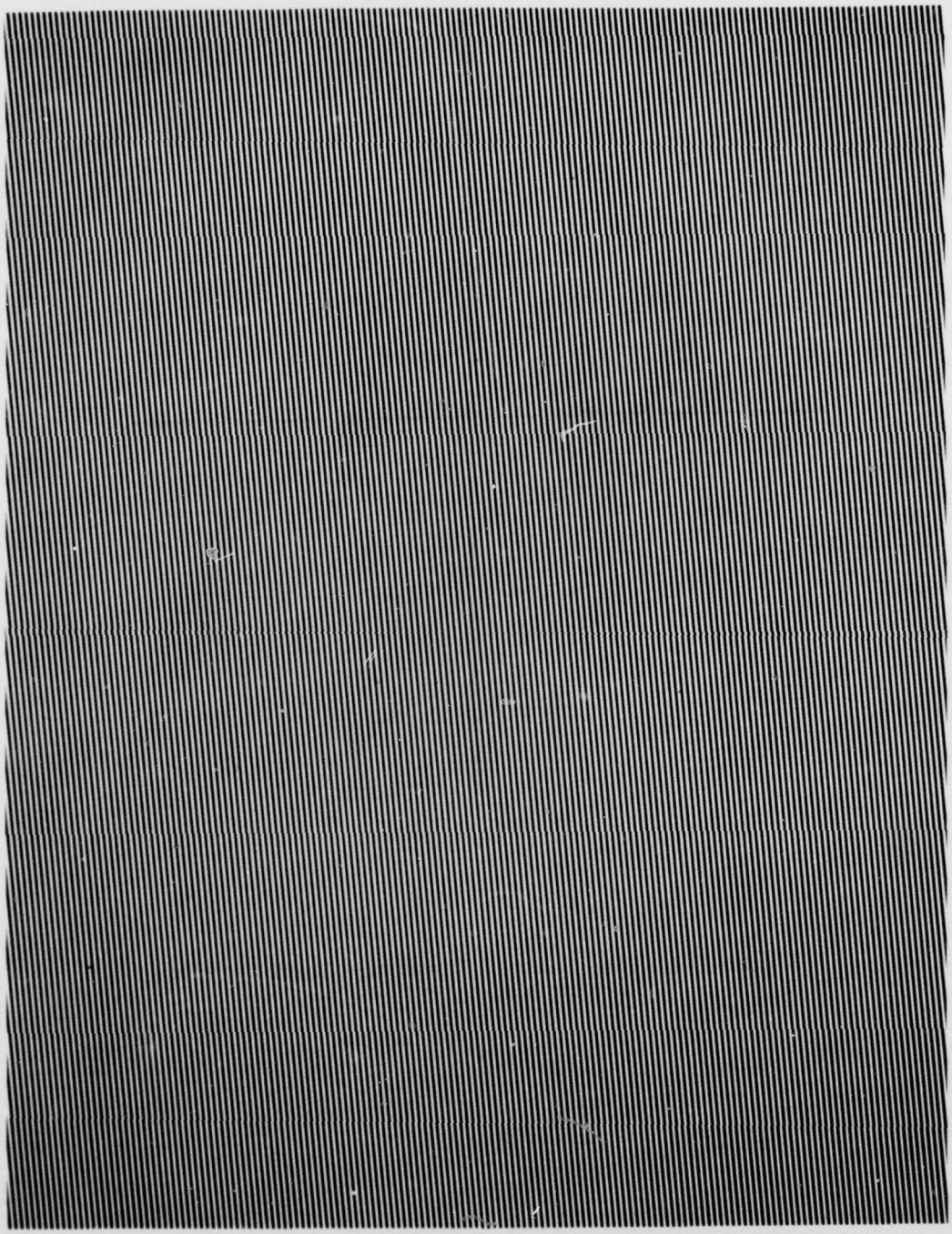


Figure C-2. Rotated Version of the Input Test Pattern of Figure 5-1

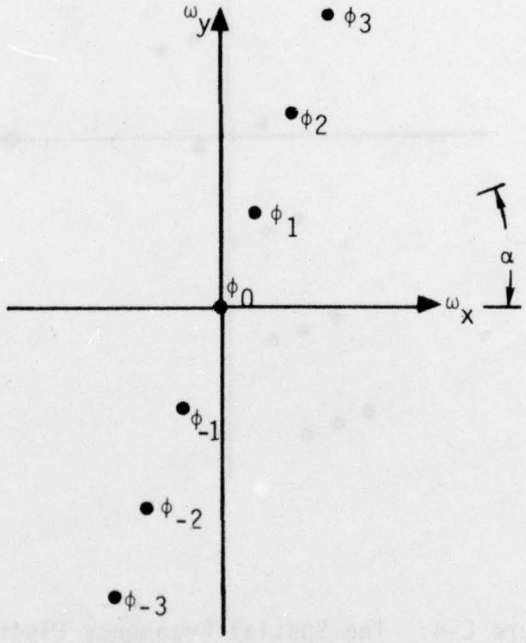


Figure C-3. The Local Origins of the Replicating Effects of the Image of Figure C-2 Used as a Sampler

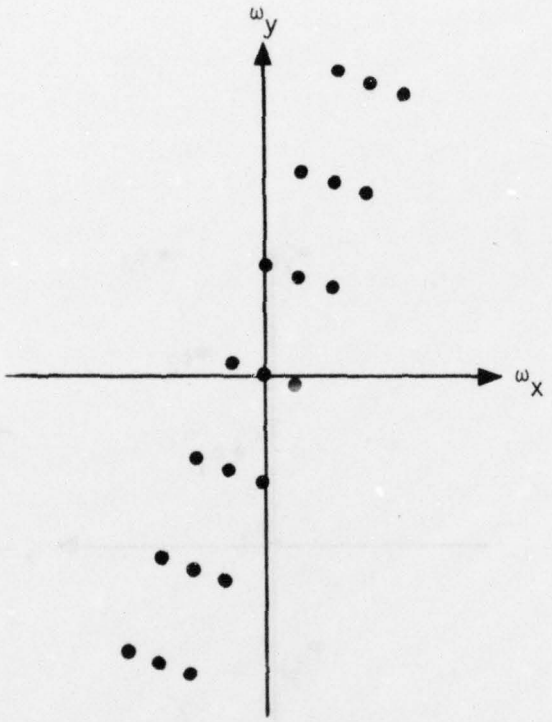


Figure C-4. The Spatial Frequency Distribution of the Image of Figure 5-4

Figure 5-4 closer to or further from the eye it is possible to superimpose contours of MTF response onto Figure C-5, as shown in Figure C-6. Thus the spatial frequency components of Figure 5-4 which are most apparent are D, E, and F. E is the average brightness while D and F form an aliased low frequency nearly vertical spatial sine wave. This sine wave is the quite evident Moire' pattern observed in Figure 5-4. Thus Moire' patterns are seen to be the aliased phenomena of a digital image sampling process and are subject to the laws and properties thereof. For instance the reason that the Moire' pattern is horizontal while the original patterns are vertical is apparent in the spectral plane of Figure C-6.

Very complex and rich forms of digital image testing procedures can thus be developed using the specialized aliasing properties of digital image systems and the MTF properties of the eye. Section V considers a few of the possibilities.

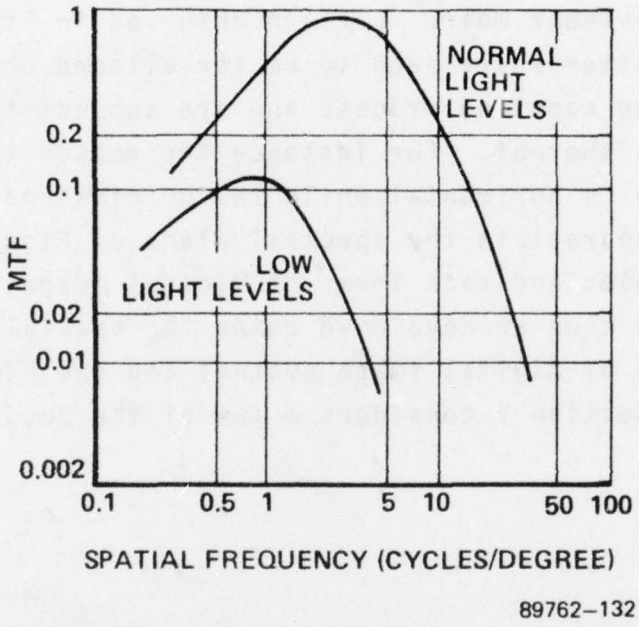


Figure C-5. Modulation Transfer Functions of Visual System (at Retina)

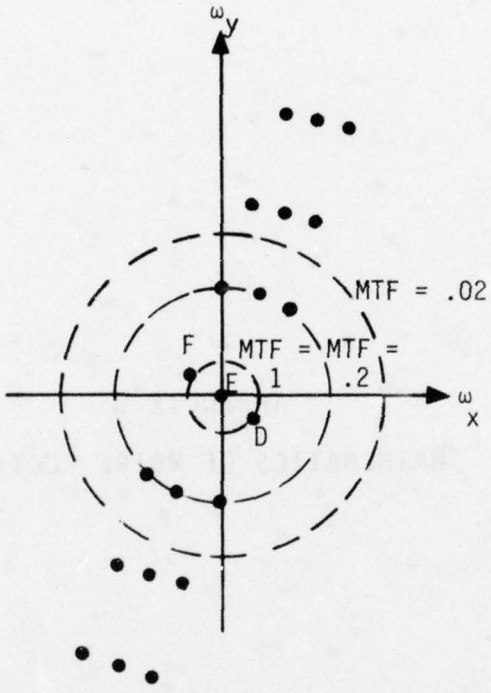


Figure C-6. Relative Response of the Eye to the Spatial Frequency Distribution of Figure 5-4

APPENDIX D

MATHEMATICS OF MOIRE' PLOTTING

APPENDIX D

MATHEMATICS OF MOIRE' PLOTTING

A mathematical understanding of the means by which Moire' patterns can be used to plot function is developed here.

Let the lines of the test image, Figure 5-9, consisting of horizontal lines be indexed by the sequenced

$$h = ... -2, -1, 0, 1, 2, ...$$

and the lines of Figure be indexed by the sequence

$$k = ... -2, -1, 0, 1, 2, ...$$

as shown there. It will be seen in Figure that the Moire' patterns will be observed at the locus of the points of intersection of the two patterns of Figures 5-9 and 5-10 where h-k is another integer p

$$p = ... -2, 1, 0, 1, 2 ....$$

That is, the Moire' patterns are solutions of the subtractive indicial equation

$$h - k = p \qquad (D-1)$$

Now the equation for the lines of Figure is

$$y = bh + tf(bh) \qquad (D-2)$$

Where

y = the vertical position of any point on the line

b = the normal spacing of the lines

h = is defined above

t = a constant, the scale factor

$f(.)$ = the function by which the line spacing deviates from the normal spacing, b

The equation for the lines of the figure consisting of horizontal lines when canted at angle α is

$$x = y \cot \alpha - bk \cos \alpha / \sin \alpha \qquad \text{(D-3)}$$

where

x = the horizontal position of any points on the line and all other values are defined above

Equation (D-2) can not in general be solved for h. Instead, solving Equation (D-3) for k gives

$$k = \frac{y \cot\alpha - x}{b \tan \theta} \qquad \text{(D-4)}$$

Inserting Equation (D-4) into Equation (D-1) gives

$$hb = \frac{y \cos\alpha - x \sin\alpha}{\cos\alpha} + pb \qquad \text{(D-5)}$$

Now rotating the coordinate system clockwise through an angle α gives the old coordinates x, y in terms of the new coordinates x', y'

$$y = y' \cos\alpha + x' \sin\alpha \qquad \text{(D-6)}$$

$$x = y' \sin\alpha + x' \cos\alpha \qquad \text{(D-7)}$$

Combining Equations (D-6) and (D-7) into Equation (D-5) gives

$$hb = \frac{y'}{\cos\alpha} + pb \qquad \text{(D-8)}$$

Substituting Equations (D-8) and (D-6) into Equation (D-2) gives

$$x' = \frac{1}{\sin\alpha}\left[y'\left(\frac{1}{\cos\alpha} - \cos\alpha\right) + pb + tf\left(\frac{y'}{\cos\alpha} + bp\right)\right]$$

Now as $\alpha \to 0$

$$x' \approx \frac{1}{\alpha}\left[pb + tf(y+bp)\right]$$

Upon appropriately shifting the origin and dropping primes, the Moire' pattern obeys the equation

$$x' \approx \frac{t}{\alpha} f(y)$$

Thus it is seen that the Moire' pattern plots the function $f(\cdot)$ at an amplification inversely proportional to α, the angle of cant, of the original patterns of Figures 5-9 and 5-10.

APPENDIX E

MEASUREMENT OF MTF BY THE OBSERVER

APPENDIX E

MEASUREMENT OF MTF BY THE OBSERVER

Section V-B described an approach by which the MTF of a digital system could be determined by an observer without test equipment. The mathematical justification is given here.

Let $A_{IN}(x,y)$ and $A_{OUT}(x,y)$ be the amplitude of the sine wave at location (x,y) in the original and reproduced test images.

Now from Equation (1) x is also the spatial frequency of the sine wave at the point (x,y). Thus

$$A_{IN}\ (x,y) = y$$

Now from the definition of MTF it is seen that

$$A_{OUT}(x,y) = MTF(x)\ A_{IN}(x,y)$$

$$= MTF(x)y$$

For any given conditions, there exists a minimum amplitude d(x) of any spatial sine wave of frequency which any given human can perceive. Thus there exists a b(x), Figure 5-7, such that

$$A_{OUT}(x,b(x)) = d(x)$$

and there exists an a(x) such that

$$A_{IN}(x,a(x)) = d(x)$$

It follows

$$A_{OUT}(x,b(x)) = d(x) = A_{IN}(x,a(x))$$

or

$$MTF(x)b(x) = d(x) = A_{IN}(x,a(x))$$

or

$$MTF(x)b(x) = a(x)$$

or

$$MTF(x) = \frac{a(x)}{b(x)}$$

which is the results obtained at Step 4 of the procedure of Section V-B.